

Report of simulation investigations, a base of statement that life evolves in the half-chaos

Andrzej Gecow

<http://viXra.org/abs/1603.0220> <https://sites.google.com/site/andrzejgecow/home> gecow@op.pl andrzejgecow@gmail.com

Investigations were done in 2011-2015. Description based on wider Polish version. It is simultaneously a publication and a supplementary data for publications (e.g. [Naaj](#)). Specific form is dedicated for reading from screen which allows to enlarge particular figures for analysis. It contains over 400 graphs and tables (formally 72+17) .

Correction 30 Nov 2017: In a met8 research described in the ‘[Report of simulation investigations, part II, a growth of half-chaotic autonomous networks](#)’, it turned out that practically every autonomous network has classical modules, so also random networks with constant structure investigated in this paper. This forced me to change the names ‘semimodule’ and ‘semimodularity’ to ‘ro-module’ and ‘ro-modularity’ because they incorrectly suggested that ro clusters (Ch. 5) are not also classic modules.

Abstract

Half-chaos is a specific state of deterministic dynamic networks with parameters which random network make strongly chaotic. In the half-chaos small disturbance may give chaotic or ordered reaction in similar probability. Existence of such network state was up till now problematic, described investigations prove it existence in networks with random, constant structure and show methods to create it and its properties. Version of half-chaos based on “ro-modularity” mechanism is especially interesting. Ro-module is a relatively small, isolated, functioning (nodes change their states) network segment when the majority of nodes of this network do not change their state. Ro-modules are also classic modules. Half-chaos is kept while small changes are accumulated but vanish when one large change is accepted. Half-chaos state is much more adequate for living and civilization objects description, therefore known Kauffman hypothesis “life on the edge of chaos” may be deepen and reinterpreted to “life in the half-chaos”, which is the main purpose of the investigations.

Keywords: chaos; complex networks; dynamic networks; deterministic networks; Kauffman networks; computer simulation.

Contents

Abstract	1
Contents.....	1
Some strange names or shorts and typical parameters	4
1 Introduction	5
1.1 Short view of problem.....	5
1.2 About form.....	6
2 Negative feedback density increasing - met1 & 2	7
2.1 Introduction.....	7
2.1.1 Task.....	7
2.1.2 General assumptions.....	7
2.1.3 met1.....	8
2.1.4 met2.....	8
2.2 First experiment	9
2.3 Second experiment – influence of parameter tmx in met2.....	12
2.4 Third experiment – nets behaviour for large t , met2 200.....	14
2.4.1 Tasks and assumptions	14
2.4.2 Results.....	17
2.4.3 Secondary initiations	19

30 November 2017	Andrzej Gecow	andrzejgecow@gmail.com	Report of simulation investigation... half-chaos	Introduction	2
2.4.4	Crocodiles				20
2.5	Fourth experiment - interactive narrowing of function by met2				33
2.6	Summary				38
3	Modularity – met3				39
3.1	Aims and premises				39
3.2	Provisional reconnaissance				39
3.2.1	Primitive simulations, chaos on nodes level, tmx=60				39
3.2.2	Estimation of N1 for short attractor in the module				39
3.3	Simulation after met2 200, chaos on module level, tmx=20000				41
3.3.1	Investigation of stability				41
3.3.2	Attractors in the modules and global ones				42
3.3.3	Crocodiles				43
3.4	Conclusion				47
4	Point attractor – met4				48
4.1	Introduction				48
4.1.1	General aims				48
4.1.2	Premises from earlier investigations met1, 2 and met3				48
4.1.3	Interpretive basis				48
4.2	Investigated models				49
4.2.1	Models without regulation: c for 4,3 $f(0,0,0)=0$, and d for 2,4 $f(0,0,0,0)=0$				49
4.2.2	Model with minimal regulation b for 4,3 $f(0,0,0)=f(0,0,1)=f(0,1,0)=f(1,0,0)=0$				49
4.2.3	Model a with strong regulation for 4,3				49
4.2.4	Simulations done				49
4.3	Basic results				49
4.3.1	Clearly separated, similar capacity 2 peaks – ordered and chaotic events in damage size distribution				50
4.3.2	Fraction of PAS in accepted events, investigation of secondary initiation				51
4.4	Conclusion from crocodiles				54
4.5	More important problems of simulations, A1-4 and threshold				60
4.6	Summary				61
5	Accumulation of ordered changes does not lead to chaos, ro-modularity – met5				62
5.1	Introduction				62
5.1.1	Aims				62
5.1.2	Interpretive view				62
5.2	Accumulated changes, passes N1,N2,M, formulas bf,br,cf,cr, s,K=4,3				62
5.3	Problem of shift and of fade out type, series 34				63
5.3.1	Results of investigations				63
5.3.2	Explanatory example				65
5.3.3	Ice and independence of loops				65
5.4	Advanced series 44 – passes M free & with blockade of smearing, shift=50, steps of attractor length				65
5.5	Simplified series 45 to bring nearer to chaos, shift=2, not diminished attractors, $A_3 \geq 3$				74
5.6	Ro-modules – searching for premises and proof				85
5.6.1	From frequency of secondary initiations				85
5.6.2	From distribution of small attractors fractions				86
5.6.3	From distribution of P(A4), A4 – number of disturbed nodes, local cluster A4 – set of disturbed nodes				87
5.6.4	Connections of local clusters A4 into global clusters A4				89
5.6.5	From distribution of A1 for accepted on right wall of crocodiles				91
5.7	From periods of node state cycles – series of investigation clusters ‘ro’				92
5.7.1	Initial detailed investigation				92
5.7.2	Local and global clusters on example bf 103 from series 44 ‘4+7+20’				94

30 November 2017	Andrzej Gecow	andrzejgecow@gmail.com	Report of simulation investigation... half-chaos	Introduction	3
5.7.3	Series ro 44 '4+7' 100 M20, statistical investigations				97
5.8	Conclusion and summary				106
6	Start from the short attractor instead PAS0 – met6				108
6.1	Introduction				108
6.2	Short attractor				108
6.2.1	Creating of short attractor				108
6.2.2	Stability investigation of system with short attractor				108
6.3	Investigation of evolution – accumulation of changes as in passes M of met5 ro 44				109
6.4	Half-chaos in met6 and conception of ro-modules				113
6.4.1	In met6 is lack of ro-modules				113
6.4.2	Clusters A4				113
6.5	Conclusion				116
7	Controlled creation of ro-modules – met7				117
7.1	Introduction				117
7.2	Constructing of ro-modules				118
7.2.1	Basic algorithm				118
7.2.2	Increasing active ro-modules number				118
7.2.3	Short attractor forcing, tax in met7b and met7eb				118
7.2.4	Limitations for algorithm of ro-modularity creation				118
7.3	Ro-modules investigations directly after creation – met7a and met7b				119
7.3.1	Assumptions				119
7.3.2	Damage size distribution as the main result of met7				119
7.3.3	Testing effectiveness of algorithm				124
7.3.4	Basic mechanism of ro-modularity				126
7.3.5	Comparison of met7a and met7b models				129
7.4	Investigation of evolution – accumulation of changes – met7e				137
7.4.1	Left peak and parameters selection				137
7.4.2	Clusters ro – ice and local cluster size distribution, additional disturbing mechanism 'mech2' similar to met6				142
7.4.3	Global clusters ro and their comparison to generated ro-modules				151
7.4.4	Similarity of ro-modules attractors after accumulation				157
7.4.5	Fade out as factor of mech2				159
7.4.6	Clusters A4 and their connection				161
7.4.7	Attempts to find in pass N an indicator of later deviations from met5 of net f				165
7.5	Summarising				169
7.5.1	Ro-modularity creation				169
7.5.2	Stability of obtained ro-modularity without evolution				169
7.5.3	Confirmation of the blocking mechanism of explosion by small local attractors in spite of the large global attractor				170
7.5.4	Stability of ro-modularity during evolution - accumulation of 'small' changes				170
7.5.5	Other mechanisms detected				170
7.5.6	Clusters ro and A4 - check interpretation of ro-modularity				170
References					171

Some strange names or shorts and typical parameters

s – number of signal variants. They should have the same probability. **K** – number of input links in each node of network. **s,K** – two dimensional parameter (s,K).

N – number of nodes in network. **tmx** – number of observer time steps, maximal time, length of investigated section of trajectory.

net types: **f** – scale free (sf), [Barabasi-Albert](#), **s** – single scale (ss), **r** – “Random” [Erdos-Renyi](#) (er). **reversed-annealed algorithm** see [\[arj ch.3\]](#) [\[dgec, bics, fgec, it\]](#)

ini – initiation, permanent change of function value for one node, for one input state (particular signals on all K node inputs).

PAS – Point Attractor System, network where each current node state is equal the node function value for current input state. Attractor length =1. See ch.4.

PAS0 – PAS where each current node state = 0 (and each current node input state contain all K input signals=0).

d – **damage** – fraction of nodes which node state differs between observed disturbed network and pattern – original, not disturbed network. $d=A/N$,

A – **Avalanche** – number of damaged node (state of the node differ to pattern).

Threshold – arbitrarily taken number (from the gap between **left** and **right peak** in damage size distribution) which differs small (ordered) and large (chaotic) effective change in $A(tmx)$. **Accepted ini (akc)** - which has $A(tmx) < \text{threshold}$.

q = (number of accepted ini)/(all ini). Stability is measured using **order degree q** (symbol used as in [\[Ramo06 see ch.2\]](#)).

met2 – Method 2 of half-chaos search. From met2 to met7 they are described in chapter 2 to ch.7 respectively.

explosion – rapid come of process from small difference to pattern (order) to large difference (chaos).

crocodile – useful form of image of simulation, see ch.4.4.

half-chaos, ro-modularity – see ch.1.1 and other introductions.

1 Introduction

1.1 Short view of problem

This study is a working wide description of simulation investigations conducted by me to explain problem of Kauffman hypothesis that life is on the edge of chaos and order. I admire of Kauffman, he makes a large step in similar time, when I also have try to do something in this direction. Currently I use Kauffman networks in my investigation. Unfortunately, of this subject we have different outlook, and for each of us ours thesis are especially important. My reason to pick up these investigations is a contradiction of current form of this hypothesis to my assumptions for my model of structural tendencies, which come into being in 1974 before Kauffman hypothesis has arise. Who is right – me or Kauffman? Shown results indicate, that me, but difference is small and Kauffman hypothesis is not refuted, but deeply reinterpreted.

[Kauffman in 1969 - 71](#) has proposed Boolean networks (called also Kauffman networks) for living systems description. Only after decade physicists have spot them. In such networks build fully random has been found phase transition between order and chaos, in few general parameters. It is a rapid change of system properties in stability aspect after a small disturbance. Kauffman indicates, that necessary for life evolution small changes of function are accessible only near this phase transition, but it considers only fully random systems in all remaining aspects and parameters.

I have published in 1974 in Polish and in 1975 in English on Fifth International Congress of Biomathematics in Paris certain model of extremely controversial recapitulation of phylogeny in the ontogeny. In this model and its simulation I use my network, similar to Kauffman network, which I call aggregate of automata. Basing on complex, justified estimation I take, that life evolves in chaos – as currently we can shortly say. That time notion ‘deterministic chaos’ in limited networks does not exist yet. Effective publication of this model find two obstacle: an aversion in the biology and conflict with Kauffman hypothesis. Up till now nobody indicate this conflict, but nobody pick up discussion despite lot of publications. All that's left for me to do is to prove, that life evolves in chaos, more exactly – in half-chaos. At last few years I make deeper investigation, I have such prove and just in this study I describe it in the most widely form (only Polish version is a little wider). Part of arguments for this thesis I have already published, but the main are shown fully first time here (<http://viXra.org/abs/1603.0220>). It state a basis for shorter publications [Naaj](#) (<http://vixra.org/abs/1612.0390>).

Kauffman uses for his model several parameters and he build on them a space of conceivable systems. In this space there is the phase transition, and the best area for the life lies near this transition, on order side, which implies from needs of small effective changes. There evolution based on small permanent changes which initiate effective changes of function, should have the best results, therefore observed living objects should be the systems belonging to this area. That is the hypothesis ‘life on the edge of chaos’.

There is no error in this model and reasoning, but as in any model, lot of elements are simplified by assumptions. Here lot of parameters, which are not openly considered, are treated as random. The system space contains any variants of system and has small number of dimension. This also is correct.

Problem lies in adequate selection of the most influencing parameters for consideration in model. But evolution detects any possible means of adaptation, which especially make limitation to small number of parameters difficult. Passing over such dimensions results that possibility which they offer are invisible. In such a case the conclusion, that life tends to indicated area of parameters (when remain are random) is correct, but that life achieves this area, may not be correct, because these remain parameters can give more attractive offers.

Kauffman has investigated mainly parameter K (number of inputs to the node) fixing N (number of nodes in the network), but functions and node’s states were random. However, question: ‘what lack of randomness of these elements effects’ was investigated. Conclusion does not challenge view of phase transition nor the Kauffman hypothesis.

My investigation took less formal way. I try to base an increased stability of chaotic systems on negative feedbacks, whose Kauffman practically did not take into consideration in his model, however he discusses them in his book [ooKauf](#). My effects confirm their important role, but they suggest simultaneous necessity of short attractors and probably modularity also. The modularity also looks not enough in investigated area, however, factor of short attractor turns to be sufficient.

Extremely short attractor – point attractor, as start point of evolution gives not only a specific state of strongly increased stability which is proper for evolution and can be hold freely long by condition of small effective change, but it also creates properties similar to modularity, despite even connection of nodes. I call this state ‘ro-modularity’. Its properties are very similar to liquid state described by Kauffman, where he saw living objects, but system has here chaotic parameters (if system is random, they give mature chaos, i.e. damage size distribution is properly described by [Derrida](#) balance level). Acceptance of small effective changes does not take out of half-ordered state but one acceptance of large effective change is enough to disappearing of this specificity and system stays typically chaotic in agreement with parameters. This area associates to

overheating liquid. There is no phase transition here, which needs that system is chaotic or ordered, but not together. Here these two form of reaction on small initiating change have similar probability – chaos in mature form and order exist here simultaneously in similar degree.

Because parameters of system are chaotic (in sense of random system), generally this state should be called 'half-chaotic', but more adequate is to say that life evolves in second half – in 'half-order'. On distribution of the damage size (size of effective change) measured using number of node states which differs to control system, there are two peaks separated by gap of counts. Left peak for ordered changes (small) and right peak for chaotic changes near [Derrida](#) equilibrium. Existence of such two peaks is typical for liquid region, especially for its part lying in chaos, but there left peak of ordered cases is very small and for more chaotic systems can be neglected. In half-chaos despite systems have 'more chaotic' parameters, both peaks are similar. When we call 'chaotic' a finite deterministic network, we do not clime, that each small initiation gives a large effective change, but that nearly all do so. The Kauffman hypothesis also do not clime that evolution is impossible in chaos range, but that there is harder to evolve. Even if all initiations lead to large change, then it is possible that before change has grown up to such size, will be enough time to evolving object replicates and mutates. An assumption that damage avalanche grows rapidly after initiation must not be always true.

The point attractor is an extreme, therefore I have check, that ro-modularity can be build basing on received description which confirm that description is complete. I check also, that for half-chaos small attractor is enough, but in such a case it is not a ro-modularity and a shape of left peak is especially narrow and not so suitable for evolution. In both cases a long cumulating of small effective changes does not lead to leave half-order state. In most investigations as small initiating change a point change of function was used (for one input state), but I check also, that structure change (addition or subtraction of node) leads to similar effects.

From the beginning, I have reservations about number of signal variants to Kauffman assumptions. On the simple example of a thermostat I show [\[ari.it\]](#) that Boolean networks are not always adequate enough to statistical investigations. I also show there other interpretive arguments for higher number of signal variants. In below described simulation experiments I also use more than two equally probable signal variants. As in earlier publications, I stand by suggestion, that in such a case name 'Kauffman network' should be still used.

Described results are sufficient basis to deep reinterpretation of Kauffman hypothesis 'life on the edge of chaos', which for distinguish should take sound 'life in half-chaos'. This way the 'reversed annealed algorithm' used in my earlier simulation of structural tendencies gets sufficient basis and gets rid of collision with proper place for life. The half-chaos gives a new view on the life, a definition of small change which is a base for natural identity criterion of evolving object, a core of Darwinian mechanism.

1.2 About form

This is a provisory description of my simulation experiments, report of these investigations. They are long, took more than 5 years, and were no so linear, like this description. Obviously, much more experiments, calculations and graphs are done, here only the most important are shown. I often have come back to early closed theme due to finding new tools or new understanding. So 'crocodiles' are introduce in met4, but much advanced are used in met2. Also description grows not simultaneously to experiments, however, this data are also to me too large to make them in one consistent form. It is not a book to read, it is for study on screen a particular problem if something is not clear in publication, but may be, some forced students will have to read it. I ask then for forgiveness, especially because my English is as it is and cannot be better, because I have not a money for help, I am pensioner only. Be happy, that you must not read it in Polish. I apologize for the remains of a mess, but it's only small remnants. They are complex. Many theme are only provisionally recognized, despite their attractiveness perspectives, but I can not do everything, because something should be leaved for Followers, and it is worth ever come to an interesting 'end' and be able to show it. Besides, I should also make it on time because counting to finishing at the age over 70 years is rather an excess of optimism. So you not only can, but even should choose a topic and some unfinished and wade through the virgin bush. In met3, e.g. there is no check whether the resulting increase in stability is permanent with accumulation of evolutionary change. I did these notes so faithfully es I can, I noted things 'obvious', but when it came to use them after a time, I had usually a lot of trouble. However, without this report all this work would vanished like a cloud.

All particular materials exist, such as documentation and the results of simulations and Exel files and their development. If you will need to delve into these materials, it is possible, but for that I am needed. I hope that I will find everything and every detail can be checked. There are also programs in Pascal and .exe for each experiment, they would be shared, but without my help rather no one come through the swamp. Maybe it will have a sense of returning to such sources, if someone's recurring results of my research will get a little different effects. Then we would need to find out why.

Figures and tables are numbered within chapters 'met', a reference to another chapter and met is: [m3.fig.2](#), means met3, chapter 3 and in it the [fig2](#). References to figures and tables are marked in red, to easily find them in the text. To study a figure should be enlarged. **Important sentences are marked.** [Reference to literature](#) as well, but later I resigned from it, it should be in the publications.

2 Negative feedback density increasing - met1 & 2

2.1 Introduction

2.1.1 Task

Interpretive consideration of living object suggests that really random reactions are chaotic, but stability is achieved by naturally selected reaction, means – not random.

I expect, that these reactions are negative feedbacks. This view should be confirmed by simulation.

Then let us take a random chaotic system and change a part of its feedbacks from random to negative. We expect in the effects, that in damage size distribution the right peak of Derrida balance of chaotic reaction will stay as before, but left peak of ordered reaction containing small effective reaction should be much stronger. In random chaotic systems this left peak is very small and can be neglected, but for not random systems it may be similar to right peak, and in such a case system is simultaneously ordered and chaotic. **I call such a system ‘half-chaotic’**. This view was a basis of my ‘reversed-annealed algorithm’ (see ch.1.1), but conflict with currently taken view of ‘life on the edge of chaos’ needs decide.

This is a particular task – to check a particular first expected answer for wider question: ‘exist such ‘half-chaotic’ systems simultaneously ordered and chaotic?’ and ‘what is a difference between them and typically chaotic?’

From assumption, these series of investigation (**method 1 and 2 of stability increasing for chaotic systems, in short: met1 & 2**), we limit to function selection and we leave without changes the random structure of connectivity and random initial states of nodes.

We expect, that such a structure contains enough feedbacks which we will be able to change into negative.

Another assumption included in such a program, is that it is possible to change something not very complicated in random system to get ‘half-chaotic’ system. (This assumption turns to be problematic.)

The main effects turn to be generally negative, what was a surprise, but some exceptions suggest, that problem lies in length of attractor and path to it. These observations are a basis for next methods of stability increasing for chaotic systems.

2.1.2 General assumptions

We extinguish damage in disturbed system on a section of trajectory, which length is **tmx** steps, by suitable change of function. We do not care is it feedback, but damage is an effect of initiation.

After random creation of network of given parameters N (number of nodes), s (number of equally probable signal variants), K (number of input to any node) and type (network type: sf – scale-free, er – Erdos-Renyi ...) which defines connections, functions and initial states of nodes, we record a trajectory of tmx steps calculated in synchronous mode.

Next, consecutively each node is initiated in all s-1 possible cases. Initiation (ini) is a change of function of this node only for initial input state. Because there are s variants of function value for any input state, that can be only s-1 possible initiations for any node. Initiation is permanent – means it is for whole tmx steps, but for one initiation. Such small permanent changes model evolutionary changes.

First such complete of initiations gives a measure of stability of a wild system – still fully random system, without correcting changes yet. During next complete of initiations correcting changes are imposed using method 1 (**met1**). Method 2 (**met2**) needs several complete of initiations. A measurement of stability after correction needs next complete of initiations. In met1 two passes of correction and measurement are made for answer help something a second pass or not.

Stability is measured using order degree q (symbol used as in [\[Ramo06\]](#), changed from ‘r’ used in my earlier works [\[it,ari,brj\]](#)). $q = (\text{number of accepted ini}) / (\text{all ini})$.

Accepted ini (akc) - which has $A(\text{tmx}) < \text{threshold}$. A(t) is a number of damaged nodes in time t – nodes which have other state than in not disturbed system, here – in table of recorded trajectory. Threshold – arbitrarily taken number which differs small (ordered) and large (chaotic) effective change in A(tmx) - number of damaged nodes in tmx.

Later threshold will be taken from the gap between left and right peak on damage size distribution. If q(tmx) does not change after small random permanent changes, then replication 1/q times with such changes should keeps number of evolving systems, despite that they are chaotic.

2.1.3 met1

First variant of method of stability increasing for chaotic systems is called ‘**met1**’. To hold trajectory unchanged, function corrections for given node can concern only node input states which are not used in trajectory of undisturbed system and not yet used in disturbed system. Then for each of node a set of unused input states is found. This set is decreasing while tmx grows, but it is not a linear dependency.

When after ini during calculation a node gets up till now unused input state and function for it gives damaged state, then function take for it value from undisturbed system. This is correction, it will stay if this ini is accepted ($A(tmx) < \text{threshold}$).

Due to reserve of unused input states will be distributed evenly for all ini, function correction is made if $A < 3$ and for one ini only 15 correction can be made. In the second pass these limitations are: $A < 7$ and 30 correction for one ini. Second pass results less than 1% better, and this effect is taken as effect of method. Such procedure generate system (in function range) which is more stable, but for particular initial state.

The met1 was tested for $tmx=60$, $N=400$ and 4000, $\text{threshold}=60$. Effects (fig.2) for $s=2$, $K=4$ are significantly worse than expectation, but for $s=4$, $K=3$ better than expectation based on algorithm ‘reversed annealed’ used in my earlier works. For higher tmx (e.g. $=2000$) the set of unused input state are very small and most of ini explode to chaos on first short section of trajectory.

2.1.4 met2

In met2 I abandon random undisturbed system and corrected system is build recursively for consecutive section of 10 time steps, but still for one initial state. Limitations as in first pass of met1 ($A < 3$, up to 15 correction for ini). After completion of all ini on the section, a new trajectory is calculated, longer by 10 steps ($\text{length}=tx$), up to reaching of $tx=tmx$. (Number of correction in condition of t is in fig.12 for modified method met2 200.) The met2 gives much stronger effects for the same parameters, as met1 (fig.2). Remark, that modifications of random functions convert random values into used for other input states, then functions become narrowed, which should increase of stability, without connection of function to particular nodes in network structure. Stability of corrected system is then compared to wild system and to system, where obtained function are shifted into other nodes (f2 in fig.2).

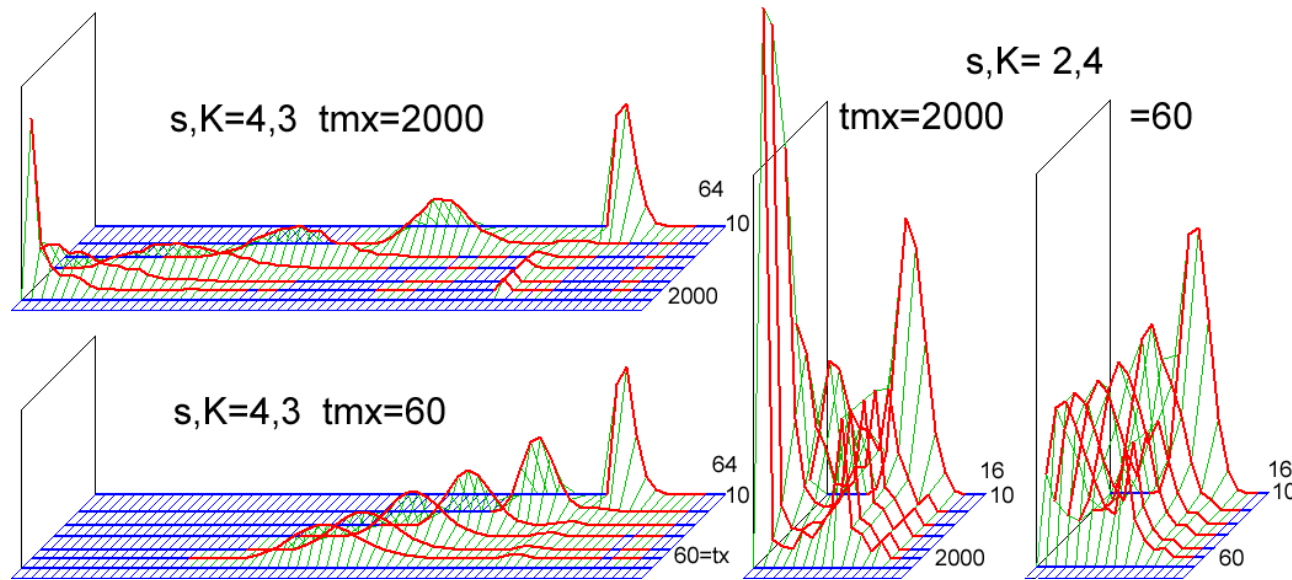


Fig.1. Distributions of number of unused input states for networks type f for 6 different tx . For networks r they are similar. For $tmx=60$ all 6 steps are shown, for $tmx=2000$ are shown selected $tx=10, 40, 90, 200, 600$ i 2000. In each case, stable peaks for larger number of unused input states are visible. They are an effect of short loops. For last sections and $tmx=2000$ unused states there are only few. Sharp cut in 54 for $s,K=4,3$ and $tx=10$ effects from possibility of used only 10 states from 64 in 10 steps.

Accessibility of unused input states is an important condition of described methods. For $s, K=2,4$ all input states for node there are $2^4=16$ but for $s, K=4,3$ there are $4^3=64$. Distribution of number of unused input states (fig.1) is similar for networks f and r, then I show it only for f, when higher fluctuations appear. Small peaks for higher number of unused input states stay for consecutive tx. They are an effect of short loops. For $tmx=60$ a 6 distribution are shown for tx increased by 10. For $tmx=2000$ tx=10, 40, 90, 200, 600 and 2000, for tx= 600 and 2000 the number are small, but significant number stay in loops, which length is near 20. These nodes have lot of unused input states, but they cannot use them for correction because they should not destroy loop. For r network there are less such short loops. In investigation on relationship of got stability and length tmx correction for all section tmx for each section of 10 steps is applied. It effects a large time of simulation, however in later sections it brings small number of corrections. In later investigations, for much higher tmx (e.g. 4000 to 20000) section of correction is 200, what is included in name of method (met2 200).

2.2 First experiment

In a first experiment $tmx=60$ and $N=400$ or 4000 . Degree of order q is watched for $s, K= 4,3$ i $2,4$; for 6 network types earlier investigated in [\[arj.brj.it\]](http://arj.brj.it) using Comparison of q for systems: wild, met1, met2, fn2 (function after met2 shifted into other nodes) and earlier results for autonomic and open networks using reversed-annealed algorithm are shown in fig.2. Results for 400 nets $N=400$ and for 20 nets $N=4000$ are practically identical.

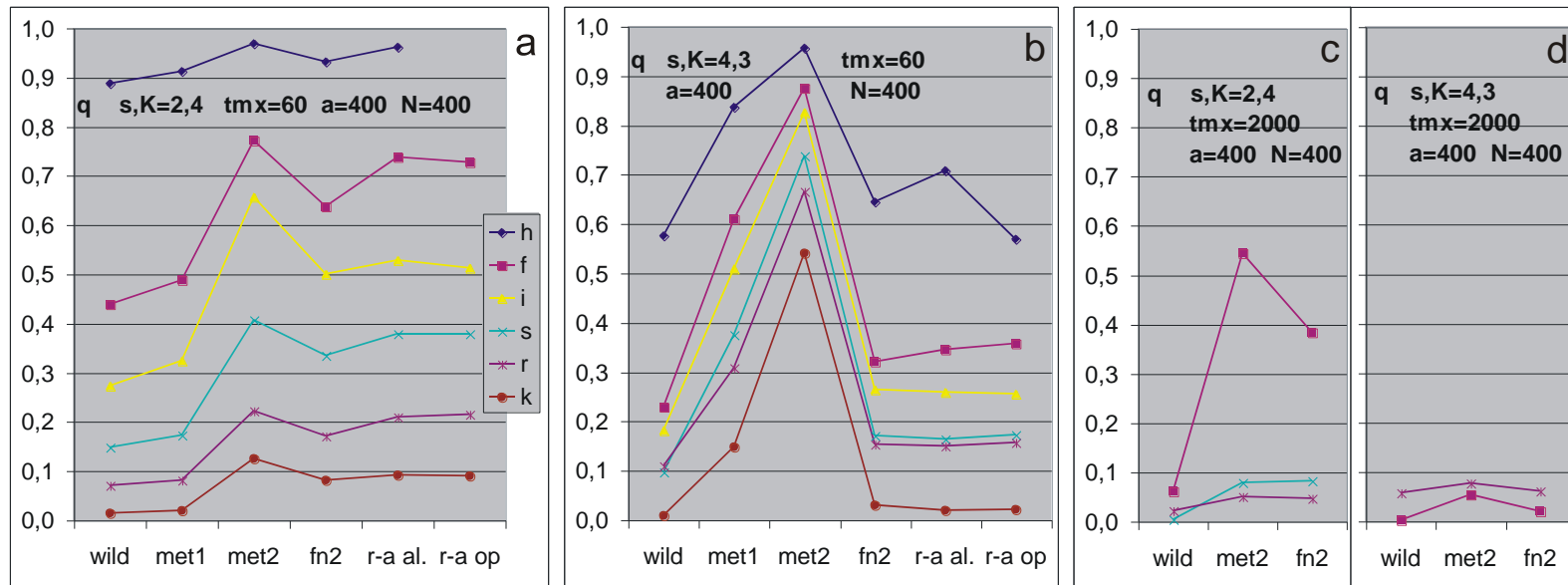


Fig.2. Comparison of degree of order q got in met1 and met2, for wild system, effected from function narrowing in met2 (fn2) and results of reversed-annealed algorithm for autonomic (r-a al) and open (r-a op) networks; for different network types used in [\[arj.brj.it\]](http://arj.brj.it). More important of the types: f-scale free, s-single scale, r-Random Erdos-Renyi. Unfortunately, comparison to r-a old results lost sense when results for $tmx=2000$ (c,d) are got (see also fig.4). It suggests, that met2 may be interesting if attractor length will be similar to $tmx=60$.

Such results allow to limits most of investigations to $N=400$ and f and r network types, which are more famous and moderately extreme. Net f is more ordered but r more chaotic, which is in agreement with investigation using reversed-annealed algorithm. For met2 assessment the fn2 effect is important. It is a necessary side effect of method, but met2 is stronger. For $s, K=2,4$ the effect is significant, but for 4,3 – small. Analysing it, an **internal homogeneity P** [\[ooKauf\]](http://ooKauf) is measured (table 1), which for wild is exact as should be, but for met1&2 are significantly higher. For $s, K=4,3$ it needs 4 numbers, which tell not much.

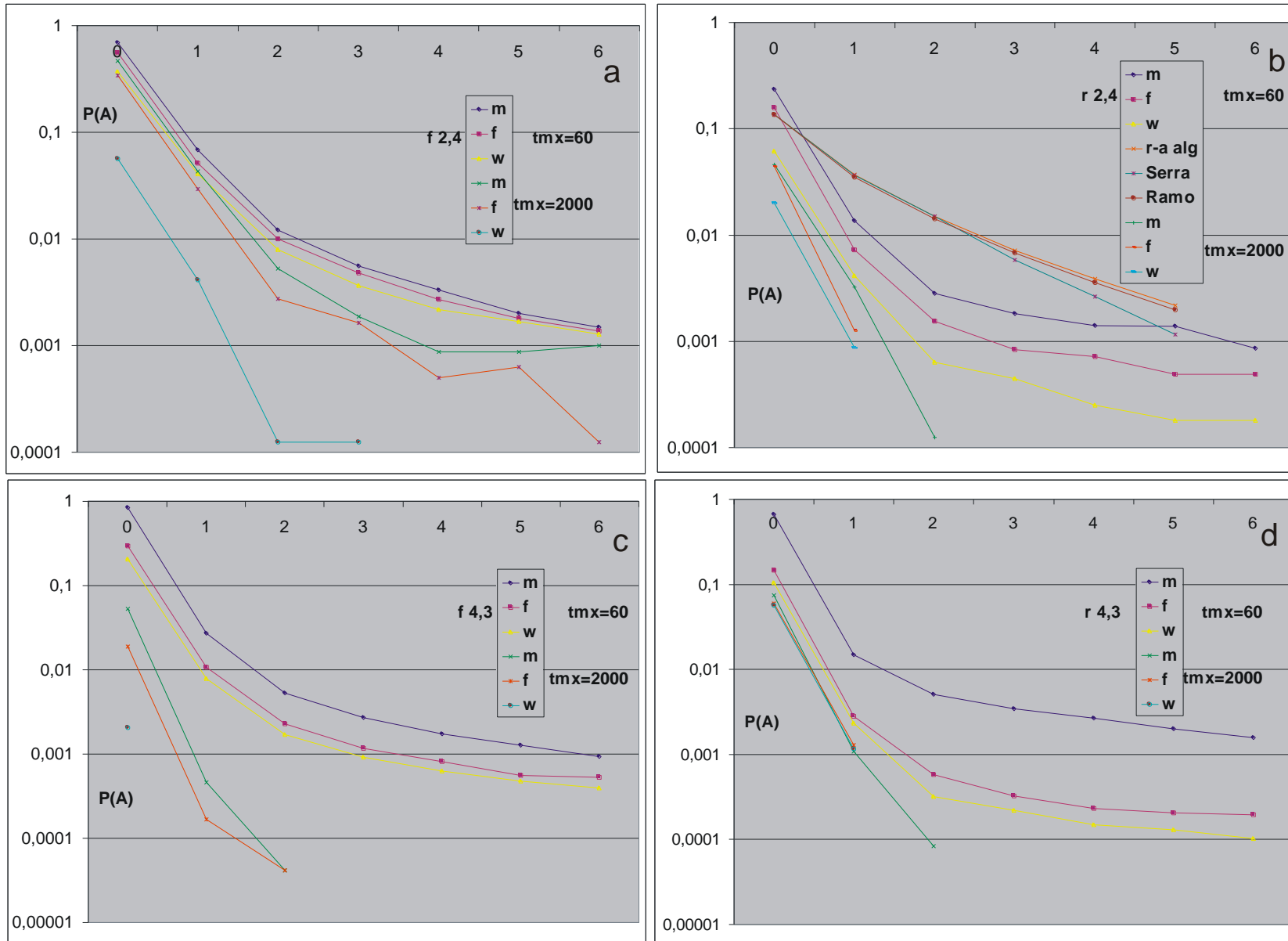
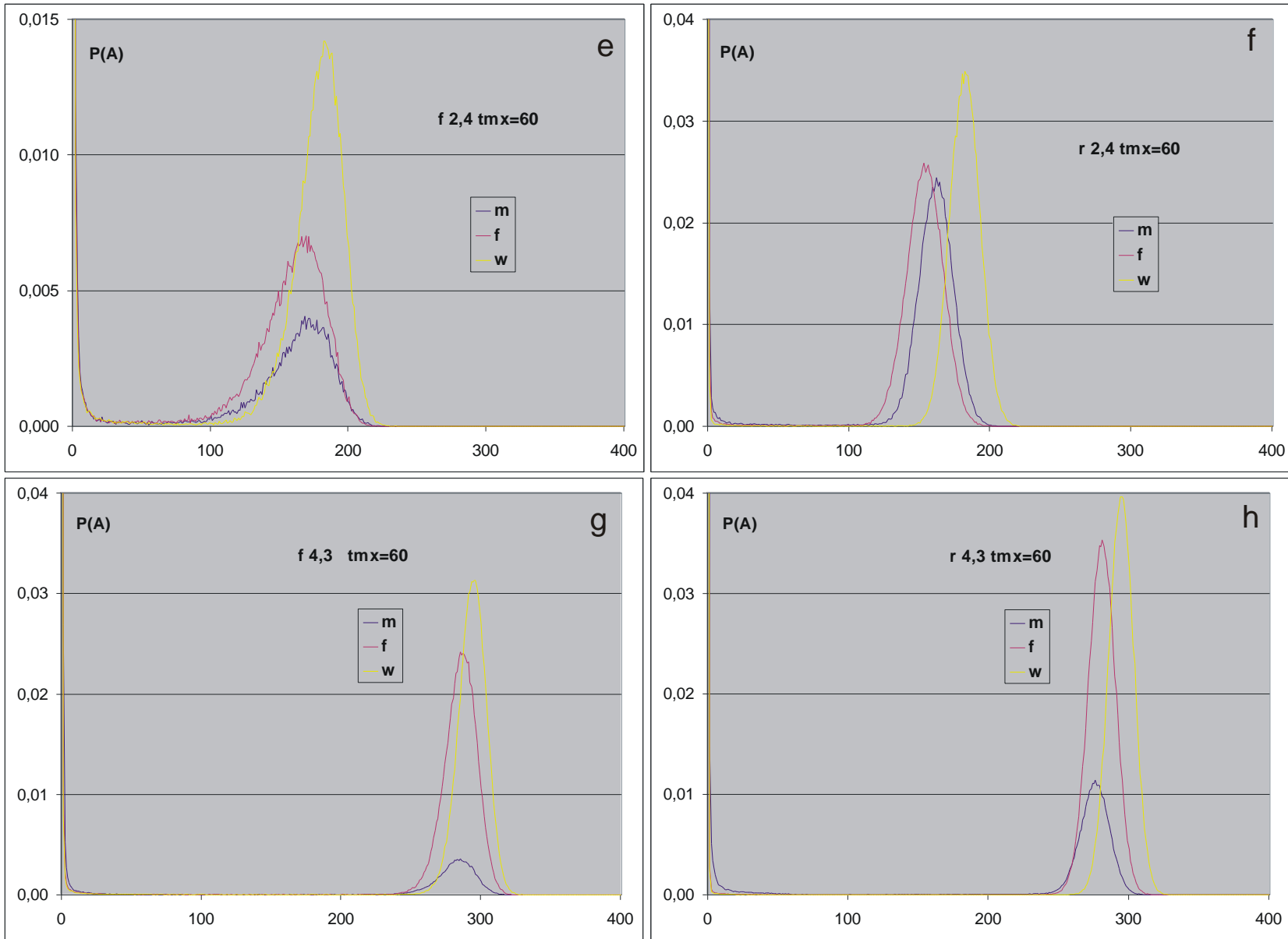


Fig.3. $P(A)$ - damage size distribution, in $tmx=60$ for networks scale-free (f) and Random Erdos-Renyi (r), $s, K=2,4$ and $4,3$. m-met2, f-fn2 effect of function narrowing after met2, w-wild random network without corrections. (a-d) - left peak in log-scale. For $r=2,4$ in addition distribution from reversed-annealed algorithm, theoretical distribution [Serrajtb07], $p(A)=b_A w^{A-1} e^{-wA}$ eq. (4.11) (where $b_1=b_2=1$, $b_3=3/2$, $b_4=13/6$, $b_5=29/8$, $b_6=237/40$, here A starts from 1 what is our $A=0$) and [Ramo06], $\sqrt{\pi} w^{A-1} A^{-3/2} e^{-(1-w)A}$ eq. (9). Unfortunately, results strongly depend on tmx – e.g. results for $tmx=2000$ is added (see fig.4). In next page (e-h).



(e-h) – full $P(A(tmx))$ - damage size distribution for $tmx=60$ in first experiment met2. m-met2, f-fn2, w-wild. Shift into left in comparison to wild of right peak of [Derrida](#) chaotic balance is an effect of function narrowing. Compare to fig.5 in [\[arj\]](#).

Table 1. Internal homogeneity P for s,K=2,4 tmx=60

wild=0,59827	h	f	i	s	r	k
met1	0,6098	0,6040	0,6060	0,6049	0,6046	0,6041
met2	0,6161	0,6286	0,6379	0,6429	0,6446	0,6462

Comparison to results of reversed-annealed algorithm turn to be too early, but they are an important indication. Experiment gives also distribution of damage size, which in left peak is compared in [fig.3a-d](#) also (in [fig.3b](#)) for reversed-annealed algorithm and for theoretical expectation [[Serrajtb07, eq. \(4.11\)](#)] and [[Ramo06, eq. \(9\)](#)] for ordered phase. The right peak of Derrida balance is shown in [fig.3e-h](#). Remark, that these results consider tmx=60, which occurs to be not adequate (what is shown in [fig.2c,d](#) and in [fig.3a-d](#) for tmx=2000, which is an effect of second experiment), however, if attractor length be similar to tmx=60, then such view may be adequate...

2.3 Second experiment – influence of parameter tmx in met2

Random networks, especially with $s > 2$, typically have very long attractors. At the time of experiment conducting, they look as impossible to monitor. Arbitrary defining of length of monitored section was then necessary. Extinguish of damage by increasing of negative feedbacks gives awaiting of shorting a global attractor length by local cycles, which may effected in reaching of higher stability area. Experiences of first experiment allow for complete – check for effect of large tmx=2000 for selected network types. Time of simulation strongly increases with tmx, simultaneously numbers of unused input states and of new corrections decrease ([fig.1](#) and [fig.12](#)). Dependency of degree of order q on tmx is shown in [fig.4](#). Unfortunately, when increasing tmx, q effectively drops down without stop on any increased level of stability. Only f 2,4 seems to reach such plateau. For r level of stability from blind nodes (without outputs, $k=0$) is depicted.

Results for f and r 2,4 suggest to check ‘middle’ network type s 2,4. It really gives middle result, which gives hope for small level of increased stability, however, it seems to be an effect of function narrowing. This experiment for s 2,4 gives amazing cut of m2 and fn2 before tmx=2000 for several independent simulations. The tmx was then enlarged to 3000 and next 20 nets are simulated.

Unused input states practically ended ([fig.1](#)), but maximal tmx=2000 or 3000 was still very small in comparison to average attractor. In [[ooKauf](#)] attractor for RBN is estimated (for $K > 5$) on $0.5 * 2^{BN}$ where $B = (1/P)^{1/2}$, then for $N=400$ and $P=0.5982$ ($K=4$) is over 2^{500} . I expect that such value is blurred and after met2 can be much lower. It may be an explanation of f 2,4. For 200 nets r 2,4 of weaker method (third experiment) there was no any attractor for tmx=10000, but for f 2,4 only 19% does not overcome one cycle of attractor. Entrance into second revolution of attractor ends decreasing of number $A < \text{threshold}$, then short attractor is a method on stable level of stability, which we are going to reach.

In [fig.4](#) q for different tmx is an average of different set of systems. Corrections are added in whole section of tmx. For consecutive points of tmx there are different numbers of simulated and averaged nets: 400, 80, 40, 20. It gives higher exactness where it is possible, but comparison may be misleading. Horizontal axis is similar to log-scale. In [fig.5](#) results of simulation for maximal tmx is depicted, it is for small number of nets (20, only for s 2,4 is 40), but they are the same nets for any t, and they have the same correction section – the highest tmx. It allows for comparison of slope, and of values for consecutive t. In [fig.6](#), however, the results of correction in section 200 for tmx=20000 are shown, but point $t=200$ does not change slope of curves.

In [fig. 2-6](#) averaged effects are presented, such pictures more say about methods, but less create intuition about process and statistical phenomena. For this a dynamical picture of simulation process called ‘crocodile’ is much more legible and richer ([fig.13-16](#)). It is first of all a dynamical picture of avalanche history $A(t)$ drawn on the screen for each ini. Certain other event are dynamically reported. After complete of all ini a graphic and in numbers summary of statistic is added like: (red) $L(t)$ - number of $A(t) < \text{threshold}$, remark, that $q(t) = L(t)/(s-1)N$, where $(s-1)N$ is a number of ini; number of damage faded out (blue) – $A(t)=0$. Dependences $q(\text{tmx})$ in [fig.4](#) and $q(t)$ in [fig.5,6,7](#) and in crocodiles are similar, but should be remembered, that crocodile and $q(t)$ in it, is for all ini in one, particular system.

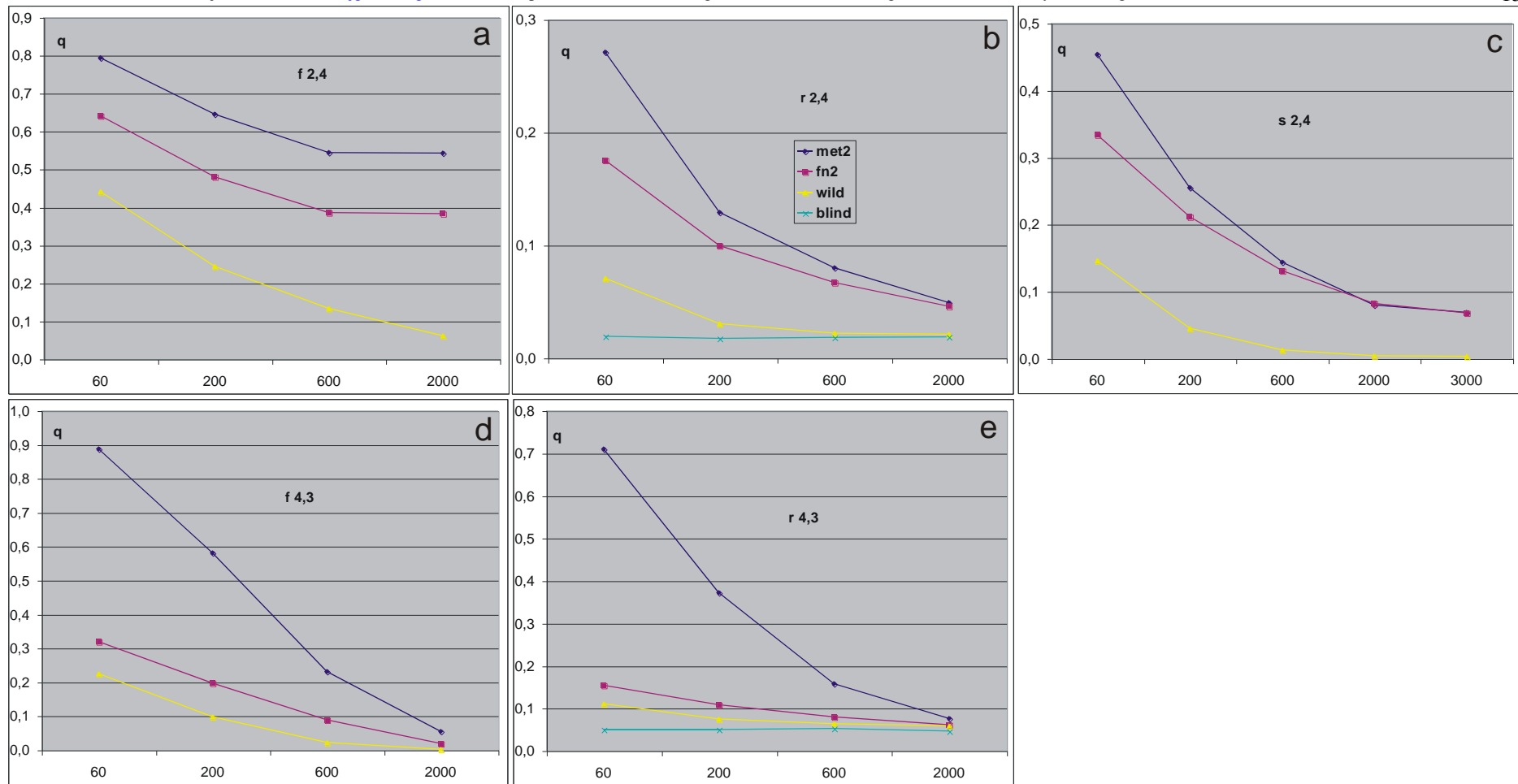


Fig.4. Dependency $q(tm_x)$ – degree of order q from tm_x for: met2, fn2 - narrowing of function after met2 and wild network, for net types: f and r; s, $K=2,4$ and $4,3$. In addition for s $2,4$. For r network (RBN) level of asymptote effected from blind nodes ($k=0$, i.e. without outputs) is shown. $N=400$. Number of nets for consecutive tm_x is: 400, 80, 40, 20. Only f $2,4$ seems to reach plateau. Remain nets f and r are in $tm_x=2000$ near to hypothetic asymptote, these asymptotes are not higher than wild. Additional net s $2,4$, which is in middle between f and r, may be, has increased level of asymptote. An amazing cut of m2 and fn2 before $tm_x=2000$ leads to enlarge tm_x to 3000 and here 40 nets are simulated for $tm_x=2000$ and 3000.

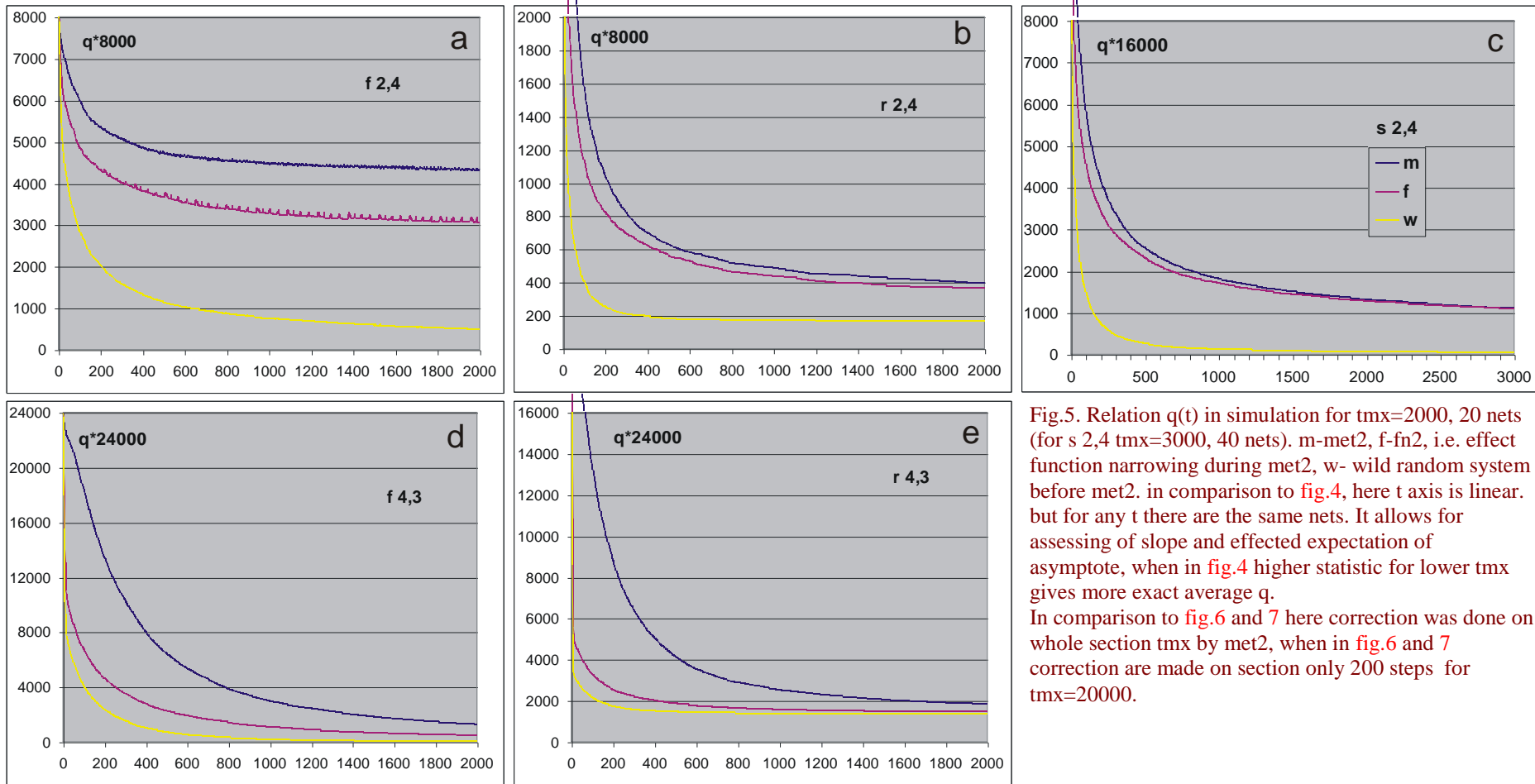


Fig.5. Relation $q(t)$ in simulation for $tmx=2000$, 20 nets (for $s\ 2,4\ tmx=3000$, 40 nets). m -met2, f -fn2, i.e. effect function narrowing during met2, w - wild random system before met2. In comparison to fig.4, here t axis is linear. but for any t there are the same nets. It allows for assessing of slope and effected expectation of asymptote, when in fig.4 higher statistic for lower tmx gives more exact average q . In comparison to fig.6 and 7 here correction was done on whole section tmx by met2, when in fig.6 and 7 correction are made on section only 200 steps for $tmx=20000$.

2.4 Third experiment – nets behaviour for large t , met2 200.

2.4.1 Tasks and assumptions

The results $q(tmx)$ for $f\ 2,4$ (fig.4a, 5a) suggest to check $q(t)$ in longer section tmx , because small slope for higher tmx must not be an effect of higher number of met2 corrections, but rather entering area of attractors. In a third experiment (its symbol is 'met2 200') the section of correction is shorted to 200 steps (20 sections of 10 steps) which radically decreases time of simulations. Limitations are weaker, as in second pass of met1: ($A < 7$, up to 30 corrections on one ini). $N=400$, as previously, but tmx is extended up to 20 000 in last simulations. After random creation of network, function and initial state, the wild (w) net was investigated, later this net was corrected by met2 200 and its stability was investigated (m) up to tmx . Counting on entry into attractor, state of network in tmx was taken as initial and stability investigation was repeated (x). It is not an extension to $2tmx$, because initiation was imposed in other initial states of nodes and of network. On the end, effect of narrowing of function (f instead of $fn2$) was measured. Here functions are swapped between first and second half of network and in addition input states of function were arranged in reversed sequence. It leaves statistics of functions like internal homogeneity P , but destroys any connection of corrections with structure, which stays without change. Also new initial states are randomly drawn.

Change of initial states only (investigated in other series s,K=2,4 than shown in fig.6) typically should (I have think) change of trajectory and basin of attraction. This curve is similar to f for nets s and r 2,4, but for f 2,4 it lies significantly higher and unexpectedly change of initial states only (after met2, means with corrected functions) gives similar effects as m and x. Really, 56% of such events enter attractor of undisturbed trajectory which length is the same as for m, probably the same attractor.

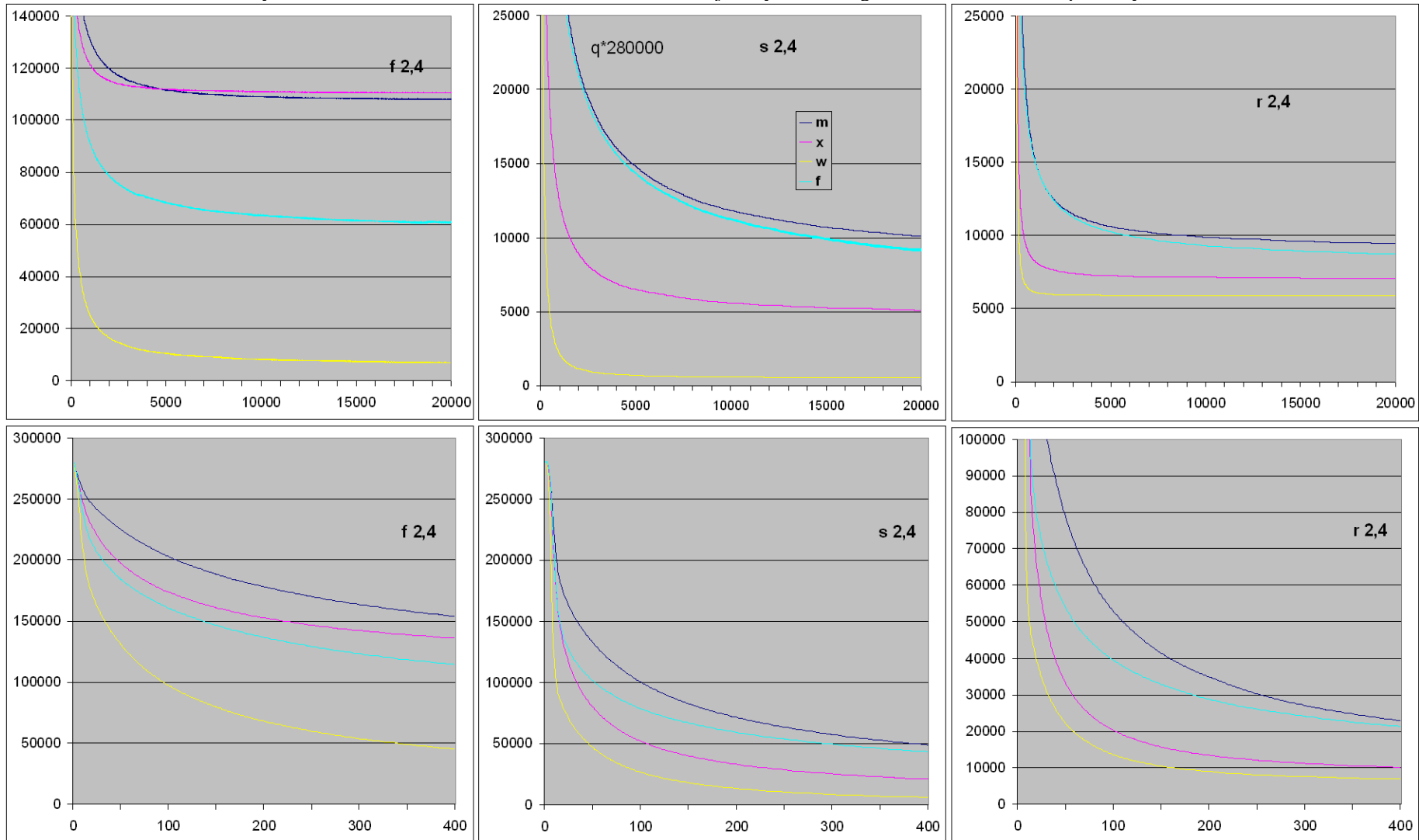


Fig.6. Result $q(t)$ of simulation of 700 nets **f, r, s 2,4** met2 200. Upper – in whole range $t_{mx}=20000$, lower – first section up till $t=400$; w – wild, m – met2 200, x – after shift of initial point by t_{mx} , f – narrowing of function, by-product of met2, after swapping of function for nodes, reversing sequence of input states of function and random changing of initial state. For net types s and r: perversity effect - $x < f$. Similarity of m and f shows, that achievements of met2 are only an effect of function narrowing. In lower row at point $t=200$ (end of corrections) there are no changes of curve slope. For f 2,4 the met2 gives expected strong increasing of stability q and shift of initial point gives larger increasing of stability than decreasing from perversity effect.

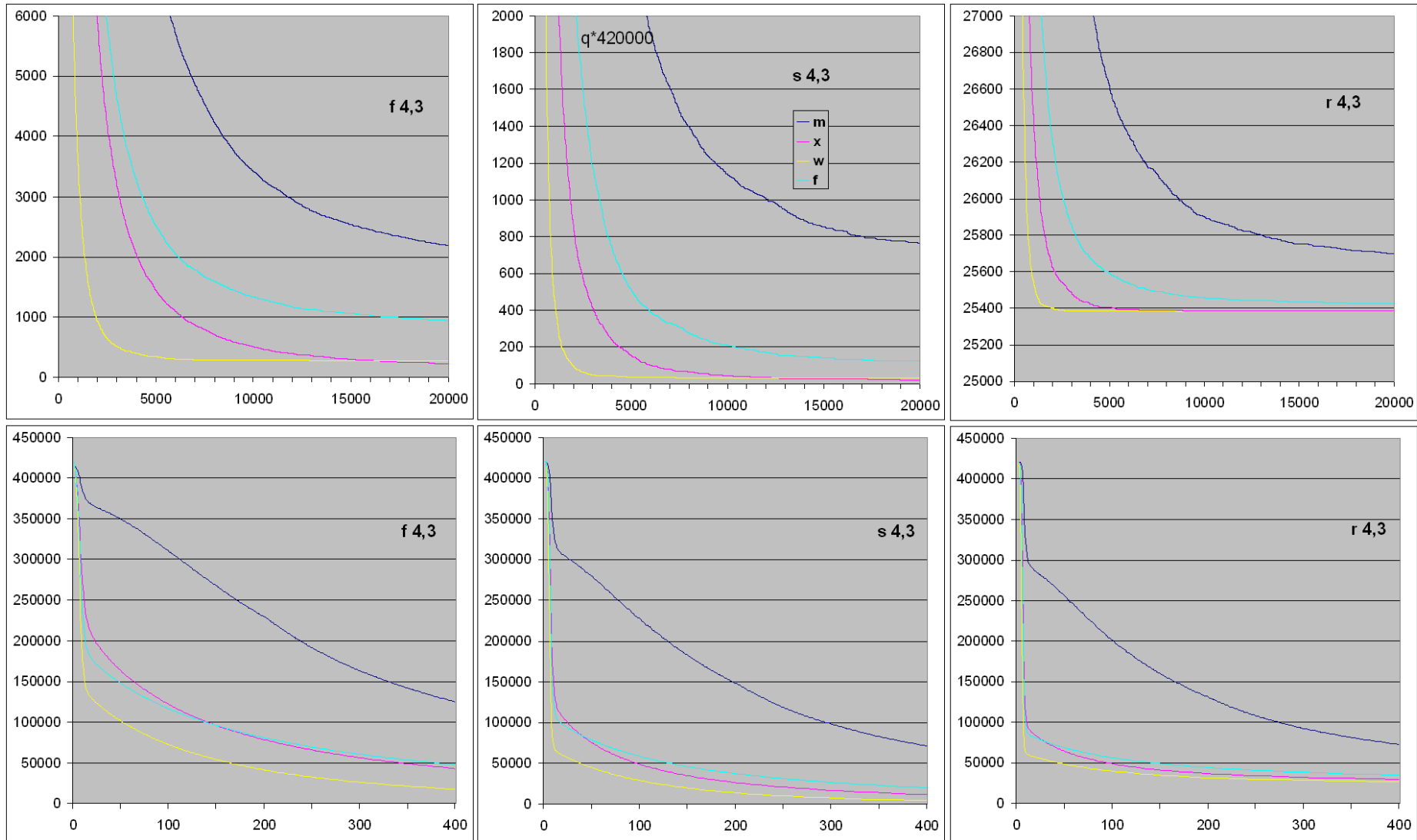


Fig.7. Result $q(t)$ for $s, K=4,3$, in simulation met2 200 of 350 nets, $N=400$. Near $t=10$ change of slope can be seen, what mistakenly suggests connection to end of first section of correction. Curve x cross f for $f 4,3$ near $t=200$ (end of corrections area), but for nets s and r these cross appear near $t=40$. In most of investigated range of t the perversity effect occurs ($f > x$) for all three nets, x even drops lower than w . Narrowing of function turn out significantly weaker than met2 in opposition to $s, K=2,4$, where m and f are similar (fig.6).

2.4.2 Results

In **fig.6** results of the **basic simulation series of 700 nets s,K=2,4** are shown. It are joined results of 300 nets of fast simulation without watching after chaotic explosion. and 2 full simulation of 200 nets, totally 280000ini. In upper row q(t) is shown for whole range of tmx=20000. First section of 400 is shown much precisely below to depict end point of correction at t=200, but there is no any change of slope.

For net type r and s 2,4 the curves m and x are very different. Not only x<m, but also x<f, in approximation x=m/2, which was surprising. It turn out, that shift of initial state for x by t=2 from point for m is enough so that x drops to half of m, and shift t=1 gives x about 2/3m. This effect is connected to met2 procedure and to particular connection of states and function to the structure. Any mix of these connections increase stability ! I call it '**perversity**' – correction of function in order to extinguish damage for particular place in trajectory as initial state results for other points on the same trajectory that system is less stable, than it imply from statistical properties of functions. Its has influence on secondary initiation (after fade out of damage). Source of perversity effect becomes unknown.

Table 2. Number of attractors for accepted (A(tmx)<60) and average attractor length in simulation of 700 nets N=400, tmx=20000, type f, r, s 2,4, (totally 280000 ini per investigation) for w – wild, m – met2 200, x – after shift of initial point by tmx, f – narrowing of function. In column: a – accepted, n – not accepted, 0 – attractor not found, 1 – one revolution of attractor, 2 – two or more revolution of attractor. Average attractor length only for f 2,4, because for the rest (including all s,K=4,3) attractors are not found. The only exception is s 2,4 for function narrowing where attractor was found in undisturbed network (**fig,16f**). For summary of f 2,4 see also **fig.8**. These results explain specific behaviour of net f 2.4 (seen already in **fig.6**) by entry in area of attractors. One revolution of attractor on section tmx=20000 typically effects not from long way to attractor and late found it, but from large length. After met2 much more attractors are found, extension of trajectory (x) makes this effect faster. Accepted events prefer shorter attractors, what is seen for many revolutions. Attractors with one revolution are so long that they do not correlate with acceptance.

		w	m	x	f
f 2,4	a0	5525	3639	1500	12699
	a1	0	1617	875	1015
	a2	1597	102775	108188	47254
attr.length f 2,4	a1		9935,3	14320,3	10157,5
	a2	26,6	662,7	600,5	785,7
	n1	9946,4	9981,1	10237,4	9967,5
	n2	274,8	1555,0	1614,7	2130,5
r 2,4	a0	5870	9437	7067	8732
	a1	0	0	0	0
	a2	0	0	0	0
s 2,4	a0	558	10097	5106	8996
	a1	0	0	0	23
	a2	0	0	0	168

For s and r networks s,K=2,4: **Tab.2** shows, that there is no any attractor found in the range of accepted events (which was calculated up till tmx). Similarly, there is lack of attractors for chaotic events, but they are calculated up till tmx only for 400 form 700 nets, therefore I do not add them to the **table 2**. In **fig.6**, m and f curves are similar, means the most of **stabilising effect results from function narrowing only**. Showed in **fig.9** distribution of L(tmx) size (remembering: L(t) - number of A(t)<threshold, q(t)=L(t)/(s-1)N, where (s-1)N is a number of ini) is easier for interpretation for net s 2,4 than r 2,4 because in the last effect of blind nodes interferes. Here curves m,x,f significantly differ from w, but also f and m are similar. The perversity effect is visible. Its source was not searched.

For net f (scale-free) s,K=2,4 met2 gives strong and stable effects, compatible with aims of met2. The net f works significantly in other way than s and r. The expectation, that extension of trajectory gives increasing of effect by entering range of often attractors occurrence turns to be accurate for f 2,4 and curve x is clearly, but not

much higher than m (from about t=5000). Probably perversity effect here also exist, but its power is less than effect from earlier finding of attractor. In table 2 the f 2,4 event is especially interesting. There are many attractors found in the range of accepted processes, especially in x. It is much exactly shown in fig.8, where strong increasing of repeated revolution participation as effect of met2 and difference of the participation in function narrowing are visible. However, length of attractors do not differ. Only for f 2,4 the L(tmx) distribution has so long tail, that in fig.9 it needs summarizing for higher L. Even wild system has single counts in this area. For comparison, f 4,3 is shown in the same picture. It occupies left side lower than L=22, where are no m and x for f 2,4. Both this curves (m and x for f 2,4) lie much higher than w and f in fig.6. This effect, which is the aim of met2, is clearly visible while results in form of crocodiles are studied (fig.15, 16a,b), but only for f 2,4. Success of met2 for f 2,4 suggests, that while chance of shorter attractors will be increased in the method, then direction may occurs accurate, but in current range, the correcting of random system by damage extinguish only turns out to be insufficient.

Results for s,K=4,3 are shown in fig.7. In this series 3 net types (f,s,r) are investigated using tmx=20000 and 350 nets (300 in fast simulation and 50 in full simulation). The perversity effect (x<f) is here strong, even x falls lower wild a little bit. An effect of met2 is clear, m always much higher than w and f, but also much lower than expectation. In fig.7 the curve m has a little to w, but its slope do not suggests significant increasing of q level. For f 4,3 q(tmx) is about 0.5% but for s 4,3 about 0.2%. In the last series, similarly as for s and r 2,4 (tab.2), there was no attractor found. Distribution L in fig.9 is shown only for f 4,3, but for s it is similar, only curve m is slightly different. In comparison to f 2,4 here is two time less events. For wild f 4,3 q(9000)=1/1500 and slowly fall to 1/1556 at tmx. If between t=9000 and tmx a process which did not exploded is replicated to 1560 descendants, each with small change like ini, then such evolution can roll infinitely and population will grow, despite that systems are chaotic. Net s 4,3 needs about 10 time more but s 2,4 2 time less descendants. Considering such possibility in plateau (fig.7) is more sensible, but numbers are really great. However, for f 2,4 only 60 is enough – chaos is different. Remark, such evolution need not correction of met2.

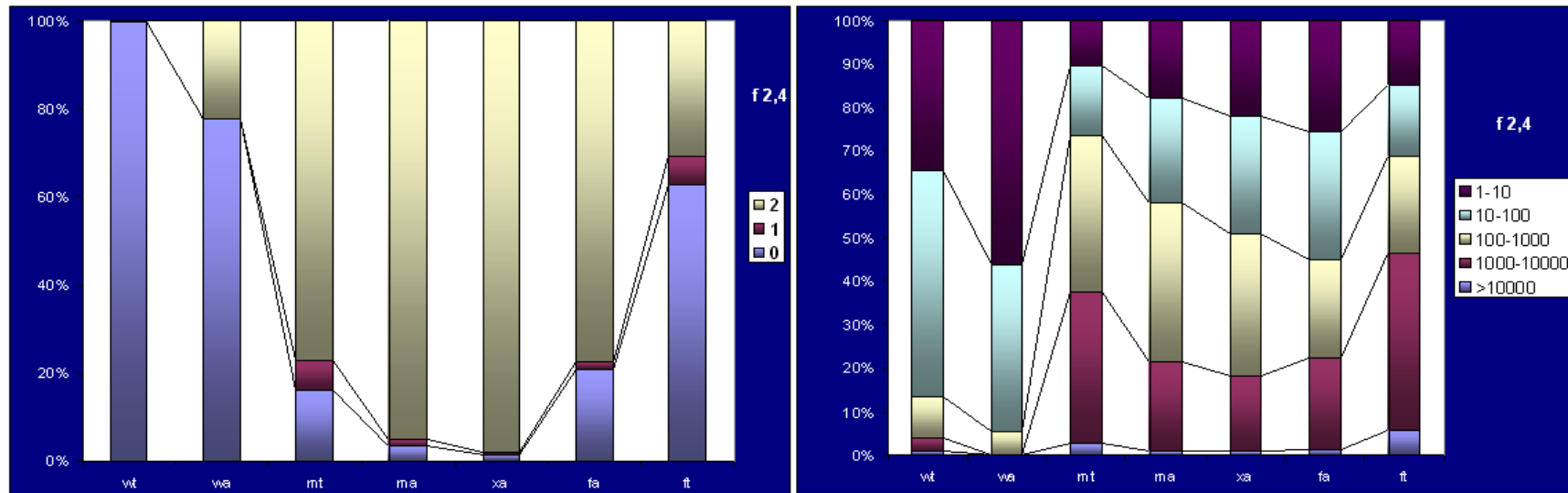


Fig.8. Comparison of frequency: 0- attractor not found, 1- one revolution of attractor, 2- two or more revolution of attractor, and distribution of attractor length. Simulation results of met2 200 for 700 nets (a - accepted) or 400 nets (t - total) f 2,4, tmx=20000. The first letter of column symbol: w, m, x, f, as in table 2.

Using met2 200 gives significant increasing of found attractors and increasing of fraction of attractors > 100. Limitation to accepted (ma or fa) decreases fraction of greater than 1000 and increase smaller than 100. Extension of trajectory xa decreases fraction of 'not found' and 'one revolution' increasing fraction of the smallest. Also effects of structural connection of selected functions give significant difference in increasing of number of found attractors. It is visible comparing m and x to f.

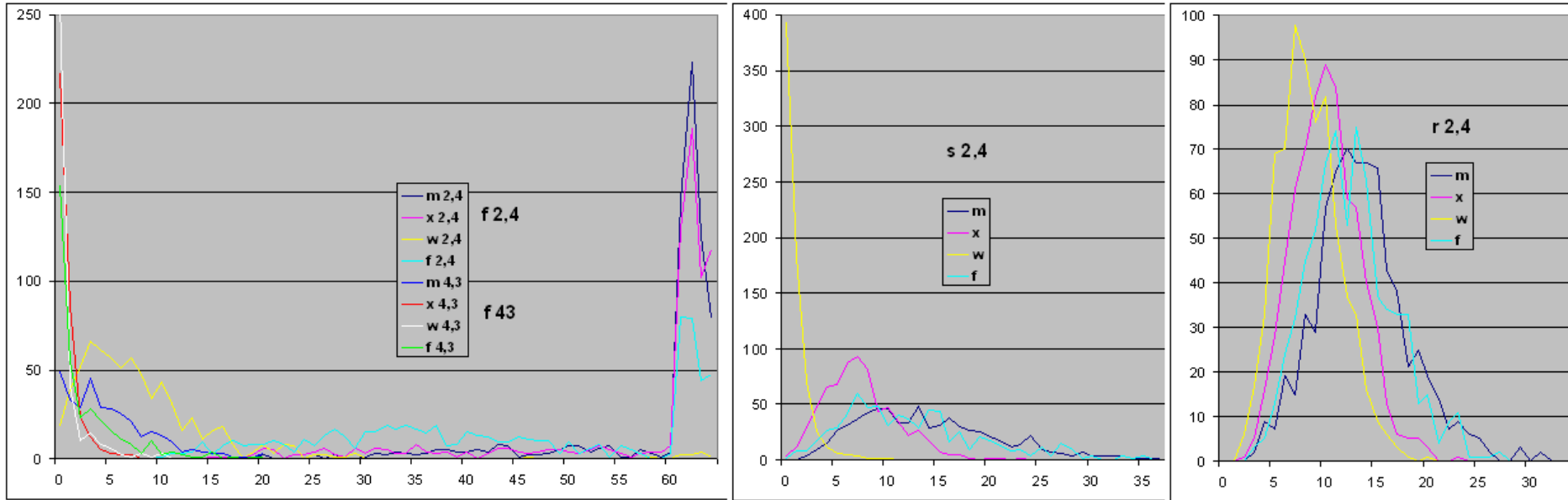
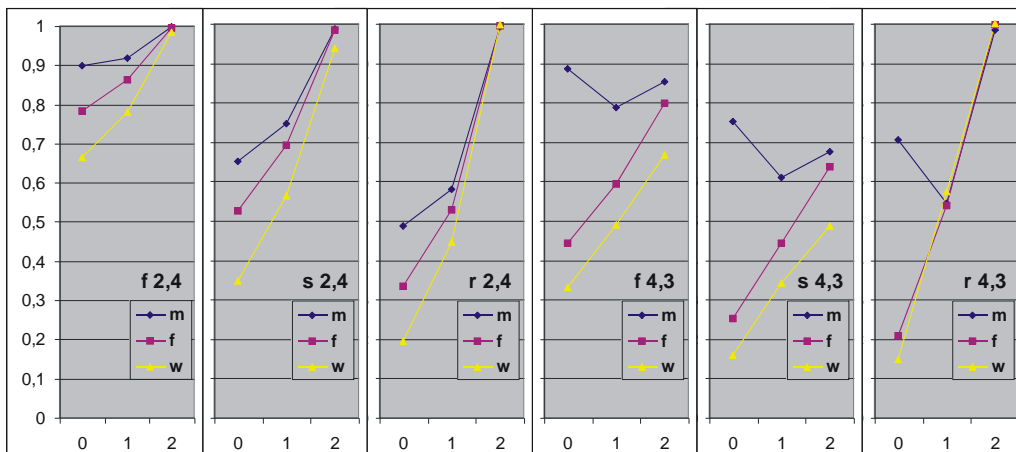


Fig.9. Distribution of $L(tmX)$ (horizontal axis) for f,s,r 2,4, 700 nets and f 4,3, 350 nets. For f 2,4, $L > 60$ in sections: to 100 (61), to 200 (62), to 300 (63) and to 400 (64). Even wild system has single counts in this section though its shape is similar to met2 result for s . Excluding f 2,4 always perversity effect is visible. For s and r 2,4 m and f curves are similar, which confirms small meaning of matching function to damage extinguish. The picture for net r is deformed by blind nodes. For net f 4,3 (similar to s 4,3) only m is slightly similar to wild f 2,4.

2.4.3 Secondary initiations

Searching for stability q increasing we can count for damage fade out or for keeping damage on very low level. Crocodiles show, that typically red line is very near to blue, which means, that nearly all accepted events for given t are a damage fade out $A=0$. However, typically both these curves fall down, means – fade out events become active typically in other circumstances and it can lead to chaotic explosions. This circumstances begin to repeat when second revolution of attractor starts. Therefore attractors are

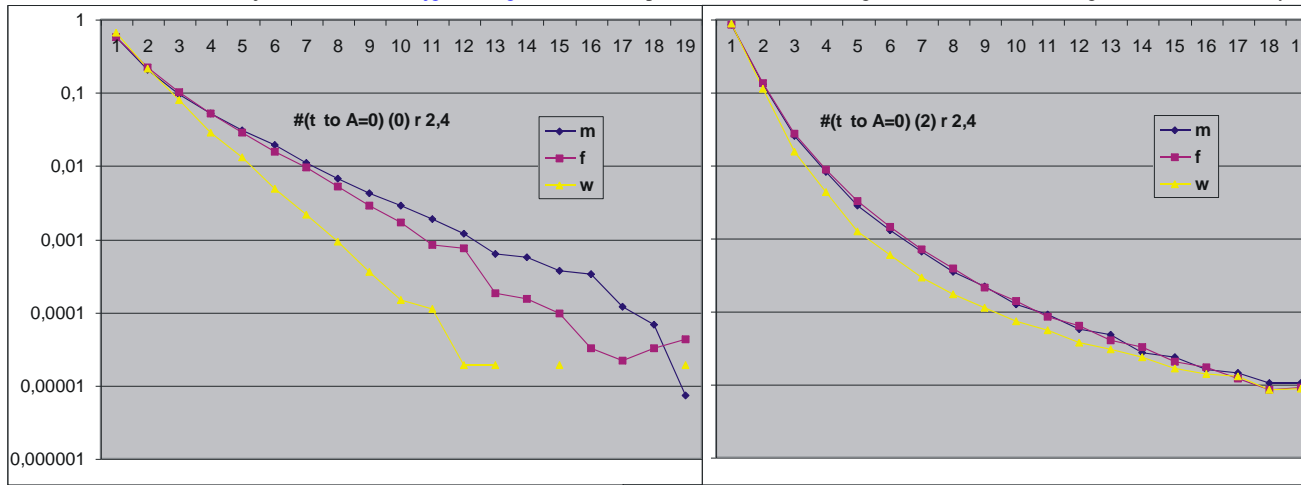


investigated.

However, is it true, that only attractors change chance for fade out? Therefore it was observed, what fade out events do, if after secondary initiation they have similar probability for fadeout or explosion, as before. How met2 or function narrowing influence on these probabilities.

Fig.10. Probability of fade out after first initiation (0), after second initiation (1) and after third an later initiations (2); for accepted.

In fig.10 results of these investigations are shown. Probabilities of fade out really differ. For $s, K=2,4$ after second initiation the probability is much higher, but after third initiation it is practically sure. In nets 4,3 later ini also have higher chance to fade out, but fare to sure except r 4,3. When behaviour of nets 2,4 are qualitatively similar, then fig.10 for r 4,3 differ to f and s 4,3. Result m (met2 200) for 4,3 have minimum for second ini



which effects from forced by met2 increasing for first ini. In conclusion, consecutive ini have significantly higher chance for fade out, despite attractors do not appear. It means, that some mechanisms exist, may be they can be intensify. Fig.11. Fraction of number of steps t after ini to fade out on example r 2,4. Left – after first ini, right – after later than second ini (here shorter periods appears more times in period tmx).

In fig.11 is shown for r 2,4 how often particular number of steps t after ini to fade out (A=0) appears. After first ini (left) each of m,f,w differs significantly. The faster is wild. However, for later than second ini (right), all 3 curves are very similar. For s 2,4 and 4,3 and r 4,3 pictures are similar. For f 2,4 and 4,3 first and later ini the pictures are similar to right.

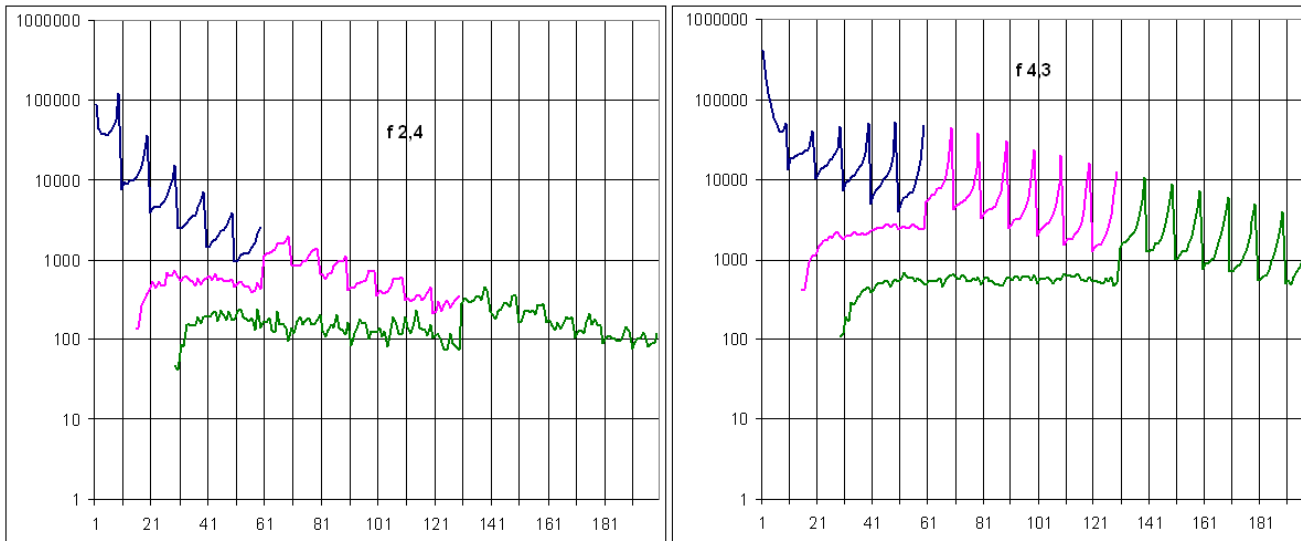


Fig.12. Number of corrections in met2 200 on period 200 t for f 2,4 (700 nets) and 4,3 (350 nets). For remaining nets pictures are similar. Data are collected in 3 sections: 10- 60, 70-130, 140-200, what differ by colour. The corrections in section just corrected are rare, which shows effectiveness of method. This data contradict an explanation of perversity effect, that most of correction are cumulated near t=1. Comparing left and right picture should be remembered, that for s=4 there are 3 time more ini/net and 2 time less nets.

2.4.4 Crocodiles

Looking through very large number of crocodiles turn out to be especially useful. It allows for roughly realizing of abundance of phenomena participating in such simulations and influencing on investigated parameters, especially on their exactness and interpretation. Several examples are shown in fig.13-16. The phenomena should be filed and investigated separately, but it must be leaved for future.

Crocodiles are used starting from third experiment, when lot of independent series of met2 200 simulations (f, r 2,4 i 4,3 – for tmx= 1000, 4000, 8000, 10000 and 20000) was made. The crocodile are most legible for tmx=1000 where one pixel shows one step of t as in fig.15, (for tmx=20000 it shows 20 steps). Estimation of stop of falling down of A(t) on the higher level needs much longer periods, then last series uses tmx=20000. Such estimation, however, is often subjective, because long periods without chaotic explosions happen. Only criterion of entry into second revolution of attractor turns to be sure, which was state after lengthen tmx.

From 6 last variants of simulation met2 200, $tmx=20000$, 700 nets: $f,s,r,K=2,4$ and $4,3$, **only $f 2,4$** reaches indisputable stable and significantly higher q level. From this 700 $f 2,4$ nets, only 71 leaves chaotic on tmx (10%), from this 26 finds attractor of pattern in the next period tmx (investigation x). Including of these events to chaotic is based on tmx , but tmx is taken arbitrary and $L(tmx)$ for m happens high. Average L (number of $A<60$ on tmx) is 44.7 (range 20-135) for these 71 chaotic nets. are not No event reaches full chaos ($L=0$) on this tmx . Obviously, for shorter tmx there are more nets estimated as chaotic, e.g. for $tmx=1000$ 2/3 of nets should be estimated as chaotic, but for $tmx=10000$ and 200 nets there are 39 chaotic (19.5%). In each event estimated as not chaotic an attractor of pattern was found.

Looking through remain nets all events are estimated as chaotic.

Nearness of curves: (red) $L(t)$ and (blue) number of fade out ($A=0$) for t , is an important information from looking through crocodiles. It shows, that **falling down the curves stem from secondary initiations, which exhaust their diversity after first revolution of attractor**. Remark, that recorded finding of attractor means finding the state from tmx , attractor may appear earlier. Crocodiles with recorded attractors are shown in [fig.16](#).

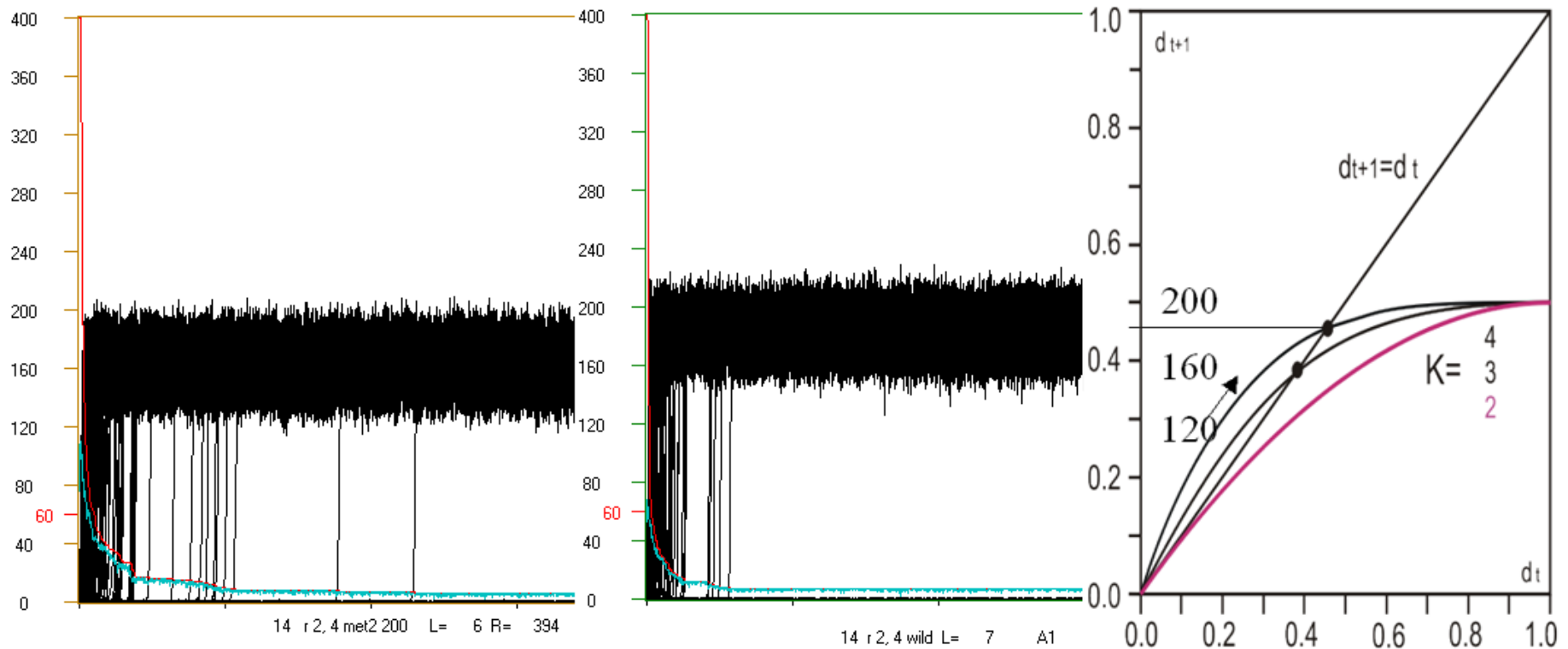


Fig.13. Comparison of beginning of avalanche for typical $r 2,4$ after met2 200 (left – later explosions, slower falling down of: red - $L(t)$ and blue – fade out), wild before met2 (middle – the same net). Black – number of damaged nodes $A(t)$ – avalanche. Under horizontal axis periods of 400 t are indicated. Right - 'Derrida plot' which shows theoretical level of chaotic avalanche ($d=A/N$, here $N=400$)

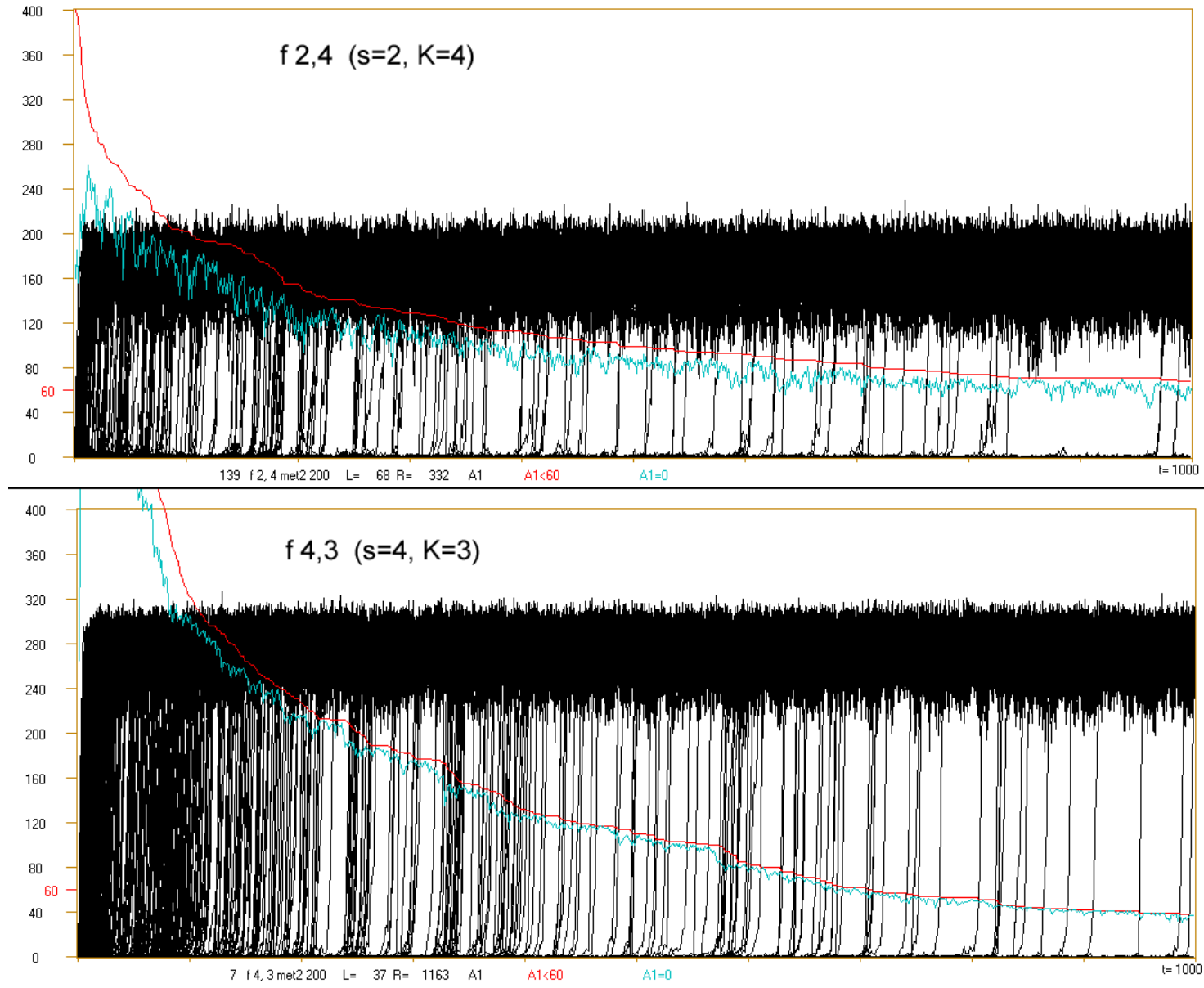


Fig.14. Typical chaotic avalanche $A(t)$ for network type scale-free (f). ($N=400$) In both cases curves: red = number of $A < 60$ at t (ordered events) and blue = number of $A = 0$ at t (fade out of avalanche) show node number in left scale, but for $s=4$ there are 3 initiations per node, for $s=2$ only one. To get frequency connected with probability $P(A < 60 | t) = q(t)$ and $P(A = 0 | t)$ node numbers should be divided by 1200 or 400. For $s=2$ taking 400 on scale as 1 we get probability. Description in bottom: number, type of net, s, K , symbol of method (met2 200), L – number of $A < 60$ at tmx (here $tmx=1000$) and number of remain events of initiations R , which have exploded creating Derrida balance state. Later colour description of curves. ($A1 = A$) Remember, however, that initiating change is permanent and next appearance of initial input state for the node leads to next avalanche, but in other circumstances. This causes that met2 is not sufficient, but also suggests, that a length of attractor is the crucial parameter. If here first revolution of attractor will end near tmx , then left peak (fig.3) will be satisfying. When $f 2,4$ often is not similar to shown typical case, so for $f 4,3$ it do not happen: for 700 nets and $tmx=20000$ there are no one.

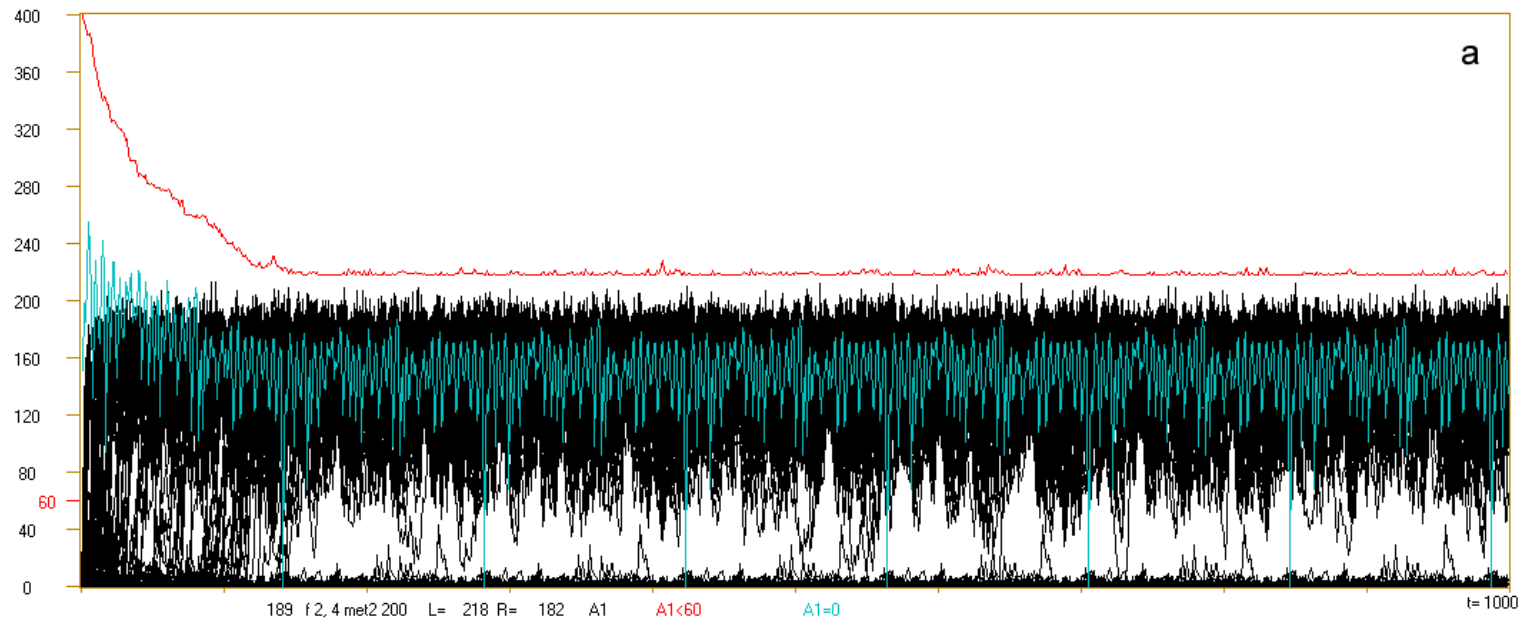
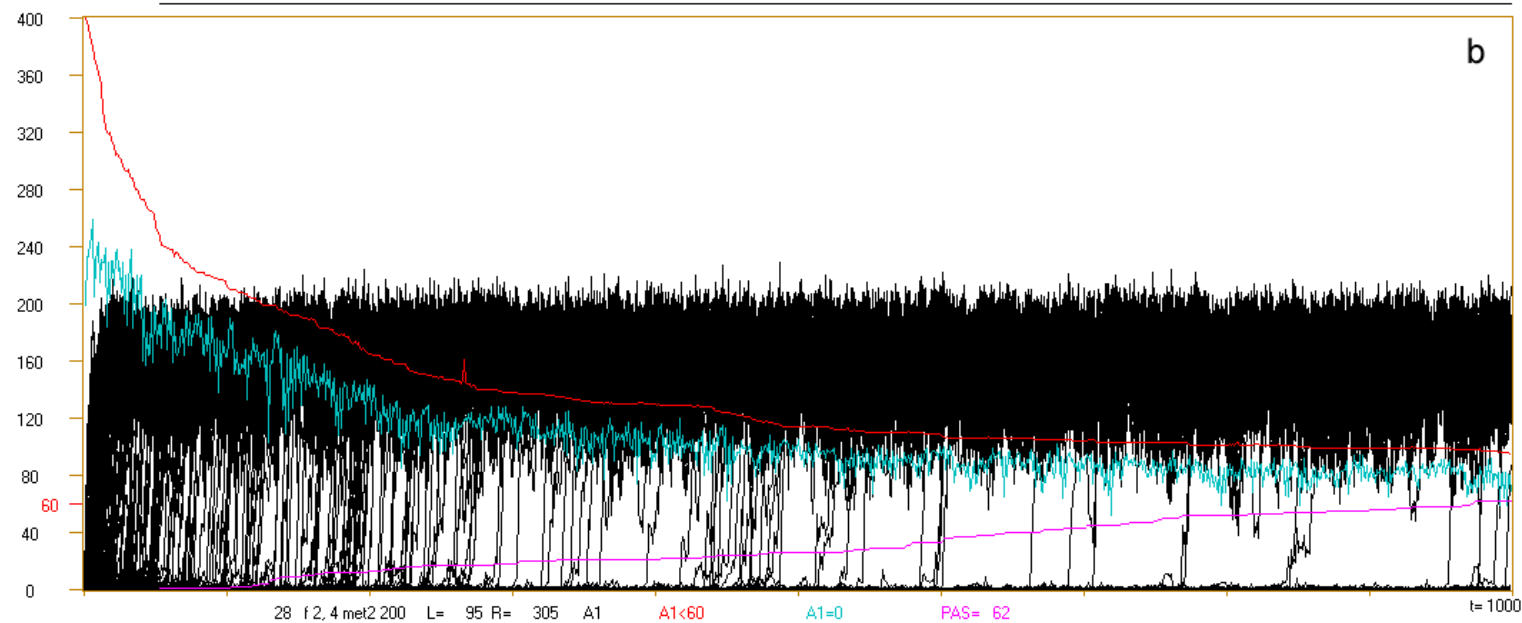
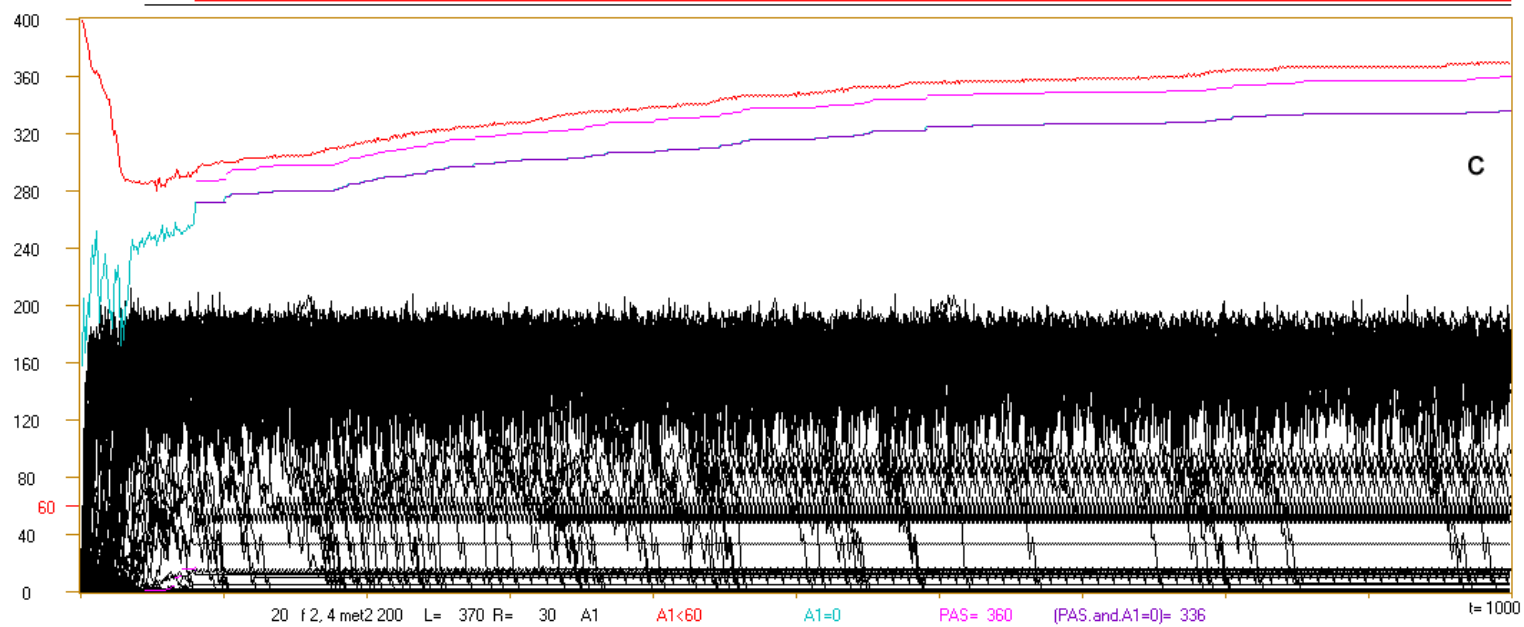


Fig.15. Simulation examples of met2 200 for $f 2,4$ $tmx=1000$.

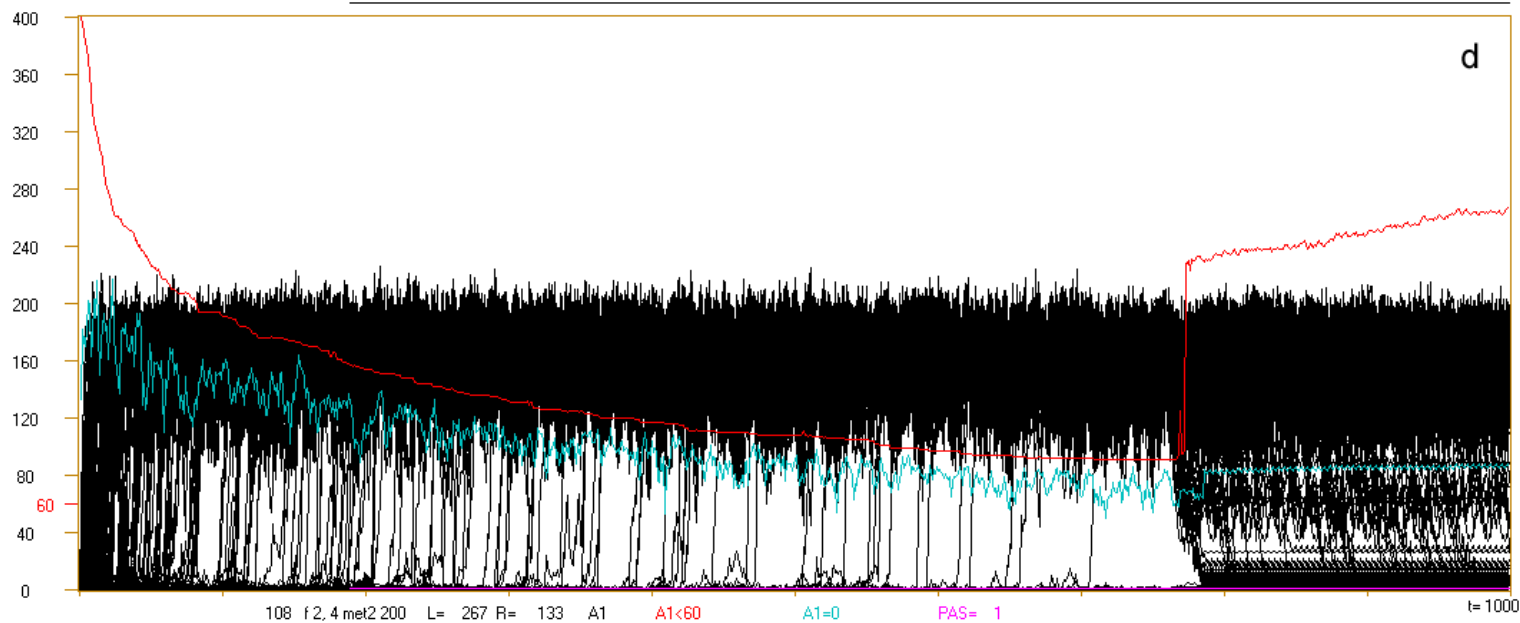
a - stable state of high order, significantly lower Derrida level and lot of cross of threshold=60 from Derrida balance. Despite width of [Derrida](#) balance, thin layer below it contains more cases.



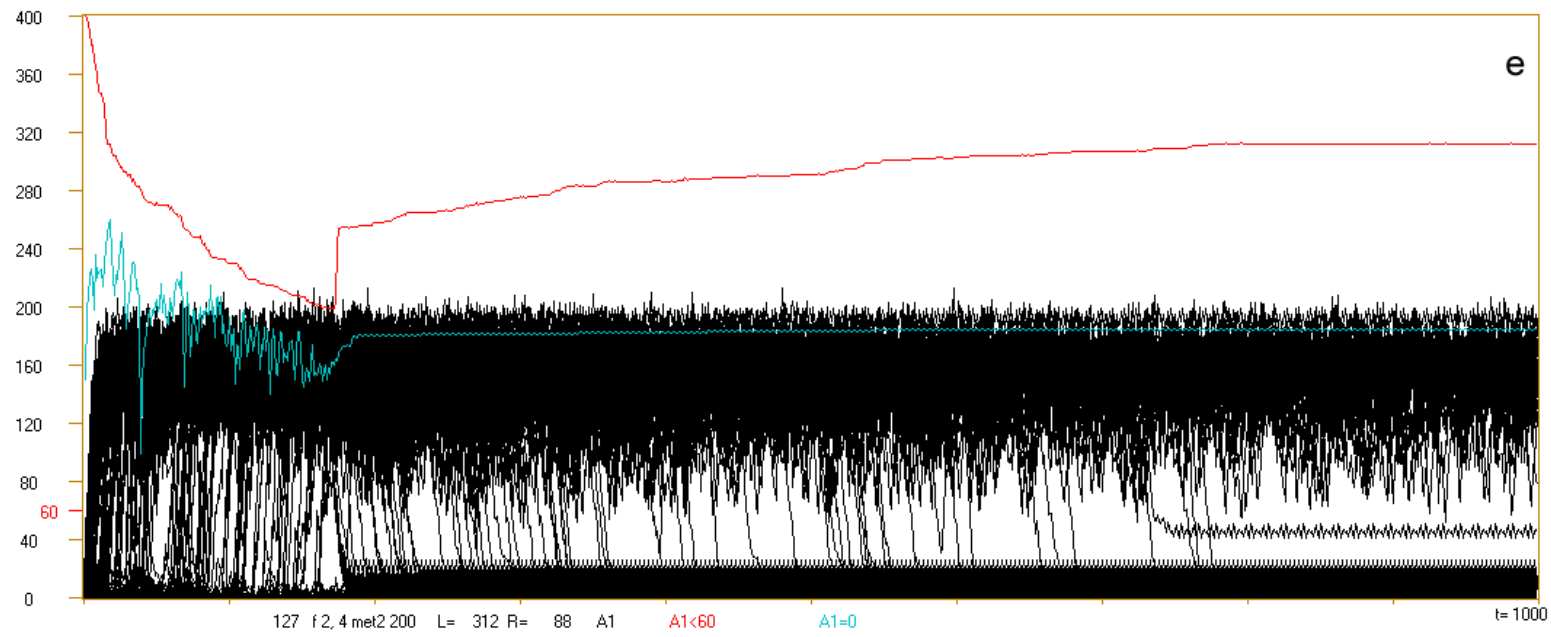
b - similar to typical chaotic case but stable increasing of point attractors up to 62 which guarantee stable high level of order. Black line over box indicates rage of point attractor after initiations.



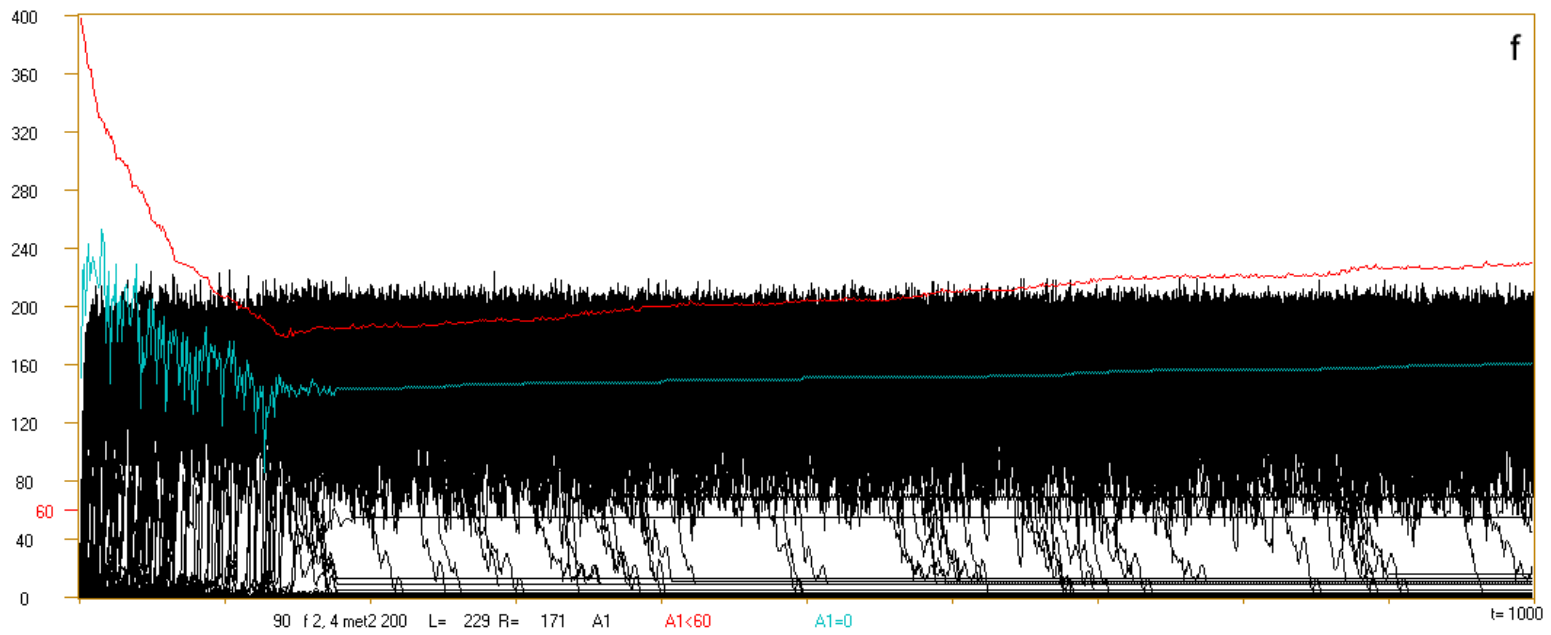
c - There are point attractors after initiation. Number of them reach 360 of 400 ini. As many as 336 are full fade out ($A1=0$) which indicates pattern attractor shown over box as red line. Point attractor of pattern is rare ($3/200$). After short period when $A1(t)$ comes down from the top (damage explodes to chaos) becomes opposite process falling down from chaotic Derrida level to ordered level.

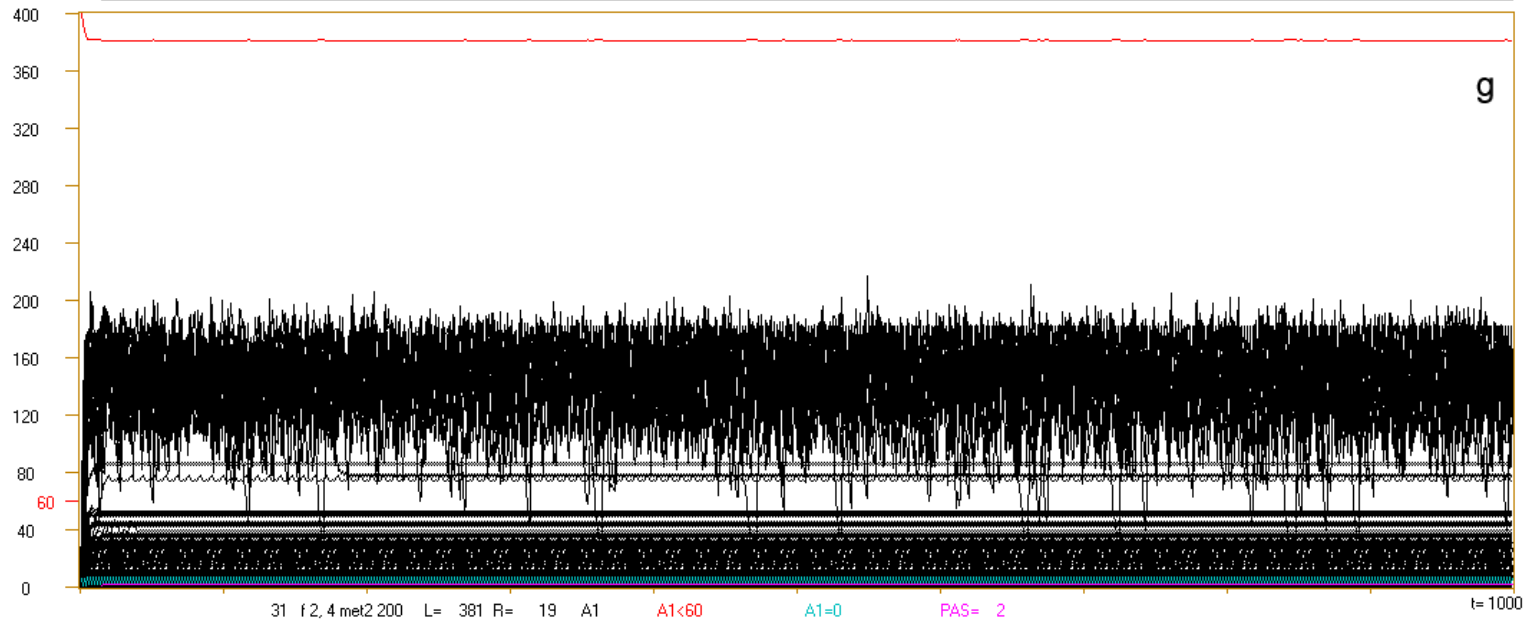


d - After long period of typical chaotic behaviour rapid change occurs – enter into order.



e,f - Cases similar to d, but change is much earlier and jump of order is smaller. Probably short attractor of pattern is an explanation.





g,h - Very high order level. It is clearly visible, that it is connected to short loops of attractors.

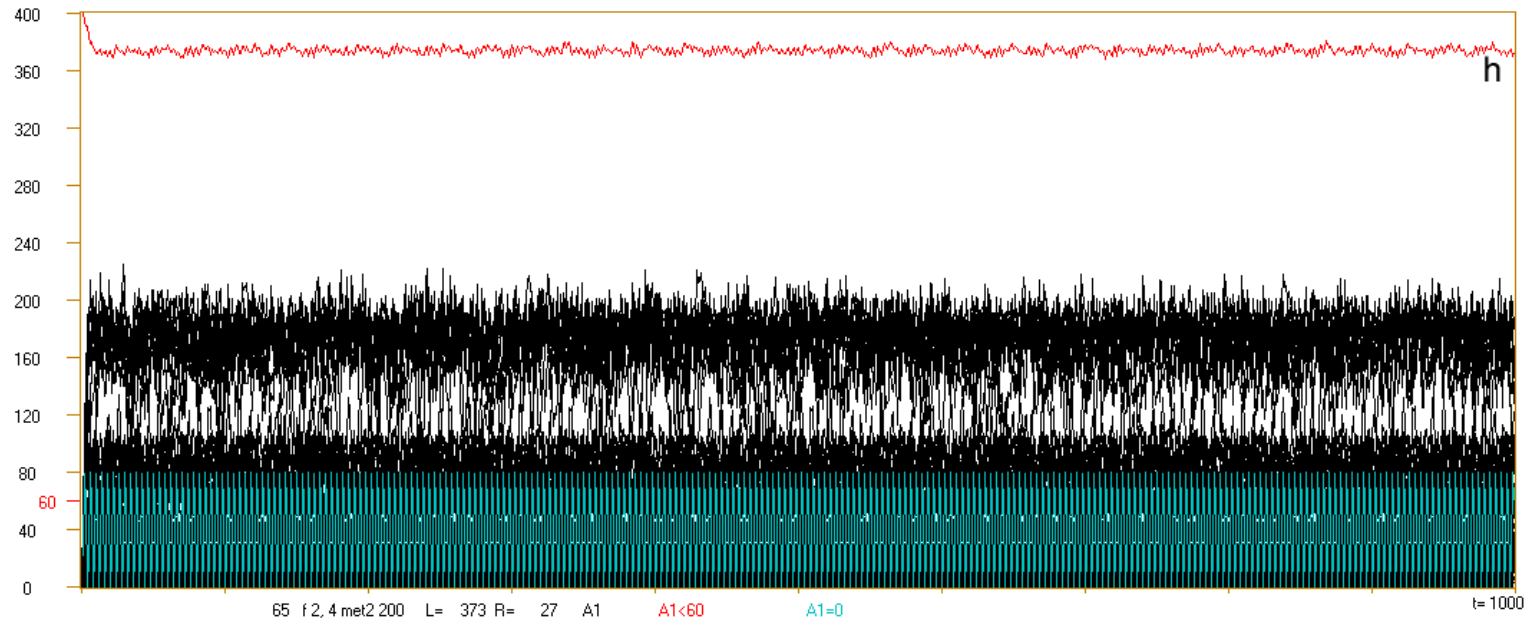
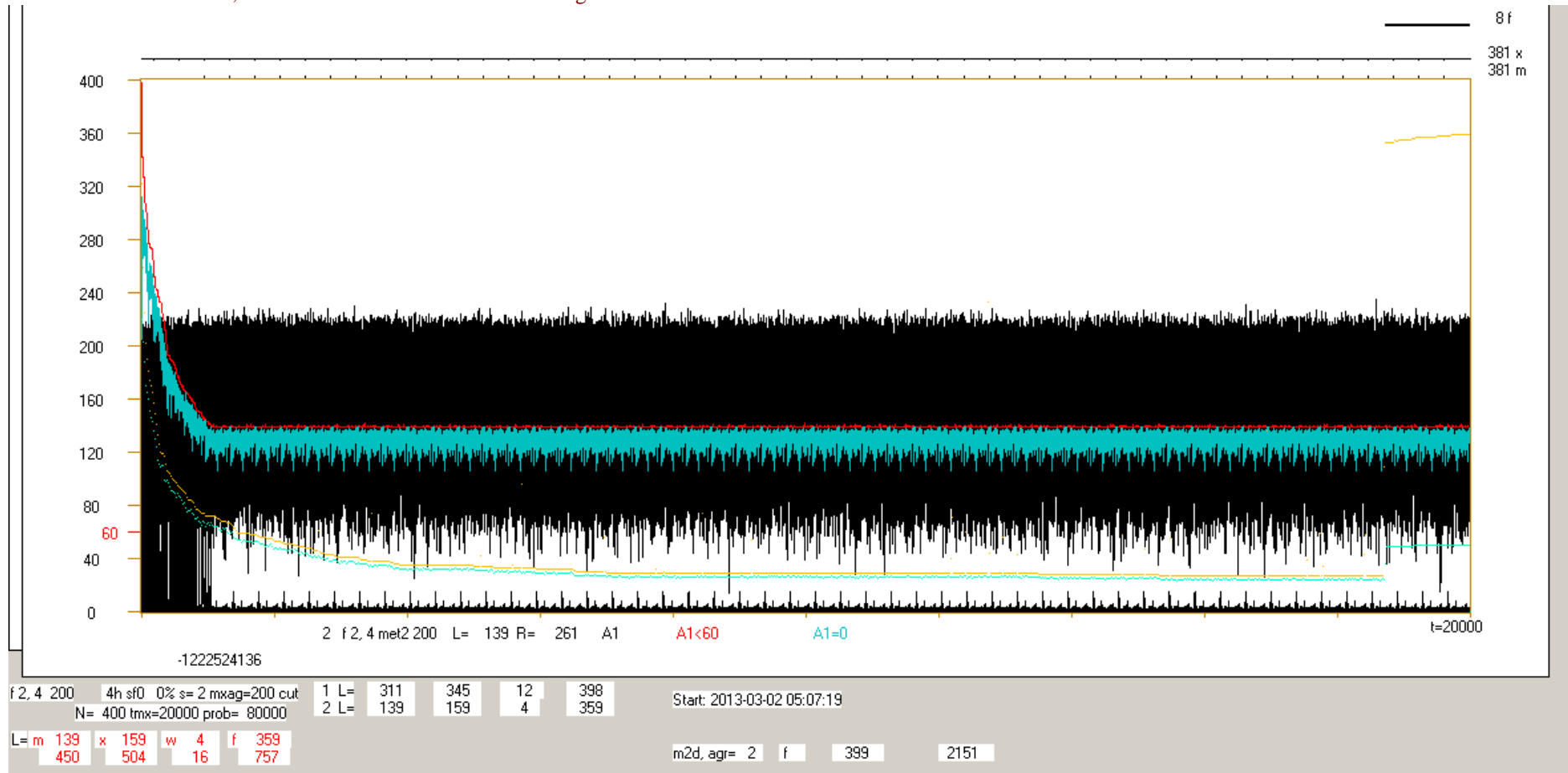
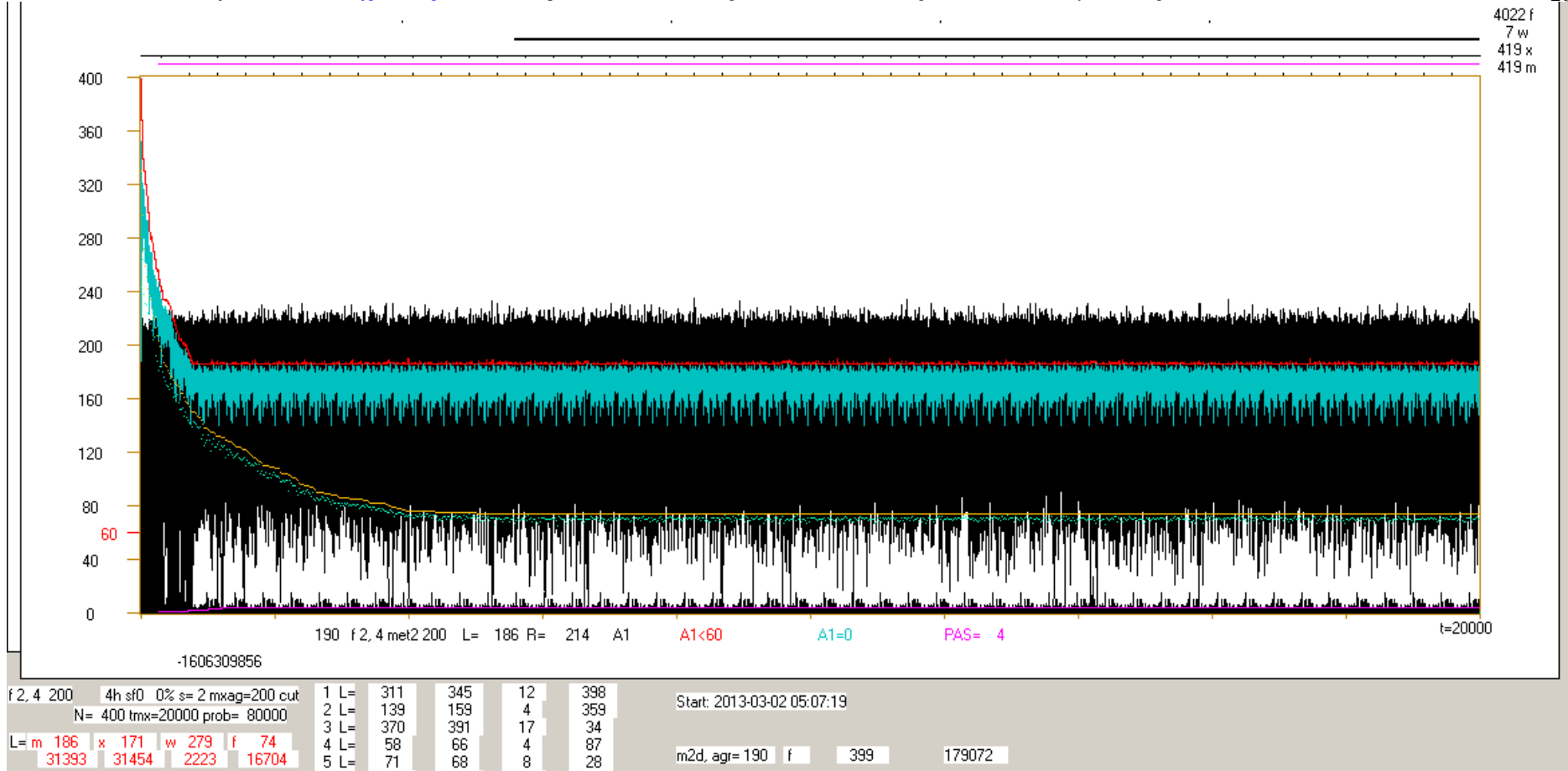


Fig.16. Examples of crocodiles from last simulation series: $tmx=20\ 000$; net type f,s,r; s,K= 2,4 and 4,3. One pixel of horizontal axis shows here 20 steps t. For one net there are investigated: wild (w) before met2 200, after met2 200 (m), after initial state shift by tmx (x), after change of connection node-function and sequence of input state for function and initial state on random (f). Attractors (state from tmx) found for this 4 simulations are shown over box and length of attractors are typed on the right. However, entry into attractor may appear earlier. The basic set of $A(t)$ (black) and red curve $q(t)$ and blue curve of fade out ($A=0$) concern of m. These curves connect consecutive points for each t. For f investigation in accordance yellow and green line show averaged points for consecutive 20 step t. Results $L(tmx)$ for m,x,w,f for consecutive nets in black, current and sums for all nets including current one in red.

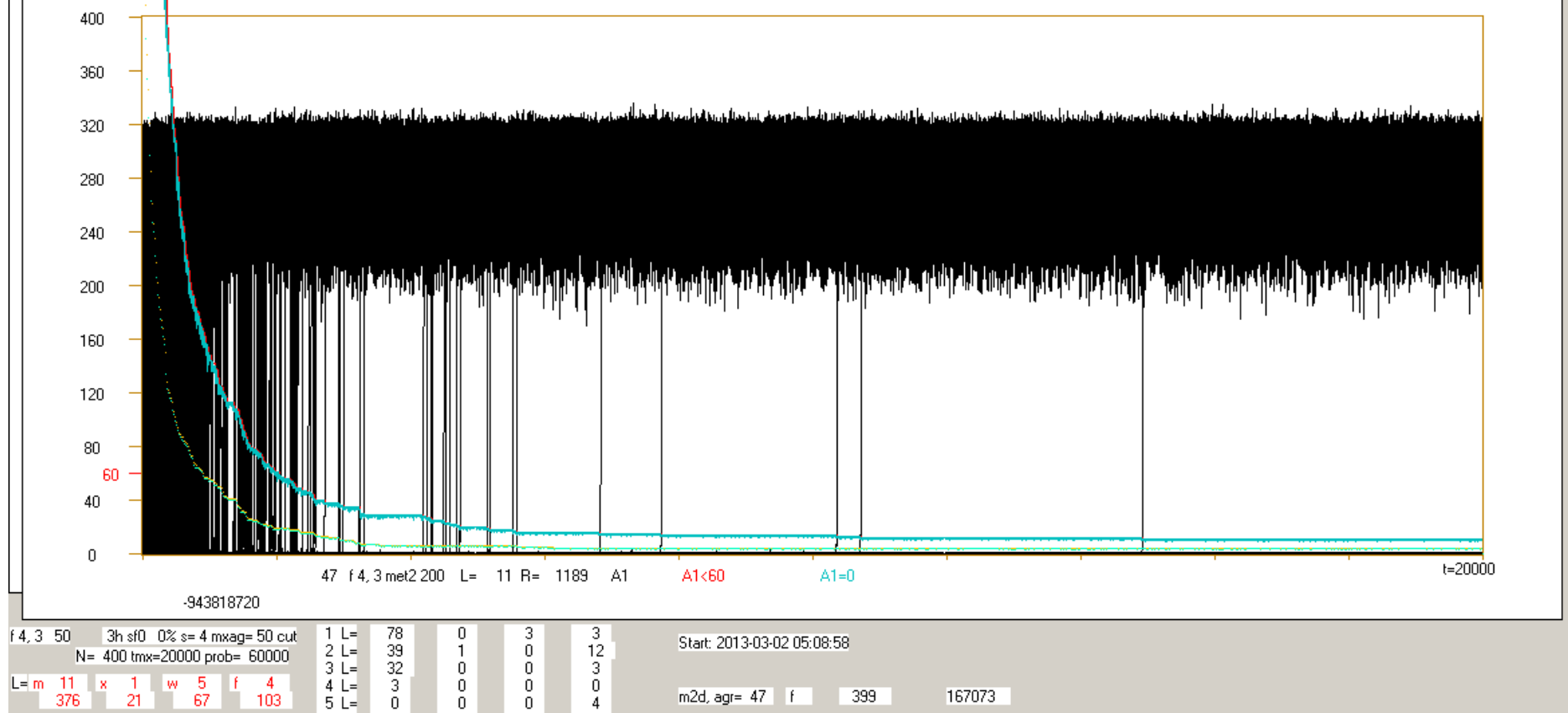


a. Typical example of f 2,4; but exceptionally attractor for f found on the end of trajectory, which effects especially high L for f. Explosions stop while attractor occurs. Arbitrary chosen threshold=60 is crossed many times (down and up) by event included to chaotic which creates misleading fluctuation of red curve. Blue curve is wide but lies near red without blocking of red. Ordered events (on box floor) and blue curve exhibit period of pattern attractor. Attractor for x is the same as for m, but appear from the beginning, which enlarge L and q for x.

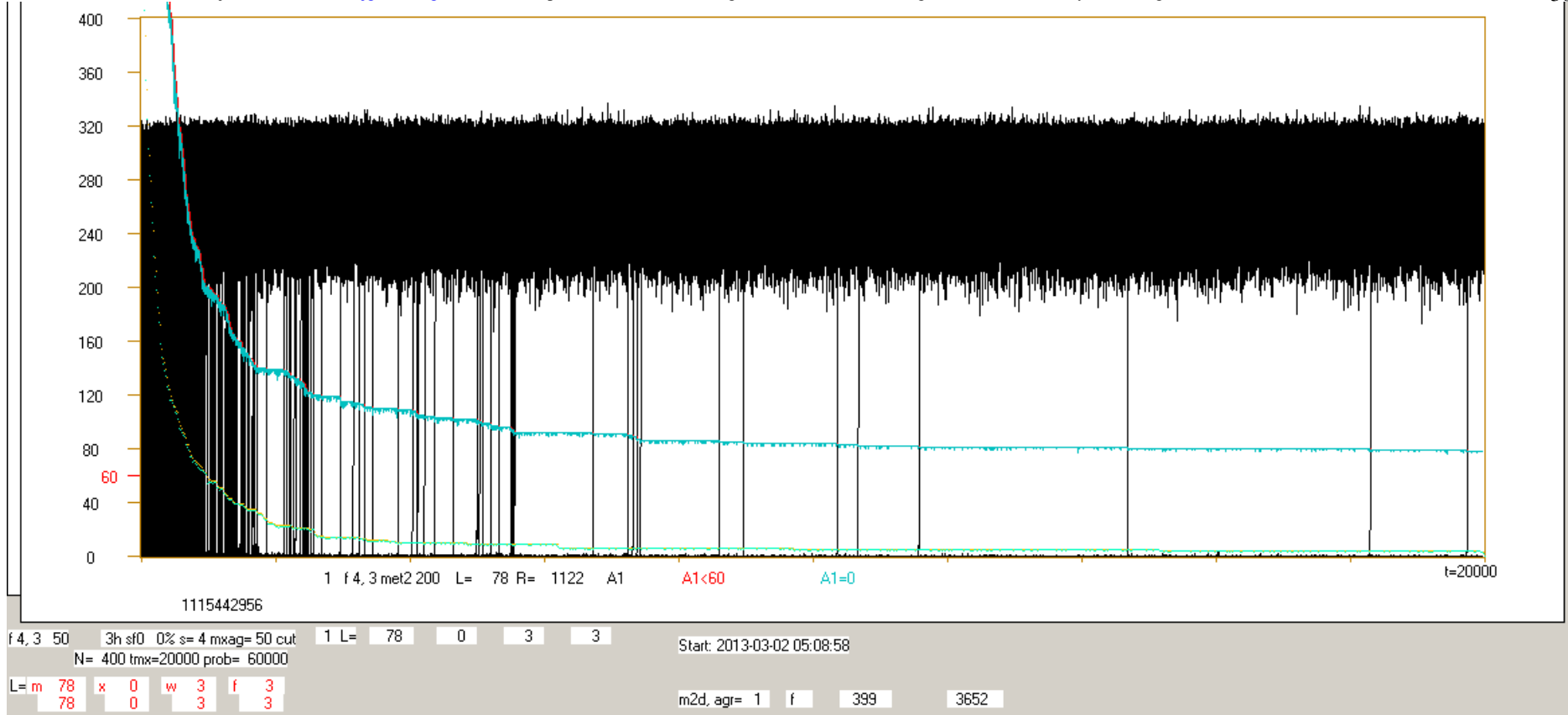
4022 f
7 w
419 x
419 m



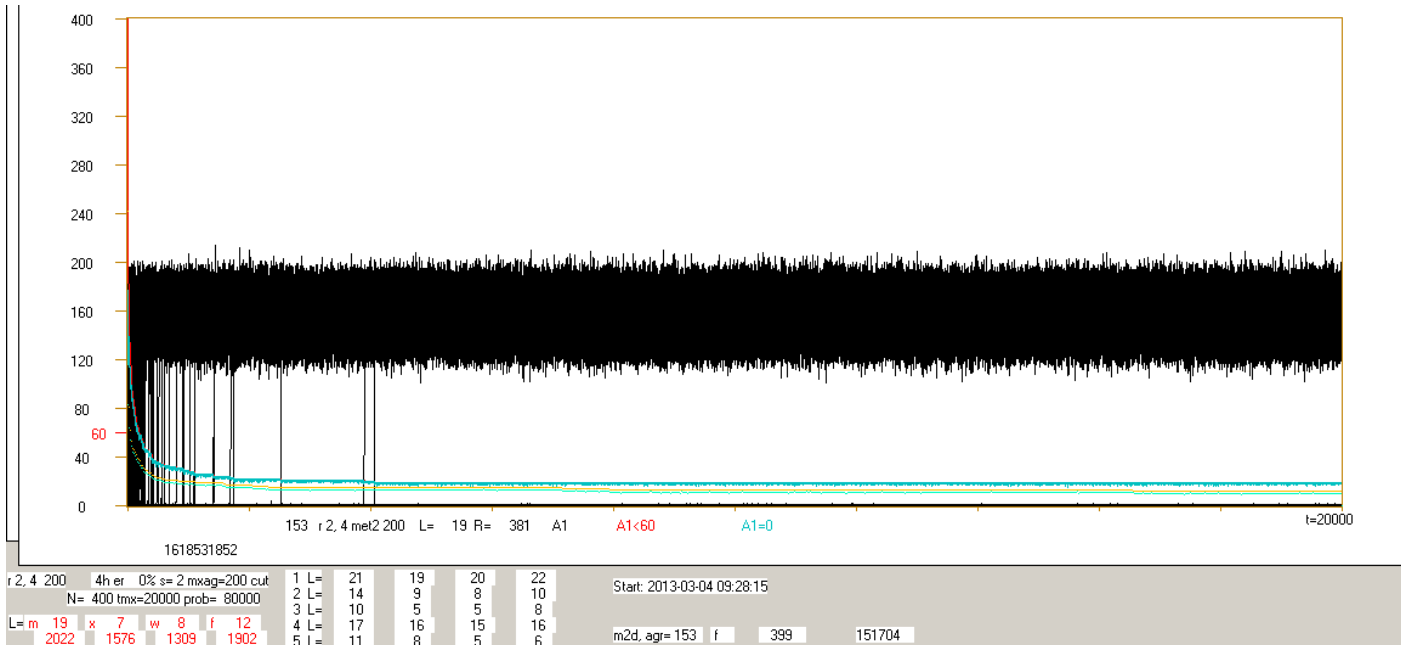
b. One of few cases where attractor for w is found. In addition, there is in m 4 point attractors (PAS=4), their range is indicated in the same colour as 'PAS=4'.



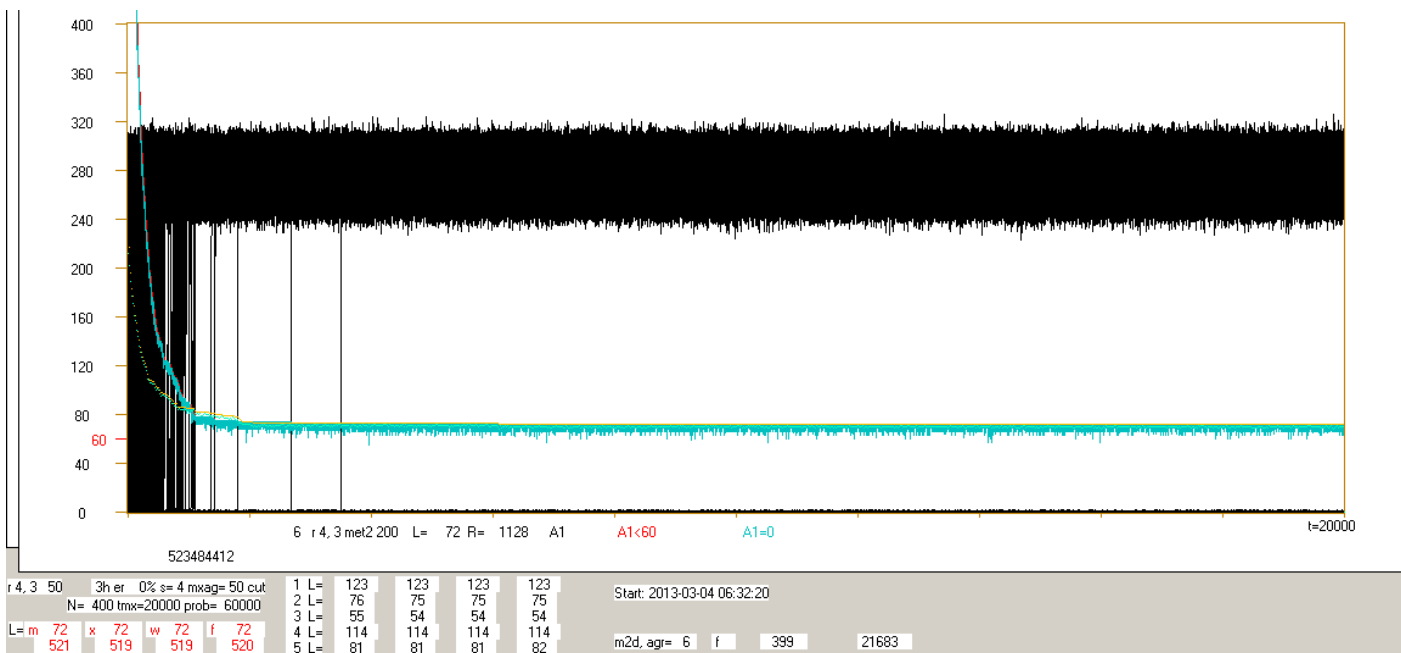
c. Typical picture of f 4,3. Red curve is blocked by blue one, which shows that events $A < 60$ are $A = 0$, means – fully fade out. Decreasing of their number effects from secondary ini in other circumstances. Despite long last periods without explosion we cannot hope that constant level of L is reached. Here on the end $L = 11$ only, what is near average. For net 1 there were as many as 78 of 1200 ini, but as can be seen in next fig.d also this event is not an entry into searched stable level of L.

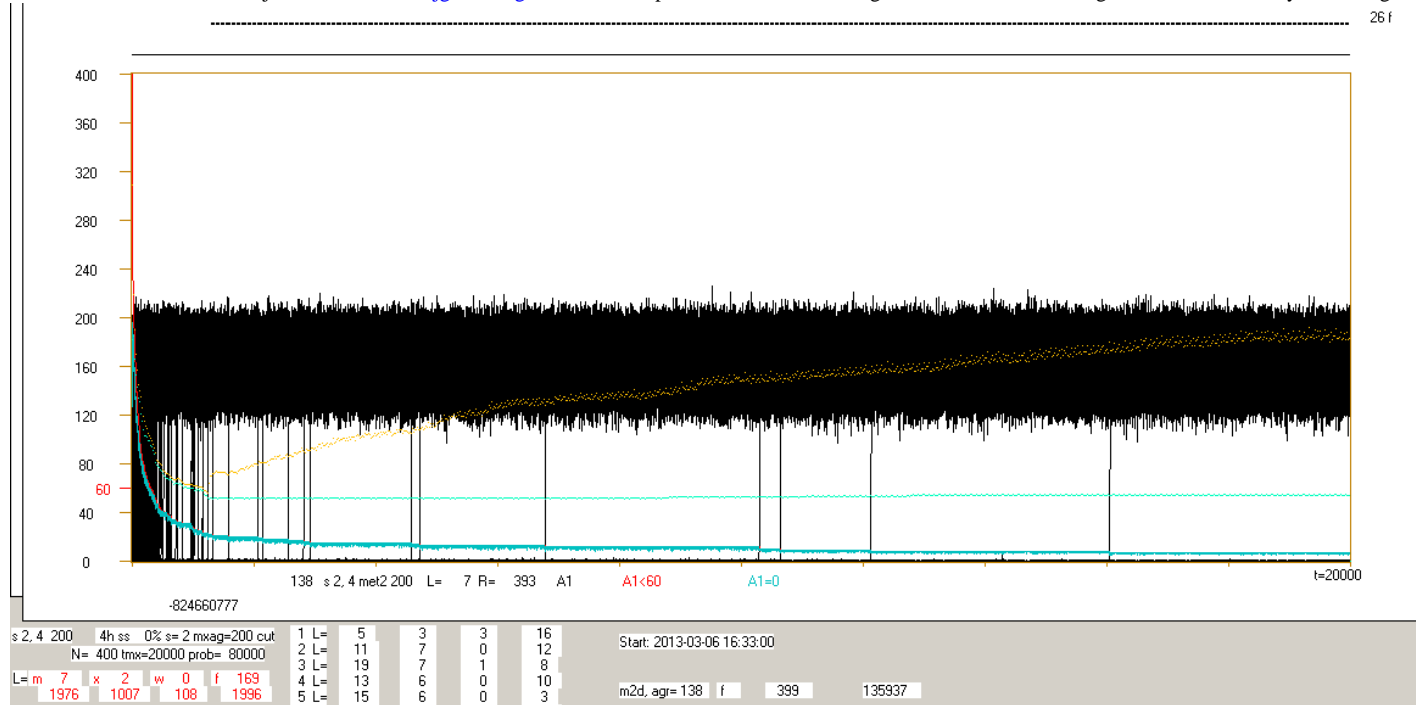


d. Especially high level L for m (f 4,3), but there is no basis to state that it will be stable in the next tmx period. Investigation x does not answer for it, x can only show, that for pattern attractor should be waited slightly more. However, for s,K=4,3 no one pattern attractor was found in over 1000 investigated nets of different tmx (from tmx=1000) for each net type (f,r,s) and in 4 investigation (m,x,w,f) for each net. Together about 12 000 events. Also for 60% of this events no one (of 1200) process after ini reach attractor. Remark, high level of L is here not a result of function narrowing, which show yellow and green lines.

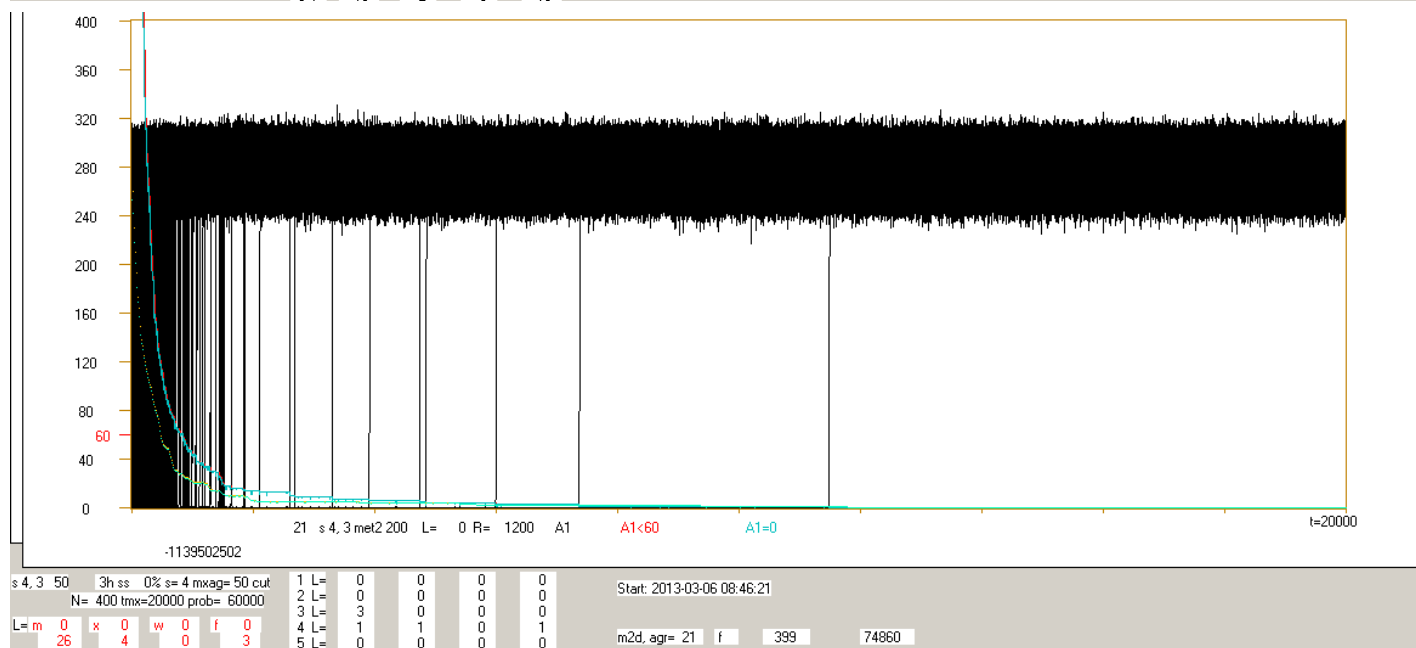


e,f. Typical picture for r 2,4 and 4,3. Stably increased level L results here from blind nodes (without outputs). It is not this higher lever we search.





g. Typical picture for m investigation for s 2,4, but exceptional appearance for r i s 2,4 of attractor. Here it appears in pattern of f investigation.



h. Typical picture of s 4,3. all 1200 initiations in each of 4 investigations give chaotic explosion and L=0. As is visible for 21 just simulated nets only 26 accepted ini occur in m investigations. The picture for r 4,3 would be similar, but blind node block similarity.

2.5 Fourth experiment - interactive narrowing of function by met2

Indication what is a difference between network describing living object and random network is a general aim of this investigation. Increased stability is taken as the main property of living object. That random network is modified. In met1 and 2 function correction to extinguish damage was such a modification. Narrowing of function was a side-effect of method. It alone leads to increasing of stability. Connection of this effect with attractor length was already shown in [ooKauf]. Using ready tools I recognize what gives intensify of this effect. Evolution uses any possibility to increase of stability, then it uses also this one, however, I do not believe, that it is one of the main.

In fourth, additional experiment for next net corrected functions by met2 200 are uses instead random ones. Before prepared investigations (w,m,f) were not changed, then f and next w give statistically the same results and they are summarized. For 2,4 nets 5 iteration was made. After such complete new random functions for next net were drawn. For s 2,4 40 completes but for r 2,4 20 completes were simulated while for s and f 4,3 – 10 completes of 12 iteration.

In third experiment for s 2,4 were 700 nets, only one pattern attractor was found there in f investigation (fig.16g) but now attractors appear in 2 cases of 80 (40 f +40 w) after first iteration (tab.3). After second iteration 11 attractors were found, after third and fourth: 59 and 72. In r 2,4 pattern attractor happened after 3 iterations of 40 investigations but in f 4,3 - after 7 iterations, after 11 there were 9 attractors of 20 investigations. More detailed in table 3. For s 4,3 there was no attractor found.

The fourth experiment is reconnaissance only, statistics are small due to simulation time, more exact analysis are given up. In tab.3 data usable for planning of new investigation are collected.

As in previous experiments, the great fraction of $A(tmx)=0$ is observed in the range of accepted ($A(tmx)<60$). For comparison to previous experiments threshold=60 is left, however in fig.17 can be seen that now it should be smaller. Such arbitrary choice influences on increasing of q presented in fig.18 and table 3. Pattern attractor finding is the most important factor of increasing of q. For Boolean nets (2,4) function practically contain only 0 or only 1, and Internal homogeneity P reach over 0.73. (See also tab.1 and [ooKauf]).

Summarizing: function narrowing effect gives first of all increasing of number of attractor findings which is the main factor of q increasing.

Table 3. Preliminary results about attractors in dependency of iteration. For s 2,4 were 5 iterations (0 – without correction; 5 - 40 nets, remain 80 nets). For r 2,4 also 5 iterations but half number of nets, (see fig.19). For f 4,3 – 20 nets, iterations 7-11 of 12 shown, before iteration 7 lack of attractors. For s 4,3 investigated as f 4,3 attractors are not found.. Near all accepted are full fade out ($A=0$), see also fig.19 and earlier fig.14-16. For accepted ($A(tmx)<60$); fade out at tmx ($A(tmx)=0$); pattern: 0 – attractor not found, 1 – one revolution of attractor, 2 – two or more revolution of attractor. Lower: range of attractor length, Internal homogeneity P and q.

	s 2,4	0	1	2	3	4	5	r 2,4	0	1	2	3	4	5	f 4,3	7	8	9	10	11
accep.	0	23	893	4208	2482	1157	188	147	476	1490	2846	3022	502	5254	6389	8535	8571	5879		
	1	0	0	256	1267	151	0	0	0	0	0	162	193	0	0	0	1066	1285		
	2	0	149	1875	12132	20907	13497	0	0	0	1333	3683	4350	1539	1608	1027	803	6145		
A=0	0	23	870	4118	2434	1130	181	139	451	1456	2802	2981	487	5244	6375	8506	8546	5849		
	1	0	0	252	1237	150	0	0	0	0	0	162	188	0	0	0	1060	1285		
	2	0	140	1744	11469	19210	12015	0	0	0	1311	3555	3980	1509	1593	991	803	5982		
pattern	0	40	78	69	21	8	1	20	40	40	32	23	3	18	17	19	17	11		
	1	0	0	2	8	1	0	0	0	0	0	1	1	0	0	0	2	2		
	2	0	2	9	51	71	39	0	0	0	8	16	16	2	3	1	1	7		
>10 000		0	0	0	363	151	0	0	0	0	0	162	0	0	0	0	1066	0		
1000-10000		0	0	256	2405	1553	676	0	0	0	175	370	902	0	0	0	0	3357		
100 -1000		0	149	542	3605	4722	1798	0	0	0	0	1346	681	735	586	0	803	0		
10 -100		0	0	276	4209	6303	4096	0	0	0	727	1071	1278	1	644	0	0	1079		
1 - 10		0	0	1057	2817	8329	6927	0	0	0	431	896	1682	803	378	1027	0	2994		
P		0,5974	0,6426	0,6753	0,6996	0,7181	0,7323	0,5986	0,6428	0,6735	0,6992	0,7179	0,7336							
q		0,001	0,033	0,198	0,496	0,694	0,855	0,018	0,030	0,093	0,261	0,429	0,631	0,28	0,33	0,40	0,44	0,55		

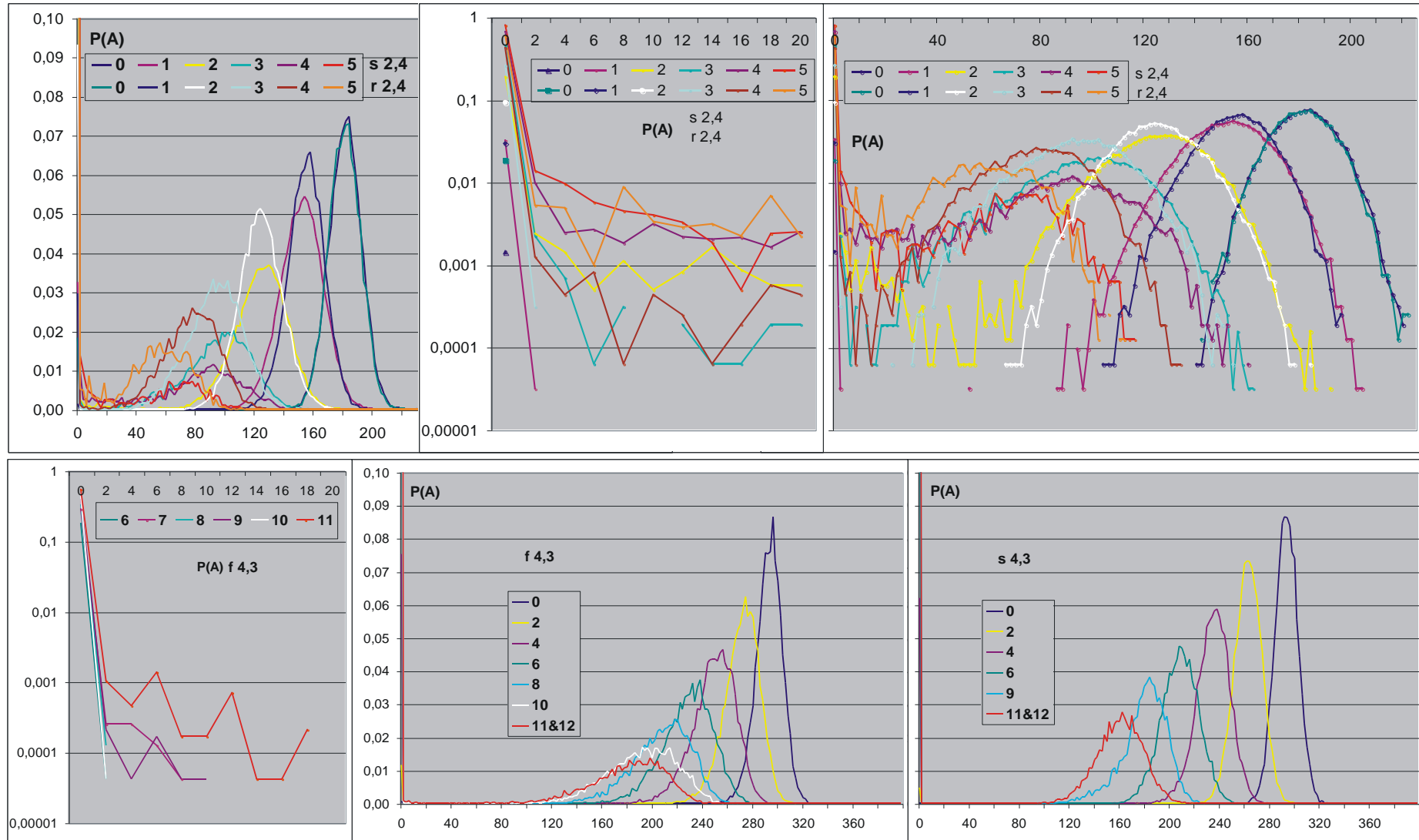


Fig.17. $P(A)$ from iteration of function narrowing met2 200 for s 2,4 & r 2,4 (40 & 20 completes of 5 iteration), f 4,3 & s 4,3 (10 completes of 12 iterations). Iteration 0 – random system before first function corrections using met2 200. Iterations 0 i last (5 or 12) in comparison to remaining have half number of events. For f & s 4,3 only part iterations are shown. Two values of A are summarized, iterations 11 & 12 summarized and 8 & 10 for s 4,3 are rejected due to large fluctuations. The most important left peak is narrow, in the beginning it is limited to one value. Second value appears for 2,4 after second iteration, for f 4,3 after 6 iterations, for s 4,3 after 12 iterations. For 2,4 between peaks there is no gap, more adequate threshold should be 20. Right peak of Derrida balance moves into left. Capacity of peaks is shown in fig.18.

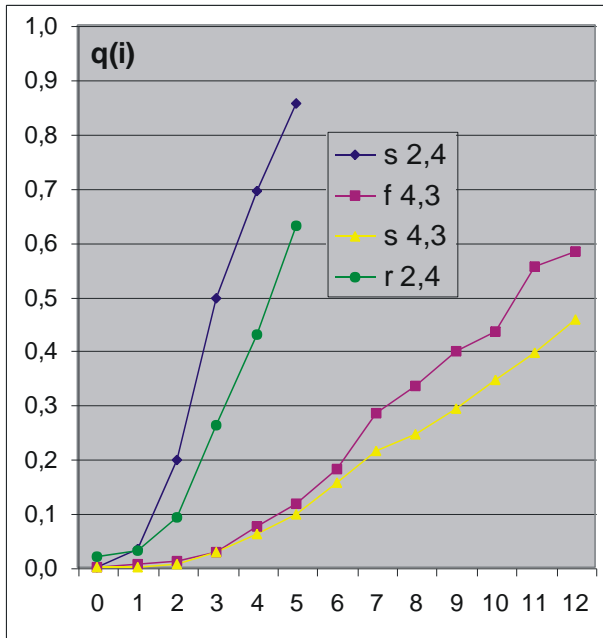


Fig.18. Degree of order (q) in effect of iteration (i) grows strongly. In most cases it effects from full damage fade out, i.e. $A(t_{mx})=0$, what can be seen in [tab.3](#). Arbitrary choice of threshold=60 for s 2,4 significantly influences q . In [fig.17](#) threshold for s 2,4 should be estimated on 20. (See also [fig.19](#) and [tab.3](#)).

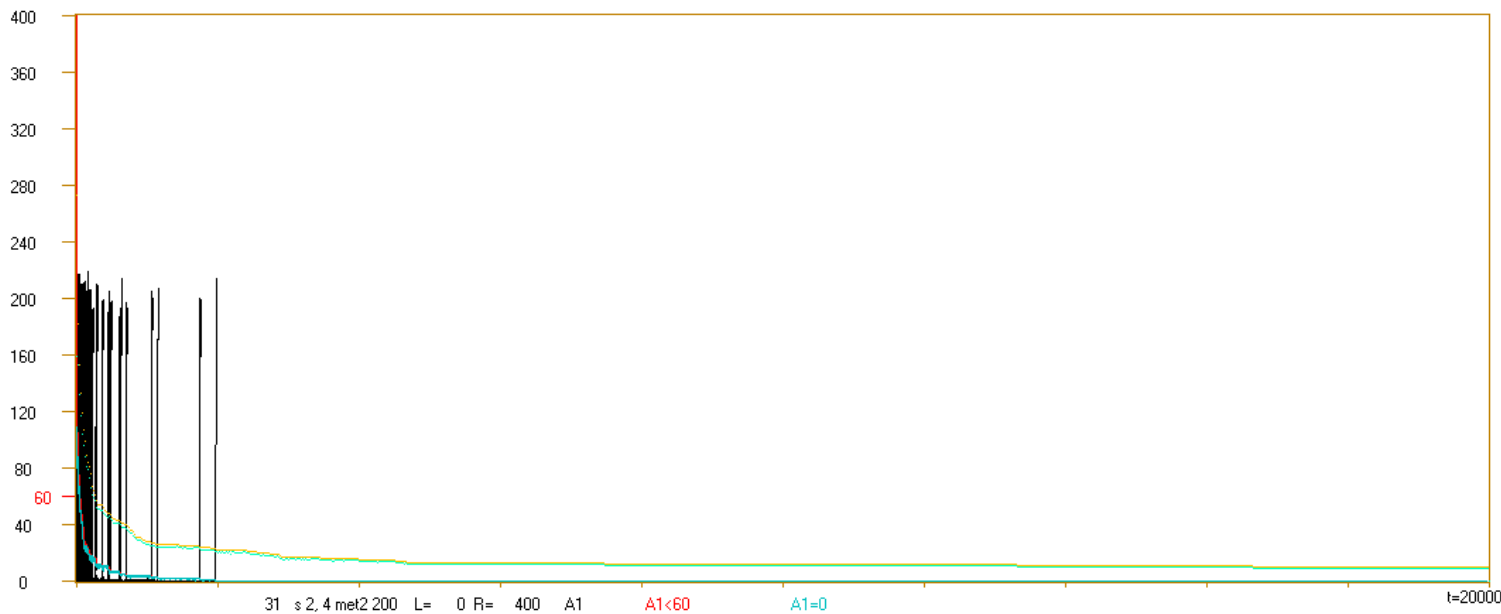
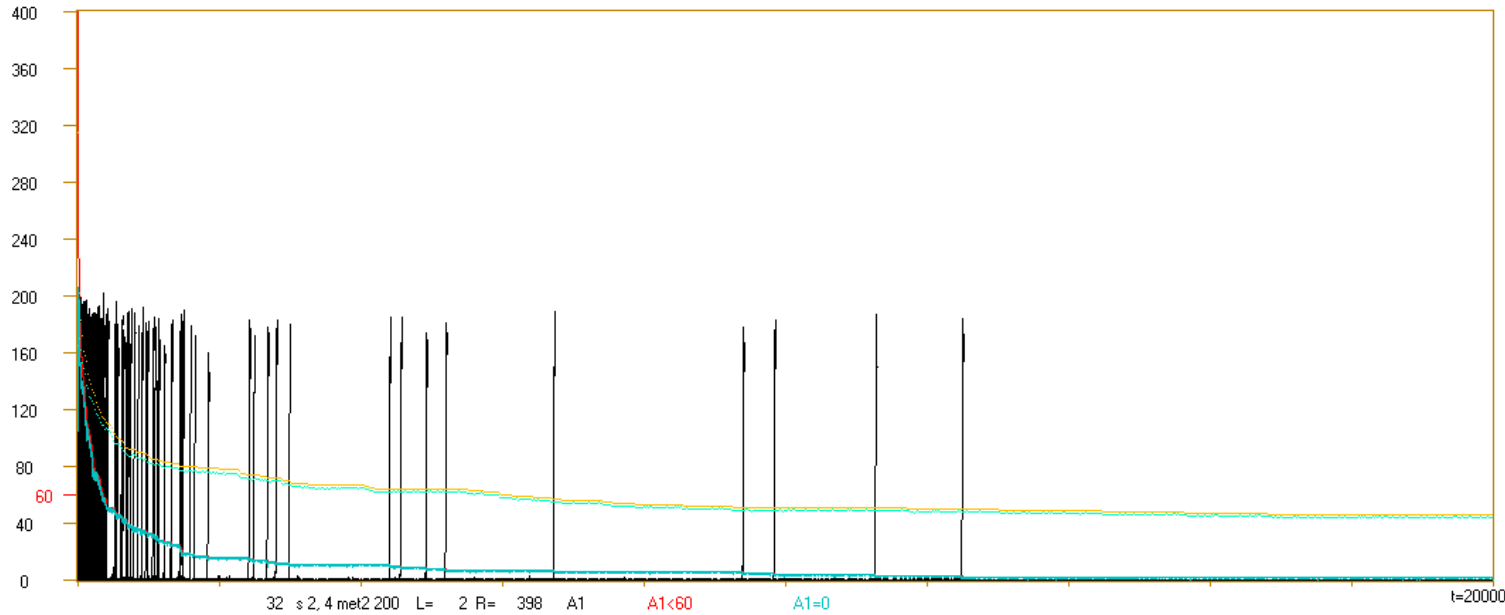
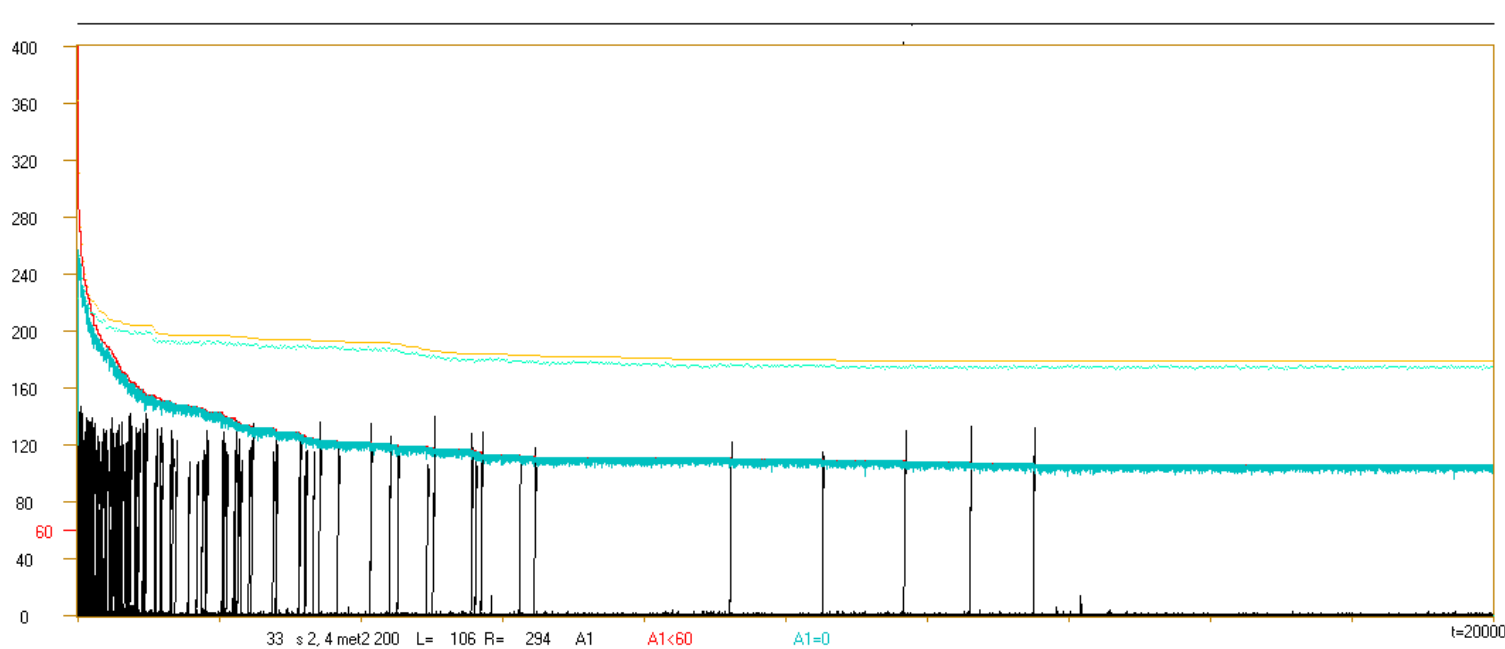


Fig.19. Example of complete of 5 iteration for s 2,4 shown in form of crocodiles. Simulation was optimised on simulation time –processes which exploded are ignored after 20 steps. For net 31 random functions are drawn and such wild system are investigated in first crocodile (black - $A(t)$; red - $L(t)$; blue - number of $A(t)=0$). Next after function corrections by met2 200 functions and initial states are shifted for other nodes as in third experiment (see [tab.2](#)) and using next complete of ini $L(t)$ (yellow) for f investigation is taken.

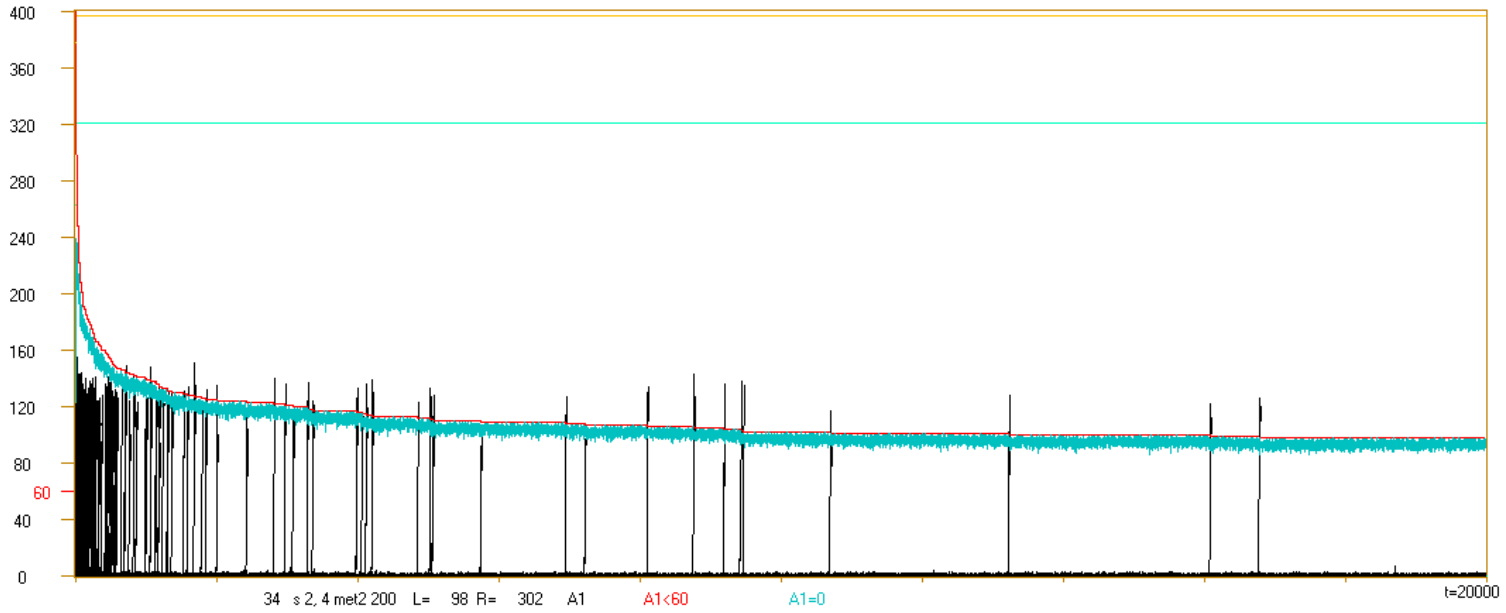


It is first investigation of first iteration. Next new random net no. 32 is drawn (its structure and initial states), but functions are leaved without change. Now, in the next crocodile, w is the second investigation of first iteration. After it the second iteration using met2 200 and its first investigation f are add (L(t) - yellow & A(t)=0 - green) into crocodile 32. Also L (L(tmx)) & R (400-L(tmx)) under box concerns w investigation. Consecutive nets also take functions from previous one. Investigation f for net 35 is the only investigation of fifth

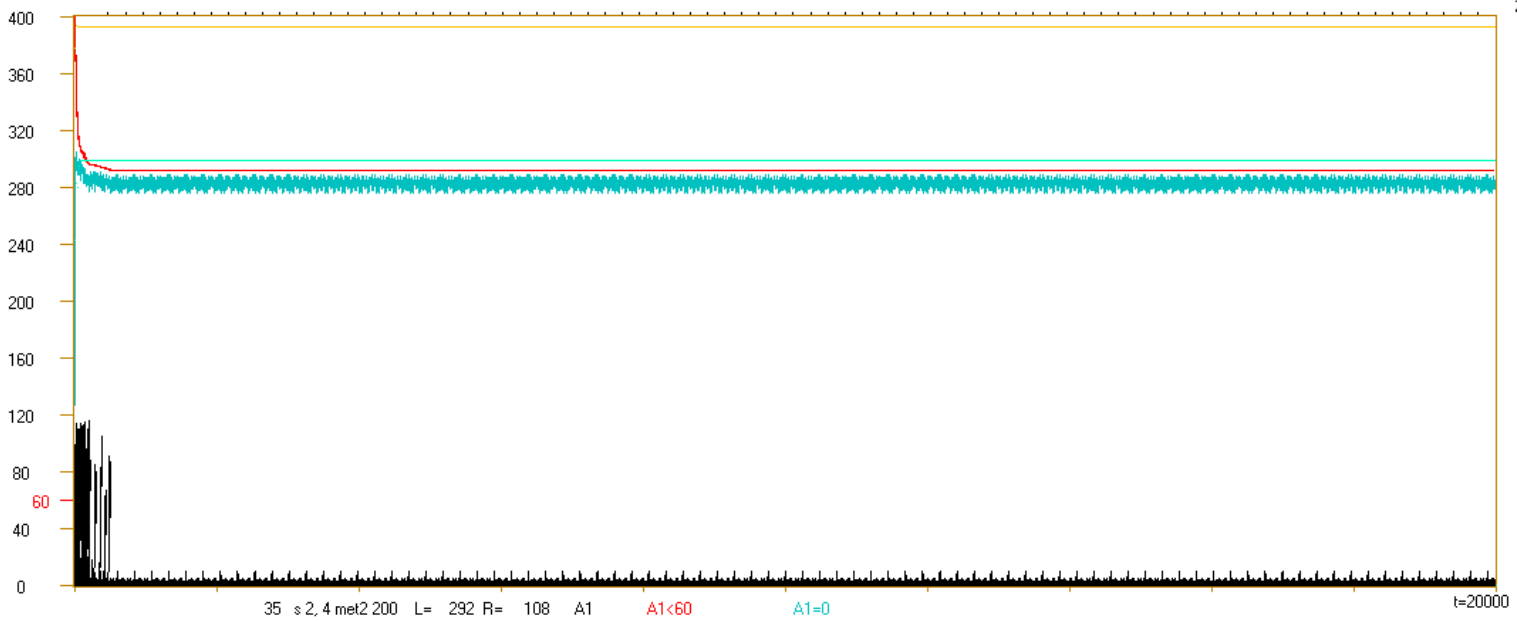


iteration, next net 36 has random functions as 31. Random functions (net 31) give L=0 (at tmx), even L=1. Such a network is fully chaotic. In fig.18 ($q=L/400$) for first iteration L is little higher. Next L grows even in cases, where attractor does not appear and net stays chaotic. It effects from function narrowing and too small tmx, for L reach 0 or attractor cuts falling down.

6f



5f
241 w



2.6 Summary

Method 1 and 2 of damage extinguish effect from expectation that active, not random because selected homeostatic reaction based on negative feed backs is a stability source of living objects. In assumptions of these methods random systems are modified changing existing feedbacks into negative, however, evolution modifies system not random, effects of long natural selection before. It may be too large simplification which leads to results much smaller than expected.

Expected effect occurs only in stronger met2 for network f 24, however effect of function narrowing only is here similar. In the remain nets s & r 2,4 and all three nets f,s,r 4,3 met2 give observed effects in right direction, but much less than expected and needed, not entering into area of stable increasing level of order.

For s & r 2,4 effect of met2 turn out to be nearly in full result of function narrowing, which is a hard to avoid side effect of method. However, for s,K=4,3 effects of method are significantly stronger than of function narrowing, which save reputation and sense of the method. **Generally, function corrections for damage extinguish occurs not enough.**

The investigations give wide reconnaissance of phenomena and of possibility of further investigation. First of all they show the basic role of short attractors in stability problem. The second conclusion is importance of function narrowing, which was already indicated by considering of P – internal homogeneity [ooKauf] and “so-called canalising functions” [Serra04, Serrajtb07]. Power of this phenomenon is different for s,K=2,4 and 4,3. It is possible, that this parameter has significant influence on stability increasing but I think that not so basic like negative feed backs and now appreciated short attractors. This way also leads to shorter attractors, but other ways should be searched.

3 Modularity – met3

3.1 Aims and premises

We come from interpretive premise about living objects that random reaction is chaotic but stability is reached by construction and active non-random reaction selected by natural selection. We expect, that it is done by negative feedbacks working in short loops which are more independent each other. We observe system in longer period than local attractors. A global attractor can be assembled from such local attractors and can be therefore much longer. Small initiating change is permanent but it fadeout ones or few times because local attractor is short. From assumption met1 & 2 were limited to function corrections leaving random homogeneous structure and random initial states. If met1 and 2 are not satisfactory then we should obtain as a next search a structure which leads to short local attractors. It is typically taken view, that in the living objects a modularity is seen. It just should lead to short local attractors. As completion of met1 & 2 (function selection) now we should build network modular by assumption which is a structure selection.

Let us build N2=16 module (small nets N1=25 of nodes each) of particular type and connect them as higher level nodes using the same or other net type. Remaining parameters (functions and initial state of first level nodes) are random (or additionally functions may be corrected by met2). Then we get net N=400 like previously, but connection between modules (if they have K2=4 or 3) are significantly weaker than previously. K1 and K2 may be different, but s must be common.

3.2 Provisional reconnaissance

3.2.1 Primitive simulations, chaos on nodes level, tmx=60

Initial expectations are: damage fade out in the module because attractor is short due to small N1. If damage explodes (chaotic development after ini), then it probably comes out of module and probably initiates neighbouring modules. There it may fadeout, but it is of small probability, because initiations repeat in nearly each step. It is assumption that modules are so great, that chaotic and ordered behaviour can be observed. Basing on other researches [brj] it was estimated, that N1>20.

Provisional reconnaissance was done for networks in the modules: type er 2,4 & 4,3 for N1=20,40,80 & 200. N2 = 400/N1. It was not important for so small networks, that net type was er, it was easier, net types sf & ss for so small N1 (mainly near 20) are not correct due to problem of start.

Intermodule connection cannot be type er due to blind modules which for so small N2 would be interpretively wrong. For modules as nodes k2=K2 was used (type ak in [arj,brj,it]). K2 = 0,1,2,3,6,9, part of it has control meaning. This connection are not random: K2 input links are connected to consecutive K2 modules. As you see, lot of parameters are arbitrary chosen, including tmx=60.

Results of this provisional reconnaissance were discouraged – in investigated range an significant effect of modularity in stability increasing was not found. Observations of weak effects suggest significant decreasing of modules (N1), what seems to be incompatible to expectations and interpretation. In effect of investigation of next method (met4) a tools are developed which allows to come back to met2 200 and met3.

3.2.2 Estimation of N1 for short attractor in the module

Investigation was done: How large should be N1 for short attractors appears often enough. 100 nets of N=40,20 & 16 are checked for nets f,r,s 2,4 & 4,3 using met2 200 with tmx=1000. Results – numbers of attractors found in pattern trajectories for m (after met2 200), f (function narrowing), w (wild) are shown in table 1:

Table 1. Numbers of pattern attractors found for 100 nets, tmx=1000, consecutively: m (after met2 200), f (function narrowing), w (wild) (as in met2 200). Simulation for nets types f, r, s; with parameters: s,K= 2,4 & 4,3 and N=40, 20 & 16. There are the less attractors for r but s,K=4,3 needs smaller N for the same number of attractors as 2,4. For r 2,4 we can expect modularity effects even for N=40 when for 4,3 similar state appears for N1=16. Using met2 200 or function narrowing only significantly increases number of found attractors.

m,f,w	N=40	2,4	4,3	N=20	2,4	4,3	N=16	4,3
f	100,100,100;		50,9,0;	100,100,100;		100,93,44;		100,100,81;
r	87,82,25;		0,0,0;	100,100,100;		53,24,1;		91,71,35;
s	100,100,87;		3,0,0;	100,100,100;		90,58,5;		99,93,47;

It is seen in table 1 that wild net r 4,3 is especially resistant. using met2 200 gives chance for N1=20 r 4,3, but only N1=16 for 4,3 is promising even without met2. Wild net r 2,4 investigated in provisional reconnaissance should [lguchi07] give for N1=20 significant effect, but observed effect was small. It may be an effect of too small tmx=60 (see fig.1). In a new interpretive assumptions modules with smaller N1 are allowed and distinction between ordered and chaotic behaviour inside module is not required. Now we watch probability of fade out of explosion or its limitation to smaller number of smaller modules.

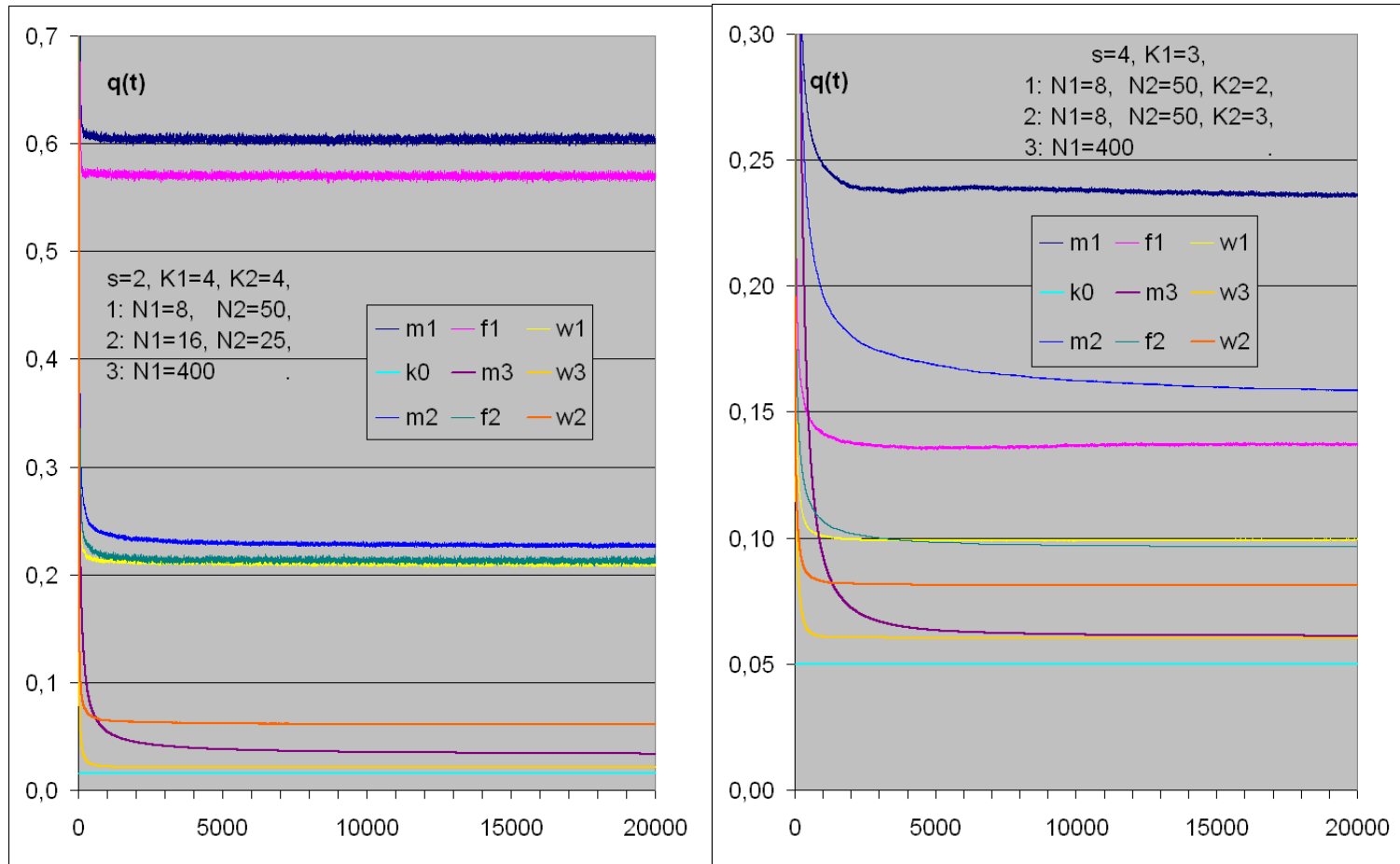


Fig.1. Dependency $q(t)$ in the main simulations of modularity effect (1) (100 nets, $N1=8$), and for more extreme parameters (2) (50 nets) in comparison to uniform net with the same size $N=400$ without modules (3) ($s=2$: 700 nets, $s=4$: 350 nets, investigations with met2). Modules as a nets (1 i 2) and net (3) type r, tmx=20000. For $s=2$: $K1=4, K2=4, N1=8$ (1) and $N1=16$ (2). For $s=4$ and $K1=3$ series (1) & (2) differ by $K2=2$ & 3 respectively. As for $s=2$ in the both series (1 i 2) there is strongly increased relatively to (3) level of q , then for $s=4$ in the range tmx=20000 it can be taken only for series (1), however series (2) exhibit significant fall for all 3 formulas m,f,w. Formula w for $s=2$ series (2) also not necessarily is stable and similarly to series (3) lies near lower limitation $k0$ resulting from existence of blind nodes in r type. Series (1) show that modularity can significantly increase q level and this increasing seems to be stable.

3.3 Simulation after met2 200, chaos on module level, $tmx=20000$

3.3.1 Investigation of stability

Now modules have $N1= 16$ or 8 nodes, $tmx=20000$ as in met2 200. The main simulation series (1) which gives significant effect of modularity has $N1=8, N2=50$. For $s=2$ $K1=4$ also $K2=4$. In addition series (2) $N1=16$. For $s=4$ $K1=3$ series (1) $K2=2$ and additional series (2) has $K2=3$. Results are shown in [fig.1 & 2](#) and [tab.2](#).

Table 2. Value q (in $tmx=20000$ see [fig.1](#)), position (A_{mx}) and value ($P(A_{mx})$) of maximum of right peak (chaotic Derrida balance, [fig.2](#)) for m, f, w and series 1, 2 i 3 described under [fig.1](#). For $s=2$ maximum shift into left of right peak appear for f (see also [fig.m2.3](#)), but for $s=4$ it is for m . Increasing of q for w shows clean effect of modularity for met3, but in opposition to clean met2, using met2 together with met3 gives strong effect in series 1 for $s=4$. In this table results are shown more exactly than in [fig.1 & 2](#).

	m1	f1	w1	m2	f2	w2	m3	f3	w3
q 2,4	0,604	0,568	0,208	0,226	0,215	0,061	0,034	0,031	0,021
A_{mx}	96	90	124	122	96	142	162	154	182
$P(A_{mx})$	0,007	0,008	0,016	0,017	0,016	0,02	0,033	0,031	0,036
q 4,3	0,709	0,412	0,298	0,476	0,290	0,244	0,061	0,061	0,060
A_{mx}	236	250	278	246	262	284	278	280	294
$P(A_{mx})$	0,017	0,023	0,030	0,024	0,030	0,036	0,038	0,039	0,041

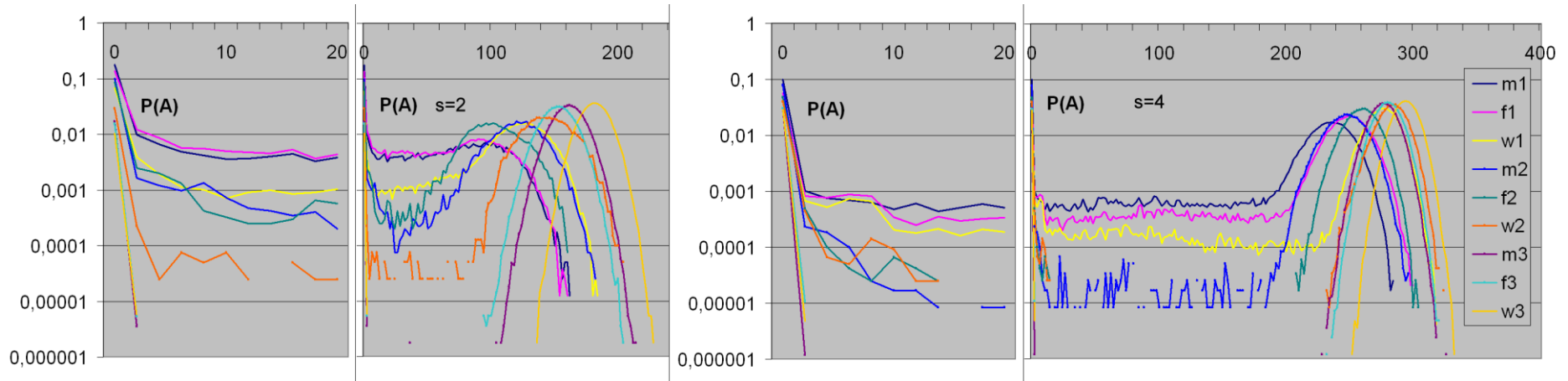


Fig.2. Distribution of probability $P(A_{mx})$ for series described in [fig.1](#). Due to decrease of fluctuations 2 consecutive values are summarized, which is visible in more exactly shown left peak. Apart from small important shift of right peak into left lack of gap between peaks appears which is more important for q defining. Here it depend on arbitrary definition of threshold.

3.3.2 Attractors in the modules and global ones

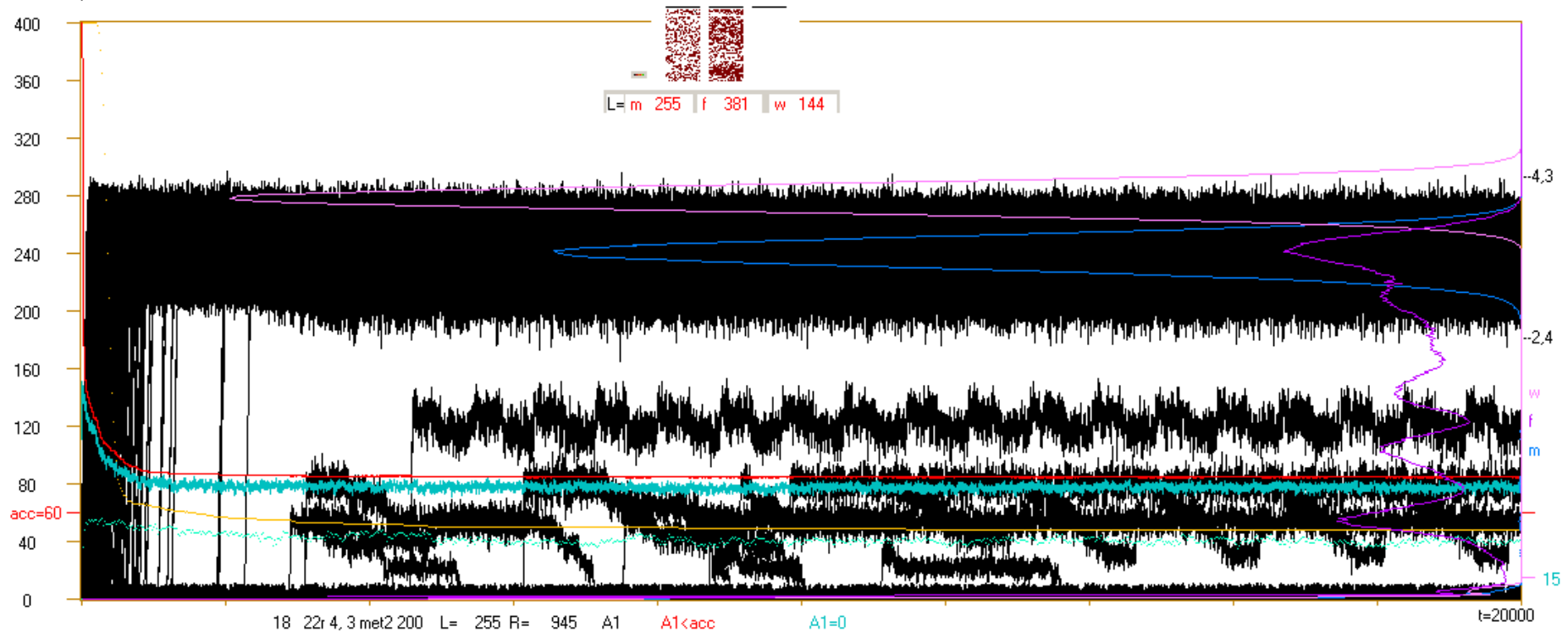
Similarly like in met2 investigations attractor appearance is correlated with existence of attractor in the pattern, but here not so strongly which was separately investigated in crocodiles (fig.3). Length of attractor is indicated by pixel colour for particular ini in given module. Similarly existence and length of pattern attractor is depicted for m,f,w. On right box wall distribution of A on section from t=400 is shown. First section is neglected because it is a region of most explosions. In fig.3 different behaviour may be seen, including clear multiplication of Derrida levels resulted from modularity. In several events damage explosion contain only so few modules (N1=8) that it is under threshold. It is the mechanism which connects left and right peaks seen in fig.2. It increase q, then it is not a lack of chaos on level 1 but limitation of it into few modules, means, lack of chaos on higher level 2. An abundance of interaction between modules due to module function complexity is so large that investigation of regularity of these interactions was given up. Generally can be stated, that modularity effectively increases stability of system despite parameters of system s, K1, K2 place random system as chaotic. In such system, as it is seen in fig.2, simultaneously exist range of damage included to chaotic and to ordered behaviours and both these ranges contain similar number of events. Between these two ranges there is no gap, only minimum.

Table 3. Number of attractor findings. First column: accepted; not accepted; total average attractor length with any time of revolutions for initiations (accepted and not accepted); in pattern. Second column: attractor not found; one revolution of attractor; two and more revolutions of attractor; average attractor length with one revolution; average attractor length with two and more revolutions.

This results should be compared to case without modularity (indicated as (3) in fig.1 & 2 and in tab.2) e.g. m12.tab.2, where for net r no attractor is found. Here is lot of attractors in effect of modularity, however, in more extreme series (2) - significantly less. It suggests that increasing K2 or N1 comparatively series (1) lead to near boundary over which effect of modularity disappears.

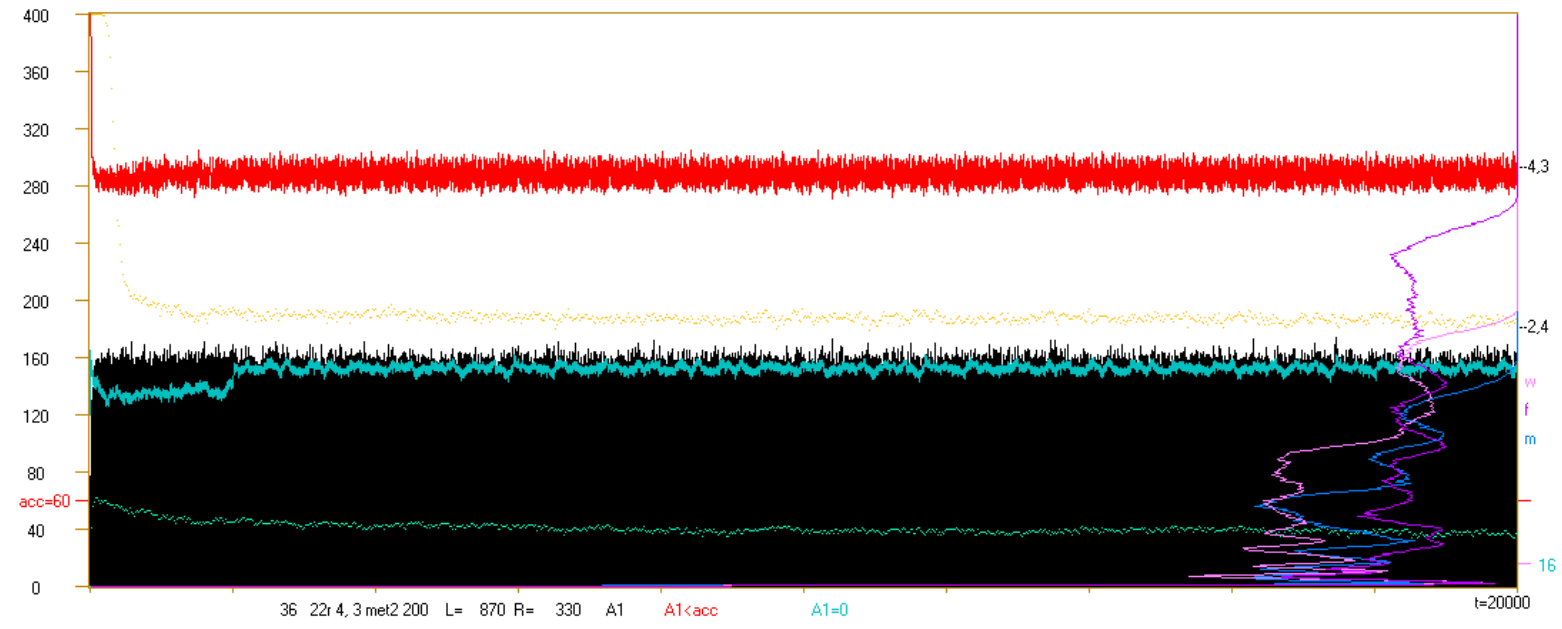
N1,K2 type s,K1 nets		8, 4 r 2.4 100 nets ini=40000			16, 4 r 2,4 50 nets ini=20000			8, 2 r 4,3 100 nets ini=120000			8, 3 r 4.3 50 nets ini=60000		
		m1	f1	w1	m2	f2	w2	m1	f1	w1	m2	f2	w2
accepted A _{tmx} <60	not found	3737	2566	2858	3170	2201	1077	19678	15222	11927	9298	5794	4874
	1	631	189	1	21	70	0	218	933	0	0	0	0
	2	19792	19979	5468	1334	2029	141	8454	329	0	224	0	0
	av.attr. 1	12000,3	12204,3	6120,0	10508,6	10072,5		8455,7	3659,9				
	av.attr. 2	1175,6	884,5	565,4	3398,1	1446,4	1601,4	1878,6	2144,0		1142,7		
not accep. A _{tmx} >=60	not found	8343	6385	21992	12682	10555	17271	71661	96499	108073	49514	54166	55126
	1	256	244	73	231	366	45	2361	3384	0	29	0	0
	2	7241	10637	9608	2562	4779	1466	17628	3633	0	935	40	0
	av.attr. 1	12291,3	11394,2	9450,8	10621,7	11179,5	11679,5	7225,8	3632,7		4661,0		
	av.attr. 2	1027,6	1040,4	689,0	1817,1	1572,2	1915,9	2014,8	2113,4		1794,8	1929,2	
tot	av.attr. tot	1483,8	1089,4	687,0	2859,9	2104,5	2155,0	2452,9	2909,9		1741,8	1929,2	
pattern	not found	29	24	62	40	31	46	78	95	100	49	50	50
	1	2	0	0	0	1	0	0	3	0	0	0	0
	2	69	76	38	10	18	4	22	2	0	1	0	0

3.3.3 Crocodiles

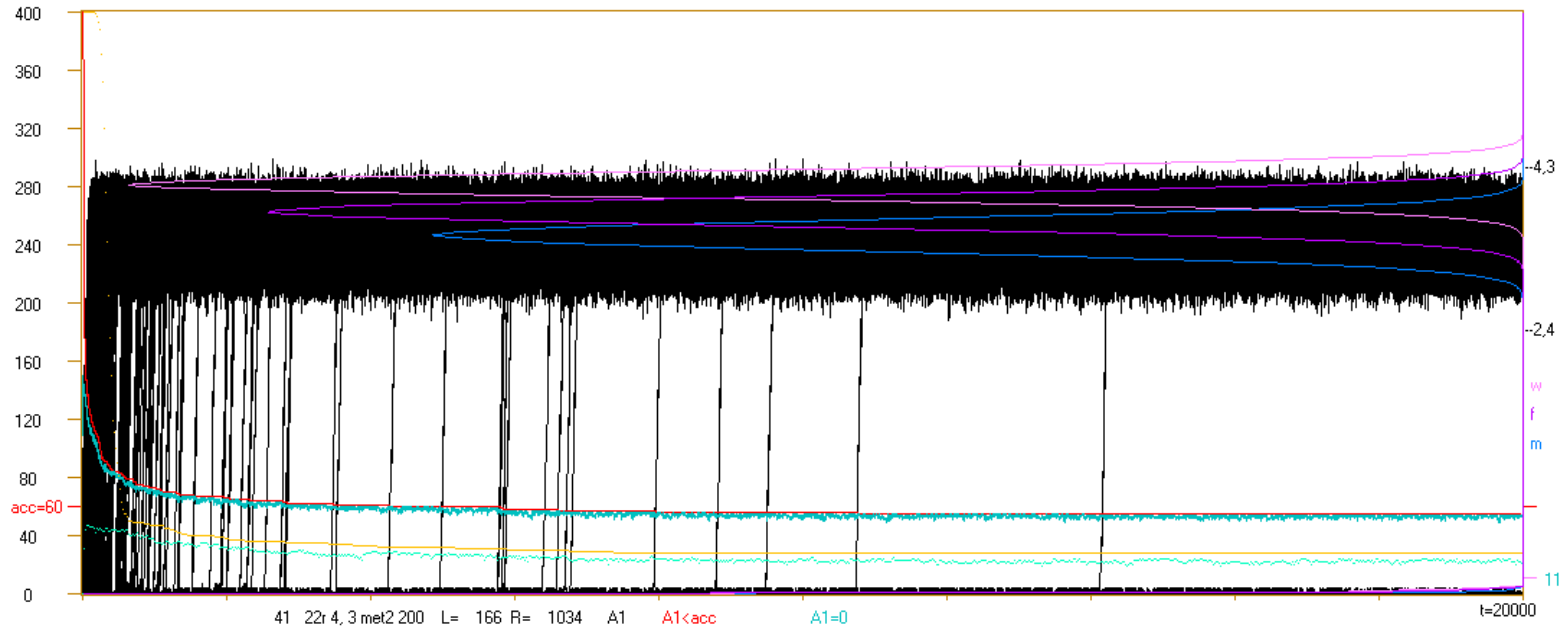


use scale 118% on the screen 1280*1024

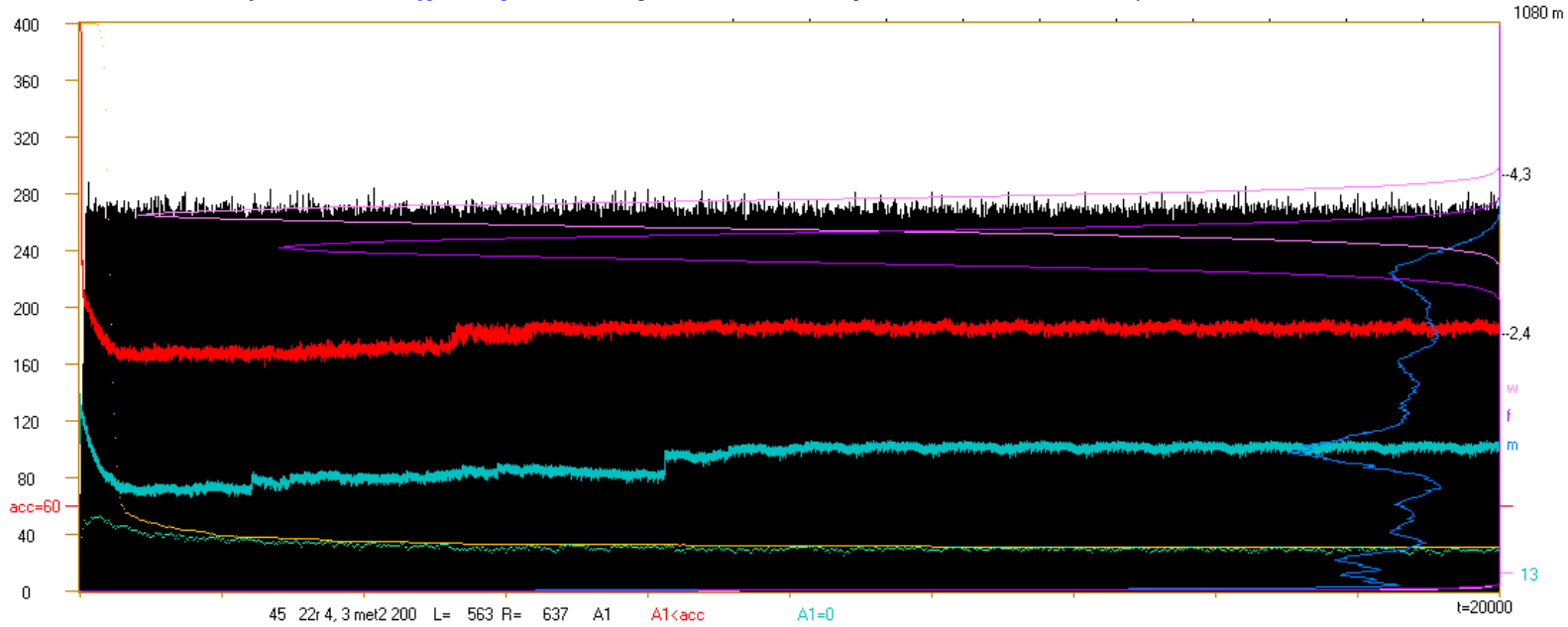
Fig.3. Examples of crocodile of simulation ‘met3 82r43a100’, i.e. $N1=8$, $K2=2$, net inside modules: type r, $s=4$, $K1=3$ 100 nets, $N2=50$ modules. (Later will be 84r24a100 series shown.) Net no 18. Investigated formula: m (met2 200), f (function narrowing as in met2 200), w (wild). Threshold (red $acc=60$). In the right consecutively from down: $t_{mx}=20000$; Number of blind nodes, here 15; threshold; colour of $P(A)$ distributions from $t=400$ to t_{mx} for formulas m, f, w; theoretic levels of Derrida balance for $s, K= 2,4$ i 4,3. Higher, for this net absent, length of pattern attractors for m, f, w. In the middle and up shifted from other place: found attractors after initiations for m, f, w. Pixel colour indicates length of attractor (in sequence: 0-10-100-1000-10000- t_{mx}). Horizontally for 2 consecutive modules. Despite lack of pattern attractors lot of attractors are found in m & f. $A(t)$ – black; $L(t)$ – red; number of $A=0$ for t - blue (line for each t, for m). Additional $A(t)$ – yellow and number $A=0$ for t – green are for w (averaged 20 consecutive values). Remark, that from near $t=2000$ to t_{mx} there is no explosion to basic Derrida balance level despite there is no pattern attractor. However, there are attractors after initiations. The basic Derrida balance level is shifted down and late explosion occurs up to $t=11000$, but they do not reach full net – part of modules is not initiated, several smaller levels of Derrida balance are seen. Such picture typically is overwritten, here visible events of them are so single, that they do not add visible effect into distribution of $P(A)$ for m. Similar phenomena much more intensive result for f lot of peaks in $P(A)$. The lowest of them lies lower than threshold, which effects $L=381$ (of 1200).



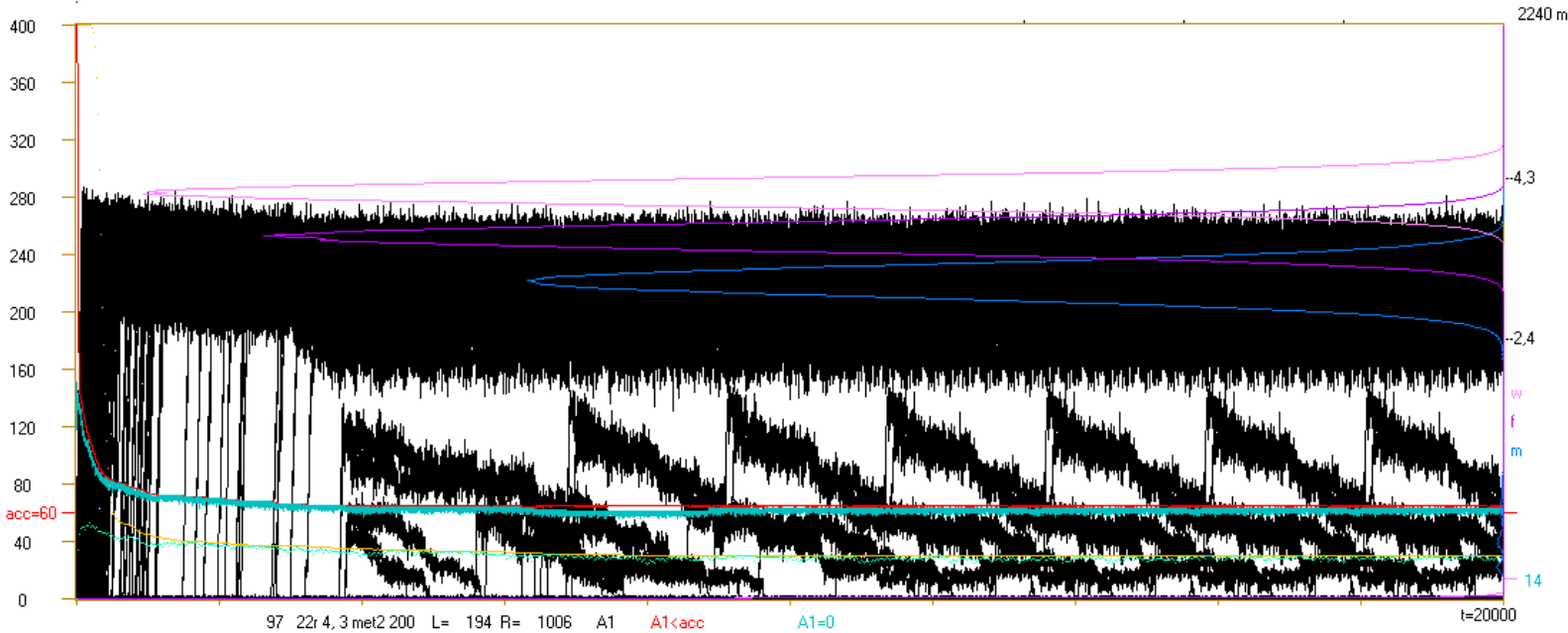
All 3 formulas have strong limitation of damage to small number of modules. Here it is lack of attractors not only in patterns but also after initiations.



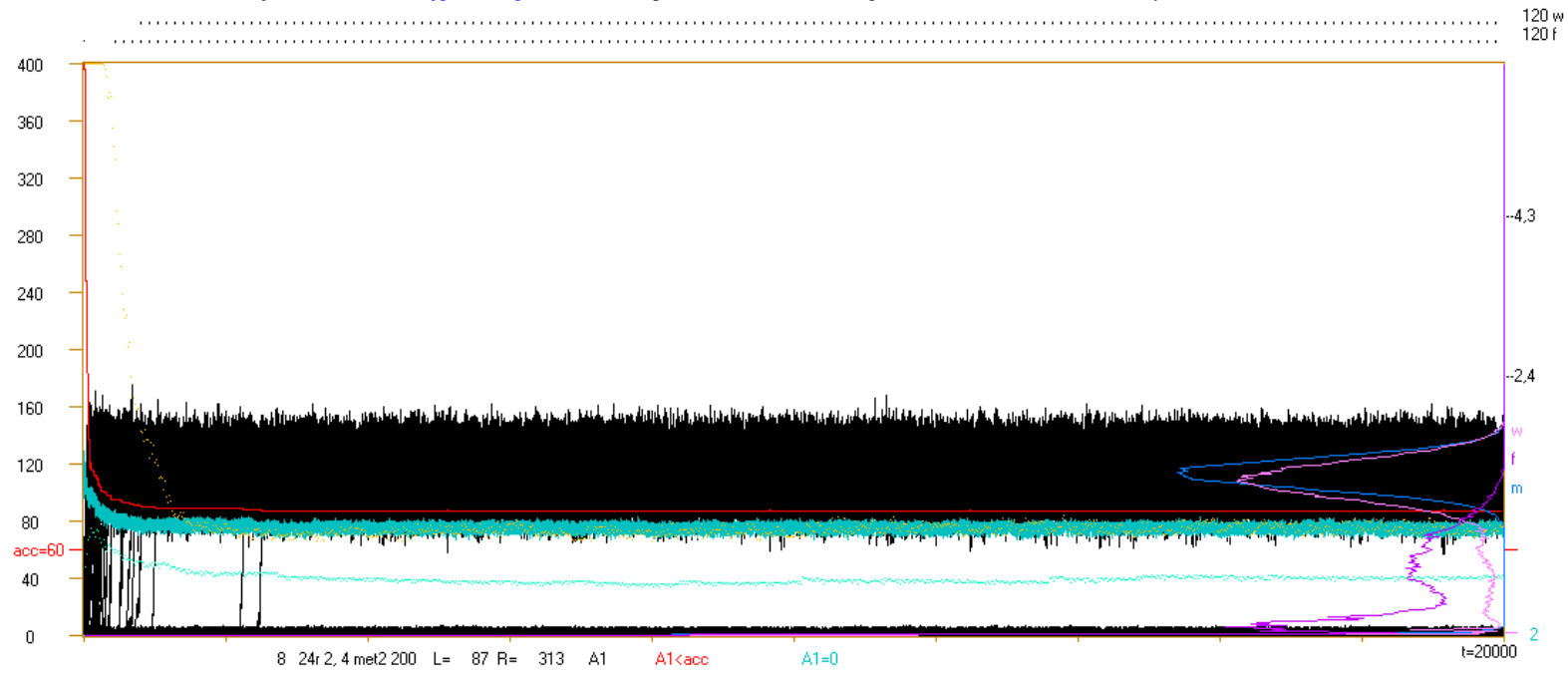
Typical chaotic event for all 3 formulas. Practically, modularity effects nothing beside slower falling of $L(t)$.



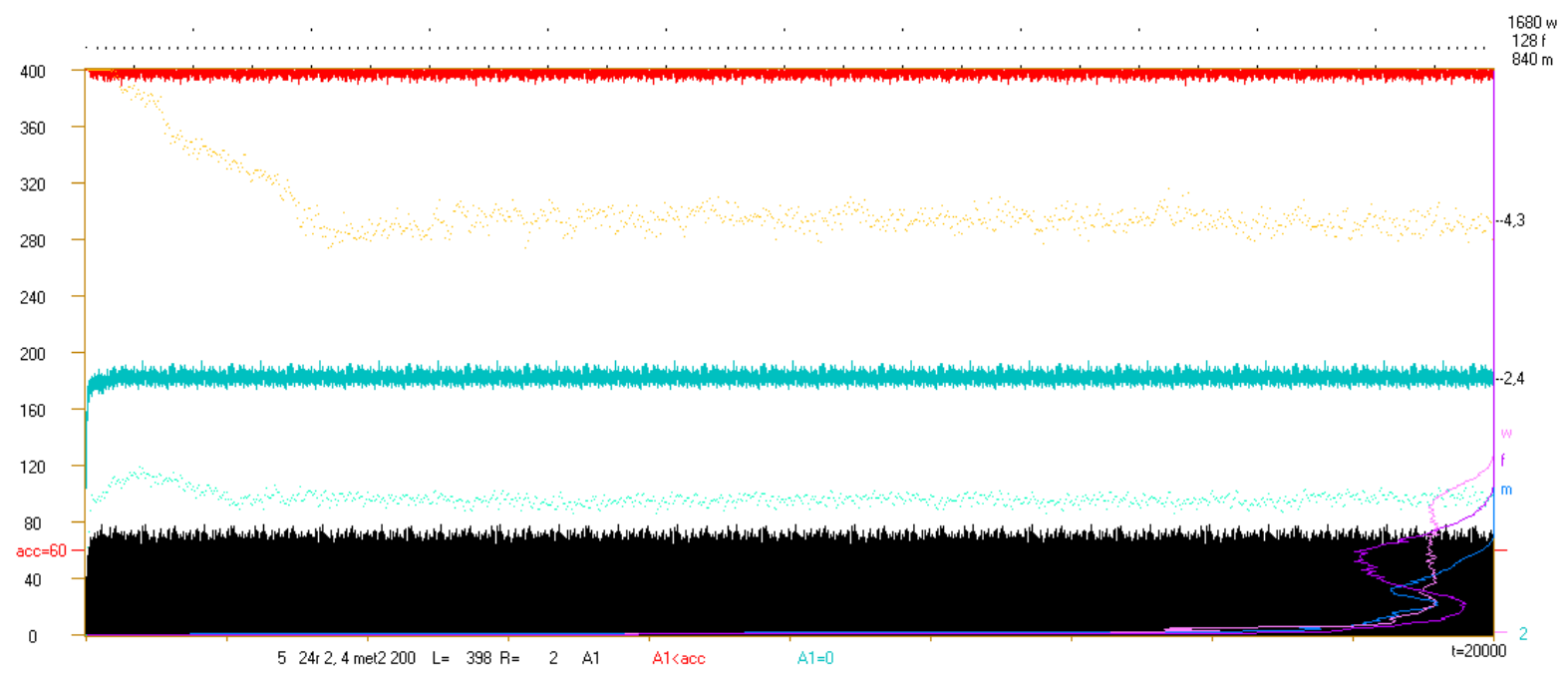
Pattern attractor is present, but in $L(t)$ and $(A=0)(t)$ correlation to second revolution of it is not visible. Earlier jumps of these curves suggest attractors in initiated modules. High level of $L(t)$ results from chaos inside modules under threshold. Minimum of $L(t)$ in first part of process like here is often present which can be read in fig.1.



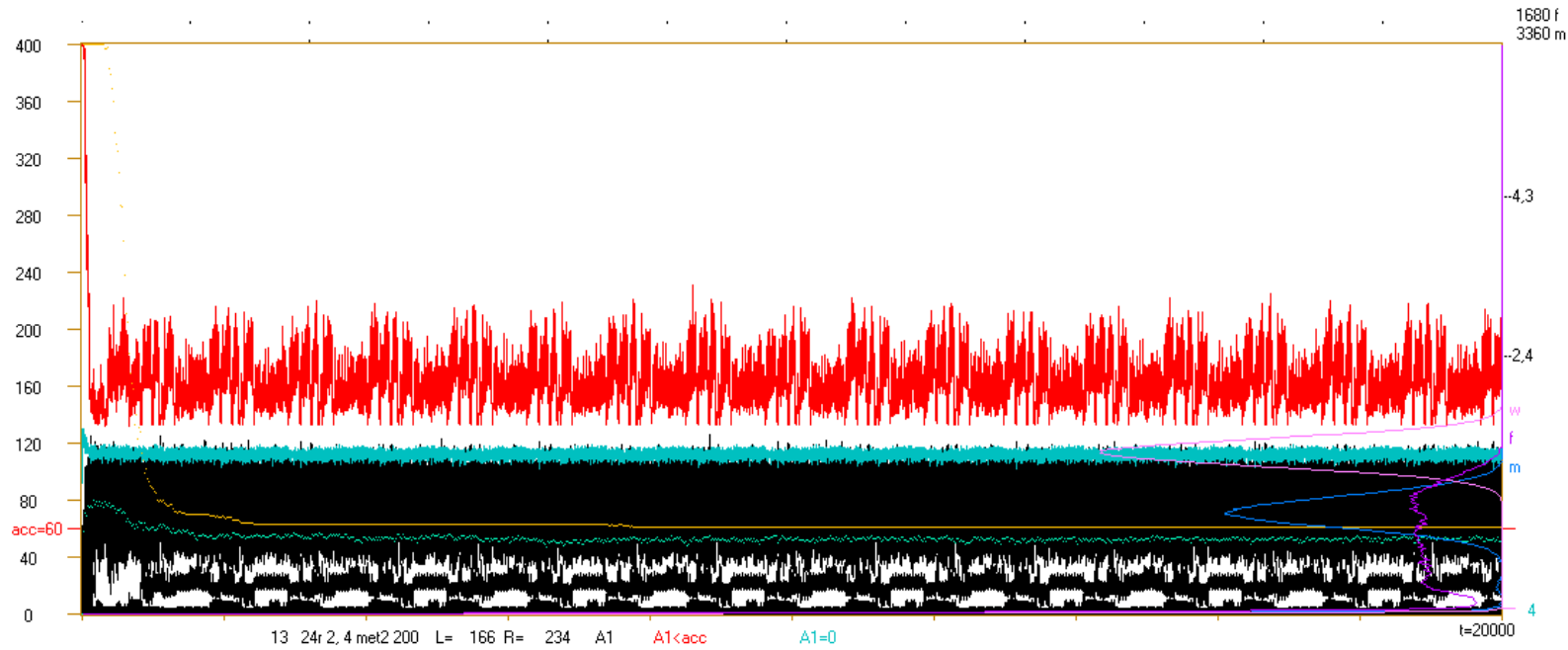
In this event repeated phenomena are visible much before pattern attractor start, however, repeating is not exact. It suggests appearing of module attractor, but later it change a little.



We start review of series **84r24a100** where $N1=8, K1=K2=4, s=2$. Here also global Derrida levels are lowered. Here is lack of pattern attractor for m , but from near $t=2500$ is lack of explosion and $L=87$ (of 400) when chaotic asymptote $=2$. Strong increasing L does not effect from Derrida levels under threshold. Then it is not chaotic event despite attractor is not found.



Here is opposite situation – all Derrida levels are under threshold, but damage does not reach many modules in one time.



Here arbitrary chosen threshold contain under itself large part of right peak, which has typical shape, but probably not for all modules in one time.

3.4 Conclusion

As can be seen in fig.3, modular structure offers abundance of phenomena which is hard to statistical analysis. Evolution has wide possibility to choice. Compound of modular structure (met3) with met2 gives stronger effects of stability increasing than single methods. However, it seems that short attractor is the basic factor leading to stability increasing.

4 Point attractor – met4

4.1 Introduction

4.1.1 General aims

The main aim of this all investigation program is to find stronger basis than interpretive only, for my reversed annealed algorithm. One of the basic assumption of this algorithm is a placing of life in area, where random system is chaotic. Living objects, however, are not random, they are an effect of Darwinian natural selection, which criterion (of this selection) is stability. In the network modelling living objects I expect two peaks in the damage size distribution – right peak connected to Derrida balance and left peak of small damage connected to stability increased by evolution. The rev-ann algorithm offers such distribution, but it is contradict to generally taken hypothesis that life is on the edge of chaos and order (in random systems). Current investigations have to show, that this hypothesis results from too simplified model and deeper analysis prove assumptions taken for rev-ann algorithm, that life evolves in generally chaotic area, however in its range in sub-areas of strongly increased stability, and that such sub-areas exist and are fit for evolution of life.

4.1.2 Premises from earlier investigations met1, 2 and met3

Earlier methods give some increasing of stability, but they are not satisfactory enough. Investigated factors turn out to be not the main. Obtained effects result from other factor, always the same – fast reaching of short attractor, however, earlier expected factors (negative feedbacks and modularity) much help and make stability stronger. Evolutionary change is a permanent change. It should be small (and should give small effective change of function), than it is modelled as ‘point’ change of one node function (change of node function value for one input state). After such initiation, damage (difference to previous functioning of system) can fade out, because next input states of changed node are typically different and doe function like previous. However, input state for which function was changed, will appear time to time, and then secondary initiation of damage appears, but it meets another circumstances, that previously. The fading out all such initiations has small probability, because it is power of value very smaller than one. Exponent of this power is connected to attractor (and way to attractor) length. Second revolution of attractor repeats previous circumstances and if up till now all initiation fade out, then it will repeat and explosion to chaos will not happen.

First attempt to receive short attractors from modularity was unsuccessful (because too large modules are supposed). After such result next method (met4) was defined: to start from so radically short attractor as point attractor. Model with point attractor has well interpretive base. In modularity aspect results of met4 change expectations shifting attention from typical module based on connection density to module in function dimension – short independent loops.

4.1.3 Interpretive basis

Point attractor is a fully frozen state of system, but radical dominate of ice is a basic property of solid and liquid phase in Kauffman description of ordered region in space of random system parameters. Now investigated system exists in this space in chaotic region, but we consider more selected (not random) parameters adding states and functions (connection only in met3). In such the space with extended searching we find specific region, similar in properties to solid region, means – ordered. We are interested in evolutionary changes and their acceptance by natural selection for which small effective change is a criterion. Between these evolutionary changes in our perspective evolving object stay without changes, it functions in the same manner, in statistically the same environment. In some high level nothing changes. Conditions which describe this duration do not change, only next evolutionary change will change them. On lower levels we observe short independent cycles, like breathing, heart rhythm, even – generation.

Describing interpretive bases of rev-ann algorithm in [[dgec](#), [bics](#), [fgec](#)] an event of open network without feedbacks was indicated, where each node on its output has a state which its function gives for current input state. In such the network, consecutive steps change nothing, which corresponds to point attractor. In [[it](#)] interpretation was described wider – it is model of system which function stably during a long time. Now we do not limit to open system without feedbacks, but we investigate autonomous system with feedbacks, because from investigation of such the system it was concluded hypothesis that life is on the edge of chaos. We assume the state of point attractor as a system state imposed evolutionary changes and model of system which function stably during a long time.

For the met1 & 2 modification of random system was investigated, however, it was not sure, that region of living objects is attainable easily enough from random system. In conclusion of these methods this assumption was indicated as a source of failure. Now we get rid of this assumption and we start from specific state.

4.2 Investigated models

It is easy to create point attractor state for given random network. For it is enough that after random draw of node states, for current input states of node its function gives its current state. More easy, however, is to assume, that states in point attractor are called ‘0’, than all functions have $f(0)=0$. Remaining input states give any function values. Share of ‘0’ in function statistic can be equalized. Both method are equivalent (which was checked). I call ‘PAS’ general ‘Point Attractor System’, but specific form with all ‘0’ states – ‘PAS0’. In met4 investigation PAS0 is used.

4.2.1 Models without regulation: c for 4,3 $f(0,0,0)=0$, and d for 2,4 $f(0,0,0)=0$.

I call such a model ‘c’ for s,K=4,3, and ‘d’ for 2,4. They do not model any regulation, only PAS0.

4.2.2 Model with minimal regulation b for 4,3 $f(0,0,0)=f(0,0,1)=f(0,1,0)=f(1,0,0)=0$

Investigations were limited to only PAS0 not from the beginning. Initially still the main attention was directed into regulation aspect. It effects of reverse sequence of model names. For 2,4 there is lack of possibility to easy introduction of regulation, but it is possible for 4,3 and it was done. Model with minimal regulation is called b. For signal value 1 interpretation was taken: swung from proper state ‘0’, but still in range of homeostasis. It leads to add to $f(0,0,0)=0$ also $f(0,0,1)=f(0,1,0)=f(1,0,0)=0$.

4.2.3 Model a with strong regulation for 4,3

On the beginning, however, model a with strong regulation was define. Obviously, here also $f(0,0,0)=0$, but description is much more complicated. Here direction of swinging in homeostasis range: 1 – positive; 3 – negative. Swinging of one of 3 input signals gives 0: $f(0,0,1)=f(0,1,0)=f(1,0,0)=f(0,0,3)=f(0,3,0)=f(3,0,0)=0$. Function also gives 0 if 2 signals are swung, but in opposite direction, and third is 0, i.e. for each combination of 0,1,3.

If 2 signals swing in the same direction but third is 0; or 3 signals swing but they are not equal, then function result is swung, i.e. is 1 or 3.

If 3 signals swing and are equal, or at least one is 2, then result of base function is 2, but such value for particular node is converted into random value in the way, that share of each function value be equal. In table 1 the base function is shown.

Table 1. Base function for model a. Upper row: first input signal; 3 signals from second input. First column: under first input signal 3 signals from third input.

0 0 1 2 3	3 0 1 2 3	2 0 1 2 3	1 0 1 2 3	Replacing of tables for first input signals 1 and 3 has interpretive base.
0 0 0 2 0	0 0 1 2 0	0 2 2 2 2	0 0 0 2 3	As can be seen, formula a model strong regulative reaction. Nature of it is negative feedback
1 0 1 2 0	1 1 2 2 1	1 2 2 2 2	1 0 1 2 3	with possibility of coming out of range of homeostasis.
2 2 2 2 2	2 2 2 2 2	2 2 2 2 2	2 2 2 2 2	
3 0 0 2 3	3 0 1 2 3	3 2 2 2 2	3 3 3 2 2	

4.2.4 Simulations done

For each of 4 models (a,b,c,d) 3 series of simulations (N=400, tmx=200; N=400, tmx=2000; N=4000, tmx=200) were done for net types f and r. In each series number of initiations was 48000. It allow to check influence of increasing N and tmx separately.

Models a,b,c,d differ in possible ‘random’ variants of initiations. Obviously, in model d it is 1 possible ini for each node. For s=4 generally 3 different values should be, from assumption of met4 for PAS0 it is not 0, but for model a values 3 and 1, and for model b value 1 must give fade out, then they are not ‘random’. For model a only value 2 remains, and for model b only 2 and 3 remain. They are changes which effect is define not by model, only by particular event. Only model c can use all 3 remaining values.

For N=4000 and one possible ini (models a & d) 12 nets are simulated. It gives 48000 ini, then for model b 6 nets and for model c 4 nets are simulated to be the same number of ini. For series with N=400 there are 10 times more nets. In effect for N=4000 influence of particular net structure is high, but influence of N increasing are the only aim of these series and for it statistics occur to be enough. The basic results are given by series tmx=2000 & 200, N=400.

Basing on provisional investigation of right end of left peak the threshold is shifted from 60 to 100 for N=400 and to 300 for N=4000. In later investigation for N=4000, model a and net type f the threshold=800 is used.

4.3 Basic results

The proper for biological evolution area in space of system parameters with chaotic parameters s,K for random systems is indicated.

In this area chaos and order do exist simultaneously with similar degrees.

4.3.1 Clearly separated, similar capacity 2 peaks – ordered and chaotic events in damage size distribution

For all 4 models a searched state of damage size distribution (fig.1 & 2) is reached. There are 2 strong peaks (tab.2): left – very small damage, and right – large damage corresponding to Derrida equilibrium of chaotic events. Between them there is gap which clearly separates both peaks.

Table 2. Division of result of initiation by permanent point change on chaotic explosion and ordered (saved) events based od $A3 < \text{threshold}$. ($A3$ – average $A1$ from last period before tmx , see ch.4.5. In fig.1 & 2 similar data based on $A1$ differ minimally.). Next division of ‘saved’ into different variants: PAS, fade out to $A1=0$ (fade) and (other). In middle model and net type is indicated. Basic results are shown in percent of ini or of saved, but for exactness estimation also in number of events. Upper part is for $N=400$ but lower for $N=4000$. The most important results are indicated in colour.

4753	18741	15111	31149	32766	41078	16983	39655	expl A3	tot ini=48000
43247	29259	32889	16851	15234	6922	31017	8345	saved A3	tmx = 200
39847	26597	31806	16293	15147	6884	30323	8266	pas	N = 400
353	430	191	180	18	13	53	39	fade	
3047	2232	892	378	69	25	641	40	other	
9,90	39,04	31,48	64,89	68,26	85,58	35,38	82,61	c = expl A3	% ini
90,10	60,96	68,52	35,11	31,74	14,42	64,62	17,39	q = saved A3	% ini
92,14	90,90	96,71	96,69	99,43	99,45	97,76	99,05	pas	%saved
0,82	1,47	0,58	1,07	0,12	0,19	0,17	0,47	fade	%saved
7,05	7,63	2,71	2,24	0,45	0,36	2,07	0,48	other	%saved
af	ar	bf	br	cf	cr	df	dr		
3373	17902	13965	30610	32805	41106	17170	39788	expl A3	tot ini=48000
44627	30098	34035	17390	15195	6894	30830	8212	saved A3	tmx = 200
43727	29655	33826	17321	15187	6891	30785	8207	pas	N = 4000
52	46	27	18	0	1	8	5	fade	
848	397	182	51	8	2	37	0	other	
7,03	37,30	29,09	63,77	68,34	85,64	35,77	82,89	expl A3	% ini
92,97	62,70	70,91	36,23	31,66	14,36	64,23	17,11	saved A3	% ini
97,98	98,53	99,39	99,60	99,95	99,96	99,85	99,94	pas	%saved
0,12	0,15	0,08	0,10	0,00	0,01	0,03	0,06	fade	%saved
1,90	1,32	0,53	0,29	0,05	0,03	0,12	0,00	other	%saved

Only **model a for net type f turns to be too effective**, i.e. regulation is here very strong and right peak is small, but exists. The same model for net r gives normal right peak similar capacity as model b – with minimal regulation for net f. Similarly as in met1 & 2, net f is much more stable than r, and this difference is similar to difference between models a & b.

For $tmx=2000$ calculated for the same nets as $tmx=200$ results in table in fig.1 for left peak differ only for af by 140 (43410-43270) and df by 2 (31019-31017). It means that **left peak practically does not decrease with tmx increasing**, and observed differences result from fluctuation between peaks. Complex nature these fluctuations show only $A(t)$ called crocodiles (fig.3 & 4). They come to existence for simulation program control, but turn to be irreplaceable source of information of complex aspects of

investigated phenomena. They show first short period of chaotic explosions and later long period of stable division on ordered and chaotic events connected to both peaks (fig.3 from which name ‘crocodile’ is taken).

An effect of of N increasing to 4000 is shown in fig.2. Comparing to N=400 (fig.1) the peaks are narrower and period between peaks more empty. Expected, searched and just found **effect increases significance when net grows**, then simulated networks are not too small.

Both peaks are present simultaneously in each single net. These networks are then simultaneously chaotic and ordered. While initiation we do not know (deterministic network ‘knows’) if the effect will be ordered or chaotic.

Stable fadeout of permanent change is here impossible, after fadeout immediately secondary initiation appears which leads to stable oscillations in short loops.

4.3.2 Fraction of PAS in accepted events, investigation of secondary initiation

Initial view about ordered events practically was limited to expectation of full fade out to $A1=0$. Falling own of q with tmx increasing in met1 & 2 turns attention on secondary initiations. A role of length of the way to beginning of second revolution of attractor was the basic conclusion. Such conclusion result met3 and current met4. In met4 any ini starts from PAS0 and after fade out to $A1=0$, immediately in next step repeating of all previous damage process starts. It is repeating ad infinite. The secondary initiations are not interesting in met4, but slightly corrected ready tools give interesting results. They are shown in tab.2. Each ini (for each column there are 48000 ini) gives explosion ($A3$ comes over threshold) or stays ‘saved’, means ‘accepted’ and ordered. There are 3 variants of saved events: PAS – point attractor (it cannot be PAS0), fade out to $A1=0$ and something else.

Saved (q) reach 93% for extreme model af, but in half of models cross over 60% all ini, it does not fall lower than 14% (cr). The most important result shown in tab.2 is **fraction of PAS in saved**, which for N=400 **does not fall lower than 90% for model a, in remaining vary between 96.7 and 99.96%.** **Because each PAS is a coming back to circumstances before permanent change, evolution can go on without coming out of point attractors, only jumping between them. It is sufficient prove of area existence, where evolution can persist long without leaving it, in the range of parameters s,K of system placing random system in chaotic region.** However, limiting description of living objects only to systems with point attractor is interpretive extreme and question arises, if remaining variants will be allowed then will we get similar possibility of long evolution without necessity to end in chaos. On this question further met5 will answer, where such changes will be cumulated. It also will give positive results, which significantly expands sub-area of chaotic systems suitable for biological evolution.

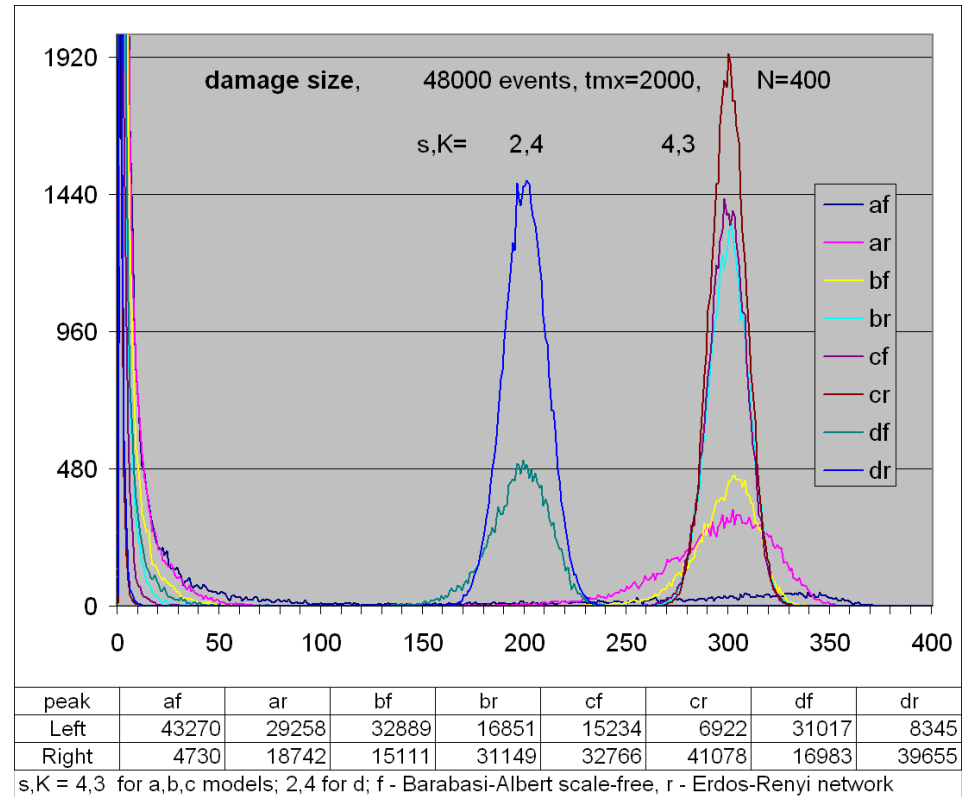
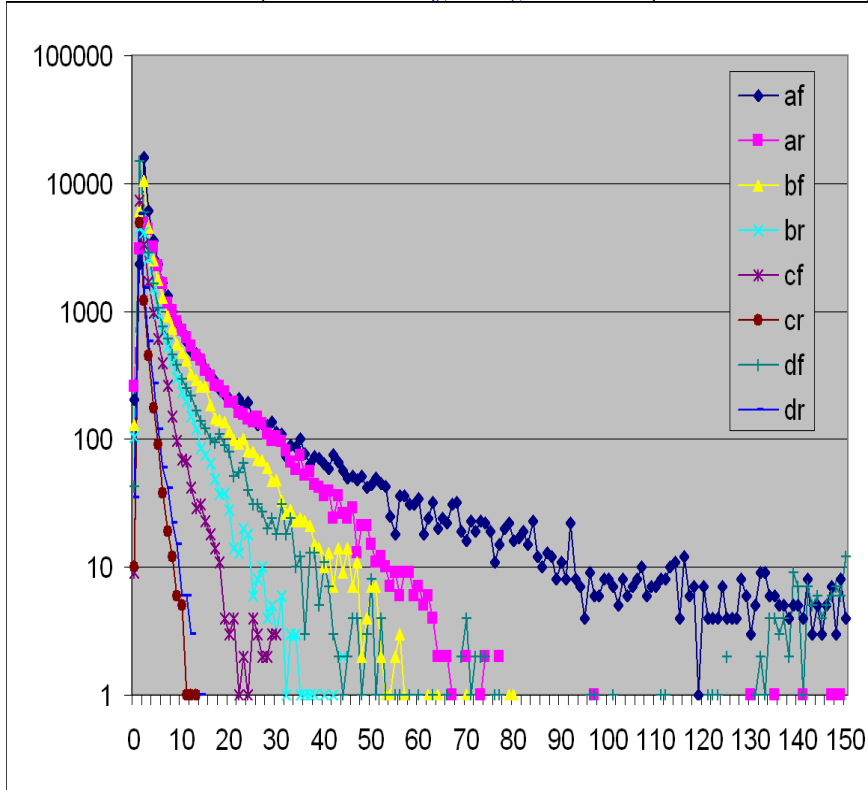
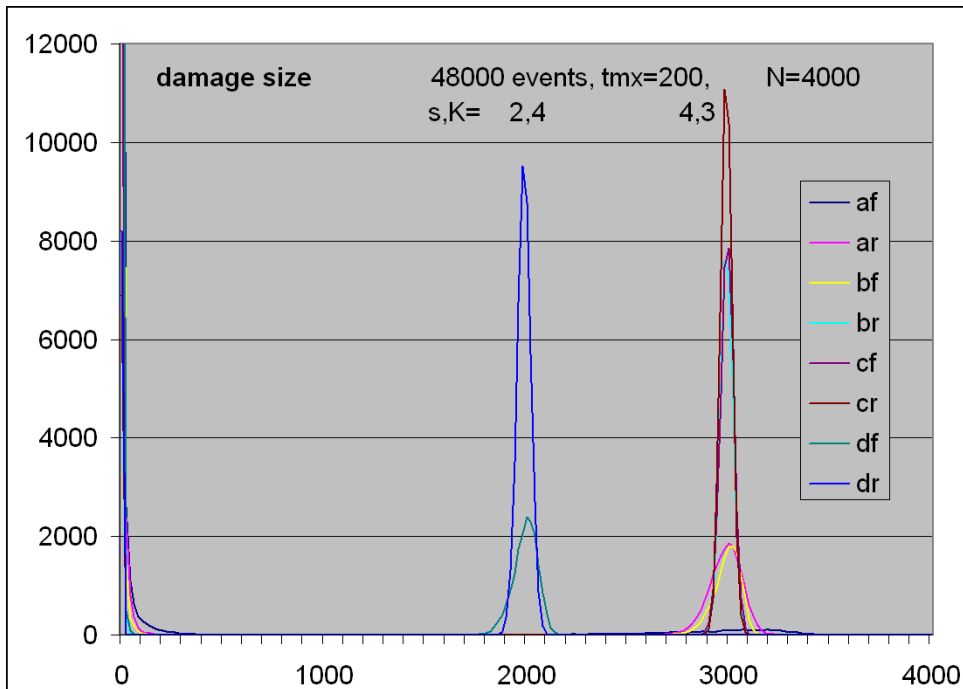
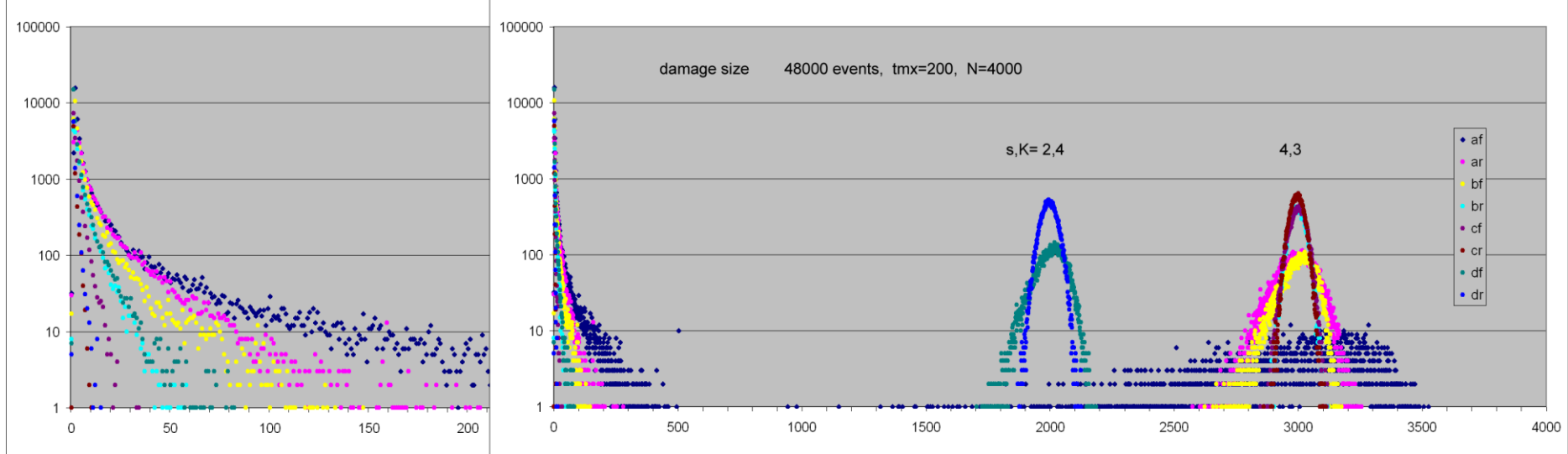


Fig.1. Basic result of met4 – distribution P(A1) (On vertical axis numbers of count are shown. To obtain probability P this number should be divided by 48000 ini.) A1 – Avalanche is a number of damaged nodes at tmx. It is result of models a,b,c,d for N=400, tmx=2000. For tmx=200 and the same set of nets results shown in table differ for left peak only for af (43410) i df (31019). It means that when tmx grow the left peak practically does not decrease. The left peak has long tail which allow small, but not extremely small evolutionary changes, making view near expected biological interpretation. Effect of N increasing to 4000 is shown in fig.2.

Remark, here results are based on A1 but in tab. 2 results are based on more exact A3. Differences are small.

Obtained distribution P(A1) with two peaks: left for small damage (ordered), and right of Derrida equilibrium (chaotic), and near empty gap between them, exactly correspond to view assumed in reversed-annealed algorithm. 480 counts is 1% when we consider probability P(A1(tmx)).

Regulation in model a is very strong, then right peak is small and flat and gap between peaks is not empty. It show, that regulation is strong and important tool of evolution to increase of stability for system which parameters categorise random system as chaotic. However, this conclusion is for very short attractor.



peak	af	ar	bf	br	cf	cr	df	dr
Left	44713	30098	34035	17390	15195	6894	30830	8212
Right	3287	17902	13965	30610	32805	41106	17170	39788



Fig.2. Distribution $P(A1)$ (when divide by 48000) of damage size (damage $d=A1/N$) in models a,b,c,d for $N=4000$, $tmx=200$. **In comparison to $N=400$ (fig.1) peaks are narrower, and gap between peaks is more empty.** In upper logarithmic diagram a horizontal axis $A1$ is shown in full exactness, but in diagram nearby one point is a sum of 20 values of $A1$. In log diagram it is clearly seen how great is difference of height of right peak between models and network types f & r. In right down chaos and order degree is shown for simulation $N=400$, $tmx=2000$. Yellow part of order is an effect of blind nodes ($k=0$) present only in network r.

4.4 Conclusion from crocodiles

Graphs $A(t)$ dynamically collected for all ini of one (or few) net are called crocodiles basing on [fig.3](#). They come to existence for control of simulation program, but they turn to be irreplaceable source of information about complex aspects of investigated phenomena. They show first of all a complex nature of gap between peaks ([fig.4](#)), a short period of chaotic explosions at the beginning and later long period of stable division on ordered and chaotic events connected to both peaks. Observation of crocodiles was the main source of tools development and allows to come back to deeper investigation of earlier met1, 2 (met2 200) and met3.

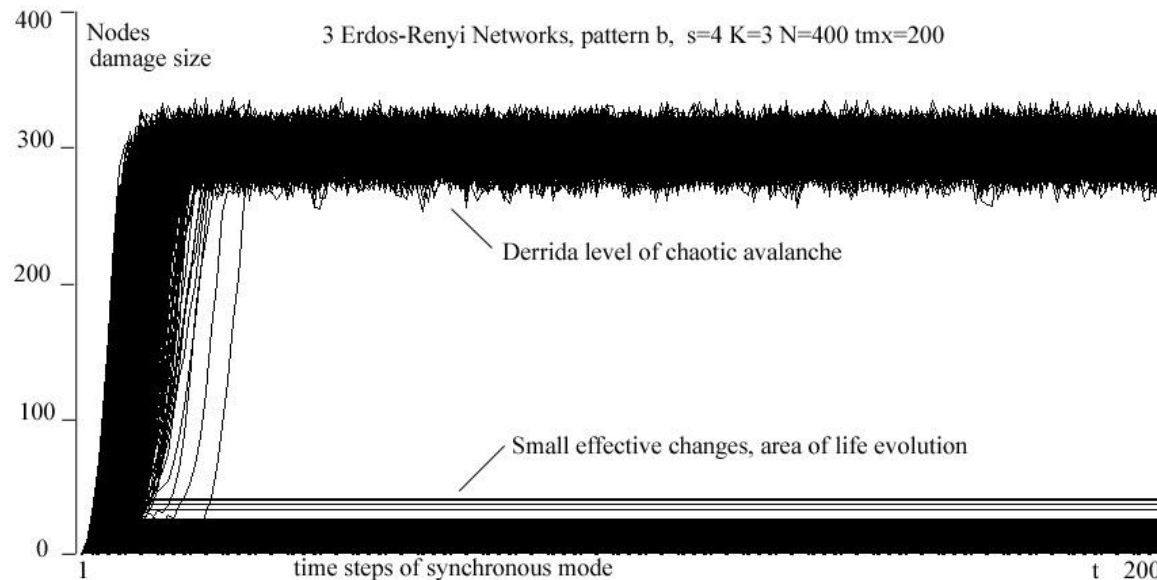
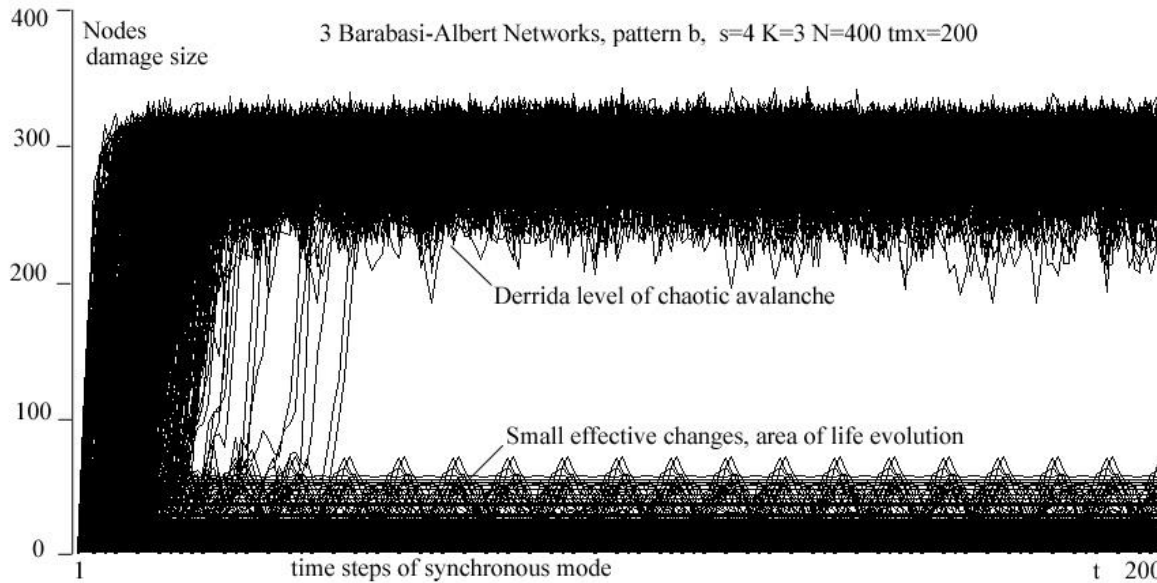


Fig. 3. Graphs of $A(t)$ for 3 nets f 4,3 which gives the name 'crocodile' to this type depictions of simulations. They turn out to be very useful.

This crocodile arises from initiations in 3 nets scale-free in model b. Here teeth of regular oscillations resulted from short loops are visible in lower jaw. Upper jaw correspond to Derrida equilibrium of chaotic events.

In opposition to such dependency of A (Avalanche) from time earlier (met1, 2, 3) shown here chaotic explosions quickly disappear and both peaks reach stable capacity. Similar picture is for models b,c,d and both net types f i r, they differs in details ([fig.4](#)). Only model af gives especially ordered events, see [fig.4](#).

Lower - similar graph for 3 nets r 4,3, (Erdos-Renyi net called „Random”, but PAS0), model b.

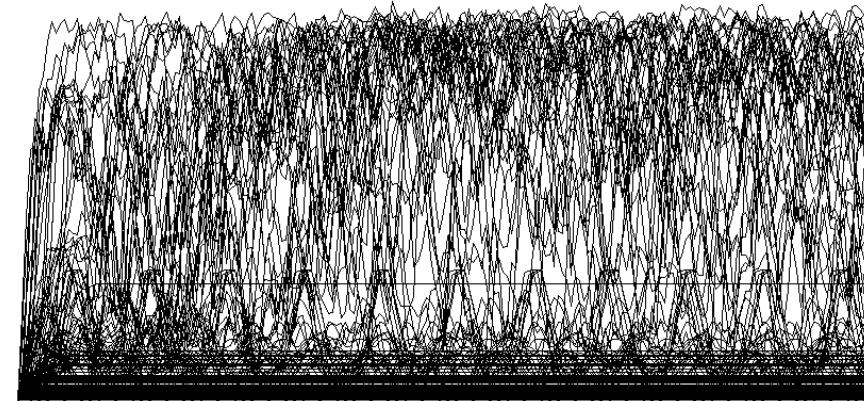
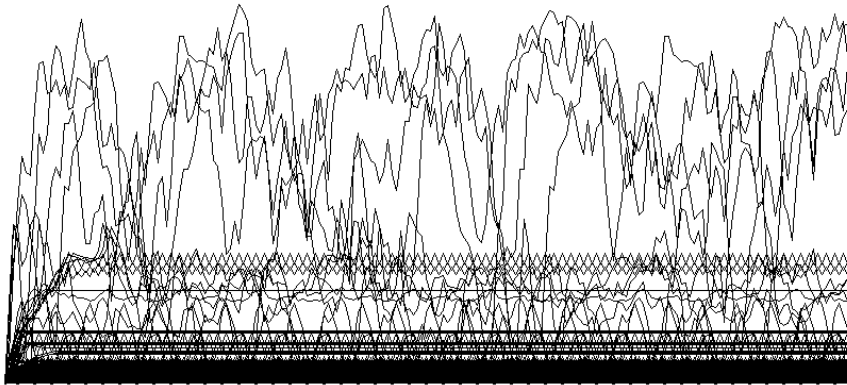
This crocodile is more safety, it has no teeth, but straight lines mostly result from point attractors (PAS) – they stably differ from pattern which is PAS0.

After short period state of both peaks (jaws) become stable, both ranges – chaotic and ordered, are narrow and gap is empty. Here only 200 steps are depicted ($tmx=200$), means one step = 5 pixels.

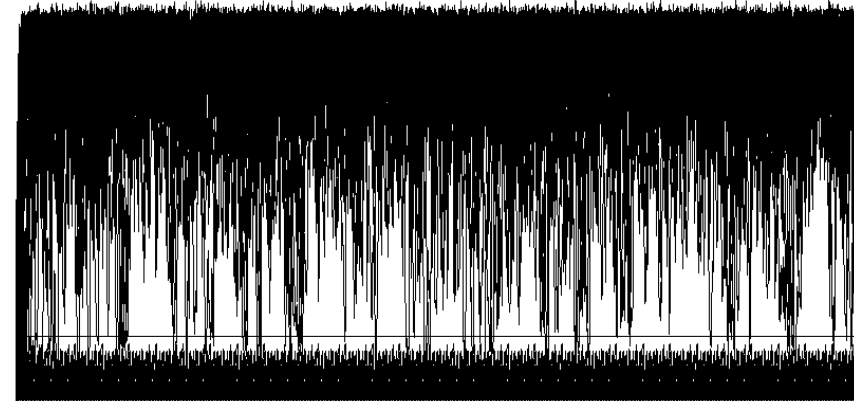
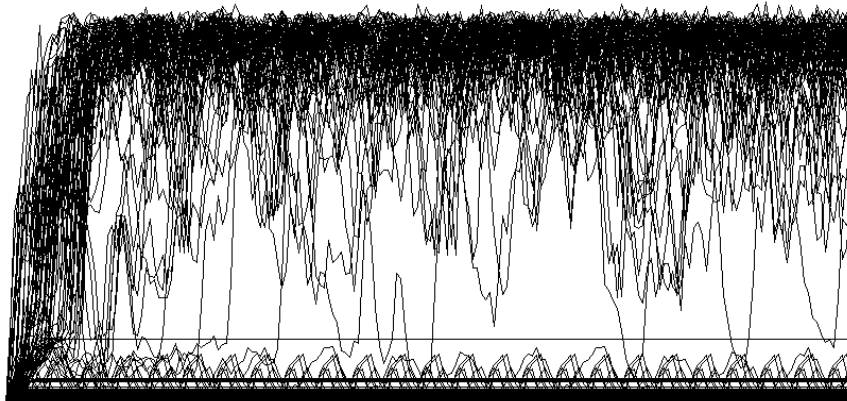
Fig.4 - begin. Review of crocodiles from simulation of models a, b, c & d. Description of examples: model (a,b,c,d); net type (f,r); net number; $tmx=200, 2000$ (t,T); $N=400, 4000$ (n,N).

Different pictures of crocodile happened, they can be much different than in fig.3. Especially in model a, where is small number of chaotic events as effect of strong regulation.

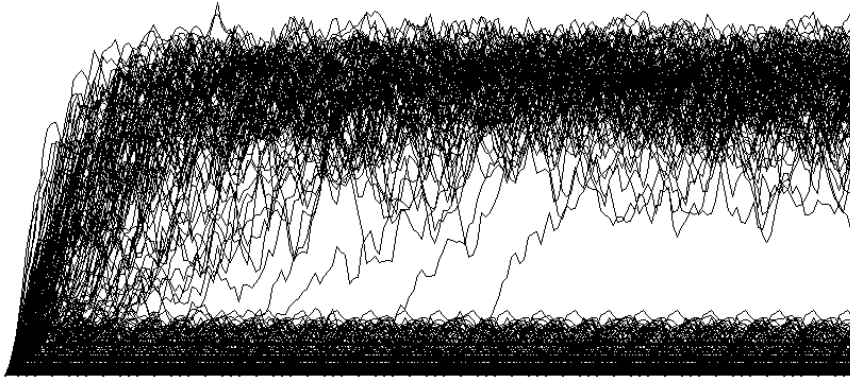
Line on the right shows provisionally scale: it uses 10 and 100 sections, vertical axis depicts N nodes. Horizontal axis depicts $tmx=1000$ pixels. Lower crocodiles for model a start (generally 'tn', i.e. $tmx=200, N=400$).



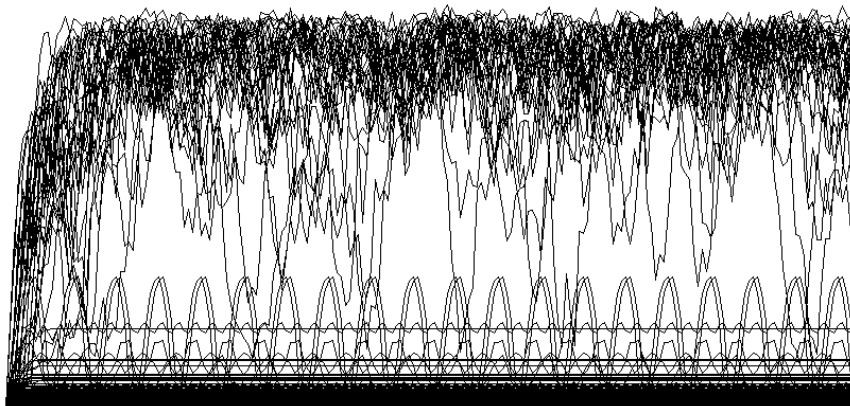
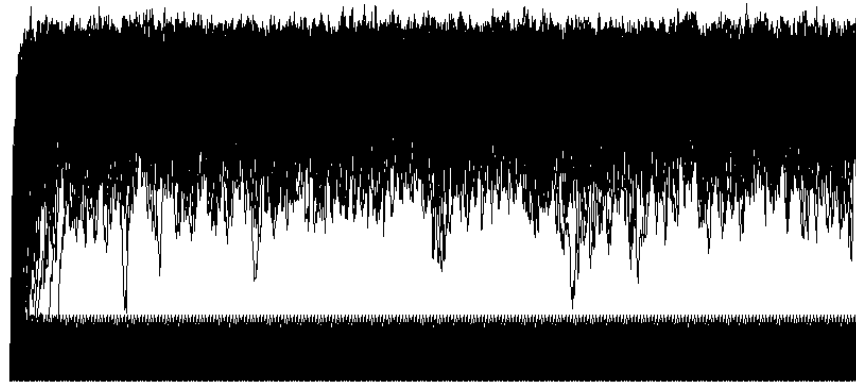
Model a $tmx=200, N=400$. af69tn, af15tn extremely ordered despite parameters $s, K=4,3$. Small number of events reach Derrida level, but they next typically back fall down. Most of events stay on low level. Lack of gap between peaks, however increasing tmx to 2000 has increased L only by 2 for af15Tn (from 360 to 362).



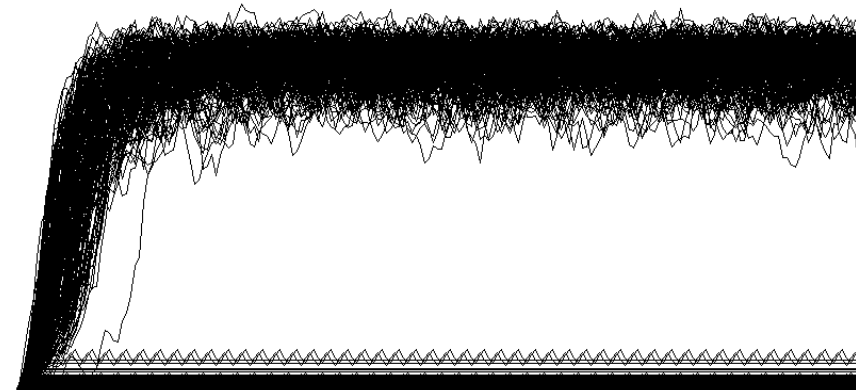
af58tn i af58Tn (this is the same net investigated in both ranges of tmx) – little more chaotic events than above, more 'empty' gap is visible between peaks. However chaotic events often drop down to small values of A1 crossing threshold, but they come back upper, near Derrida level. Still most events stay low. In af58Tn repetitions are visible up till $tmx=2000$.



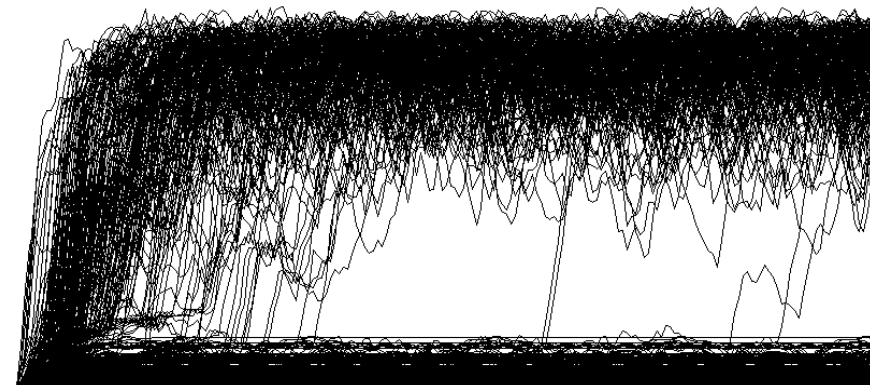
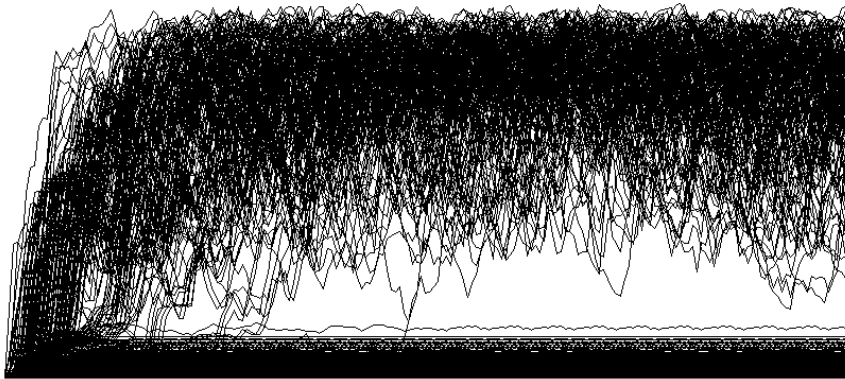
ar13tn & Tn – late explosion to Derrida equilibrium. It can be observed in model a for net r but for f all range is overwritten. Here $L=292$ for both $tmx=200$ and $tmx=2000$, then there is no explosion further.



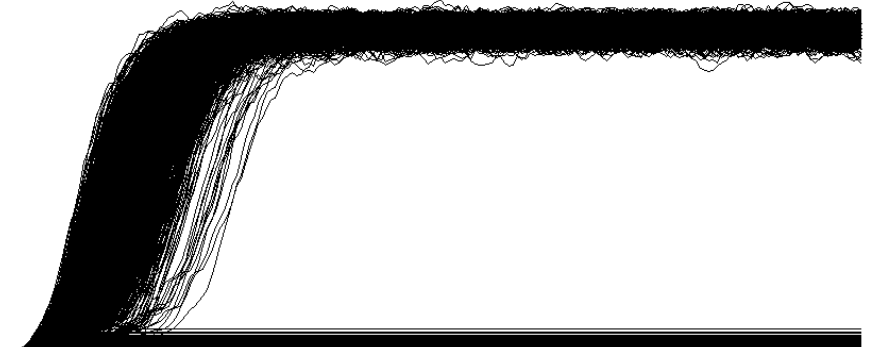
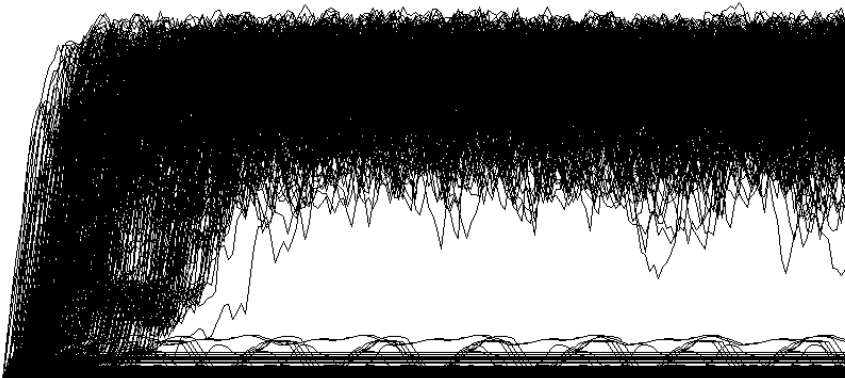
af107tn – high oscillations over threshold=100 of ordered events. Generally, but here especially, short oscillations of ordered events are clearly visible. For chaotic events there is lack of visible oscillations.



ar19tn – normal picture with well separated narrow peaks can happened in model a. For net f it happened rarely, but for r typically. Here $L=194$ for both tmx .

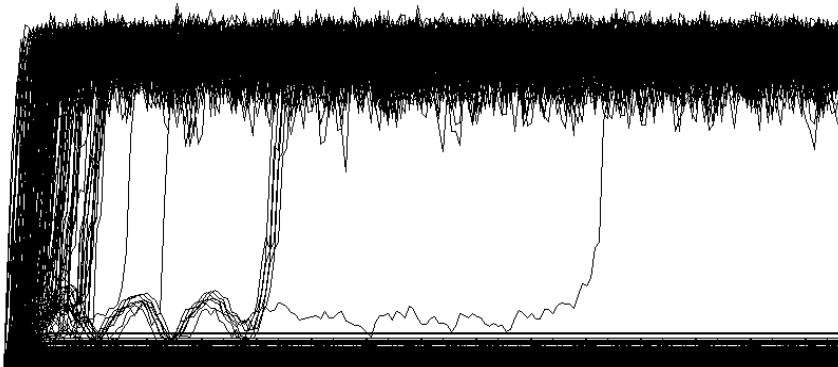


Model a $tmx=200, N=4000$ only 12 nets, all with clear separation of peaks even for f. Extreme events: **af12tN** low range of chaotic; **af7tN** late explosions.



af3tN typical, oscillations of ordered are visible.

For net r pictures are similar. **ar3tN** is typical.

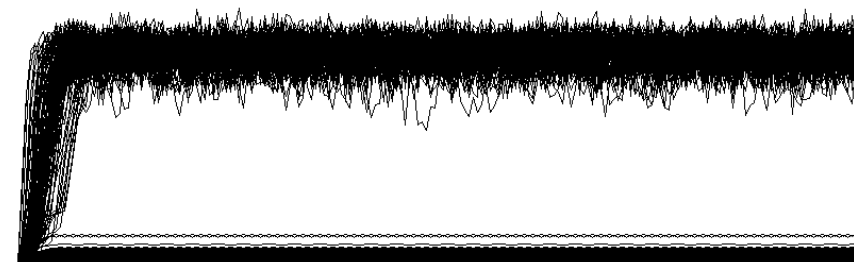
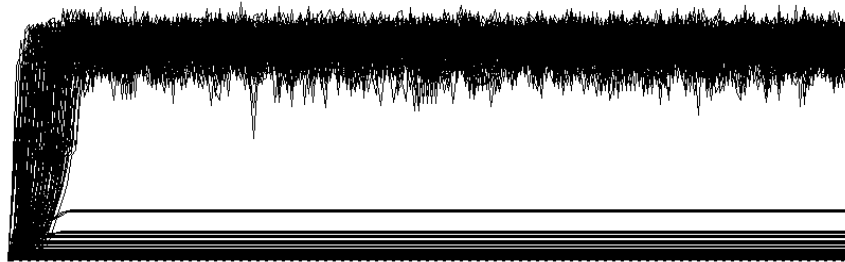


Model b $N=400$. Here both examples in fig.3 are typical. Extreme event with late explosion **bf23tn**, but in **bf23Tn** is lack them further.

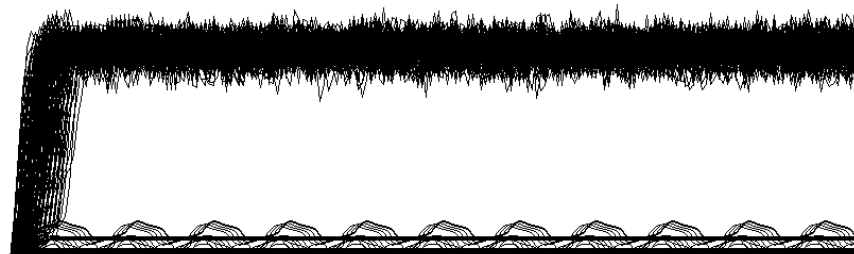
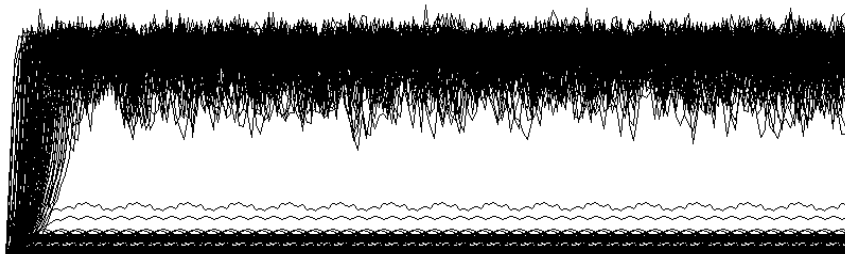


b N4000 bf6tn with oscillation of ordered. Generally both peaks (back belts) are narrow, gap between is clean. Lower belt (left peak in P(A1)) typically is straight and thicker for net f than for r . Horizontal lines happened there, like here in **br5tn**, probably PAS.

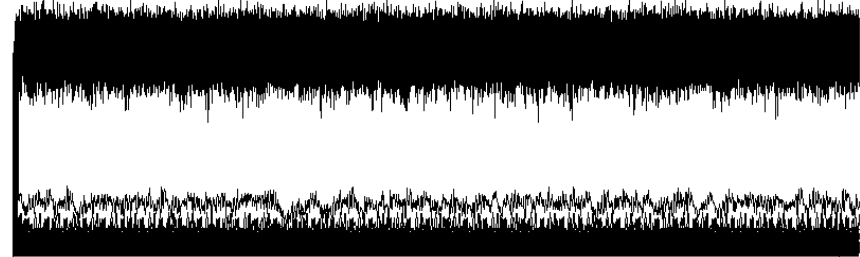
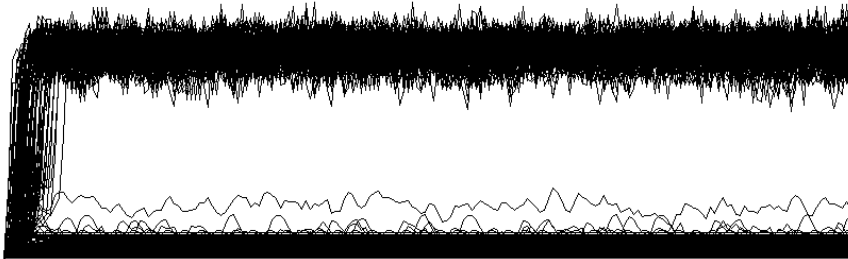
Model c – crocodiles look similarly to above shown for model b and they are not presented here. Both belts are slightly narrower than in model b.



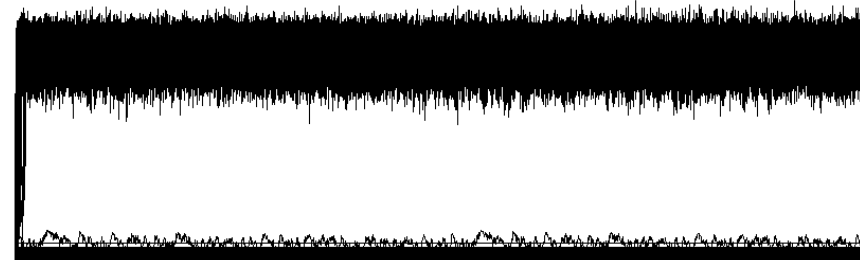
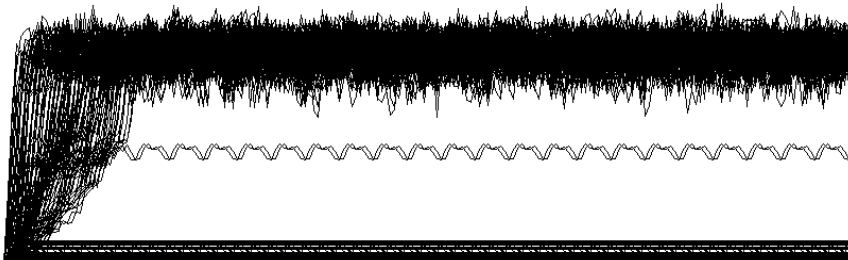
Model d, $s,K=2,4$ differs to models a,b,c where $s,K=4,3$, then Derrida level is here lower. Consecutive 6 examples $df\#tn$, here **df3tn** and **df4tn**.



df109tn & **df117tn** exhibit short loops of attractors, this is typical but not always.



Just in this example **df16tn** and in longer period **df16Tn**, the processes clearly visible over lower belts do not exhibit repetitions (loops), despite it they do not explode.



In **df72tn** we have probably 2 similar processes a little over threshold=100. I think that damage loops here in the same loop with small shift. Generally $tmx=2000$ add small; because explosion stops in the beginning. However, it happened as in **df91Tn**, that A1 reach only 30, but attractor length is near 1000. Net r in model d does not offer interesting examples.



for $N=4000$ in model d lower belt becomes extremely narrow, upper also becomes narrower, however, in these typical **df1tN** i **dr12tN** lower belts contain $L=2610$ and 699 of 4000 . Above is **fig.4** - review of crocodiles from simulation of models a, b, c & d.

4.5 More important problems of simulations, A1-4 and threshold

Already in met1,2 where tmx initially was especially short (60), and chaotic explosions occur up till end of investigated bracket, appear problem of explosions near tmx . For such the explosions, A (– number of node states which differ to states in pattern trajectory) is already large, because explosion is going, but it does not reach threshold yet. To avoid of including such the large values into set of accepted events, A was firstly taken earlier than tmx and it was rejected, if later threshold was reached. For the basic and such the new type of A name $A1$ was taken. Differences in distributions occur not important, but problem leads to take precautions.

In met4 similar problems occurs only in model a, but not with late explosions, only with great fluctuation of $A(t)$ and crossing of threshold by chaotic processes (see model af $N=400$ in [fig.4](#)). Solution of this problem needs averaging of $A1(t)$ in proper period and leads to define $A3$. For stable $A1$ processes a beginning of process has influent on $A3$, typically decreasing value, which was important for short tmx . In other hand, a late explosion after half of tmx period, allowed $A3$ to hold under threshold. Concluding, $A3$ was calculated on a last period before tmx , which much corrected the base of decision of acceptance.

$A2$ had its source in reversed-annealed algorithm, where left peak had interpretation of sum of $A1$ to fade out. In met4 the fade out turn out to be a small part of ordered events (see [tab.2](#)), and for remaining events $A2$ has no sensible interpretation. In met4, i.e. PAS, fade out to $A1=0$ immediately initiate next avalanche of identical way, then $A3$ properly take previous interpretation of $A2$ for fading out, and simultaneously it has correct sense for all types of processes after initiation. However, it occurs, that for global statistical results difference between $A1$ and $A3$ is not significant, but $A1$ has significantly simpler interpretation and definition, it does not depend on arbitrary defined period of $A3$ taking. Therefore results for $A1$ are frequently described as for A . The differences can be seen in [fig.2 & 2](#) where $A1$ is used and [tab.2](#) where $A3$ is used and [differing values are indicated](#).

In further investigations (met5) also $A4$ is used, which is a number of nodes which was damaged during full process after initiation. It have to show size of loop where damage rotates.

One of the basic parameters of the investigations is arbitrary defined threshold of events selection on accepted and not accepted (ordered and chaotic). The definition is however, not any. The threshold has to separate two difference types of behaviour of damage. If long, empty gap between left (ordered) and right (chaotic) peaks is present in the distribution of damage size, then choice of point in the range of the gap is any. But not always this minimum is empty, which depends on investigated models and their parameters. Also a slope and place of right peak change by the same reasons, which change of circumstances of correct threshold definition. When last, long simulations are preparing, a data for threshold definition should be collected, but in crucial period the probability of events is the smallest, then for collection of necessary statistic long time of simulation is needed. Therefore it happened, that the threshold turns out to be not correct enough after 'last' simulation. So, defined in met1 & 2 universal threshold=60 must be changed in met4 on 100 for $N=400$ and 300 for $N=4000$, but for model af $N=4000$ it turns out that threshold should be raised up to 800, which is visible in [fig.2](#).

Many problems with correct interpretation of results, accurate questions and data acquisitions the dynamical visualisation of simulated process called crocodile help to solve. It come to being during met4 investigations, was later developed which allowed to come back to earlier themes and improved investigations e.g. met2 200 or met3.

4.6 Summary

The results of met4 (**tab.2, fig.1, 2**) indicate sub-area of random chaotic systems available for biological evolution. In the sub-area chaos and order are present simultaneously. These systems are in state of point attractor (PAS). For any random connectivity structure we can construct PAS by function definition for each node for one, initial input state.

For all 4 models (model a with strong regulation, model b with weak, minimal regulation, models c and d without regulation; models a,b,c for $s,K=4,3$, d for 2,4) a searched state of damage size distribution is reached (**fig.1 & 2, tab.2**). The state contains 2 strong peaks: left – very small damage (ordered events) and right – large damage (chaotic events in [Derrida](#) equilibrium). Between peaks is deep minimum, typically empty gap without counts.

Only **model a for net type f turn out to have too effective regulation**, i.e. right peak is small, but exists. Despite ‘chaotic parameters’ of system (if it would be random), the system is practically fully ordered, **which indicate importance of regulation as one of effective methods of stability increasing**.

Left peak (ordered events) practically does not decrease when tmx (length of investigated trajectory) increases. Found effect increases intensity when network increases, means – simulated networks are not too small.

Order degree q (accepted, ordered events) reaches 93% for extreme model af, but in half of models q cross 60% of all initiations **and does not decrease under 14%** (model cr). **A fraction of PAS in ordered events is an important result (tab.2)**. The fraction for $N=400$ is **over 90% for model a, and for remaining models it is between 96.7 and 99.96%**. **Because any PAS is a coming back to state before permanent change, then evolution can roll without coming out of PAS, only jumping between different them. It is sufficient prove for existence of sub-area available for evolution in range of parameters s,K of system, which place the random system in chaotic area.** However, limitation for living objects description to only PASs is an interpretive extreme and question arises if we allow for remaining ordered events to be collected during an evolution, then will evolution also have no limitation and will not need to reach chaos? This is the question for met5.

The proper for biological evolution area of systems with chaotic parameters s,K for random systems is indicated.

5 Accumulation of ordered changes does not lead to chaos, ro-modularity – met5

5.1 Introduction

5.1.1 Aims

All investigated here systems have chaotic parameters s, K , means, random system with such the parameters are chaotic. This chapter describe investigations called met5. They are a continuation of met4, which started from PAS – point attractor system. PAS0 was used, its all initial node states are 0 and all node functions for input state 0 gives value 0. Such the system after small initiations exhibits simultaneously order and chaos in similar degree. A fraction of PAS in ordered events is over 90% for model a, and for remaining models b,c,d it is between 96.7 and 99.96%, then evolution can roll without coming out of PAS. However, what happen, if we allow for remaining ordered events to be collected during an evolution? Will evolution be similarly stable? Answer for these questions is the main aim of met5. Acceptation of PAS during change cumulating is a come back to the beginning, therefore only changes which give longer attractors than 4 or their attractors are not found are cumulated.

The second aim is to reach of boundary of stable and chaotic regions using selected parameters of such evolution, it means - to reach the chaos in order to define range of safety parameters for the evolution and character of limitations. How the boundary of this “liquid” region looks like? Is it a form of phase transition – the rapid change of behaviour? In such a case the liquid region is a phase. Or a gradual, then description in term ‘phase’ is inadequate.

The third aim is to check thesis called “ro-modularity”, that specificity of this area consist in many short and almost independent loops. Such awaiting has many interpretive premises. The Kauffman description of liquid region as independent lakes in the eis is one of them. However, now it cannot be only the modularity based on intensity of links. Deeper interpretation is limited by model, where structure, links and functions are separated too strongly, process algebra will be more adequate [\[GdM\]](#).

In met5 only models b and c from met4 are investigated. They have $s, K=4,3$, $N=400$. Only net types f -scale free [Barabasi-Albert](#) and r -,,Random” [Erdos-Renyi](#) are used.

5.1.2 Interpretive view

We do not know how modelled system works, but we assume, that it works stably. PAS0 is a initial state of model. If system is based on small loops, then in the PAS0 they are “inside” nodes. Now we observe evolution which change the system. This evolution is assembled from small changes. If such criterion turn out to be enough to keep system stable and system become not the PAS, then we can investigate properties which allow system to be stable. Now they are outside nodes, but probably for another such elements they will look like previously node – a stably working elements. Such elements consist of few nodes, we will call them ‘clusters’ and we will search for them. How dense can be such a network of clusters? Is such the evolution limited and ends in chaos?

Existence of chaotic part of reaction on small disturbance is similar to cross of boundary of homeostasis and collapse of system. Such the possibility adds to model a death of selected objects - very important for mechanism of selection. It really is well described by chaotic explosion to Derrida level.

As in met1 - 4 I try to show, that there are more possibilities which Darwinian evolution can use for stability, than only proper parameters s, K finding. I think, that selection of structure (like in met3), of functions and state like in met4 and met5 are much easier than selection of parameters s, K , especially K which is used in current form of hypothesis ‘life on the edge of chaos’. Therefore evolution uses such the possibilities more often than tuning of K and stability found in living objects is not based on K .

5.2 Accumulated changes, passes $N1, N2, M$, formulas bf, br, cf, cr , $s, K=4,3$

Simulations in met5 are limited only to models b and c defined in met4, that $s, K=4,3$. Only net types f and r (i.e. formulas bf, br, cf & cr are investigated). Always $N=400$ nodes. The basic $tmx=1000$. Initiation (ini) is a permanent point change in function value for (point=) initial input state. This value is changed by adding ‘initdam’ which for $s=4$ can be 1,2,3, and cutting the result mod s . Such the mechanism gives all possible ini, it was used in all met1-4.

The first pass of ini and (changes) accumulation starts from PAS0 state, then all initial node states are 0. The point changes are made typically for input (0,0,0), this significantly decreases the basic exceptionality common for models c and b that $f(0,0,0)=0$ together with huge advantage of state 0 in trajectory. Average shares of any of 4 function values are equalized. In the first pass (N1) there was no possibility to omit this destruction of exceptionality, but in passes N2, after great shift of initial point on trajectory, for initiation only other input states than (0,0,0) were taken. Exceptionality of model b contain over above also $f(0,0,1)=f(0,1,0)=f(1,0,0)=0$ which models minimal regulation. In N1 for (0,0,0) change on function value from 0 to 1 (initdam=1) makes nothing, because receiver typically has in remaining inputs still 0 and disturbance fades out. Such changes are unused in model b (for N1 only).

For accumulation, after acceptance of change for particular node, there is no sense to try remaining initdam's, they are omitted (not in free passes in series 44). Similarly, if in several next passes this node has the same input state, then initiations are omitted. It is 'blockade of smearing and reversing' of accumulated changes. Two initial passes of accumulation are specific. Their results are shown together in crocodiles N. In series 45 of met5 a number of **accumulated** (i.e. accumulated changes) in these 2 passes were too small and repeating of pass was introduced. N1 was accepted if at least 30 changes were accumulated, N2 was repeated 3 times and new net was drawn if number of accumulated was less than 100. Before N2 shift of initial state by 498 time steps of trajectory was made. (In [Naaj](#) passes N are called J.) Next 20 passes M (numbered 1 to 20) are made, each depicted in its own crocodile.

The 'blockade of smearing and reversing' quickly exhaust possible **changes which may be accumulated (accumable)** and number of accumulated decreases. Statistics in such the circumstances do not describe parameter q adequately. It is needed to allow any ini in some passes M for 2 reason: to measure q, and to unblock accumable. It can be taken, that after lot of accumulations a new change of function for input state, for which change was accumulated, works in enough different circumstances to say, that it is a new, even it is coming back to function before this old accumulation. Therefore passes M 1,7,13,19 and 20 are defined as **free** - without limitations of blockade of smearing. After M1,7,13 information about input states for which accumulation was done, are collected for each node and blockade of smearing is used. Also **abbreviation 'akc'** for words **acceptation or accepted**, and **'cum', 'cumul' or 'cumulated'** for **accumulation or accumulated** will be further used, especially in figures, to distinguish them in short.

5.3 Problem of shift and of fade out type, series 34

5.3.1 Results of investigations

An evolutionary change happened in nature in stable circumstances which we can model as (short) attractor, but directly after the change a system is typically on a way before entering its attractor. In order to next changes be tested in attractor we should shift initial point of pattern trajectory. However, it turns out ([fig.1](#)), that even small such shift significantly changes a system behaviour after ini. The final series of these investigation has symbol 34 (problem 3, version 4). Accumulations are here done only in passes N. Consecutive passes M differ only in shift increased by 2 up to 38 (without accumulations and any limitations). For each formula (of bf,br,cf,cr) 50 nets are simulated which give 60000 ini / formula.

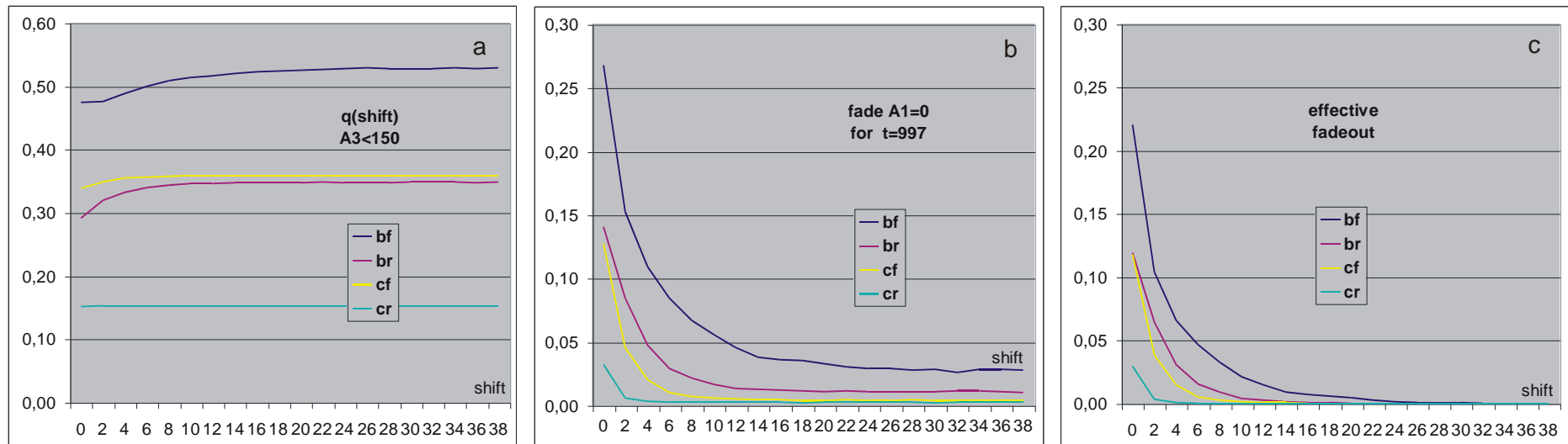


fig.1. Influence of shift of initial point after change accumulation for formulas bf,br,cf,cr (model,net type).
 (a) - q(shift) – probability of acceptance (A3<150) when shift - P(akc|shift).
 (b,c) – Probability of fade out of damage after initiation. (b) – in any way, also with lot of secondary ini, but A1=0 in t=997.
 (c) – effective fade out after first ini, i.e. without secondary ini. This possibility disappear totally.

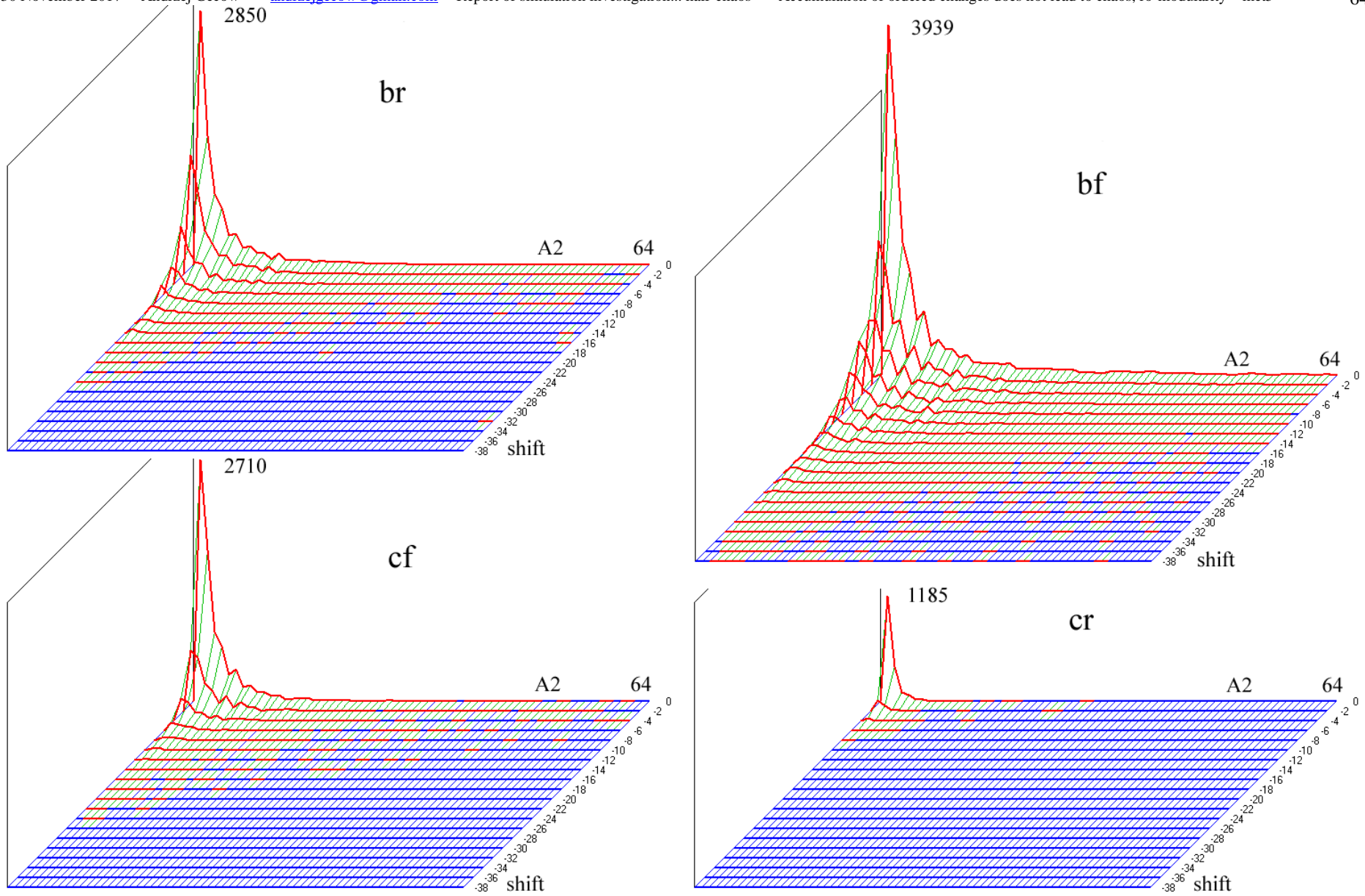


Fig.2. Influence of shift on P(A2), in the range A2<65. So small A2 appear only for effective fade out. Radical change of phenomena character with shift quantity is visible. Near peaks in A2=1 shift=0 number of counts is shown.

This investigation shows that great fraction of effective (full) fade out (reach and stay on $A1=0$) observed in the beginning quickly decreases with shift (fig.1.bc). As is shown in fig.1a shift influences q – the most important parameter, degree of order, however it is not great influence. Effective fade out allows small $A2$ (sum of $A1$ on tmx). Distribution of $A2$ in the range of small $A2$ for different shifts (fig.2) is a well depiction of phenomena, giving more information than (fig.1c). For comparison, in (fig.1b) together are mixed events with secondary initiations and fadeout which in $t=997$ ($tmx=1000$) have $A1=0$. In crocodiles (fig.8) level of $A1=0$ for each t is shown by blue curve. At the beginning, without shift, the fade out is near half of accepted changes. Next, the effective fade out falls down to 0, simultaneously degree of order q become stable (fig.1a). Lack of shift or small shift allow for full reverse of effects of earlier changes, but time flow eliminates such possibility. It is surprising, that q increases even so simple mechanism of full reversing of ini results is blocked by shift. Basing on these results in series 44 for passes M shift is taken 50 after each accumulation.

5.3.2 Explanatory example

Understanding of shift phenomenon is especially important for interpretation of met5 results. Extremely simple example will help for it, however, it is no so simple to trace. Let us use economical positional notation: one letter or digit is on the position, if we need more, then we take them in []. **nlt** = ('nod')('link' = **i-input** | **o-output**)('time'); input and output signals are indicated by digit from the range 0-3 or by letter; input state for $K=3$ needs 3 letters or digits;

not is a result of function of node **n** for argument **ni[t-1]**, we can write **not=n[ni[t-1]]t=n[xyz]t**.

Initially anywhere (in **n** and **t** dimensions) is state 0 from definition of PAS0 (**nit=000**; **not=0** for any **n** and **t**).

Node **6** gives its result on input of node **9**: **9it=xy[6ot]**. For the time being **x=y=0**.

Initiation of node **6** (permanent change) for **6i0=000** is **6[000]t=3**, before was **=0**. It is visible starting from **t=1**, in **6o1=3**.

Let this damage fades out on a way to **6it**, that always **6it=000** and **6o[t>0]=3** (are constant for any **t>0**).

After this ini **9i1=003**. If **x** and **y** in **9it=xy[6ot]** do not change, then always **9i[t>0]=003** (is constant for any **t>0**, not for **t=0**), but before was **=000** also constant for any **t**.

Also **9[003]?=9o[t>1]=c** is constant, but **9i0=000** then **9[000]0=9[000]1=9o1=0**.

Now ini of node **9**: **9[000]?=1** (was **=0**), then **9o1=1**, but **9it=000** is only for **t=0** (see above) and damage effectively fade out in one step, there is no secondary ini.

If, however, after ini of node 6 and accumulation would be a shift, even by 1, then ini of node 9 will use 9i0=003 but not 000.

In such the case if damage would fade out, then immediately secondary ini occurs, because **9it=003** is for any **t>1**.

Remark, that most of changes in trajectory is a change of constant state 0 into another constant value. This gives state similar to PAS. The minority of changes is a departure from PAS, but its size is limited by condition of small effective change. For this reason PAS'es are so frequent, which is visible in fig.7b, 9f2,h1.

5.3.3 Ice and independence of loops

To check of thesis called 'ro-modularity' is a third aim of met5. This view is based on many short, almost independent loops. Analysis of this vague conception shows that two loops with different periods, e.g. small prime numbers, cannot to have common nodes, because conditions of function of these nodes are too hard, it means, that probability of meeting of such the case can be neglected. Then such independent loops must be separated by an 'ice' – this term Kauffman has used, i.e. by nodes with constant output state. Above described example, and view effected from it, give hope on such the small loops separated by ice. This view is practically identical to description of ordered area for RBN: small lakes of activity in the ice, however, RBN is a random system, but our systems have parameters, which make random systems chaotic. Investigated here systems are not random, they start from specific state PAS. In met5 the theme of many small loops is investigated in several ways.

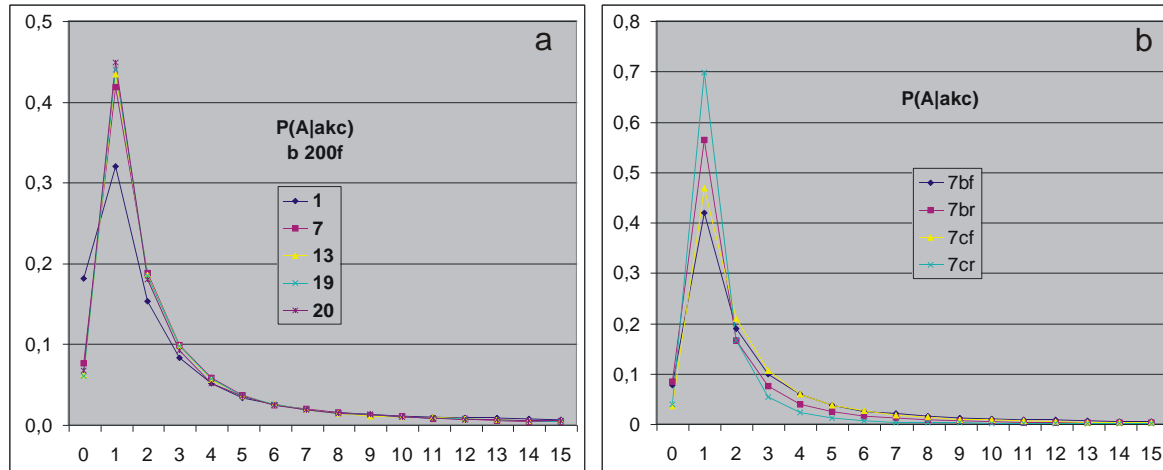
5.4 Advanced series 44 – passes M free & with blockade of smearing, shift=50, steps of attractor length

Investigated phenomena have many aspects, which should be considered when we tend to deeper and more adequate interpretation. This way, however, complexity of description increases and results become to be hard to pass on in sensible short report. Series 44, recognized as the main, rather cross this threshold of complexity. Symbols of series result from history of investigation and are placed in such simulation results as e.g. crocodiles. Symbol 44 is completed by ('4+7+20') or ('4+7') where values 4,7 & 20 are thresholds of attractor length for accumulation from $N1$, $M1$ & $M7$ respectively. Attractor should be not shorter than the threshold, for $M20$ it should not decrease. 'Free' passes: $M1,7,13,19,20$, in the remain passes the blockade of smearing was used.

As in series 34, in passes N there in no shift after accumulation, but before $N2$ there is shift by $t=498$. In passes M shift=50 after any accumulation. Presented results are typically from simulation of 200 nets ('4+7+20') completed initially (fig.5) by series 5 of 100 nets ('4+7'), but near end of investigations significantly improved simulation of 100 nets effectively reaching $M20$ called ro 44 '4+7' 100M20 was done. It was more precise than first of 200 nets on the start.

First two aims of met5 (1- starting from PAS evolution can be long and must not reach chaos; 2- to reach of chaos during evolution for study of character of the boundary) seem to be contrary. However, if we try to reach chaos by selecting changes for it, and we cannot reach it, then we get a partial answer for the second question, and stronger for the first. The main way to chaos should be increasing of attractor length, therefore above mentioned threshold of attractor length and rule of M20 where attractor cannot decrease are introduced. Attractor length is defined by searching of net state from tmx back to the beginning. These findings were indicated over crocodile **fig.7a1,b1; 9b**. More precise searching is shown in **fig.7e**. When in free passes M1 or M7 with increasing step of attractor length no any accumulation was found, or after N2 number of accumulated <101, then evolution of this net was stopped.

Shapes of left peaks (in damage size distributions) for passes free are practically identical, but not for M1 which is yet like N ‘not matured’, (in **fig.3** they are shown in the form $P(A|akc)$). It is similar for all 4 investigated formulas (bf,br,cf,cr) and both series ‘4+7+20’ and ‘4+7’. Differences between formulas are shown in **fig.3b**. Probability of acceptance $P(akc)$ slightly increases during accumulation also except M1 (**fig.4a**). This does not show that accumulation bring near to chaos, for this we should expect decreasing of $P(akc)$. In series ‘4+7’ this increasing of $P(akc)$ is visible in **fig.4a** only in M20, this let us to connect it to forcing of attractor length in M7, i.e. eliminating nets with shorter attractors. This effect is reverse than expected.



It should be distinguished, that acceptance (akc) is only a condition, that $A3 < \text{threshold} = 150$, but accumulation needs more conditions – that $\text{attractor length} \geq \text{threshold}$ for particular pass (which contain that it is not PAS). Moreover, measure of $P(akc)$ for passes not free (**fig.4b**) is deformed by blockade of smearing.

Fig.3. The shape of left peak $P(A|akc)$ for passes free, series 44 ‘4+7+20’ (each 200 nets).

(a)- for formula bf but remaining are similar.

(b)- comparison of formulas in M7 .

In series 44 ‘4+7’ the results are identical.

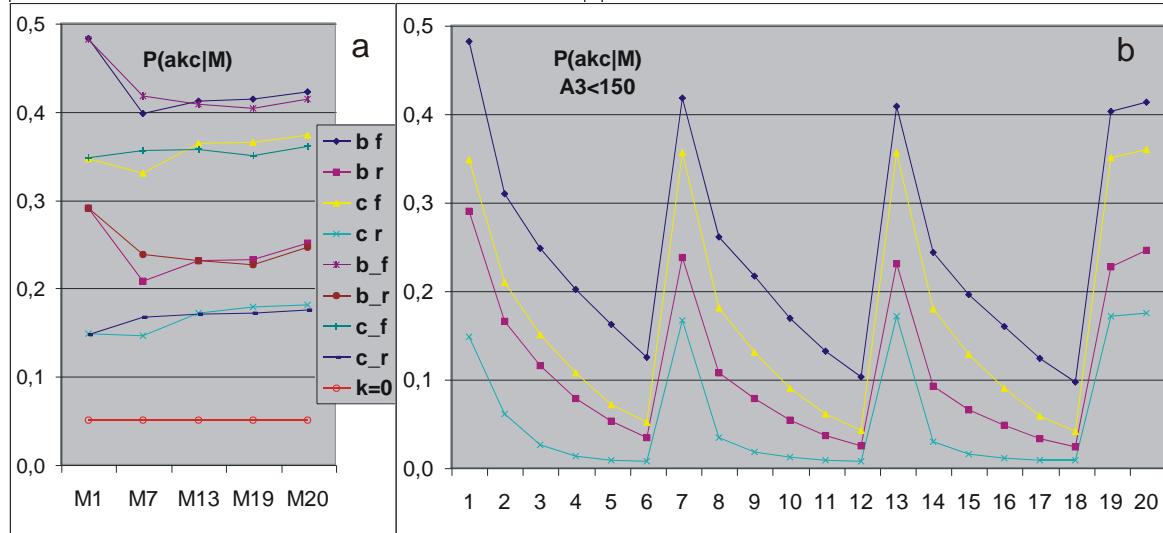


Fig.4. $P(akc|M) = q(M)$.

(a) - for passes free in series ‘4+7+20’ and later ‘4+7’ 100M20 (4 lower with ‘_’), influence of $k=0$ for net type r.

In series ‘4+7+20’ q does not decrease, but even little increases when number of accumulated increases, then chaos becomes not nearer. In ‘4+7’, where there is no elimination on $\text{attractor length} \geq 20$ in M7, there is lack of this increasing. M1 is similarly not matured as earlier passes N.

Number of events for pass free = (number of nets)*3*400 in series ‘4+7+20’, but number of nets decreases after N2, M1 and M7 (in effect of lack accumulated), i.e. nets with lower $P(akc)$ are eliminated from 200 to 198,196,200,200 after N2 respectively for formulas bf,br,cf,cr, (in model c N2 searches up to effect); to 180,145,118,45 after M1; to 110,50,47,4 after M7.

In series ‘4+7’ it counts up to 100 passes M20, but M1 is respectively: 111,132,165,434.

(b) – for all passes M series ‘4+7+20’. Here in addition a number of ini decreases from 1200 even to 0 (M12 for cr) in effect of blockade of smearing.

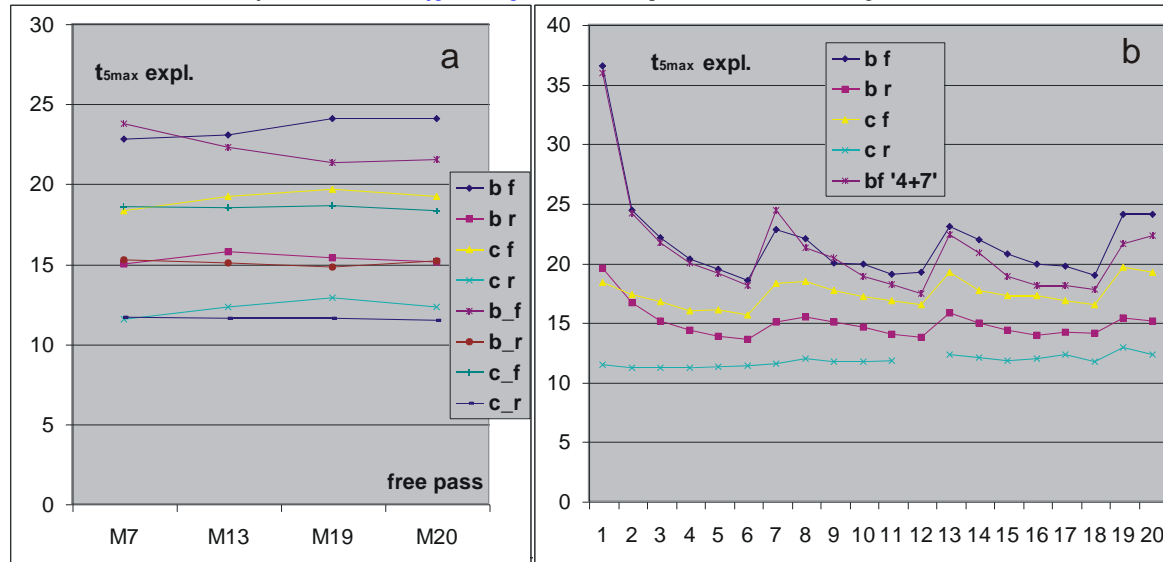


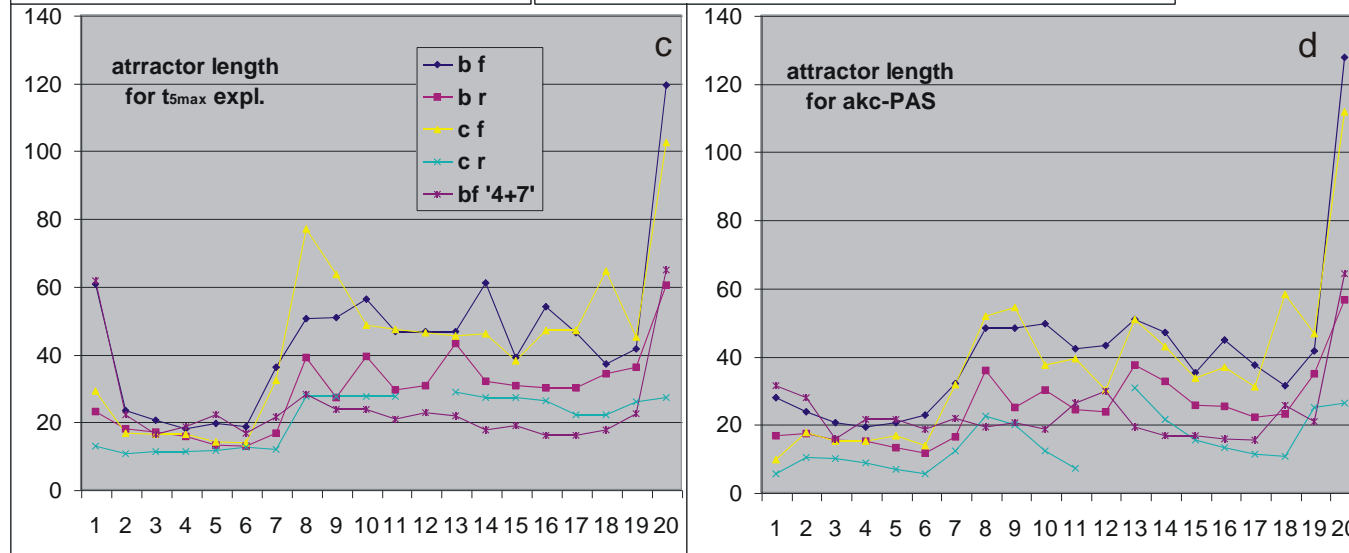
Fig.5. Average time of 5 latest explosion (a,b) and average ‘attractor length’: (c) – of pattern for 5 latest explosion, (d) - for accepted (akc) ($A3 < 150$) but not PAS, as measure of distance to chaos. 200 nets for each formulas ‘4+7+20’ (attractor ≥ 4 from N1, ≥ 7 from M1, ≥ 20 from M7) and 100 nets for bf ‘4+7’ in (b,c,d), but in (a) 4 lower (with ‘_’) from series ‘4+7’ up to 100 M20.

Degree of bring nearer to chaos boundary or entry into area close to chaos are well characterised (see [m2fig.14](#)) for particular pass by average time of 5 latest explosions ([fig.5a,b](#)). In [fig.5a](#) we do not see tendency to increase this measure, in [5b](#) in areas of blockade of smearing an explosions end earlier.

The time of latest explosion should be connected to average length of pattern attractor with way to attractor entrance. In [fig.5c](#) is used second appearance of net state frpm tmx. For way to attractor see [fig.7e](#). Remark, that at M7

condition on attractor length change: from 7 to 20. Nets which cannot fulfil this step are rejected from higher passes, but they have shorter attractors – this is a reason of increasing after M7 in [fig.5c](#) and [5d](#). Series bf ‘4+7’ has no this step (attr ≥ 20) in M7 and keeps level in [fig.5c](#) and [5d](#). In the last pass M20 the attractor length cannot decrease, then average length increase. Data for [fig.5a,b,c](#) are from pattern attractor of 5 latest explosion, but results in [fig.5d](#), for comparison to [5c](#), concern accepted ($A3 < 150$) without PAS. Not all accepted are accumulated. Despite different rule these distributions are similar.

Series bf ‘4+7’ in [fig.5b](#) has slightly decreased time of 5 latest explosion (see also [fig.5a](#)). It also shows measure exactness. The time of latest explosion turn



out to be not sensitive to substantial fluctuation of attractor length (900 replace all greater and not found). These fluctuation strongly affect the averages, especially for later passes than M7 due to small number of events (see description of [fig.4](#)). This problem is omitted in series upto 100 M20 ([fig.5a](#)). A time to entry into attractor was not investigated which is an effect of provisional evaluation of shift effectiveness, but stability got in series 34 ([fig.1](#)) generally is not an effect of bring closer to attractor which become clear later. It is explained in [ch.5.3.2](#). The way to attractor was evaluated after experiment 44 using crocodiles. For net r there is no events with this way > 100 , nor with attractors not found. For net f in model b & c (2708 & 1510 events respectively) there are only 8 & 1 ways > 100 and 10 & 5 not found attractors. They are so low fractions, that they do not influence shown results, especially in these cases there is no longer period of explosion (late explosion). Later investigations shown in [fig.7e](#)

confirm this conclusion. Decreasing of maximal t of explosion (fig.5b) after pass free is an effect of smaller number of events – in smaller set a records are smaller. For passes free the values are near identical (fig.5a). M1 is not matured enough.

Stability of maximal t of explosion and similarly stability of attractor length are kept by condition of small change ($A3 < 150$). These stabilities show that process does not tend to chaos, where these parameters should significantly grow. Initially they even decrease (M1), which is an effect of other rules of initial passes N (without shift after each accumulation). This lead to conclusion, that **shift** (which should bring nearer attractor) **stabilise, but reaching of chaos needs destabilisation**.

It occurs that near no late explosion is an effect of secondary initiation. Generally, (for bf, $t_{mx}=1000$) circa 0.06 of events of fade out to $A1=0$ in passes N ended on explosion, but in passes M only circa 0.015. This significantly influences view of mechanisms, because initially we expect, that just secondary ini are a cause of necessity to fall into chaos. Such view was the reason for which model PAS0 was build. The mechanisms turn to be much more complex than we have expect.

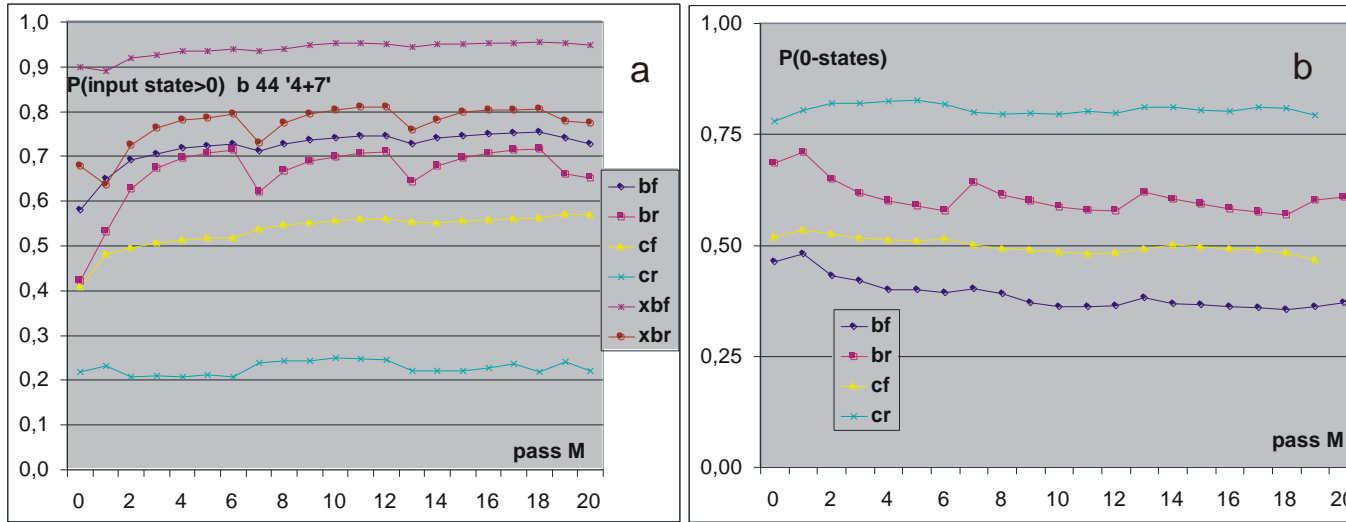


Fig.6. Difference of got system state and initial state PAS0. Data from series '4+7' 100 M20. $M0=N2$. Probability of (a) non zero input states (b) output states = 0, which are an effect of accumulation. Random state for (a) = $63/64$, but even bf is fare of this. In series '4+7+20' results are identical. These results seem not compatible to provisional results of states 0 from '4+7+20'. Such exact results for states 0 are obtained in series 100M20 '4+7'. Curves 'xbf' & 'xbr' in (a) show expected values = $1-P(0)^3$ for input states (K=3 signals) based on output states shown in (b). It turn out that greater reserve of hubs (nodes with great k) is a cause of this

'incompatibility'. The hubs is more in f than in r. Random state for (b) is $= 1/4$, bf is near to such value, despite this bf is not chaotic. Causes of differences, especially cr, are not known. We can state, that levels become stable and excluding cr they show significant shift from PAS0.

Accumulation process has to shift a system state from initial, extreme PAS0. Fraction of PAS in accepted falls down from above 0.9 in met4, initial 0.1 in passes N met5 44, to 0.01 in last passes M. Number of 0 state in net is a better measure of this shift. Initially input states assembled of K=3 signals are investigated. For random system a fraction of non zero states should be $1-(1/4)^3$, i.e. $63/64$, but, as is visible in fig.6a, even bf is fare from it. Also provisional probability of 0 state = 0.36 is incompatible to expectation, then in new series 44 '4+7' 100M20 it was measured more precisely (fig.6b,a). It turns out that hubs, especially in f, are more resistant to change.

Passes free in model b significantly reverse deviation. Degree of bring nearer to random state of bf allows to state that observed strong deviation from chaotic behaviour cannot be an effect of preservation of initial preference of states 0. Similar mechanism should be expected in all formulas. Differences visible in simpler for interpretation fig.6b may be explained basing on average numbers of accumulated on net in M20: 3976, 2300, 3086, 1267 respectively for bf, br, cf, cr; but lack of slope connected with increasing of these number complicate this explanation.

Statistical summaries of series 44 shown in fig.3-6 need wider interpretation, first of all indicating of character of qualitative fluctuation of results. This dispersion effects from great variety of summarised phenomena and their complexity. It is a cause of lack of possibility to sensible determine of errors of statistical results. Crocodiles well show in lot of different aspects a character of investigated phenomena. It is impossible to show here all $200 \times 21 \times 4 = 16800$ crocodiles from series 4+7+20 only. In fig.7 typical and specific examples of crocodiles are shown. Conclusion included in descriptions of crocodiles are not repeated in text.

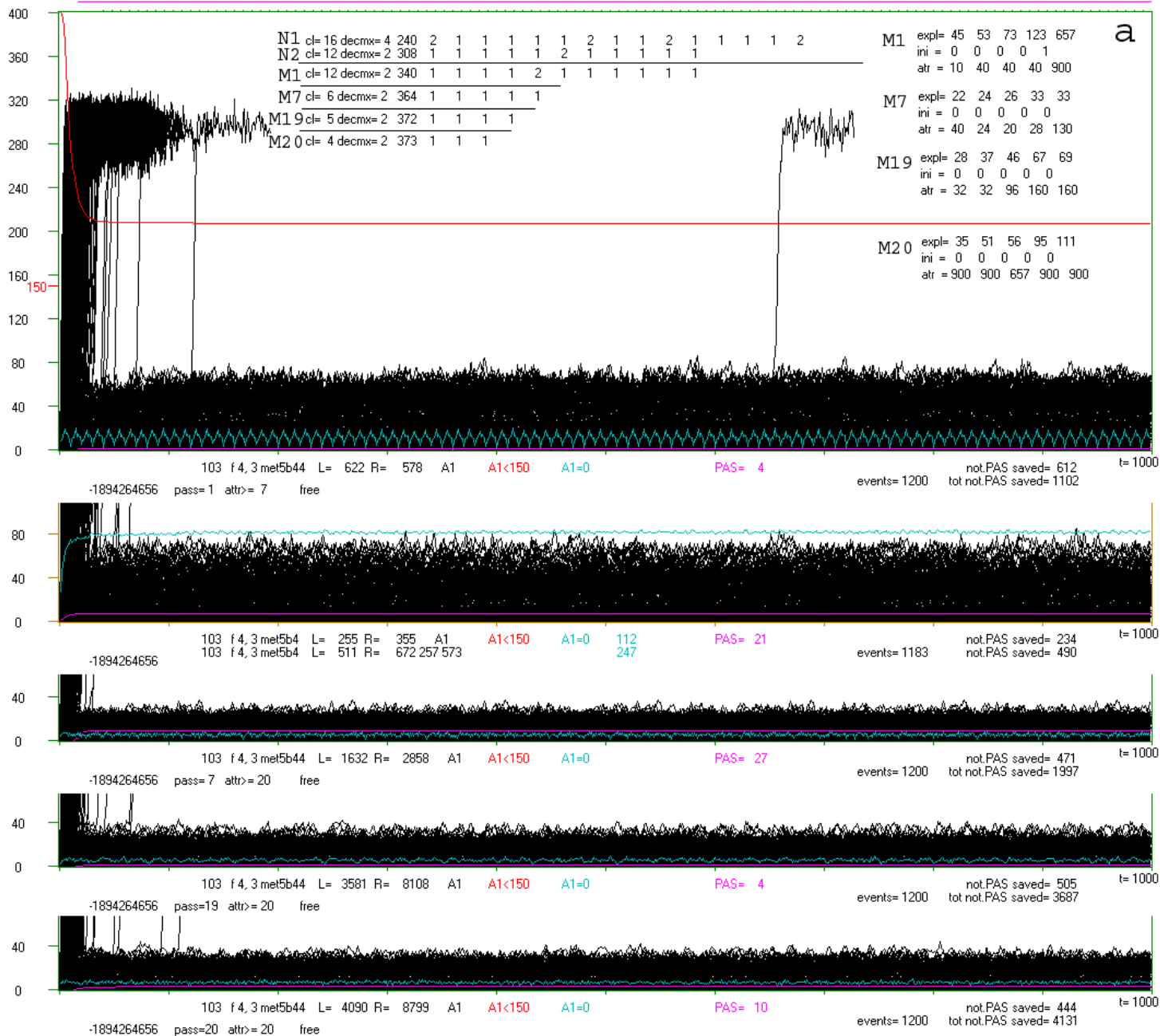
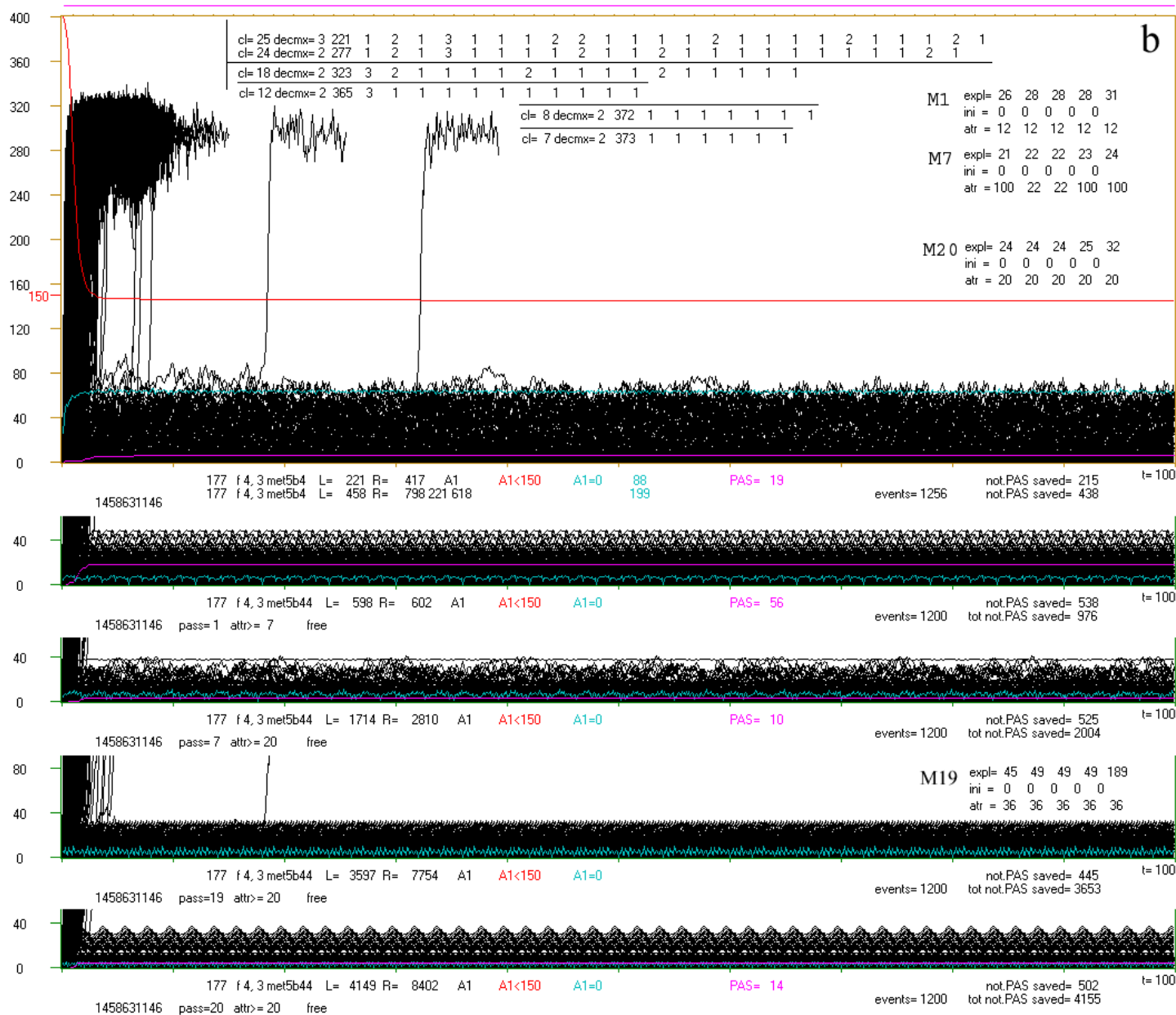


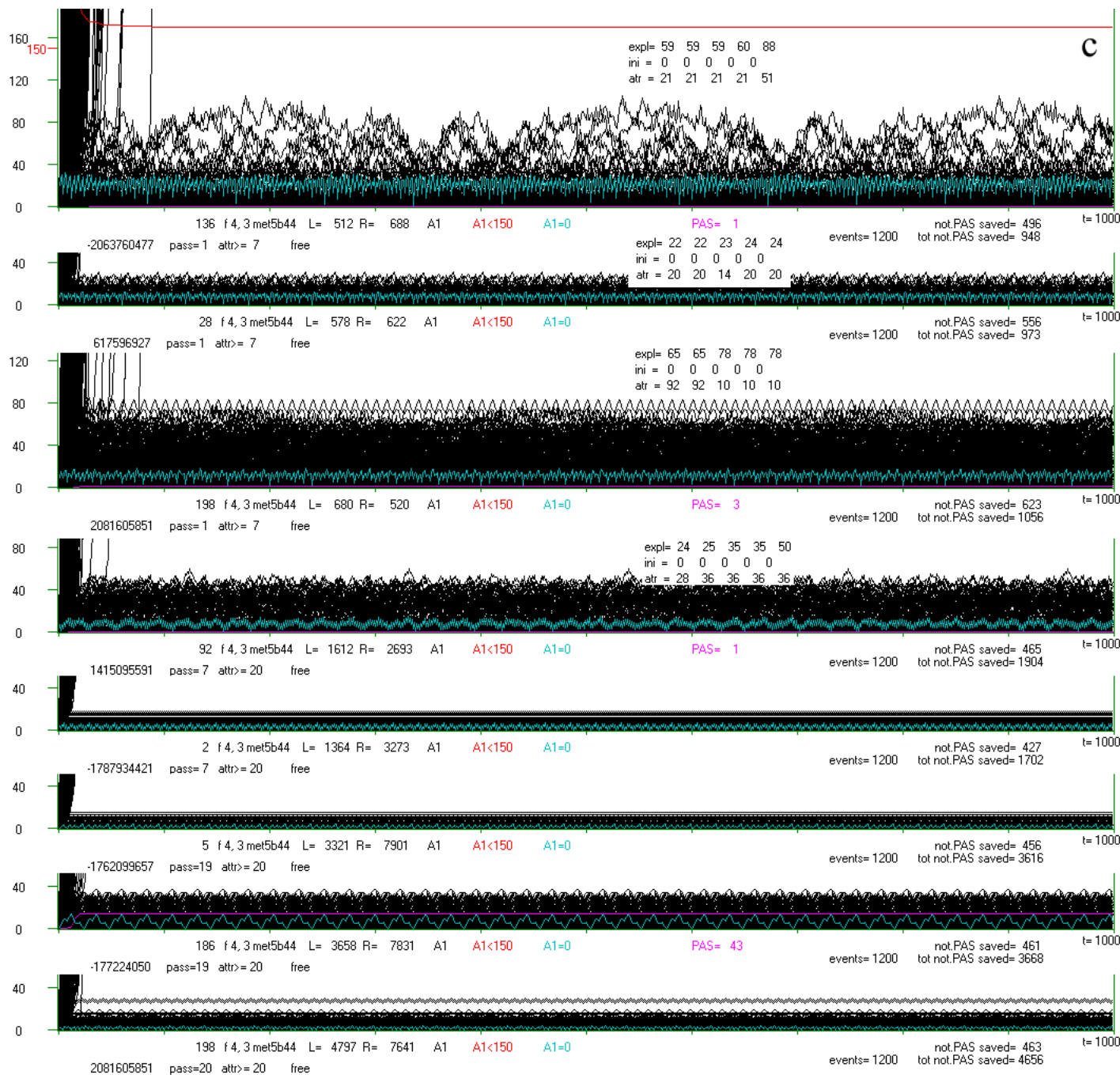
Fig.7. Selection of part of crocodiles and their additional elements from series b 44. Series c 44 is no so interesting. Figures in one page are named by digit but pages - by letter. (a) & (b) are a histories of two the most chaotic nets (103 & 177), but they are fare to chaos yet. (c) diversity of bf, generally selected for late explosion. (d) small dispersion in series br It gives view of more thin crocodiles for cf and cr which are not shown (e) attractors for f 103 (a) & f177 (b) .

(a1) the latest explosion in series 44. It is pass M1. Into box of crocodile date from outside and lower shown passes are copied. They concern of clusters and of 5 latest explosions. On upper frame a pattern attractor (=8 on the right) from beginning of the pass is indicated. **(a2-5):** (2) initial passes N1 & N2, (3) M7, (4) M19, (5) M20 where attractor does not decrease and comes out of identification range giving value 900. Despite this the latest explosion occurs in t=111. More exact depiction of attractors for passes in (a) & (b) in (e).

(b) history of net bf 177, second the latest explosion in series 44. Here this extreme feature stays longer, stronger appears in initial passes N (b1) but explosion occurs also in M19 at t=189. Pass M20 ends with attractor =20, however in pass M7 attractor =100 happened and in here omitted pass M10 even =670 with the latest explosion at t=34.



In description of 5 latest explosion there is line of number of ini before explosion. It may be 0, 1 or 2 (2 means >1). In (a,b,c) only in (a1) explosion occurs after one fade out, here attractor is not found (=900). In fig.(a & b) data about clusters are shown (see a1). cl= number of clusters at the pass end. decmx= maximal number of clusters connected simultaneously. Next numbers of nodes in consecutive clusters. In effect of this rule defining clusters typically one great cluster emerges and few very small. Over upper frame in (a1 i b1) a range of PAS is indicated and the same colour in box its fraction and under box – its number. In shown passes it is between 56 (b2) to 0 Red line described as A1<150 indicates q(t) (when instead 400 value 1 will be taken). Blue line indicate fraction of fade out to A1=0. Level of this phenomenon depend on shift investigated in series 34. For passes N (a2 & b1) it is especially high. The crocodile is 1200 black lines of A1(t) for each ini, but after explosion (coming over 150) only 70 steps are depicted, because in series 44 falling down from Derrida level to ordered level never occurs.



On right from a right frame, in vertical line changed nodes after one ini are indicated by a pixel. Their name (a number) corresponds to vertical axis on the left. It is A4 pixels in such the line. Especially in (a1) can be seen that typically they are the same nodes changed.

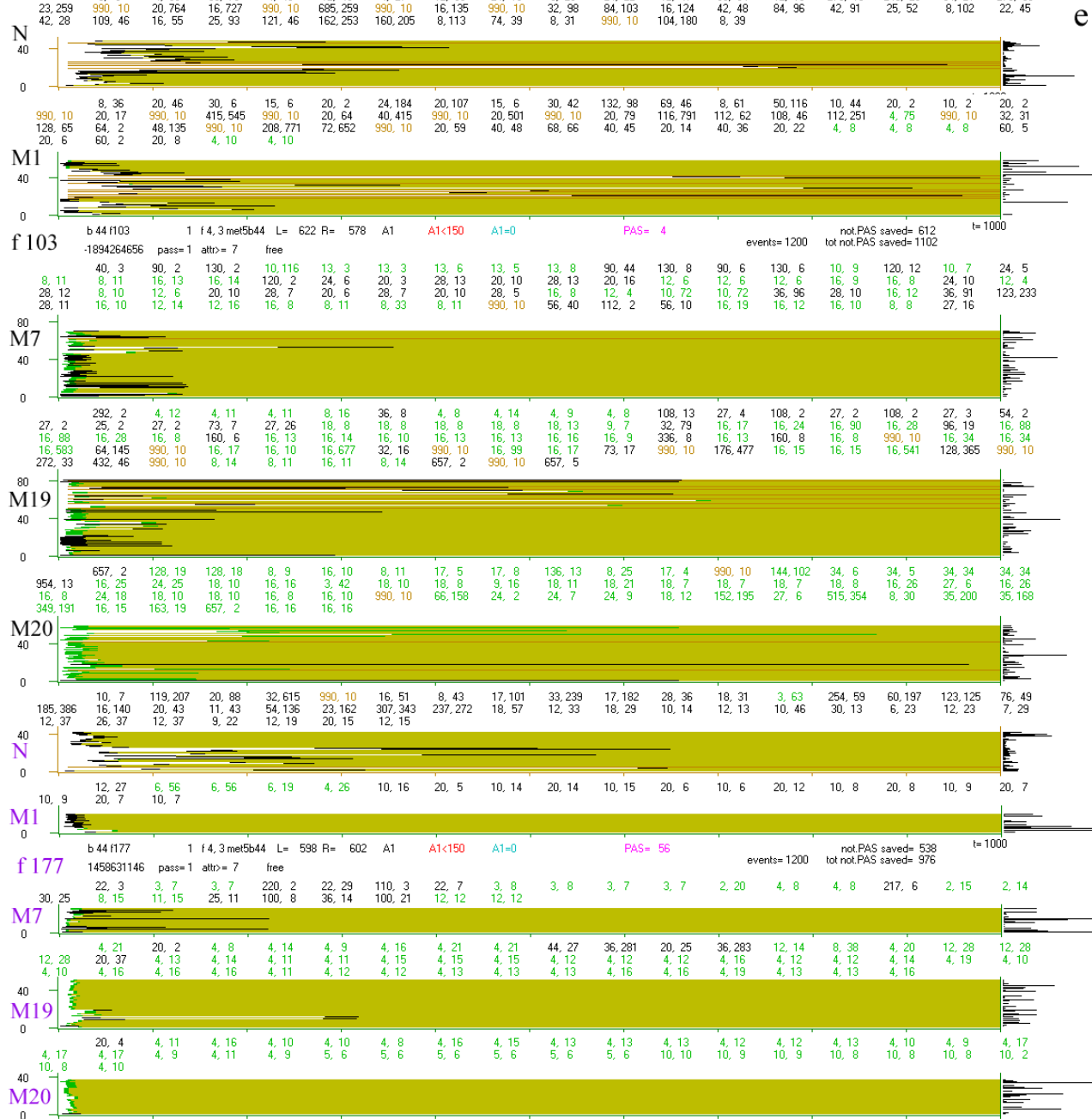
(c) diversity of bf, but (c1-4) are selected for late explosion in series 44. Despite selection of changes and events which should tend process to chaos (late explosion, longer attractors) a character of crocodiles seems very stable. Later explosions happened in early passes and in later passes explosions end in smaller t and lower belt of A1(t) (ordered) is thinner.



(d) typical crocodiles in series br 44. Net type r - 'Random' Erdos –Renyi. (It is 'Random' by name and for connections, but our nets are not random in function and states.) In comparison to net f – scale free net r is much more stable, there is no any symptoms of bring nearer chaos and there in no late explosions.

Width of lower belt (order changes, left peak in damage size distribution) is typically smaller than for net f. Extreme cases (2,6,7) are very thin in comparison to (c1,c3,c4,b1, a1,a2).

The character of crocodiles for series cf 44 if very similar to shown in (d) examples of br. Series cr 44 create crocodiles similar to (d8) or thinner and smoother, without any visible structure.



e

(e) Complementary investigation of attractors on the same examples **f 103** (a) & **f 177** (b). For each pass for consecutive attractors their length and positions of first occurrence are noted. Values **990** are depicted by another colour symbolize lack of attractor finding. **Green** depict accepted but not accumulated due to too short attractor. **Black** – accumulated and attractor found. The same colour is used below. This picture is intended to analyse in enlargement on pixels. Consecutive lines indicate finding of attractor another than in pattern, they are added on the top. Only accumulated (black) change the pattern. The line starts from **white** section of way to attractor, next section of first attractor, next ut to **tmx** attractor is present. Each accumulation without change of attractor length add pixel to right. Both examples of net belong to less stable (late explosions) which here correlates with late entrance into attractor. After each accumulation (if stay the same attractor) the beginning is shifted by 50 to left, which is not visible here, but number of this shifts is depicted on right. Then **white** section before attractor is much shorter. Late entrance happened significantly frequent in initial passes which explain late explosions. A proposals of longer attractors happened more frequently at first few passes, but in later predominate proposals **too short** attractors. Then the process has some stabilising.

5.5 Simplified series 45 to bring nearer to chaos, shift=2, not diminished attractors, $A3 \geq 3$

Series 44 has answered on basic question (1) of met5: Great accumulation of small changes, even selected intentionally to direct to chaos, does not give any visible bringing nearer to chaos, despite shift from initial PAS0 is significant. Then evolution can long processes in this area without threat of necessity of entry to chaos. It is much larger sub-area of chaotic systems, than only PAS indicated by met4. Two aims remain to do: (2) to reach chaos on this way, and (3) to see ro-modules.

The complexity of experiment 44, especially two type of passes (free and with blockade of smearing) makes interpretation hard, however, it is more adequate model. A new attempt to reach boundary of chaos was done also using simplified model, without blockade of smearing, but with stronger selection of changes which should bring closer to chaos. This series has symbol 45. Here attractor cannot diminish in all passes starting from N2 with length =4. New condition: $A3 \geq 3$ should strongly destabilize, but the main difference to series 44 in this aspect is a reduction of shift from 50 to 2.

The new conditions for accumulation significantly decrease chance for accumulation of given accepted change. This make problems to collect sensible number of accumulated in initial passes N. The main experiment should start when state of net is significantly shifted form initial PAS0 and we can expect, that it is stable. Therefore a condition for N1 was added, that it should accumulate at least 30 changes, and N2 was repeated (with shift by 498 at its start) 3 times to accumulate totally at least 100 changes. If particular net does not fulfill these conditions, then it was rejected and new net was drawn.

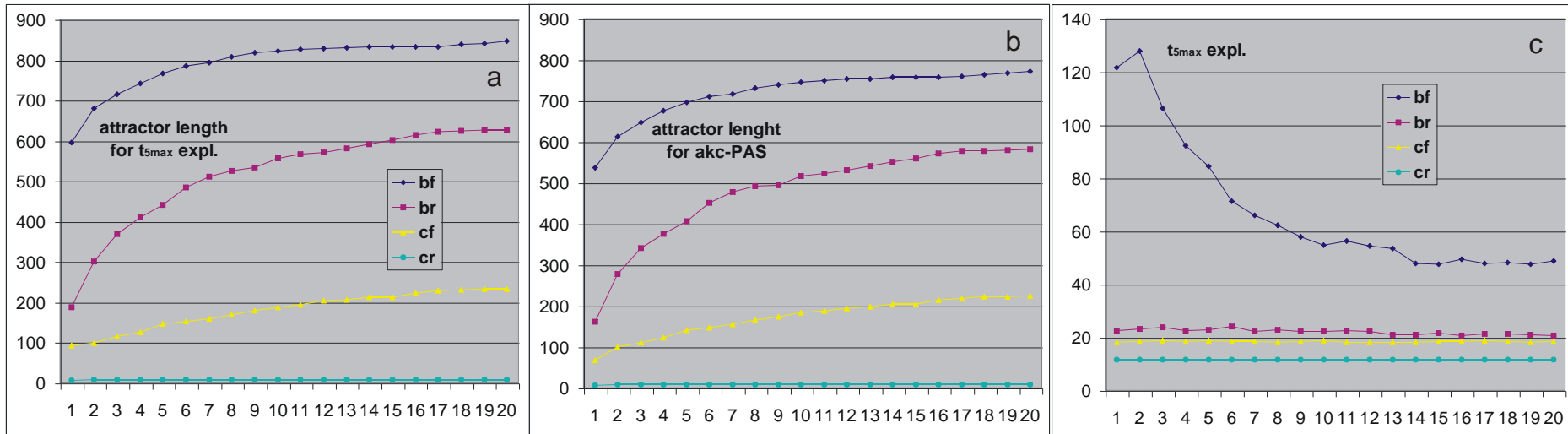


Fig.8. The lack of bringing nearer to chaos in series 45. Horizontal axis depicts passes M. (c)- Average time of 5 the latest explosions, despite (a,b) – forced growing of attractor length. (a) – for 5 the latest explosions, (b) – for accepted without PAS (akc-PAS). Parameter ‘attractor length’ turn to be based on wrong assumptions (see text and fig.9c), in approximation it now means length of a way to the end of first attractor.

In series 45 (similarly to series 44 ‘4+7+20’) 200 nets are created for each of 4 formulas bf,br,cf,cr. For br, cf & cr there is no any shift of picture to chaos (only slightly later explosions). However, the bf exhibits significant increasing of average time of 5 the latest explosions (fig.8c), but this increasing is the strongest at the beginning of accumulation process and in later passes quickly decreases from 130 to circa 48, where it reach plateau. The remaining formulas keep constant levels: br & cf circa 20 and cr circa 11.5, meanwhile, accordingly to force, ‘attractor length’ significantly grows for model b (fig.8a,b) which does not result in explosion time. Then attention was put on details of ‘attractor length’ measuring and simplification taken. Basing on observation from series 44 assumption was taken, that lack of attractor finding is an effect of attractor length, which is too large, but in series 44 the shift 50 kept short way to beginning of attractor. Now the shift is 2 and the way has much increased, which effects, that

using 900 for ‘not found’ cases describe rather way but not attractor length, which may be very short (e.g. attractor length=10, way=2918 in [fig.9c1](#) or 3, 2809 in [c2](#)). Remark that this unfortunately defined ‘attractor length’ was used in condition for accumulation, practically this parameter means in well approximation ‘way length to end of first attractor’. However, in both cases it gives view on a length of section without repetition in the pattern trajectory. These repetitions give significantly higher chance for lack of further explosion. Despite this section grows, the time to latest explosion diminishes. It does not reach the safety boundary indicated by ‘attractor length’ which show that some mechanisms exist which increase stability while accumulation so selected changes. Seen in [fig.8c](#) distinctness of pass M1 for bf is also visible in shape of left peak, which only for bf in series 45 is different for M1 than for later passes M, it is similar difference like in [fig.3a](#) for series 44.

Large growth of average time of 5 the latest explosions, visible mainly at the beginning of process ([fig.8c](#)) for bf, is clearly seen in crocodiles ([fig.9a1](#)), which strongly suggests that chaos is near. Explosions happened so frequently and late that for some events we can expect that if section tmx would be longer, then $q(t)$ will fall down to 0 which is a criterion of chaos. Therefore an additional simulation was done for 38 nets selected as ‘may be chaotic’ from 200, where $tmx=10000$ or 5000 was used. In order to investigate exactly the same processes the point of decision of accumulation must stay in the same place $t=1000$. In crocodiles consecutive attractor lengths are depicted (upper in [fig.9a2,b](#) and more exactly in [9c,d](#)), they are the net states from new, larger tmx . This experiment (symbol b45-) gives 3 important answers:

1- Obtained attractors happen short but they begin later (i.e. for $t>1000$) than end of earlier investigated section (up to $tmx=1000$). E.g. in [fig.9a2](#) attractor happened with length 10, pass M1 has begun with attractor 648 (right upper corner of green rectangle), first appearance of state from tmx happened at $t=1576$ (depicted on upper frame of thy rectangle). More and more exact such data in [fig.9.c & d](#). This changed of interpretation of the parameter earlier treated as ‘attractor length’, which was described above.

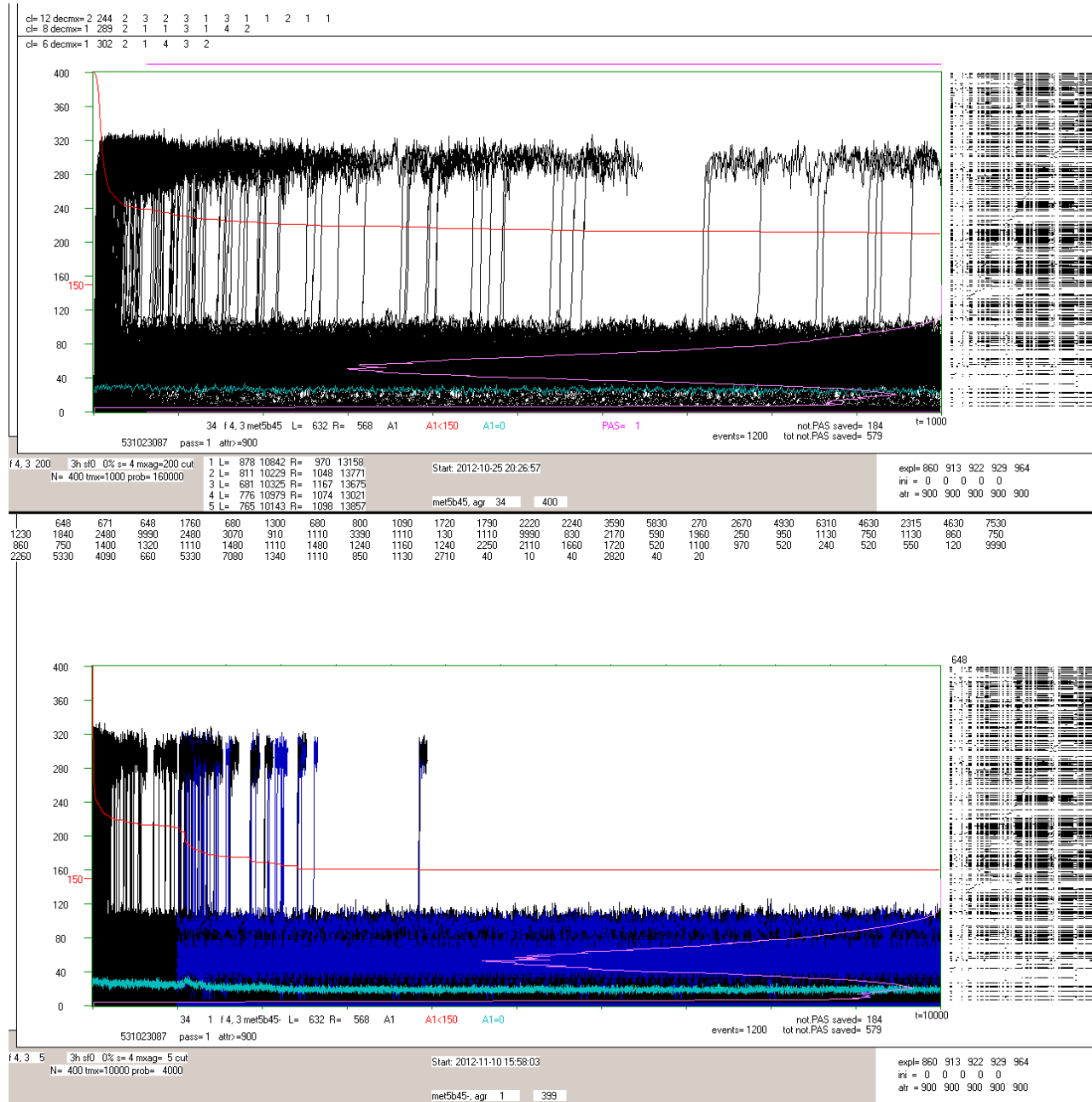
2- No one of 38 investigated events (selected as especially near to chaos) reach chaos in the range of investigated longer section. For two nets (f 176 [fig.9b](#) & f 59 [fig.9d](#)), for two passes in each of them, enlarged section was not enough to clear end of explosions. During these passes especially long or ‘not found’ (noted as 9990) attractors happened, which explain so late explosions and allow to state, that chaos was not reached here and q will stay on increased level. Event f 34 shown in [fig.9a](#) represents remain 36 of the 38, but it is the most extreme of them. All of them concern early passes M1, M4 at the most. Later passes are ‘normal’, fully or near without explosions over $t=1000$, despite the range of attractor length, fraction of ‘not found’ and time of beginning are similar. One event f 59 ([fig.9d](#)) is not compatible to this picture, it only in M9,11 & 15 has no later explosion than $t=100$, and later than $t=1000$ in M6-15, 18, 19, however passes M16, 17 and especially M20 have lot of late explosion, M16 i 20 even over $t=5000$. Despite this, q does not fall below 0.4. There are circa 40 of explosion later than $t=1000$, from these over half are a pseudo-explosion of non-accumulated or of accumulated which restore stable process. The statement, that it is significant shift into area lying near chaos has no enough base, rather it is something else.

3- Even f 103 ([fig.9e](#)) exhibits in range $tmx=1000$ rapid collapse to chaos. This is effect of overlooked aspect of shift. It happened only once and has no statistical importance, however, deeper investigation of this event help lot for understanding.

I call ‘half-chaos’ the considered state of network with chaotic parameters (fully random network with these parameters is chaotic) which exhibit similar fraction of ordered and chaotic reactions on the small disturbance. To distinguish ordered and chaotic reactions we compare trajectory of disturbed process to pattern trajectory which is of not disturbed net, but to rate changed network among half-chaotic when its reaction is ordered the pattern network and its trajectory must lie in area of ‘half-chaos’ states. In met5 I try to check is this condition enough. However, tmx limits our knowledge about last event taken as ordered, especially when very late explosions often happened and shift of initial state is used. In such case explosion can happen (with probability not to neglect) near after tmx (we do not see it) and this section of trajectory will be shifted into considered section before tmx . It is way to chaos, but it is effect of our simplification of algorithm, which neglects to check longer section, up to end of first revolution of attractors in pattern and current processes. In each ‘correct’ ordered event which does not come out of ‘half-chaos’ in this point (of earlier not detected explosion in pattern trajectory) will be ‘explosion’ and such the event will be rejected. In [fig.9e](#) in last accumulated change in pass N1 the explosion waited outside tmx . Next trajectory was shifted by 498 and the explosion of pattern become incorporated into pattern trajectory. Such obstruction is practically not to overcome.

This is similar mechanism to ‘pseudo-explosion’ considered above in [fig.9d](#) in enlarged section from $tmx=100$ to 10 000, but in this new section the pattern is not a base for elimination. Some accumulated after decision in $t=1000$ sustain explosion which next is in pattern (black explosion in crocodiles [fig.9a2,b,d](#), red in [fig.9c](#)). This not influence next events, apart that in this point they exhibit explosion, despite they do not come out of half-chaos. (In [fig.9a2,b,d](#) crocodiles events which are accepted but not accumulated are dark blue like their pseudo-explosion in [fig.9c](#).) This situation will be changed by next accumulated which is stable in this section (it does not leave half-chaos) and imitating (because is different than wrong pattern) such explosion (light blue in [fig.9c](#)) it recover correct pattern trajectory. Red line (q) diminishes after each pseudo-explosion and depicts too low q , despite this in [fig.9a2,b,d](#) q level is high. This phenomenon is interesting, however in life description explosion to chaos model death.

Fig.9. Crocodiles from series bf,r 45 including 45-. Similarly like in fig.7 pages are indicated by letters and particular passes on the page by digits. Pictures are shown in



part, typically with some copied elements inside. (a) minimally cut example bf34 short & long M1. (b) bf176, even for tmx=10000 looks like chaotic. (c) more exact analyse of attractors for above nets. (d) f59 with late explosions in late passes M16&20. (e) f103, not adequate collapse in range tmx=1000. (f,g) typical and diverse behaviour in series bf 45 (h) extreme and typical behaviour in series br 45

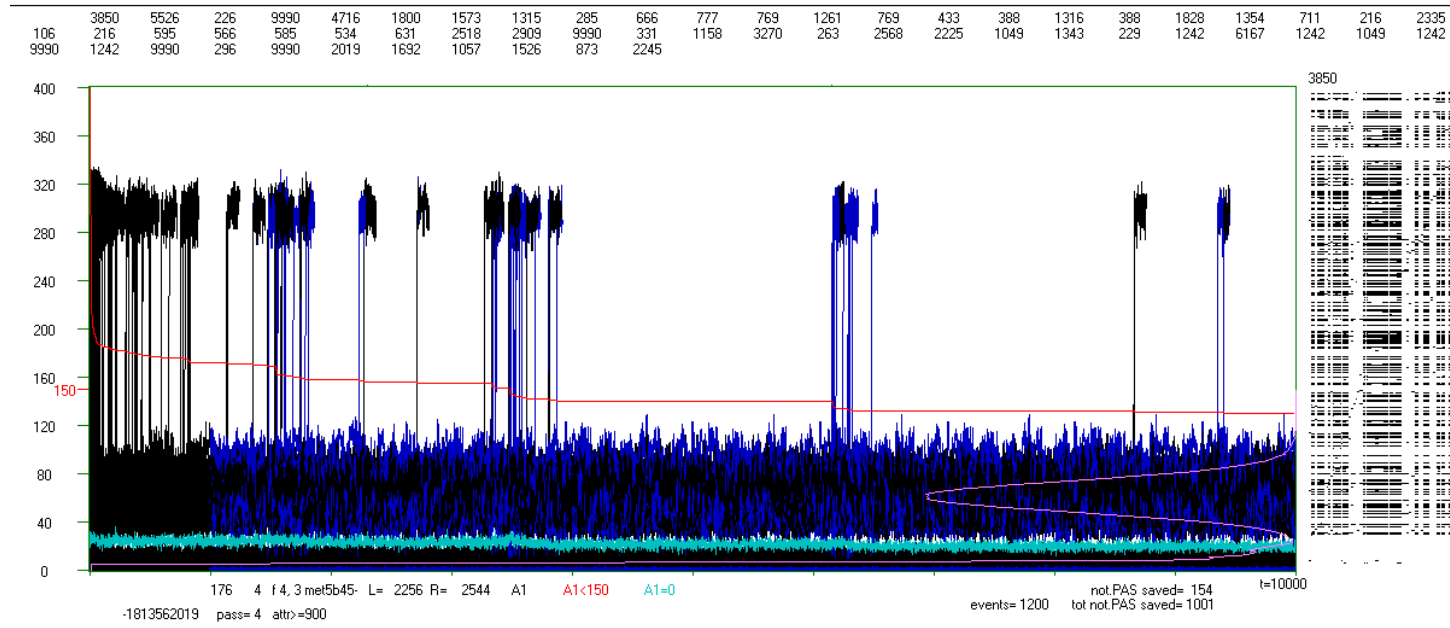
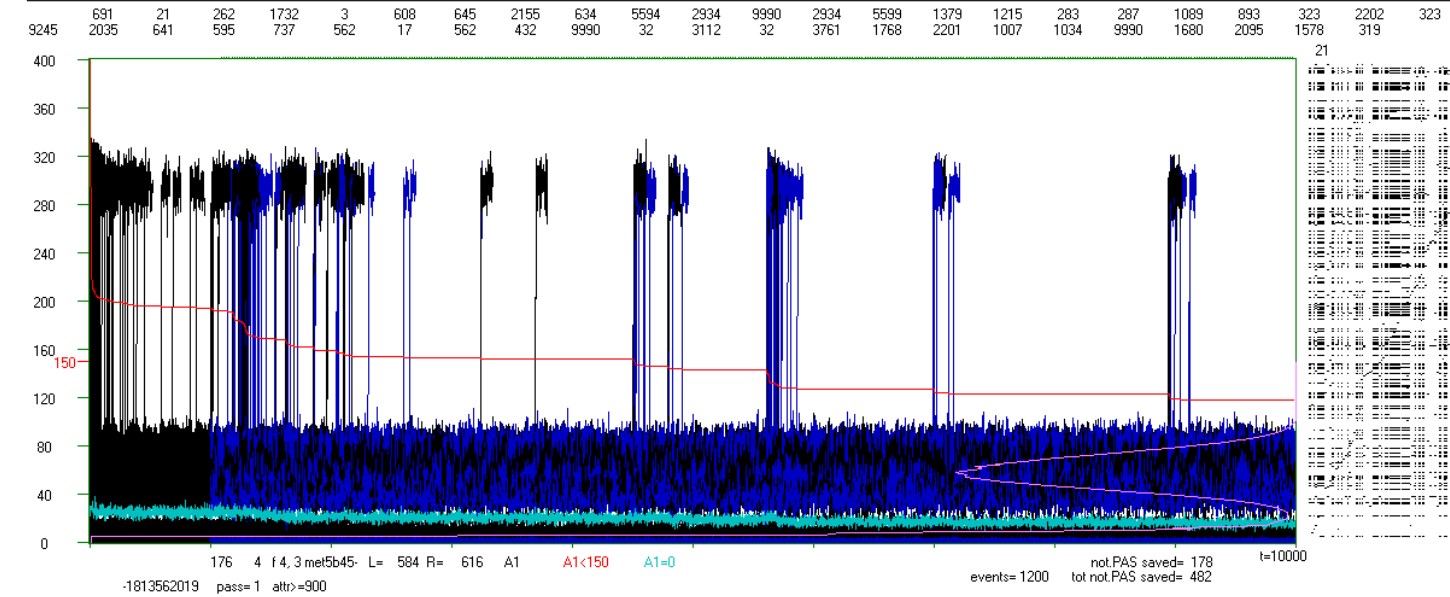
(a) Event imitating chaos in range tmx=1000, after enlargement tmx=10 000 it turns out to be stable.

(a1) f 34 M1 in range tmx=1000 suggesting chaos, because explosions do not stop before tmx. Over box of crocodile (green) range of PAS is depicted. Over it – results of clusters investigations for passes N1 i N2 over black line and for current pass M – under the line. On the right – nodes with changed states for accumulated (see end of description of fig.7b).

(a2) - The same event f 34 M1, but investigated to tmx=10000. Decision about accumulation is taken like previously at t=1000. Dark blue in the new section concern accepted events but not accumulated (later process overwrites earlier). Here over crocodile attractor length (based on state in tmx=10000) is noted.

Despite lack of attractor finding at beginning of (a1), in (a2) attractor at the beginning is 648 (right upper corner of green rectangle), but it starts at t=1576.

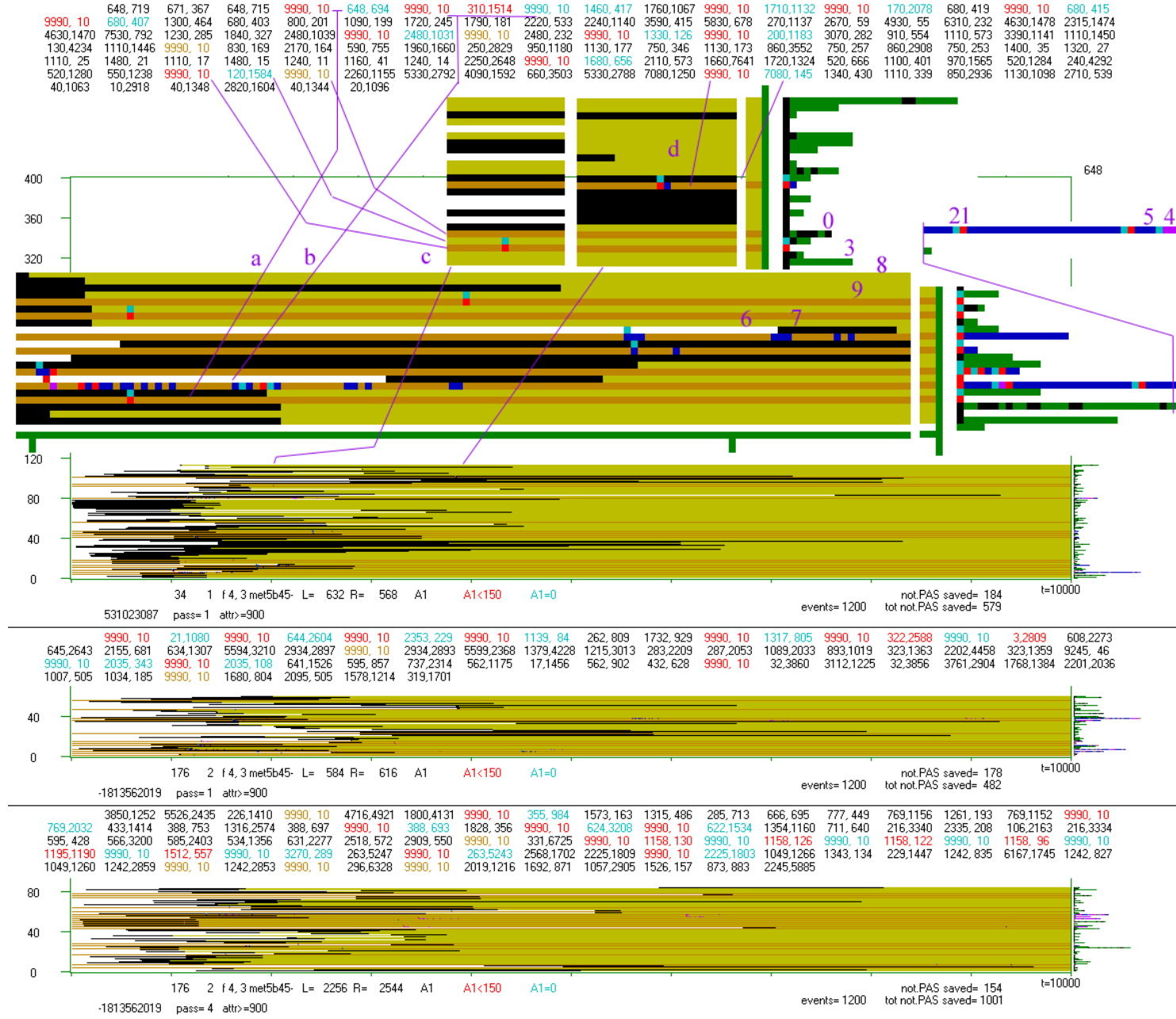
In lower (than threshold=150) part of crocodile in the right wall lies distribution of A1 taken for t≥600. It shows in (a) strong maximum near 55, and minimum near 18 which in (a1) can be seen as white gaps. It indicates presence of **ro-module**. In this ro-module Derrida level of chaos is reached, but it is under threshold.



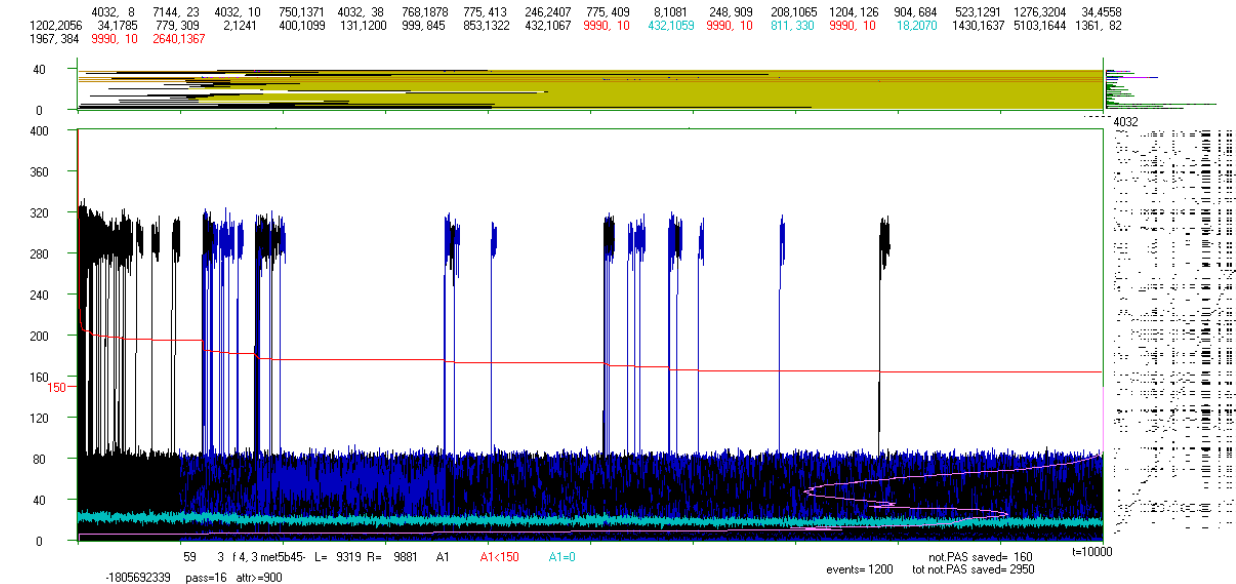
(b) f 176 passes M1 i M4. They even in range $tmx=10000$ do not exhibit end of explosions. In remaining passes there is no late explosions. Net f 34 (a) represents circa 40 similar events of 200 nets but f 176 is the only 'stronger' (later explosions) case than f 34. All they concern early passes M. Only for shown in (d) f 59 so late explosions happen in late passes.

After decision about accumulation at $t=1000$ may happened explosion to chaos (black) which land in pattern. In this place next process, however stable (not leaving half-chaos) exhibit false explosion. Red line describing q comes down after each such pseudo-explosion despite it is false due false pattern, this leads to incorrect q .

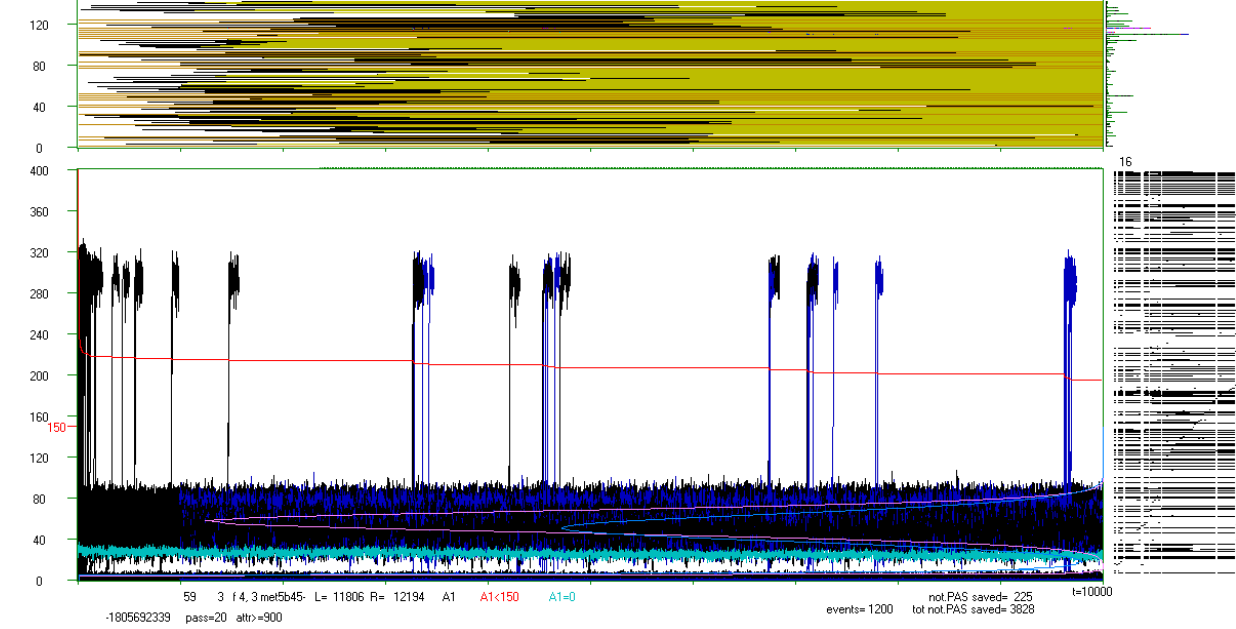
Despite this the q stays on high level. More precise analysis of attractors for this event is shown below in fig.9c2 & 3.



(c) more precise analysis of a place of first entrance into attractor, its length and of explosions and pseudo-explosions. On the top the length and entry point of attractors are noted when attractor length changes. The colour meaning as 0,1,2,9, 9990- lack of attractor finding. Instead of crocodile any accepted ini which change attractor length draws horizontal line: 6-way to attractor 7- first revolution of attractor 8- later in attractor, 9- lack of attractor finding. On the right after frame each accepted which does not change attractor length adds pixel to the right: accumulated: 0,1,2; not accumulated: 3,4,5; 0, 3 – without explosion 1, 4 – explosion 2, 5 – pseudo-explosion. It was assumed that every second explosion of accumulated is false or recovering of correct pattern. This is true in events a, c, d, but not in b. After second 9990 line of ini with explosion is taken, without change of length of attractor which is not found. Here and during next 9990 accumulated explosions happen in false state which do not recover correct pattern. Indicated places upper and lower between 1000 and 2000 are enlarged and connected with attractor descriptions.

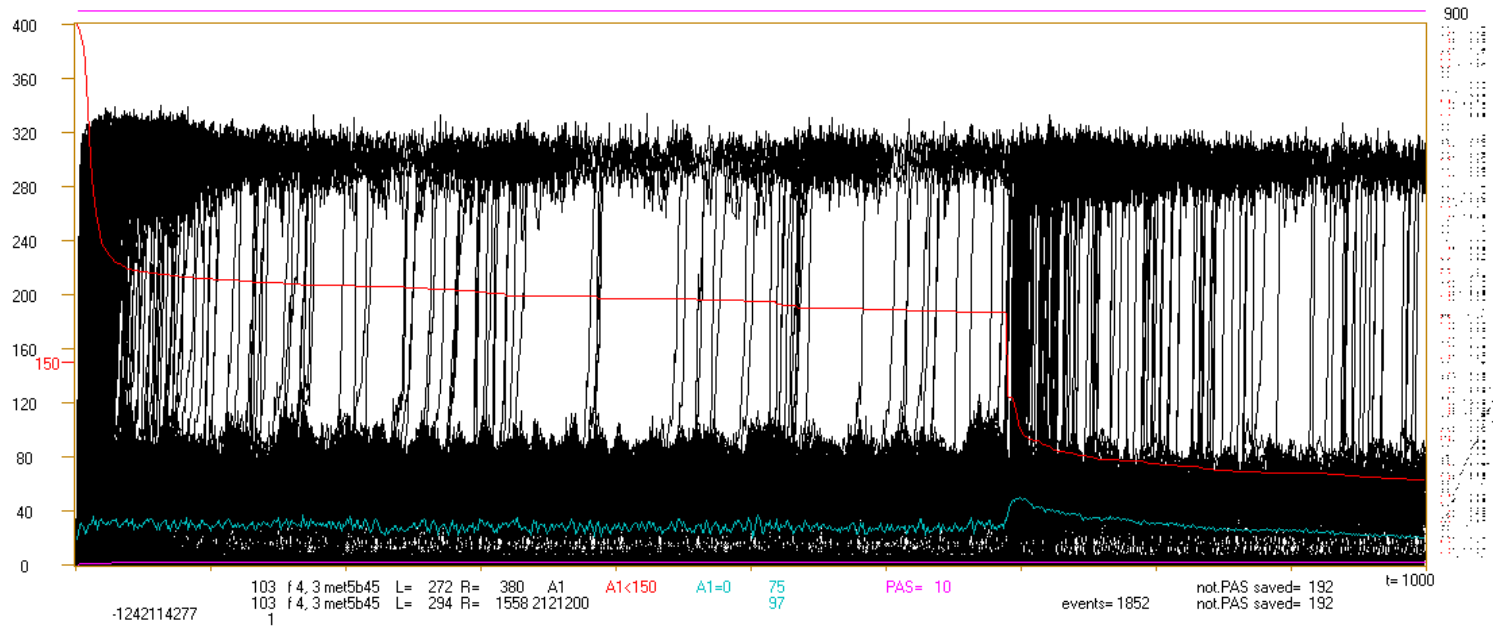


9990, 10	16,8956	1274, 477	3416,2557	2836,4020	4732,1328	9990, 10	3444,2520	9072, 269	9990, 10	4184,1970	24,9737	2076,4131	1428,2881	1188,1807	1428,1245	3716, 630	
1428,2465	3223,2517	1428,1507	936, 568	9990, 10	5292,1095	5448, 721	5292,1090	1216, 556	3080,1793	7252, 993	3080, 162	2320, 413	908, 77	9990, 10	28,2081	5656, 954	2804,1296
412,7626	1508, 622	1628, 896	9990, 10	1628,8282	9990, 10	1996, 949	4944,1325	2536, 682	4944,1321	9990, 10	120,1681	9990, 10	3512, 481	9990, 10	192,2293	9990, 10	2300,1248
3644, 384	2300,1244	7920, 793	1820, 294	24, 980	2608, 197	1176,1019	16,1013	376,2712	976, 101	908, 547	1864,3103	4352, 386	972,5003	3084, 351	4,1344	532, 919	4,2927
504,4405	1888,1130	2148,1469	500,1690	1284,1164	9990, 10	1284,7836	9990, 10	8348,1009	560,3252	8348,1005	9990, 10	4852,2705	9460, 622	4852,2701	24,1803	3200, 308	9990, 10
3338, 21	9990, 10	7136,1442	9990, 10	596,6810	2264,1167	908,3233	760, 765	936, 611	789, 604	1980, 404	148,1451	1380, 473	704,1345	1380, 225	8,1467	9990, 10	5280,3315
9990, 10	198,1755	9990, 10	2,2350	9990, 10	7492,1223	9990, 10	4999,1881	9990, 10	6049, 724	3946,2527	5096, 288	3946,2254	9990, 10	3946,1383	3522,2112	9990, 10	3522,2104
4210,2172	1231,4304	4210,4264	969,6511	4210,4260	1663, 842	4210,3980	725, 417	1707, 32	94,4373	5736, 139	794,6622	5736, 131	2139,1553	370,1083	659, 584	691,1607	

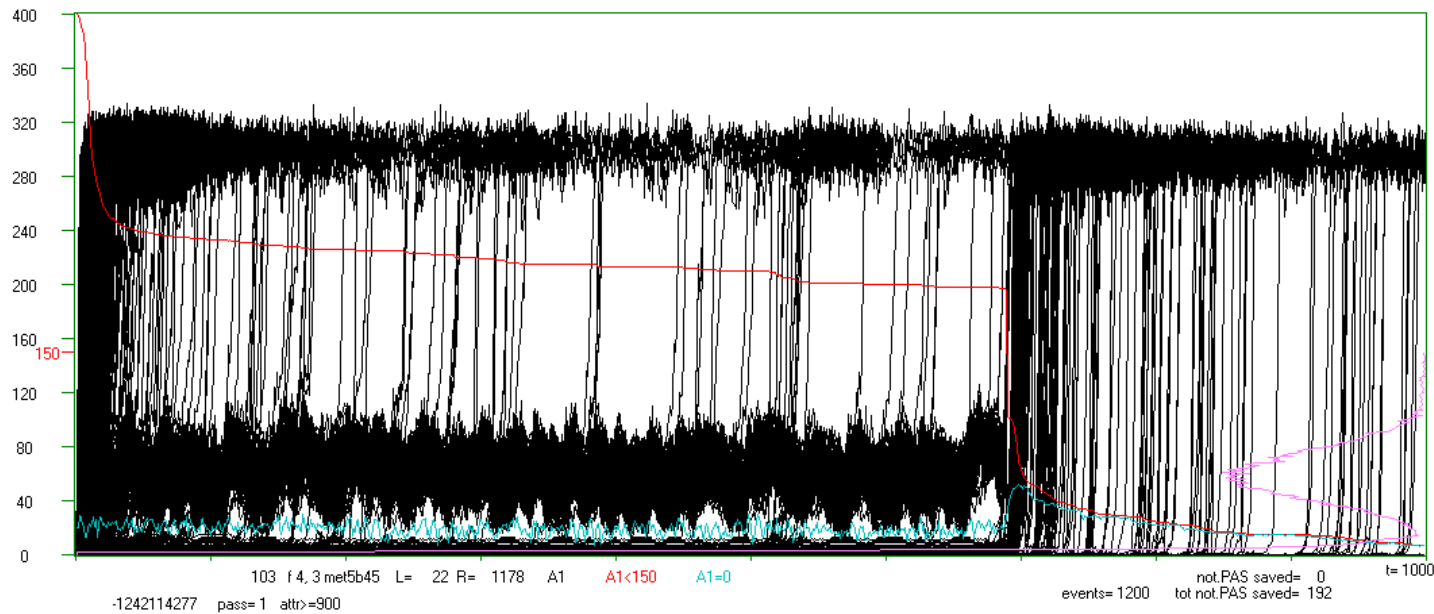


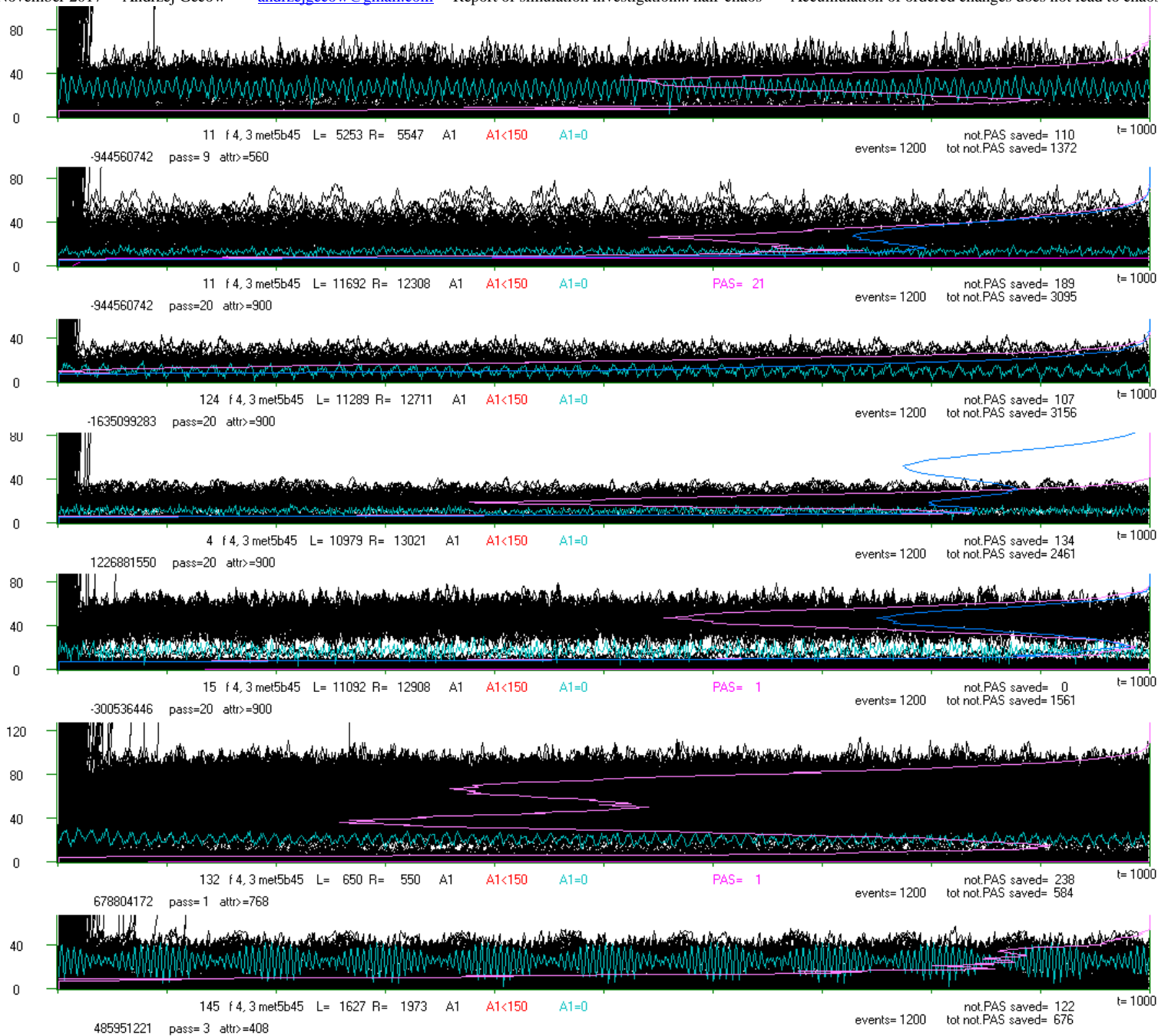
(d) exceptional net f 59 of late explosion in late passes (M16 & M20). In M9,11 & 15 there is no later explosion than $t=100$, in M6-15, 18, 19 later than $t=1000$. These late explosions are not frequent and q decrease a little despite over half of them are 'false'. Both shown passes are similar, however attractors shown over crocodiles are in both cases very different. Shown in d2 initial attractor 16 begins later than $t=2000$. Later explosion rather happen for greater attractors. Lot of times attractor was not found. In (d2) in lower area a white gap is visible in all section. Distributions of A1 on the right wall (blue is a sum by all passes M) contain minimum which is connected to above gap and maximum which is an effect of Derrida level in ro-module.

cl= 19 decmx= 3 250 1 1 1 2 1 1 1 1 1 2 1 1 1 1 2 1 1 2
 250 1 1 1 2 1 1 1 1 1 2 1 1 1 1 2 1 1 2

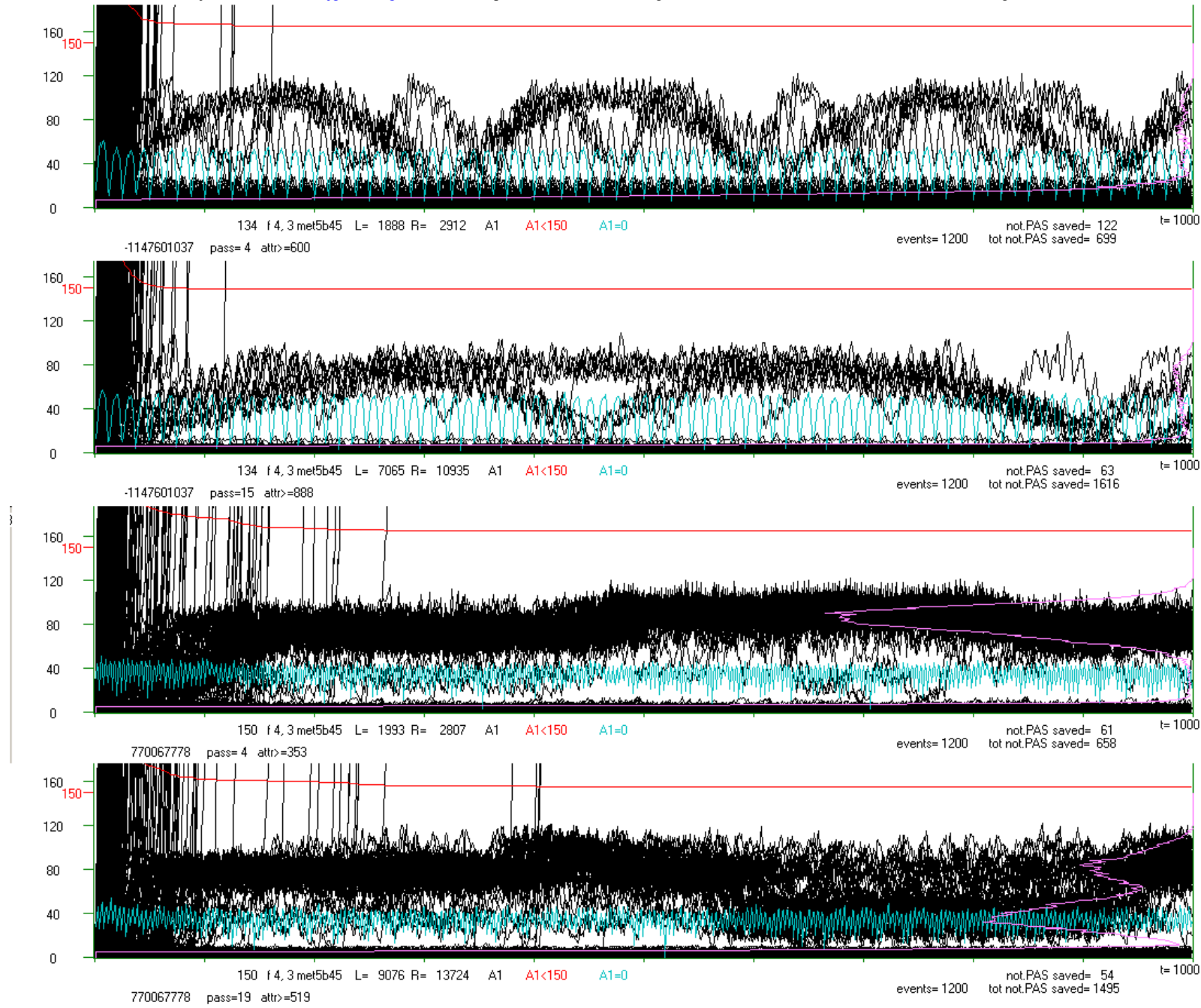


(e) f 103 – chaotic collapse in range $tmx=1000$, effect of simplification of algorithm and limitation of tmx . Later than tmx in last accumulation in N1 is explosion to chaos, but it is out of range of control. It become a pattern, but after shift by 498 at the beginning of N2 which incorporates the explosion. Therefore N2 and M1 do not find any ini able to accumulation. Contrary to added section in series 45- , here each pseudo-explosion happened in controlled range before $tmx=1000$.



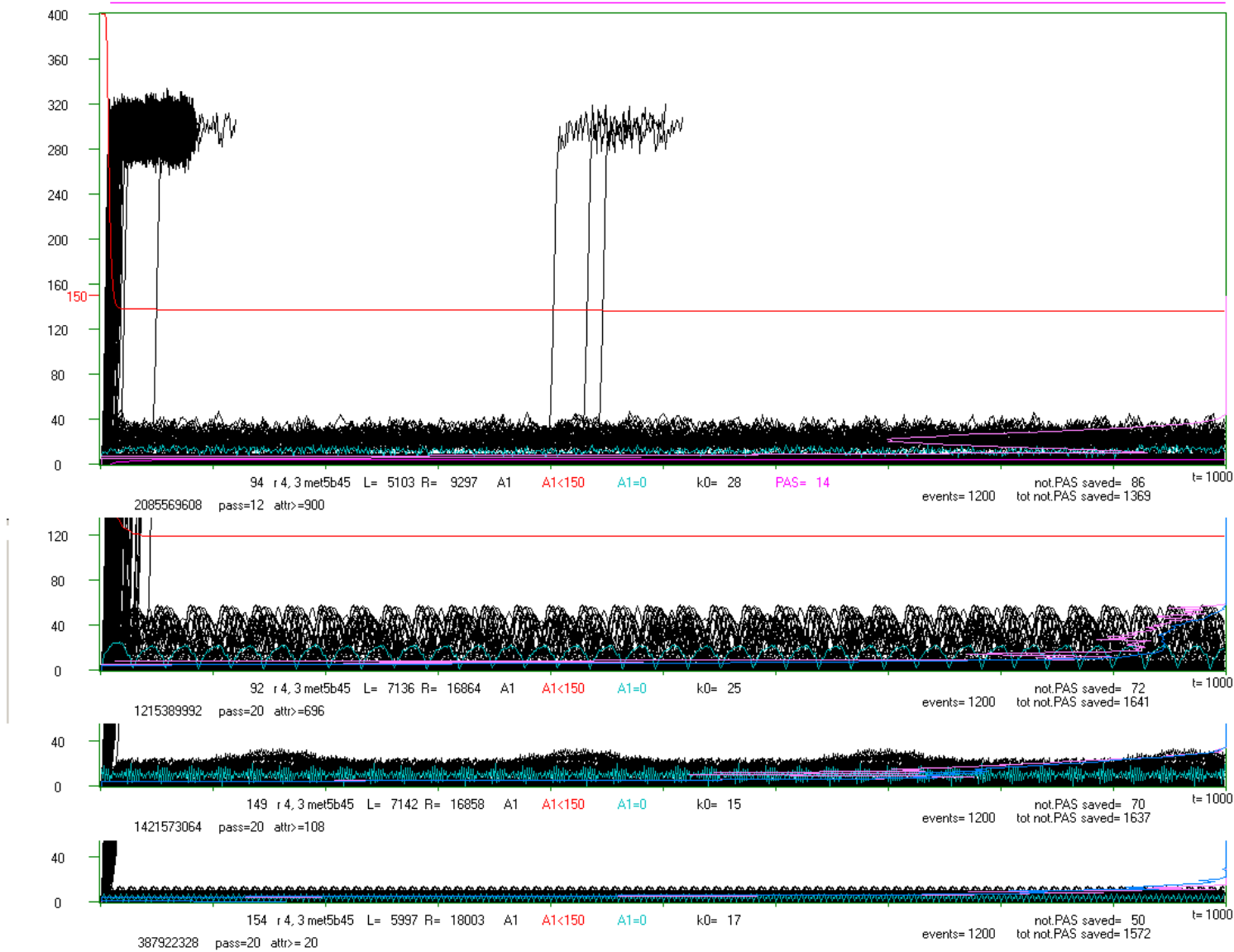


(f) typical and diverse behaviour in series bf 45. in (f1,2,4,5 i 6) clear peaks of Derrida equilibrium in ro-modules are visible in distributions on right wall. Derrida chaotic equilibrium for whole network lies much higher, near 300. In (f7) in blue line of A1=0 typical effect of two different periods of attractors is visible.



(g) specific processes of bf with visible repetitions connected to attractors length. Examples selected here shows that distributions on right wall not always adequately show ro-modules. Attractors in ro-modules may change A1 in the large range.

cl= 25 decmx= 4 1 82 1 2 2 1 4 1 1 1 1 1 3 2 2 1 4 2 1 1 1 1 3 2 1
 cl= 10 decmx= 3 174 3 4 6 1 1 2 1 1 1
 cl= 2 decmx= 3 293 1



(h) extreme and typical processes of br 45.
(h1) – exceptional, the most ‘chaotic’ event in br 45.
 The remain shown events are typical, but most of br 45 are more similar to the last two.
 Remark that density of pixels in the right out of box (changed nodes for accumulated) is much smaller than in (a,b,d).

However decreasing of maximal time of explosions is a good index that boundary of chaos not become nearer, the probability of acceptance - $P(\text{akc}|\text{M})$, i.e. degree of order $q(\text{M})$ is the basic index, but it slowly decreases for bf (fig.10a), **inversely than in fig.4a for series 44 ‘4+7+20’, where slowly grows**. For br it reach plateau in 3/4 passes M (in M14), for model c - near at the beginning. This allow to expect that also for bf q will be on similar level as for cf. We would think that small decreasing of $P(\text{akc}|\text{M})$ is an effect of growth of non zero input states (fig.10b), but complexity observed connections make hard such a expectations. We would expect that level of this parameter should reach and stay near value 390 but even bf is fare of it. The remaining reach much lower stable levels: br and cf circa 200, cr even lower than 100. These levels are slightly lower than in series 44 (fig.6), which is an effect of lack of blockade of smearing, but they are similar which lead to similar conclusion that state is significantly shifted from initial PAS0. Similarly like in series 44, fig.10b has very complex interpretation. Difference may be connected to average number of accumulated in M20 (respectively: bf,br,cf,cr = 3190,1601,2069,512). Fraction of fade out in acceptance is another element of this puzzle influencing on $P(\text{akc}|\text{M})$. As is seen in fig.10c especially for bf $P(A1=0|\text{M})$ decreases circa 0.022, but $P(\text{akc}|\text{M})$ (fig.10a) decreases in this section by 0.046.

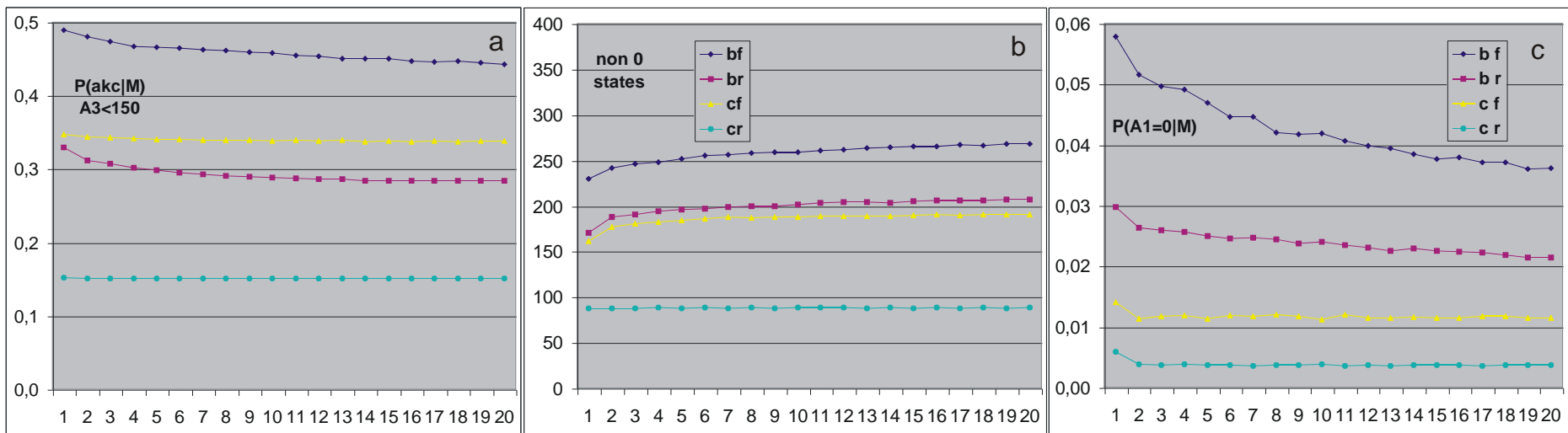


Fig.10. (a) – Level (degree) of order $q=P(\text{akc})$, as measure of distance to chaos, in condition on level of advancement of accumulation process measured by number of pass M. This level slightly decreases but only at the beginning, later it reach plateau on significantly increased level.
 (b) – Number of non zero input states ($N=400$) as measure of distance from initial PAS0. See fig.6 with discuss.
 (c) – Probability of fade out $P(A1=0)$ in consecutive passes M is a part of $P(\text{akc})$. Decreasing of $P(A1=0)$ explains only circa half of decreasing of $P(\text{akc})$.

5.6 Ro-modules – searching for premises and proof

The basic aim of series 45 and the second aim of met5 – to reach boundary of chaos on the way from PAS0 by small changes turns to be hard and is not fulfilled. It is not a failure, it is rather a more needed effect which show a power of so simple conditions of accumulated changes and reality of distinctness of state called half-chaos. The third aim of met5 remain to fulfil: to check thesis called ‘ro-modularity’ that specificity of this region of half-chaos lies in many short nearly independent loops connected to small subsets of nodes called ro-modules. This hypothetic state of system, specific type of half-chaos, I call ‘ro-modularity’ to connect it to mechanism and explanation.

Idea of many practically independent system sub-areas which have their own attractors is known as modularity, but classic modularity is based on different density of links which creates that practical independency. Such the modularity was investigated in met3. However, here we have network randomly build, we do not change connections of its nodes which stay random and even as at the begining. Modularity cannot emerge, but it is present from the beginning, which become clear for me in [met8 investigation](#). PAS0 and current state of half-chaos observed in met5 after shift from PAS0 are obtained only by defining node states and small distinctness of functions. One accumulation of small change of function giving explosion to chaos, without change of connections, is enough to this specific state disappears (e.g. [fig.9e](#)). Then it is not only classic modularity.

‘Ro-modularity’ is similar, may be the same, as state form Kauffman ‘liquid area’, but in developed model it lies not in ‘edge of chaos and order’ in random network but in specific (not random, selected) network, with chaotic parameters s, K (e.g. here used 4,3; random network with such parameters is chaotic). Still it is boundary of chaos and order, but its character is another – that was phase transition, here both forms of reactions on small perturbation are simultaneously present in the same network in similar degrees.

5.6.1 From frequency of secondary initiations

A frequent multiple fade out in stable process of damage propagation is a strong premise for explanation of half-chaos basing on ro-modularity.

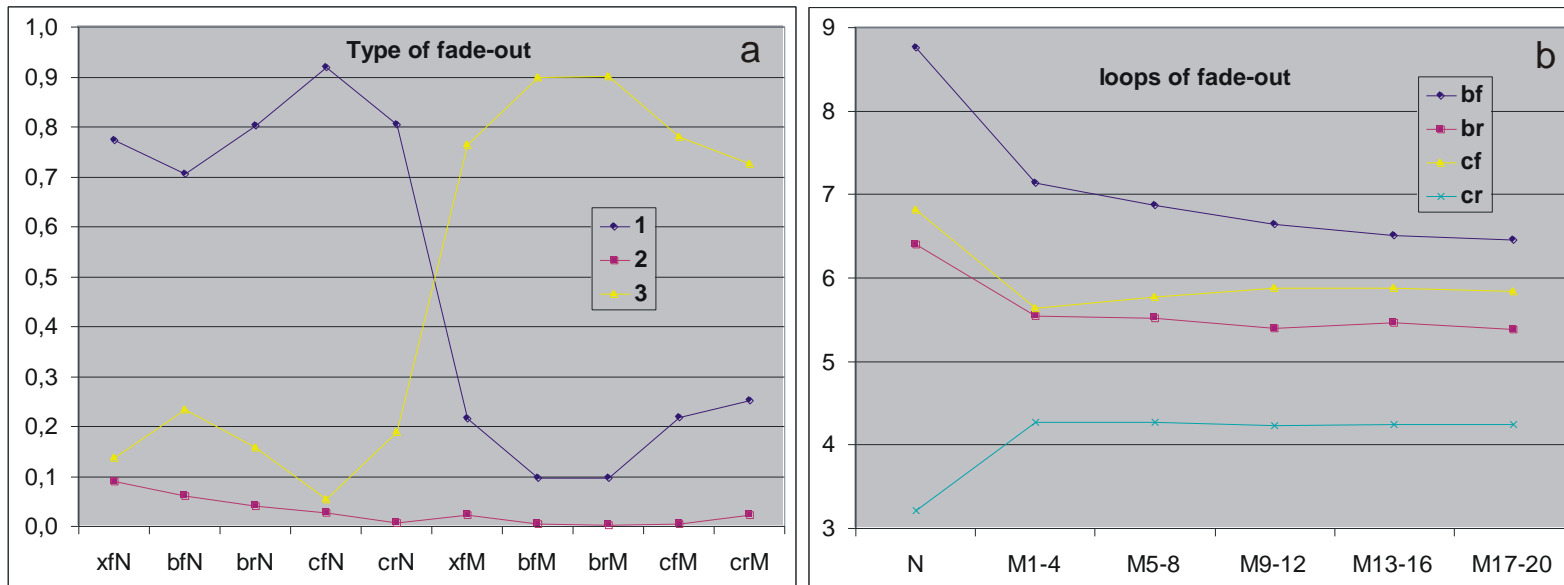


Fig.11. Types of fade out (a) and average length of loops (b) based on the multiple of fade out.

(a) relationship of fractions of fade out type and pass type (N or M) for different formulas. Symbol xf indicates series 44 bf ‘4+7’ (not 100M20), remains from series 45.

Radical difference between passes N and M is seen. In N, in accordance with the series 34, there is much more of full fade out (1), second ini as the last (2) is on small but visible level, multiple fade out (3) is slightly frequent than (2). In M passes multiple fade out radically dominates, but practically there is no (2).

(b) average period of secondary ini. It is $\ll 64$, then it is average length of loops but also radically less than average length of (global) attractors, then of local loops.

In **fig.11a**, which is a completion of distribution $P(A1=0|M)$ shown in **fig.10c**, relationship of fractions of fade out type and pass type (N or M) for different formulas is shown. Radical difference between passes N and M is seen. In the range of passes N attractors are yet short, shift before N2 is great but one then accumulations are practically done without shifts. Accordingly to results of series 34 a fraction of full fadeout is great. In passes M the multiple fade out radically dominates, despite in series 45 the shift=2 is small, but it is done after each accumulation. When double fade out practically is absent, then large multiple is expected, which suggests small loops, as short attractors of ro-modules.

Probability of appearance of node input state for which ini was done is $s^{-k} = 1/64$. If secondary ini appears in average earlier than every 64 steps, then probably short loops in ro-modules are responsible for this, because attractors are typically longer (**fig.8a,b**). Average periods of these loops calculated basing on multiple of fade out is shown in **fig.11b** for series 45. (For series 44 results are similar, but they are disrupted by diversity of passes.) For passes M the periods are small, between 4 and 7, much less than 64, then this is premise of ro-modules with such the attractors existence.

5.6.2 From distribution of small attractors fractions

Hypothesis of ro-modules suggests that global attractor of whole net is an effects of assembling of several independent loops. If so, then consecutive values in distribution of attractor length fractions should be not similar, but lengths which can be assembled from larger number of small loops should be preferred. In **fig.12** fraction of larger prime numbers which cannot be assembled, are small, but numbers assembled from small prime numbers are much more frequently used. It is strong premise for ro-modularity.

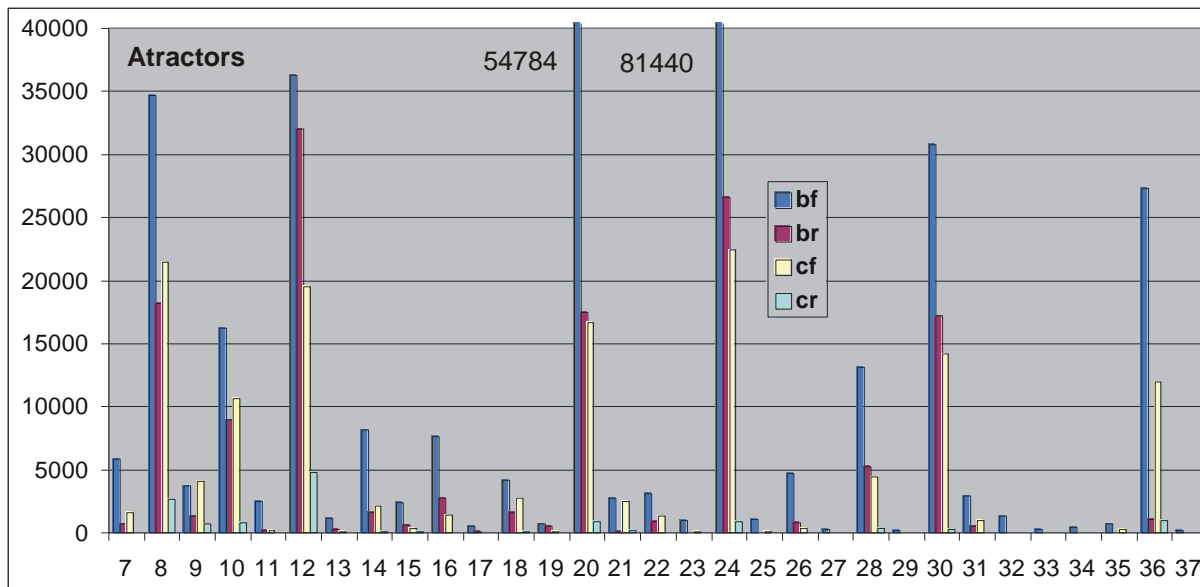


Fig.12. Numbers of using of attractor length in the range 7-37 from series 44 '4+7+20'. Lack of similarity of neighbouring length is seen. It is well explained by assembling of global length of attractor from several smaller local attractors. Higher prime numbers have smaller counts.

5.6.3 From distribution of P(A4), A4 – number of disturbed nodes, local cluster A4 – set of disturbed nodes

To see ro-modules during simulation of series 44 and 45 a set of disturbed nodes called ‘**local cluster**’ was observed. We expected that nodes from one (or a few) ro-modules participate in particular damage. Variable **A4** is a number of elements in local cluster. A4 is collected on the whole section tmx (**A41**), or from t=100 (**A4h**) without first unstable section. Both distributions really are different (fig.13). A4 was define for investigation of global clusters A4 (next chapter), distribution of A4 was checked for peaks of searched ro-modules, but **a particular size of ro-modules is a property of particular net, even it may changed during evolution**. To see it can be used method as for A1 in right wall of crocodiles (e.g. fig.9), but it was not applied in met5 (it was done in met7, see m7.fig.15g,h). In met5 attention was put to clusters ro (ch.5.7). In fig.13 distributions P(A41) and P(A4h) are shown in log form in full range of A4 and more exactly for small values of A4 in linear form. In series 44 (a, b) only A41 defined on whole section tmx for all events (calculation after explosion was limited to 70 steps t) are got. In series 45 distributions of both A41 and A4h in selection for all events and for accumulated only are available. These results are collected from N1 to M20. Values in distributions change in wide range. The first section of small A4 is the most interesting because there are peaks of local clusters expected.

Results shown in fig.13a,c,e do not confirm of provisional expectations – there is no separated peaks for different sizes of clusters what is explained above. Disturbance at the beginning in fig.13e for A4 in the range 0-2, especially large for cr, is an effect of accumulation condition $A3 \geq 3$.

A similarity of consecutive very small values in log diagrams depicts exactness of statistical measure. Significant differences of distributions for different formulas are not analysed, attention was paid for clusters ro. Peaks for greater values of A4h in fig.13d are an effect of short calculations after t=100 for explosions before t=100, A41 after explosions reach near always values 400, exceptionally 399 (tab.1, fig.13b,d). In the most adequate fig.13f excluding net cr all have a crooked tail which for bf reach circa 200. There are explosion to chaos in range of local (one or a few) clusters A4 (ro-modules), as in fig.9g. $A4=200$ does not mean that A1 cross the threshold=150. Presece of these tails is connected to mechanism of single great global clusters A4 emergence.

Table.1. The end of P(A41) in series 44 and 45 (see fig.13b,d). Explosion to chaos practically spread across all nodes of the network. For large section of lower A41 a number of events and P(A41) are exactly 0.

series	A41	bf	br	cf	cr
s 44	399	0,0039	0	0,0046	0
	400	0,6759	0,841	0,7436	0,873
s 45	398	0,000004	0	0	0
	399	0,0004	0	0,0010	0
	400	0,5420	0,7087	0,6638	0,8558

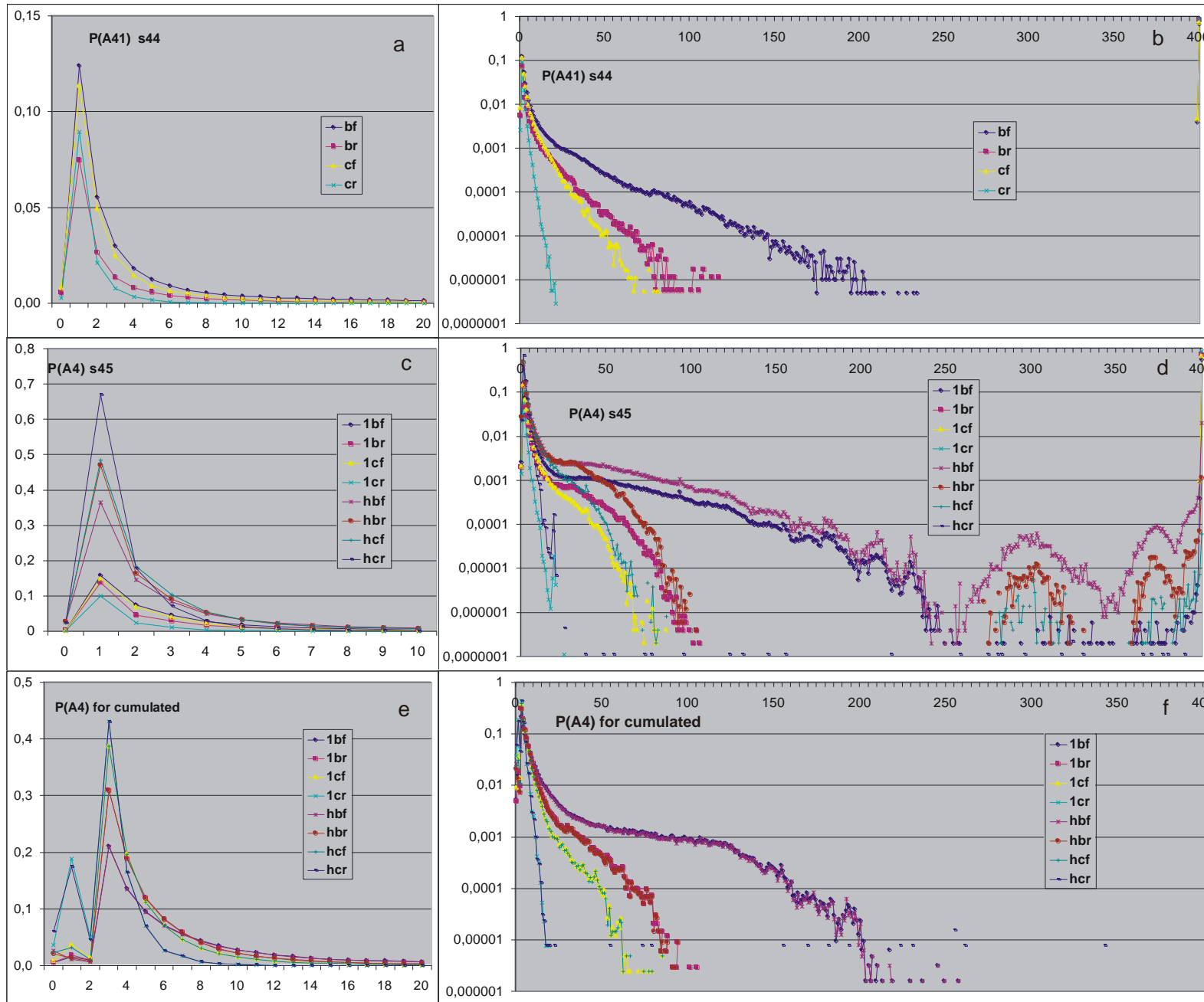


Fig.13. Distribution P(A4) for local clusters A4 in version defined on whole section tmx (without t=0) (A41), and (A4h) without first 100 steps t where explosion typically occurs. A4 is a number of damaged nodes as measure of size of ro-modules.

In series 44 (a,b) only A41 is available, later in series 44 ro '4+7' results for A4h are obtained and shown in m6.fig.3.

In series 45 (c-f) A41 and A4h for all events (including explosions) are collected (c,d) or for accumulated only (e,f). Data are collected from passes N to M20.

Simulations were optimised - after explosion only 70 steps t were calculated. For cases exploded before circa t=40 but later than t=30 it makes in A4h (d) peaks in the tails.

5.6.4 Connections of local clusters A4 into global clusters A4

As I have written above (ch.5.3.3) two loops with different periods (e.g. small prime numbers) cannot have common nodes, because conditions for their function are too hard, i.e. their probability of coexistence without explosion is too small. Basing on such the expectation during all process from N1 to M20 for accumulated local clusters A4 were connected to global clusters A4 when they have a common node. This assumption turn to be too simple, which is important for interpretation.

Results are shown over box of crocodile (see e.g. in [fig.7a,b, 9a1,d1](#) for bf and [9h](#) for br). They contain number of global clusters, maximal number of connected local clusters A4 in one accumulation and numbers of nodes in consecutive global clusters A4 starting from the oldest. **Many small global clusters A4 are expected.**

Unfortunately, **results for bf, br and cf with exception of cr is very different than expected**: at the end typically one great cluster and several very small (typically of one node) remain. Process of connection was watched from the beginning of accumulation. At the first few passes there are more global clusters ([fig.14f](#)) and the biggest is smaller.

Provisional results are shown in [table 2](#), where ‘x’ indicates number in range 1-9 and ‘1x’ – 10-19.

Only formula cr in series 44 and 45 gives result similar to expected, where number of clusters in M20 is comparatively great and clusters significantly diverse, many with size similar to the greatest, but the greatest are not great. As is shown in [fig.14f](#) the number of clusters only for cr does not change with accumulation (passes M). Also only for cr there is no right peak in [fig.14b,d](#) and long tail in [fig.13f](#).

Model b leads to the greatest connection of clusters and decreasing of their number with M ([fig.14f; 13f; tab.2](#)), so, in br45 one cluster often remain in M20, however, despite this systems stay stable, then we should change our approach.

Table 2. Provisional results of investigation global clusters A4 at the beginning of process in pass N1 and on the end in pass M20.

#cl – number of global clusters; mx cl – maximal cluster; both these values estimated as average for one net using not full data.

Symbolic values as range: x – 1-9; 1x – 10-19.

Typically maximal cluster is radically greater than remain clusters which sizes are rarely 4 or 3, typically 1 or 2. However if it is differently, then it is noted: e.g. for cf45 in N1 maximal cluster size has great dispersion: from a few to 100 and lot (may be even over 20) of clusters of size in range 10-19.

	bf44	br44	cf44	cr44	bf45	br45	cf45	cr45
N1 #cl	30	25	80	50	20	20	70	50
N1 mx cl	200	100	35+x*1x	6	200	90	x-100+?x*1x	x
M20 #cl	x	1x	40	45	3	3, often 1	35	30 or 40
M20 mx cl	350	280	240	23+x*1x	350	250	180	8+x*x

Size distributions of global clusters A4 at the beginning (passes M1 to M4) are shown in [fig.14a,b](#), and on the end (passes M17 to M20) [fig.14c,d](#). Similarly like in [fig.13](#) Beginning section of cluster size up to 10 nodes is shown more exact in linear scale ([fig.14a,c](#)), and whole section up to N=400 is shown in log scale ([b,d](#)) connecting consecutive 10 results for fluctuation decreasing. Clearly, in both ranges another mechanisms work. Right peak of larger clusters seen in [fig.14.b & d](#) significantly for model b and visible for cf shift itself to greater values – it is comprehensible. For formula cr there is lack of this peak, only left peak is wider. This direction of changes exhibits also cf. Typically, bf and cr are an extreme formulas.

In a distribution of number of clusters ([fig.14e](#)) model c exhibit clear but wide peak for greater values (circa 35 or 40), and small values are absent, but maximum for model b is near 3 and the peak ends already near 10.

[Fig.14](#) concern series 45, because diversity of passes in series 44 not allow for results summarising from several consecutive passes used here in [a,b,c,d](#). In further investigations met6 i 7 this problem is overcome, and for comparison A4h for met5c 44 ‘4+7’ are completed, which is included in [m6.fig.3 & 4](#) and [m7.fig.18 & 19](#).

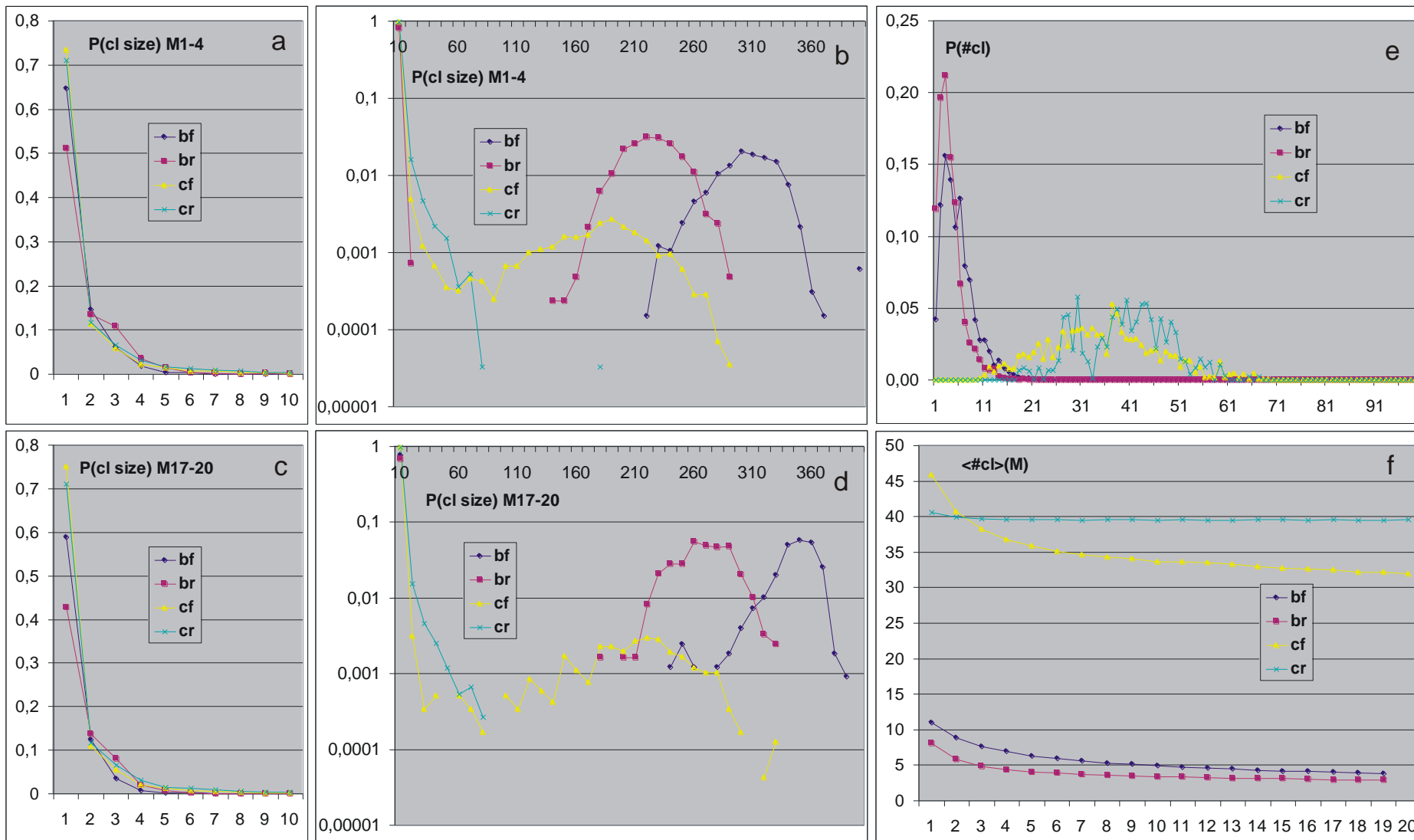


Fig.14. Series 45. Size distributions of global cluster A4 at the beginning (a,b) and at the end of accumulation process (c,d). For statistics increase the results are from 4 passes M each, and in (b,d) 10 consecutive values are added. Local clusters are connected (included) to global cluster when they have common node. Distribution of number of global clusters (e) and average number of clusters for passes M (f). For cr numbers of clusters are large (f), but the biggest cluster stays small (d). For cf numbers of clusters also are large (f), but the biggest cluster in net happens small and large too (d & crocodiles). In model b number of clusters decreases and the biggest cluster grows.

5.6.5 From distribution of A1 for accepted on right wall of crocodiles

Depiction of $A1(t)$ for whole set of ini is called crocodile (see [m4.fig.3](#)). It typically contains two belts: upper near $N(s-1)/s$ and lower between 0 and threshold which typically is defined near half of upper belt level. They correspond to two peaks in damage size distribution $P(A(tmx))$: right – of Derrida equilibrium level of chaotic reactions (upper belt) and left – of ordered reactions (accepted, lower belt). The upper belt is now not complete, because it is not interesting and simulation is optimised – only 70 steps after explosion to chaos is calculated. For typical random chaotic system the lower belt disappears – all ini explode to chaos (all depicted by $A1(t)$ processes rapidly change belts from lower to upper one) as in [m2.fig.13 & 14](#) or at the end in [fig.9e2](#).

However, in the half-chaos and its special case – ro-modularity, the lower belt (and its form: left peak of damage size distribution, $P(A(t))=q(t)$ – red line in crocodile) stays up to tmx and contains lot of events. In this lower belt two or more sub-belts often can be seen separated by white gap ([fig.7d9, 9d2,f5](#)). Hypothetic interpretation of upper sub-belt in lower belt is the chaotic Derrida level but in a range of a ro-module. Visual searching for ‘sub-belts’ is much easy in dynamical observations while crocodile is build, but even such searching is too subjective and depends on sequence of events. For more advanced searching a distribution of $A1$ on right wall of crocodile was depicted. It collect data for accepted events, i.e. lower than threshold and from $t=600$ to neglect first section full of explosions. E.g. in [fig.9a](#) strong maximum near 55 and minimum near 18 is visible, which in [fig.9a1](#) makes white gap. Probably it is an effect of chaotic behaviour of a ro-module, but Derrida level of it lies under threshold. Investigation [met8](#) turns out, that ro-modules are also a clasic modules, larger of them can fall to chaos and achieve Derrida level.

Similarly in ([fig.9d2,f1,2,4,5,6](#)) such extremes are visible and some gaps connected to minima. In passes M20 blue line is a sum by all passes M. Clarity of this distribution shows stability of such Derrida levels during all process of accumulation, but often a comparison to particular pass M shows some differences ([fig.9d](#)).

Collected in [fig.9g](#) examples show that such distributions on right wall not always adequately indicate ro-modules, because level of $A1$ can change, it must not be a Derrida level of chaotic behaviour and probably such ro-modules are too small to apply such statistical interpretation. It is really complex phenomenon. Even clear indicating of two peaks suggested 2 different ro-modules may be an effect of complex trajectory in one ro-module, which happened in [fig.9g4](#).

5.7 From periods of node state cycles – series of investigation clusters ‘ro’

5.7.1 Initial detailed investigation

Above few methods give not satisfying results – particular ro-modules are not seen, their existence is not proved, however each of these methods give convincing premises. Probably assumed view was too simple and particular examples need much more detailed investigations to define what should be statistically measured. This conclusion led to deep detail analysis of selected initiations. Just this arduous method allows to see ro-modules and has build new view, but yet without larger statistics. In order to understand a basis of this view one more important example of result types of several different investigations should be described.

In network trajectory collected after particular selected accumulated initiation (in particular net and pass M) in each node trajectory a cycle of states is searched and its period. Nodes with the same period create local cluster ‘ro’ – hypothetical ro-module. In one such simulation 25 consecutive accumulations after the indicated one were observed. Description of each of them contains: number of initiated node; attractor length (900 when ‘not found’); number of changed nodes in section of new attractor (similar to A4); number of frozen nodes (period=1); number of different periods>1; t of entry into attractor (min=2). More precise in [fig.15](#). Next (vertically) for node period>1: node number (as its name) and its period (in colour connected to period). If period was not found a 999 was used and set of nodes with such ‘pseudo-period’ was also treated as local cluster. In addition changed nodes in range of attractor are noted in red.

In order to select interesting initiations all 9 simulation (series 44 formulas bf,br,cf,cr ‘4+7+20, bf ‘4+7’, and 4 formulas of series 45) were searched firstly using crocodiles, later selected areas more detailed, which is here not described. In effect of latest analysis of circa 40 events in shown in [fig.15](#) method such **general conclusion are taken:**

- 1- Shift by 50 in series 44 after each accumulation is effective. Even when attractor appears in half of $tmx=1000$, then in 10 steps of accumulation its beginning is already in beginning of trajectory. Typically during this time attractor is not changed or changed very small. In effect **most of changes is imposed in attractor or near to entry to attractor.**
- 2- After explosion (calculated up to tmx) attractor is never found, typically $A4=400$, exceptionally =399 or 398 (compatible to [tab.1](#)).
- 3- **Changes typically concern only 1 node**, this initiated one (compatible to [fig.13](#)). Often it is 2 or 3, rarely more nodes. Because ice is the greater cluster, then change of frozen state into also frozen state (but another, frozen means period=1) is the most frequent and practically shift of node between active clusters (which are typically small) is not observed. **Appearance of local clusters ro typically in very similar set shows that such sets are real**, ‘faster connected’, not random – **these are searched ro-modules, global clusters ro.**
- 4- We do not expect another change of period of global cluster ro, than multiplication or division by small natural number, but **often change of period** (with small change of node set) **is an addition or subtracting of small number**, typically much smaller than period. (E.g. changes of period from 6 to 9; from 28 to 29; from 2 and 11 to 28 (connection of two clusters); from 120 and 20 to 140; from 24, 2 and 1 to 28; from 395 to 347 to 174; from 34 to 20 and 24 (disintegration); from 17 to 1 and 120.)
- 5- It happens relatively often, that **3 clusters are found, where 1 period=attractor and 2 remain are divisors of attractor**. Later history of these clusters indicates that **cluster=attractor is a common part of both remains.**
- 6- Some global clusters appear in many passes, they vanish and appear and change their periods many times. Other clusters do the same in the same net. It is picture near expected, but **number of simultaneously active clusters is very small, it rarely cross 4, typically is 2** (without ice).

This general conclusions have build some picture which should be supported by statistic results.

320 20	321 20	322 20	323 20	324 20	486 20	487 20	488 20	489 20	490 20	491 20	492 20	220 28	221 28	222 20	223 20	167 20	168 20	169 20	360 900	361 32	362 32	368 32	369 900	370 900	203 900	204 900	205 900	208 900	209 900	210 900	
1 396	4 966	39 339	15 339	1 339	5 382	3 382	3 382	1 382	14 382	14 382	1 382	1 372	3 372	33 373	1 373	1 393	6 393	1 393	1 350	40 351	2 351	1 350	40 350	1 351	1 362	4 362	1 362	2 362	2 362	1 362	
231 2	231 2	232 2	232 2	232 2	328 2	329 2	329 2	329 2	330 2	330 2	331 2	224 1	226 1	226 1	226 1	191 2	192 2	193 2	314 2	314 2	316 2	319 2	320 3	321 3	225 1	226 1	226 1	228 1	228 2	229 1	
49 2	49 3	49 5	49 2	49 2	49 4	49 2	49 2	49 2	49 10	49 7	49 2	35 2	35 2	49 9	49 2	49 2	49 3	49 2	0 1	0 1	0 1	0 1	0 1	0 1	0 1	0 1	0 1	0 1	0 1	0 1	
25 10	25 10	24 10	24 10	24 10	25 10	25 10	25 10	25 10	25 10	25 10	25 10	12 28	12 28	12 20	12 20	88 10	88 10	88 10	12 999	12 32	12 32	12 32	12 73	12 73	12 999	12 999	12 999	12 999	12 999	12 999	
33 10	33 10	25 10	25 10	25 10	33 10	33 10	33 10	33 10	33 10	33 10	33 10	57 28	25 1	25 1	49 20	88 10	88 10	88 10	29 999	29 32	29 32	29 32	29 73	29 73	29 999	29 999	29 999	29 999	29 999	29 999	
34 10	34 10	33 10	33 10	33 10	34 10	34 10	34 10	34 10	34 10	34 10	34 10	82 28	53 1	53 1	57 20	93 4	93 4	93 4	44 999	44 32	44 32	44 32	44 73	44 73	44 999	44 999	44 999	44 999	44 999	44 999	
38 10	38 10	34 10	34 10	34 10	38 10	38 10	38 10	38 10	38 10	38 10	38 10	91 28	57 28	49 20	82 20	102 4	102 4	102 4	62 999	62 32	62 32	62 32	62 73	62 73	49 999	49 999	49 999	49 999	49 999	49 999	
88 10	69 1	38 10	38 10	38 10	65 1	88 10	88 10	88 10	88 10	88 10	88 10	101 28	82 28	57 20	91 20	191 1	174 1	193 1	66 999	66 32	66 32	66 32	66 73	66 73	62 999	44 999	62 999	62 999	62 999	62 999	
92 10	88 10	48 10	48 10	48 10	88 10	91 10	91 10	91 10	91 10	91 10	91 10	103 28	91 28	82 20	103 20	286 10	189 1	286 10	82 999	82 32	82 32	82 32	82 999	82 999	66 999	49 999	66 999	66 999	66 999	66 999	
93 4	89 1	66 10	66 10	66 10	91 10	93 4	93 4	93 4	93 4	92 1	93 4	106 28	101 28	91 20	103 20	307 10	192 1	307 10	91 999	91 32	91 32	91 32	91 73	91 73	82 999	62 999	82 999	82 999	82 999	82 999	
100 10	92 10	83 10	83 10	83 10	93 4	102 4	102 4	102 4	93 4	93 4	102 4	112 28	103 28	101 20	106 20	325 10	209 1	325 10	103 999	103 32	103 32	103 32	103 73	103 73	91 999	66 999	91 999	91 999	91 999	91 999	
102 4	93 4	88 10	88 10	88 10	102 4	124 10	124 10	124 10	102 4	102 4	124 10	130 28	106 28	103 20	112 20	200 28	148 28	130 20	104 999	104 32	104 32	104 32	104 73	104 73	103 999	82 999	103 999	103 999	103 999	103 999	
104 10	100 10	92 10	92 10	92 10	124 10	141 1	141 1	230 10	107 1	107 1	230 10	148 28	112 28	106 20	130 20	286 10	286 10	286 10	106 999	106 32	106 32	106 32	106 73	106 73	104 999	91 999	104 999	104 999	104 999	104 999	
107 10	102 4	93 4	93 4	93 4	208 1	150 1	150 1	279 4	109 1	109 1	279 4	164 28	130 28	112 20	164 20	286 10	286 10	286 10	111 999	111 16	111 16	111 16	111 16	111 16	106 999	103 999	106 999	106 999	106 999	106 999	
109 10	104 10	100 10	100 10	100 10	230 10	230 10	230 10	206 10	124 10	124 10	206 10	200 28	148 28	130 20	200 20	307 10	307 10	307 10	116 999	116 32	116 32	116 32	116 73	116 73	112 999	104 999	112 999	112 999	112 999	112 999	
124 10	107 10	102 4	102 4	102 4	279 4	279 4	279 4	290 10	150 1	150 1	290 10	224 1	164 28	148 1	226 1	289 28	278 28	230 1	116 999	116 32	116 32	116 32	116 999	116 999	130 999	106 999	130 999	130 999	130 999	130 999	
126 10	109 10	103 10	103 10	103 10	296 10	286 10	286 10	286 10	182 1	182 1	307 10	263 28	200 28	164 20	263 20	290 28	284 28	263 20	125 16	125 16	125 16	125 16	125 16	125 16	148 999	112 999	148 999	148 999	148 999	148 999	
136 10	124 10	104 10	104 10	104 10	290 10	290 10	290 10	318 10	184 1	184 1	318 10	278 28	226 1	200 20	284 20	278 28	226 1	200 20	130 999	130 32	130 32	130 32	130 999	130 999	191 999	130 999	191 999	191 999	191 999	191 999	
174 10	126 10	107 10	107 10	107 10	307 10	307 10	307 10	307 10	223 1	223 1	325 10	284 28	263 28	226 1	289 20	289 28	278 28	230 1	130 999	137 32	137 32	137 32	137 73	137 73	196 999	148 999	196 999	196 999	196 999	196 999	
180 10	136 10	109 10	109 10	109 10	318 10	318 10	318 10	329 1	230 10	230 10	331 1	289 28	278 28	230 1	290 20	290 28	284 28	263 20	141 16	141 16	141 16	141 16	141 16	200 999	191 999	200 999	200 999	200 999	200 999	200 999	
184 10	174 10	124 10	124 10	124 10	325 10	325 10	325 10	383 10	279 4	279 4	383 10	290 28	284 28	263 20	303 20	303 28	289 28	278 1	150 16	150 16	150 16	150 16	150 16	211 999	196 999	211 999	211 999	211 999	211 999	211 999	
194 10	180 10	126 10	126 10	126 10	328 1	329 1	329 1	388 10	286 10	286 10	388 10	303 28	289 28	278 1	306 20	306 28	290 28	284 20	178 16	178 16	178 16	178 16	178 16	225 999	200 999	225 999	225 999	225 999	225 999	225 999	
211 10	184 10	136 10	136 10	136 10	383 10	383 10	383 10	290 10	290 10	290 10	388 10	306 28	290 28	284 20	312 20	312 20	312 20	312 20	182 16	182 16	182 16	182 16	182 16	278 999	211 999	226 1	226 1	226 1	226 1	226 1	
218 10	193 1	151 10	151 10	151 10	388 10	388 10	388 10	307 10	307 10	307 10	331 1	312 28	303 28	289 20	332 20	332 28	306 28	290 20	191 999	191 32	191 32	191 32	191 999	191 999	284 999	225 999	278 999	234 1	234 1	278 999	
223 10	194 10	174 10	174 10	174 10	307 10	307 10	307 10	318 10	318 10	318 10	330 1	332 28	306 28	290 20	340 20	340 28	312 28	303 20	196 999	196 32	196 32	196 32	196 73	196 73	287 999	226 1	284 999	278 999	278 999	284 999	284 999
231 1	211 10	180 10	180 10	180 10	318 10	318 10	318 10	325 10	325 10	325 10	331 1	340 28	312 28	303 20	344 20	344 28	332 28	306 20	200 999	200 32	200 32	200 32	200 73	200 73	289 999	230 1	287 999	284 999	287 999	287 999	287 999
236 10	218 10	182 10	182 10	182 10	325 10	325 10	325 10	329 1	329 1	329 1	331 1	344 28	332 28	306 20	361 20	361 28	340 28	312 20	216 16	216 16	216 16	216 16	216 16	290 999	278 999	289 999	289 999	289 999	289 999	289 999	
238 10	223 10	184 10	184 10	184 10	329 1	329 1	329 1	330 1	330 1	330 1	331 1	361 28	340 28	312 20	370 20	370 28	344 28	332 20	225 999	225 32	225 32	225 32	225 999	225 999	306 999	284 999	289 999	289 999	289 999	289 999	
243 10	231 1	187 10	187 10	187 10	330 1	330 1	330 1	350 1	350 1	350 1	350 1	370 28	344 28	332 20	382 20	382 28	361 28	340 20	259 999	259 32	259 32	259 32	259 999	259 999	312 999	289 999	312 999	312 999	312 999	312 999	
262 10	236 10	194 10	194 10	194 10	350 1	350 1	350 1	359 1	359 1	359 1	359 1	382 28	361 28	340 20	395 20	395 28	370 28	344 20	284 999	284 32	284 32	284 32	284 73	284 73	321 999	290 999	318 999	318 999	318 999	318 999	
274 10	238 10	211 10	211 10	211 10	356 1	356 1	356 1	381 1	381 1	381 1	381 1	398 28	382 28	361 20	398 20	398 28	370 28	344 20	285 999	285 32	285 32	285 32	285 73	285 73	332 999	306 999	321 999	318 999	318 999	321 999	
284 10	243 10	218 10	218 10	218 10	381 1	381 1	381 1	383 10	383 10	383 10	383 10	395 28	370 28	344 20	395 20	395 28	370 28	344 20	289 999	289 32	289 32	289 32	289 999	289 999	333 999	312 999	332 999	321 999	321 999	321 999	
286 10	262 10	223 10	223 10	223 10	383 10	383 10	383 10	383 10	383 10	383 10	383 10	398 28	382 28	370 20	398 20	398 28	382 28	370 20	290 999	290 32	290 32	290 32	290 73	290 73	340 999	318 999	333 999	332 999	332 999	332 999	332 999
290 10	274 10	224 10	224 10	224 10	383 10	383 10	383 10	383 10	383 10	383 10	383 10	398 28	382 28	370 20	398 20	398 28	382 28	370 20	306 999	306 32	306 32	306 32	306 73	306 73	344 999	321 999	340 999	333 999	333 999	333 999	333 999
292 10	284 10	227 10	227 10	227 10	383 10	383 10	383 10	383 10	383 10	383 10	383 10	398 28	382 28	370 20	398 20	398 28	382 28	370 20	312 999	312 32</											

5.7.2 Local and global clusters on example bf 103 from series 44 ‘4+7+20’

Stability of global cluster which may disappear and appear after long time is an especially important remark. Investigations of this phenomenon are especially onerous, therefore attempts were taken to automate them which give hope on statistic support. Definition of global cluster by indication of rules which local clusters belong to it is very complex and really fuzzy due to many aspects, variants and circumstances. In fig.16 are shown two conceptions. Conception based on visual show of such clusters existence is not good for statistic investigations. Second conception bases on connection of local clusters to the most similar global cluster or (if is no similar enough) creating a new global cluster. More precise description contain fig.16.

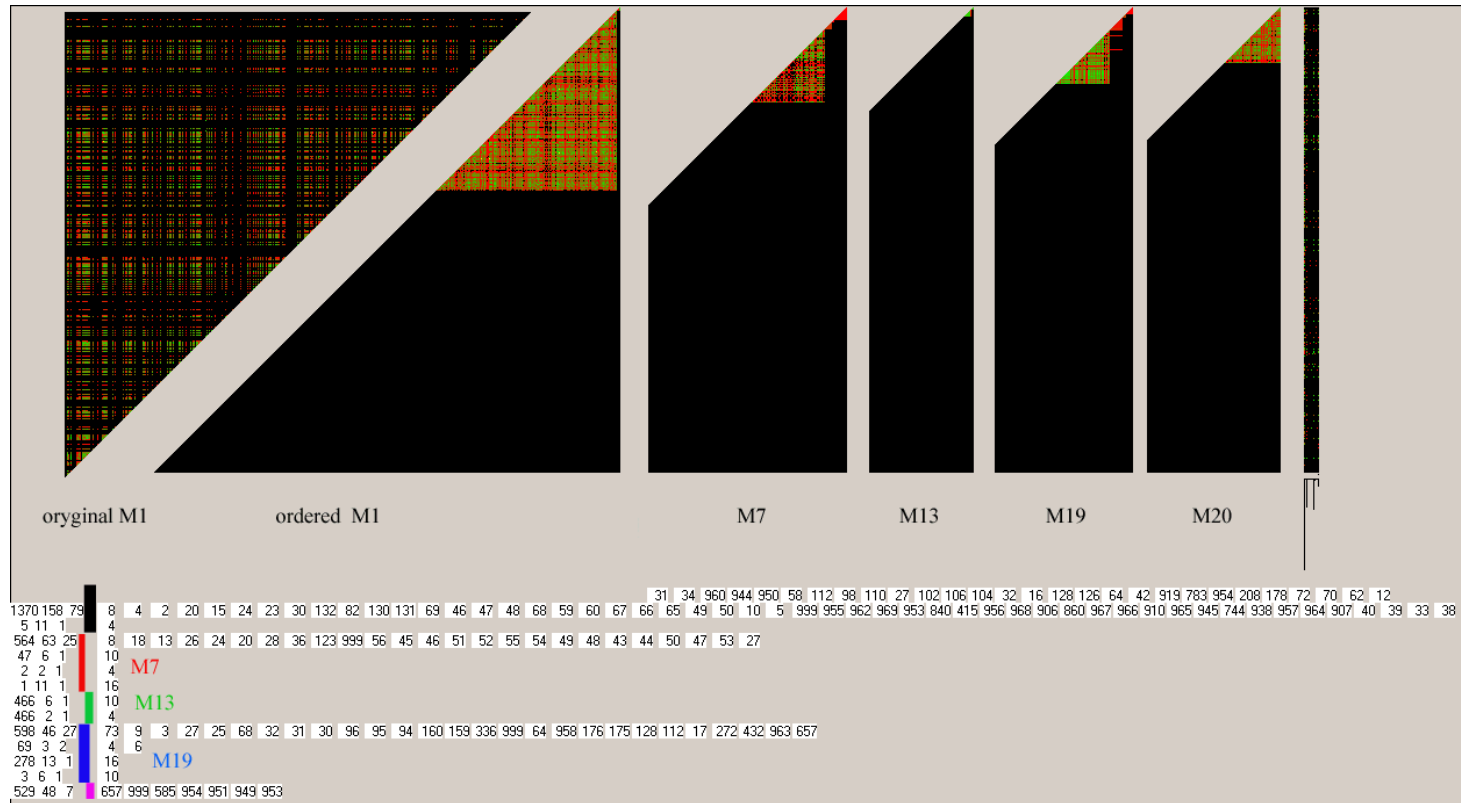


Fig.16. Correlative analysis of clusters on example bf 103 from series 44 ‘4+7+20’, (analysed before in fig.15, 7a & 7e. In table 400*400 build from the beginning of passes free 1 is added if both nodes participate in common local cluster, then table is symmetric and on the main diagonal number of node activity is recorded. Here ice is not a local cluster but lack of period is. The table for M1 is shown in original form (name is a position of node) .Black pixel means 0. Next nodes are ordered – first with 0 on diagonal. Next the greatest value in diagonal is found and in turn all its ‘companions’ in any local cluster. The last procedure is repeated up to end. In effect for particular pass free colour triangles are created in upper part of diagonal. Each the triangle shows a global cluster which is interpreted as ro-module. The second version of global clusters (further developed) effects

from connection of local cluster to global cluster if their similarity > 1/2 and is the biggest. Similarity = (number of common nodes + period in current set) / (number of nodes in local cluster). In this fig. global clusters found in consecutive passes free are indicated by colours. To the right periods are listed, on the left numbers of: appearance of global cluster; nodes in this glob.cl.; periods. As is seen in M13 always 2 the same local clusters (therefore also 2 global cluster) with periods 4 & 10 (see fig.15) are present. The picture for M1 seems to be inadequate, also in M19 first cluster contains 2 known local clusters simultaneously present. In next investigation such global cluster is divided – it is deactivate and two new global clusters are created.

It turns out that division of global cluster should be added when it is found that it is assembled from two simultaneously present local clusters. The investigation was done in several variants, including watching of global clusters in whole process of all passes M, but for many reasons the main results are for each of free passes separately.

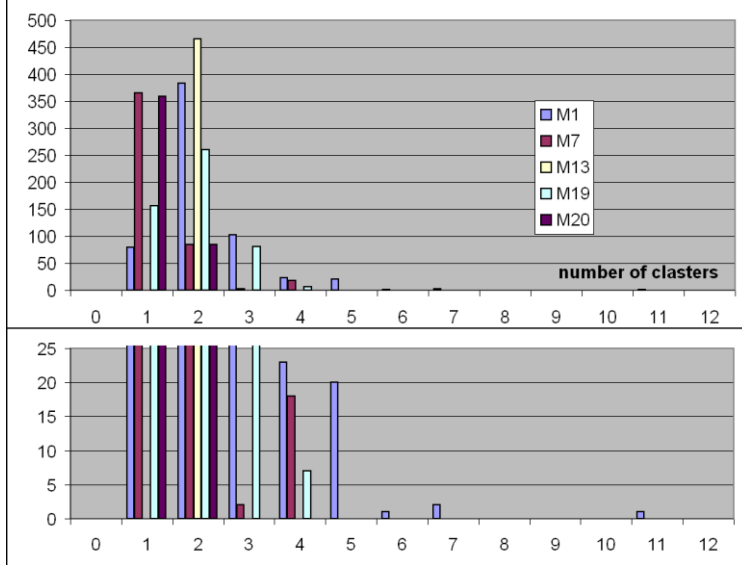
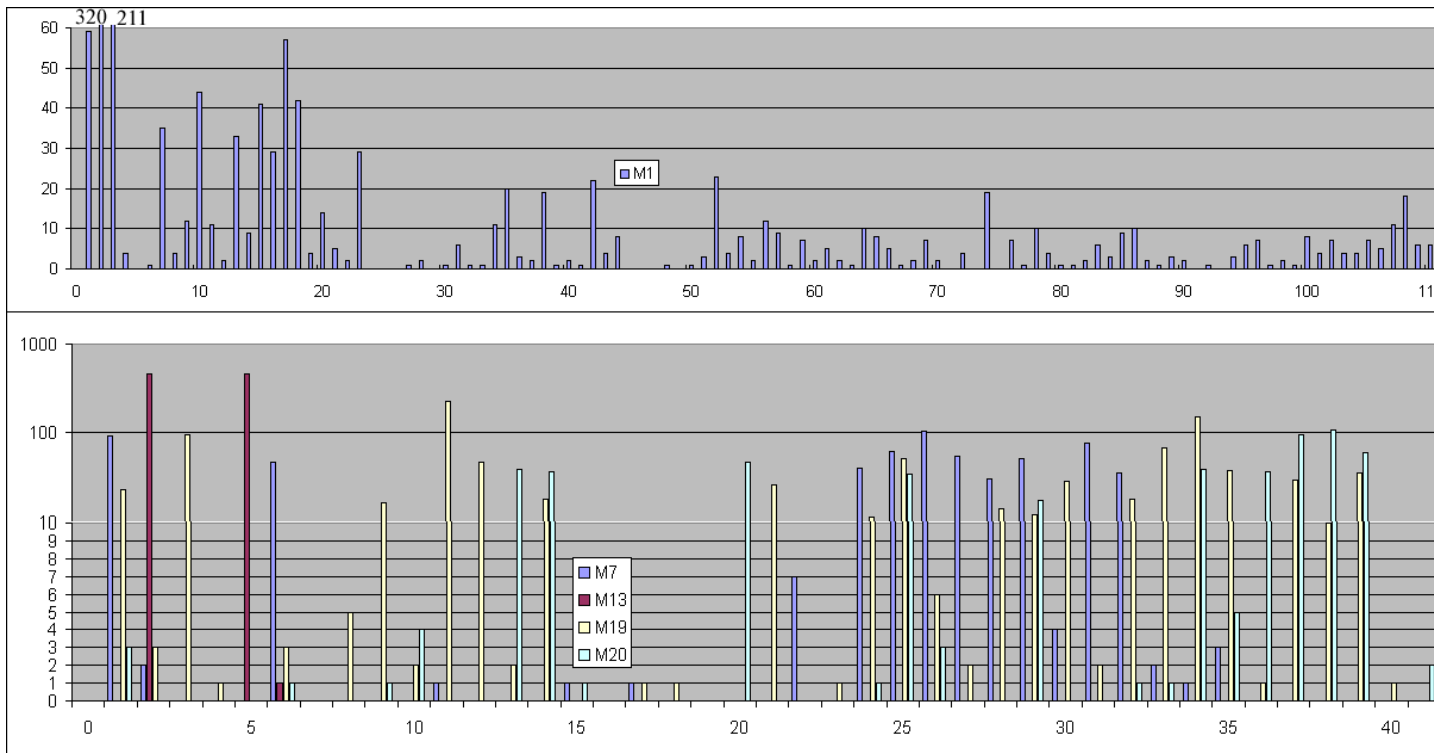
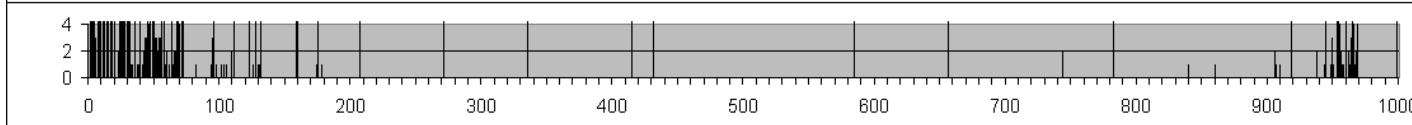
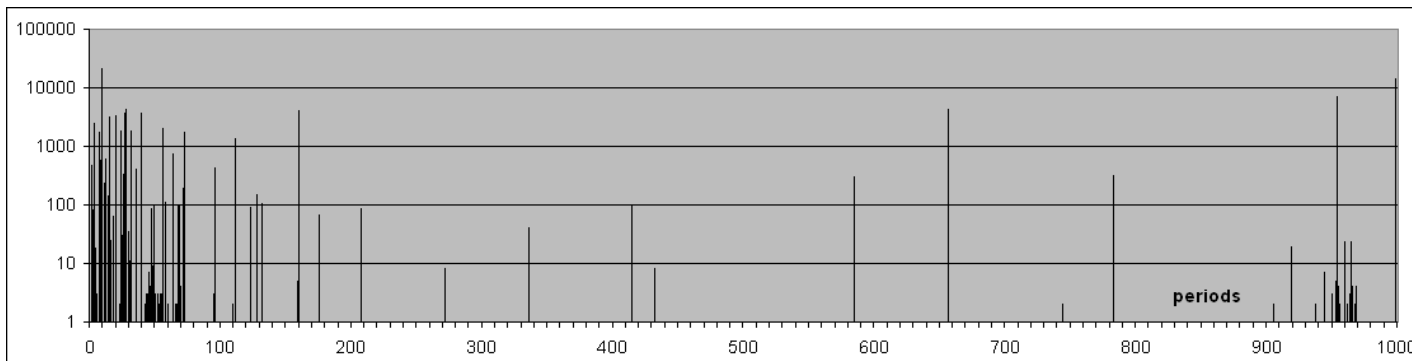
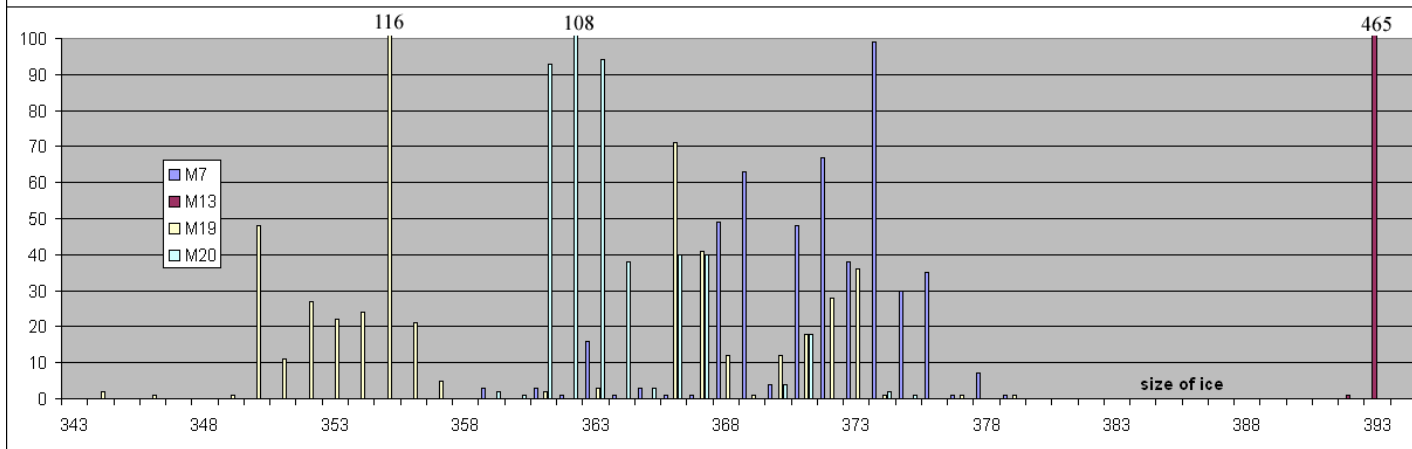
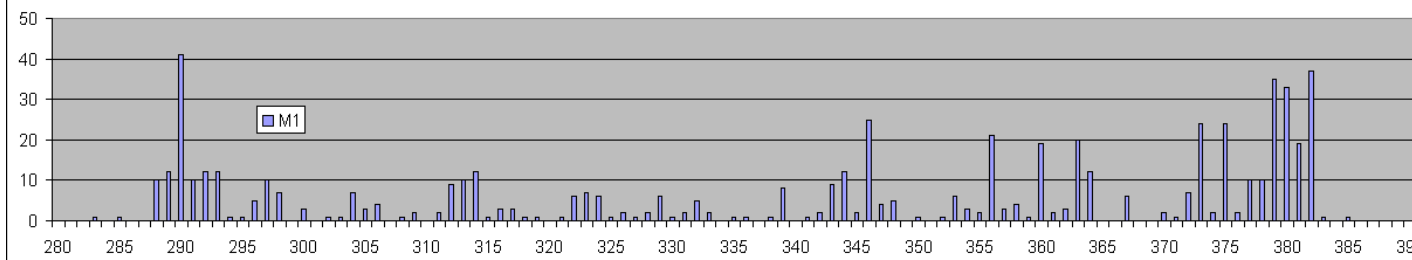


Fig.17. Examples of other analyses results. Distributions for bf 103 from series 44 of:
 (a) number of local clusters (different periods) in one accumulation in dependency on M.
 (b) local cluster size in dependency on M.
 (c) ice cluster size (period=1, i.e. lack of node state changes) in dependency on M..
 (d) periods , exact list of periods in fig.16.

(a) number of local clusters (different periods) in one accumulation in dependency on M.
 Interesting aspects: range of the parameter and typical view in dependency on advancement level of accumulation process which is measured by M.
 At the beginning of evolution, in M1 the number of local clusters has the biggest dispersion, which decreases gradually. Number 0 does not happened because PAS is excluded. Despite great numbers distributions for different M are very different which effects from specificity of particular network.



(b) distribution of local cluster size in dependency on M.
 Due to different range it is divided for M1 and remaining passes free. Out of shown range there is no counts.
 For passes M7 to M20 in the range from 10 log scale is used but lower range is shown in linear scale. Similarly to (a) the strongest influence comes from specificity of particular network.



(c) distribution of ice cluster size (period=1, i.e. lack of node state changes) in dependency on M. It is also divided for M1 and remaining passes free and it also depends on specificity of particular network. One great value for M13 is an effect of only 2, always the same local clusters in this pass (see fig. 15 & 16). In this aspect clusters M7, M19 i M20 are similar, but M1 has lot of local clusters variants, which is seen in fig.15 & 16 and 17a & b. As further data will show, it is not specific for bf 103.

(d) distribution of periods for whole evolution of particular net bf 103 from series 44. Exact list of periods in fig.16. It also strongly depends on specificity of particular network. Surprising crowd near 960 may effects from limitation of control of next revolution of node cycle.

5.7.3 Series ro 44 '4+7' 100 M20, statistical investigations

Problem of proving of presence of ro-modules as a base of stability was taken from the beginning of met5 investigation, already in series 44, but these attempts give no satisfactory results. However, strong premise described in ch.5.6 have been collected. Shown above (ch.5.7.1 & 2) detailed investigations give fast basis, but there is no yet statistical results which can be show as a simple clean proof. This need leads to new simulation series.

Detail investigations answer on few questions which previously suggest other new series '46': way to entry to attractor was problem in series 45, but not in 44; too high complexity of series 44 '4+7+20' may be reduced by resignation of attractor length threshold 20, but blockade of smearing should remain. In such a reason, new series is a small modification of series 44 '4+7' in range of rule, but significant extension in watching of particular parameters of process. In range of rules condition of 200 nets is replaced by 100 reached M20 what is important especially for cr. New series, which should be treated as the main of met5, get symbol: met5 ro 44 '4+7' 100M20.

Results of this new series are identical to earlier described results in ch. 5.4 for series 44 '4+7+20' 200 nets and '4+7' 100 nets. Small differences are described in ch.5.4 in fig.4a & 5a. More precise data allow to clear problem shown in fig.6. **Statistical basis of ro-modularity view are the basic new results of this series. They are shown in fig.18 & 19 together with descriptions**, which are not repeated in text. In fig.18 examples of simulation results of particular nets of all formulas are shown. They contains collections and history of global clusters and their graphical version in pass M20. This picture give view what is summarised in later shown statistical results in fig.19. The rules of global clusters watching are the main problem of these results. The rules are based on similarity, but it has some measure which takes under consideration lot of debatable criterions. It is not important how much it is elaborated, a relatively simple rule gives outlook of the phenomenon that global clusters – ro-modules exist. Statistical results shown in fig.19 are mainly useful for view creation about scales of various parameters of this phenomena and better intuition of mechanisms.

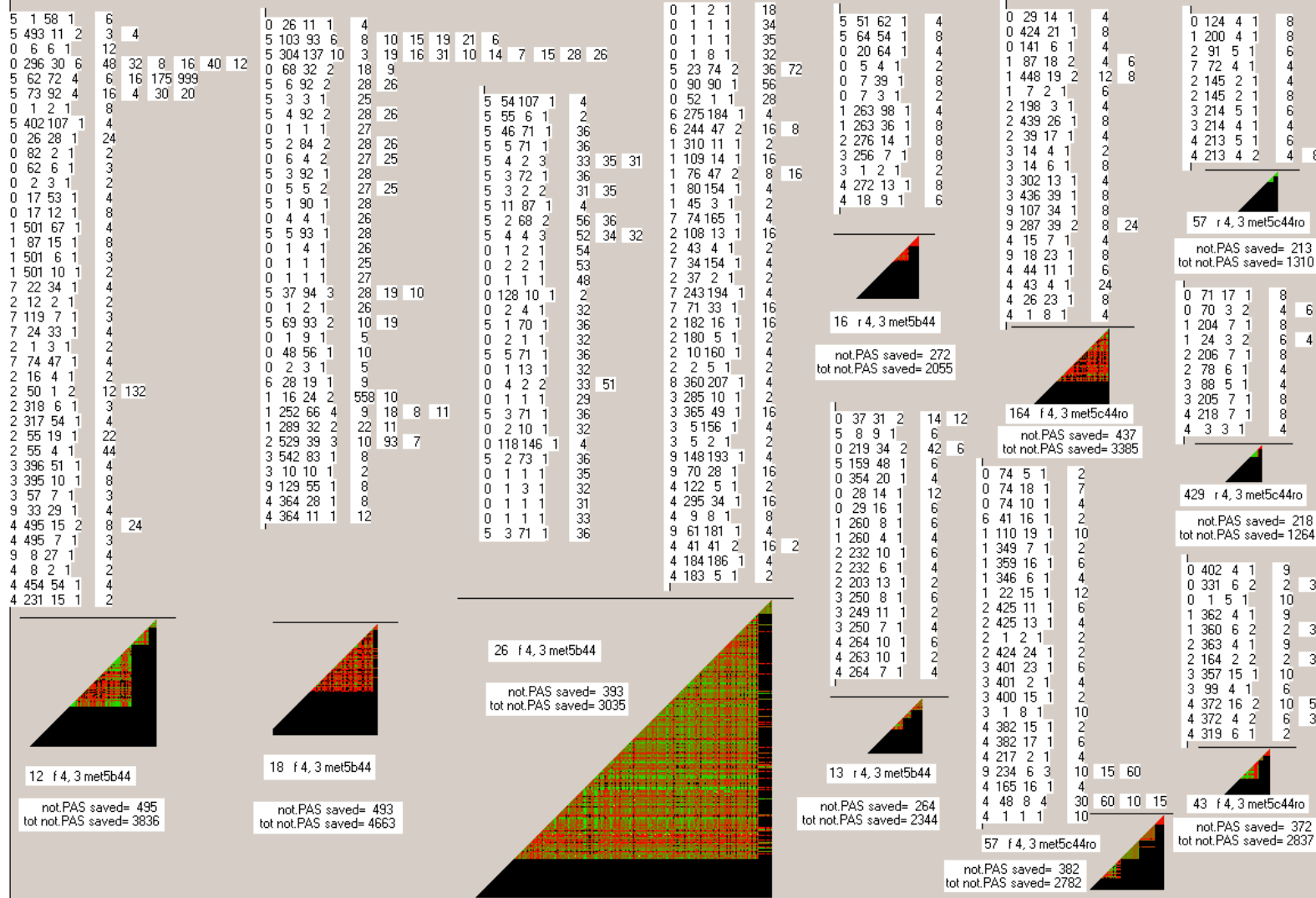
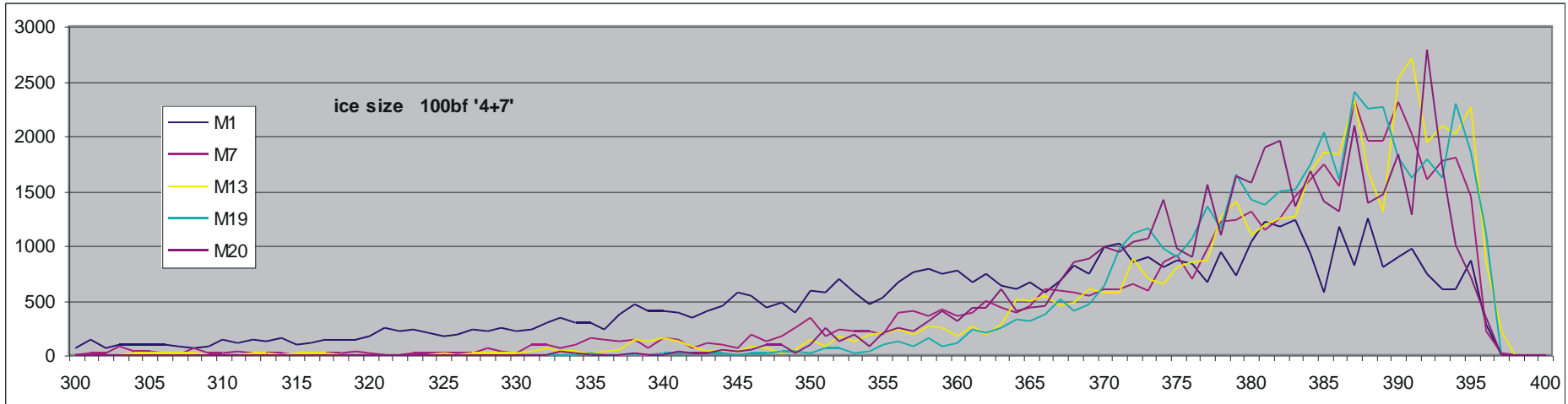
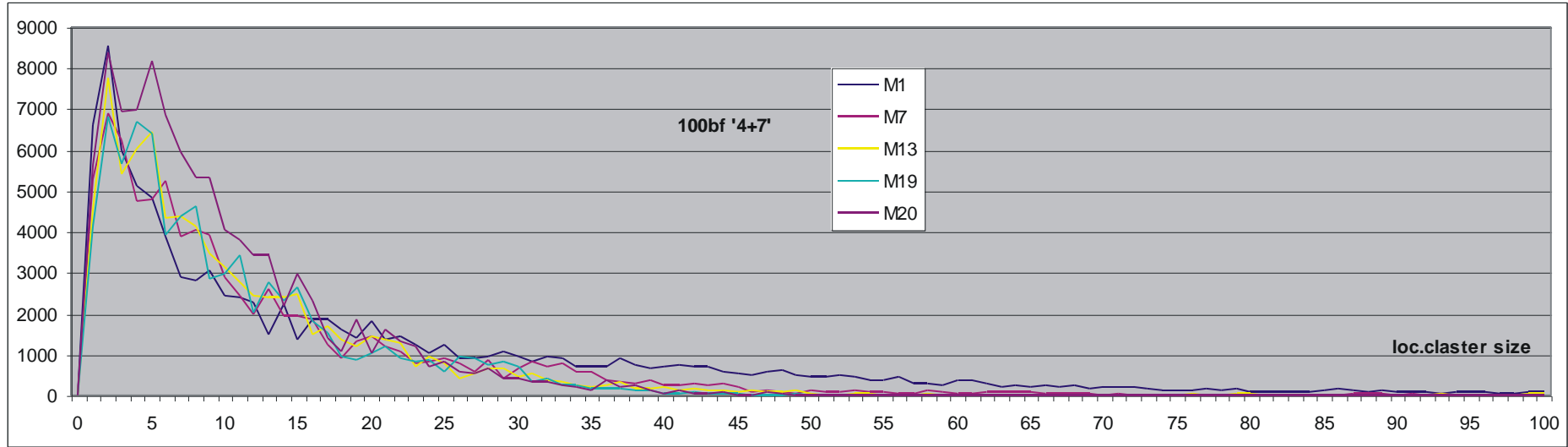


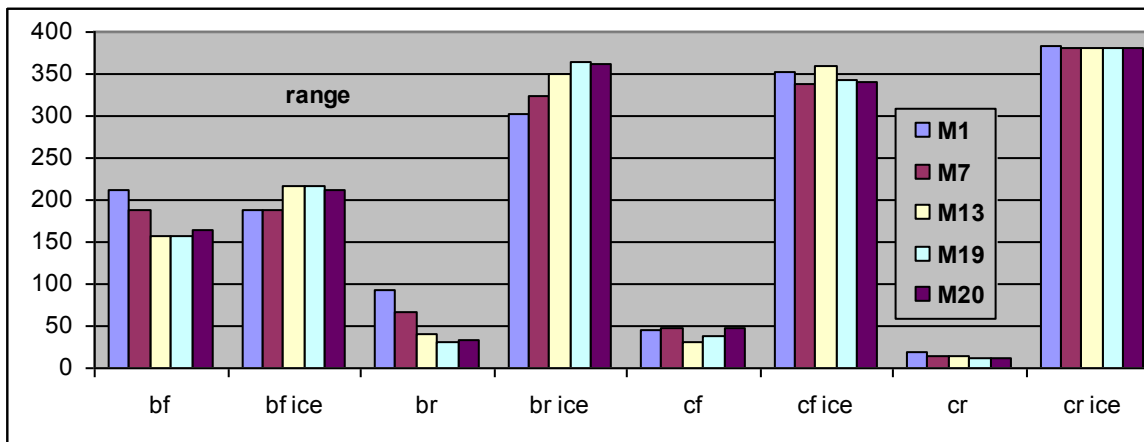
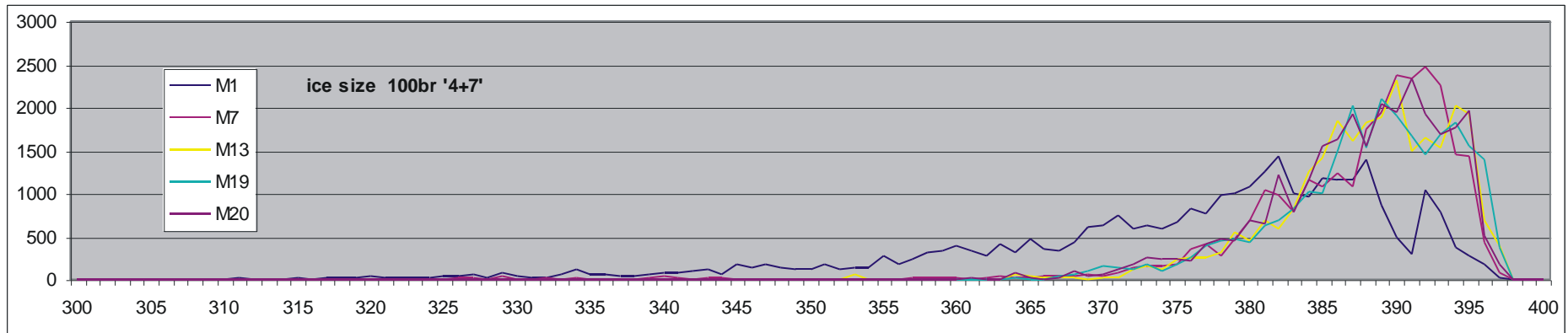
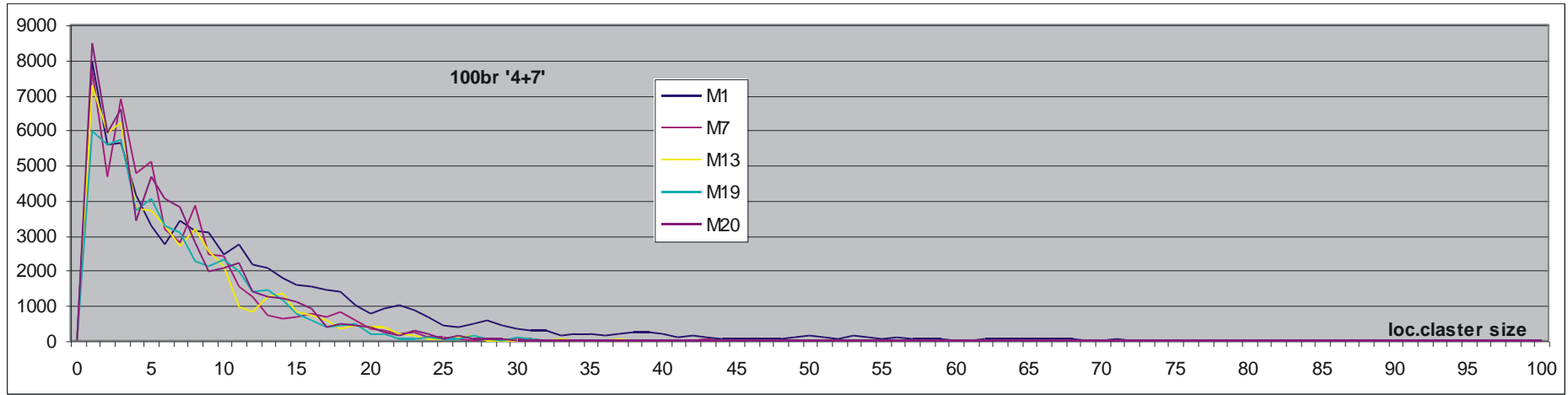
Fig. 18. Examples of history of global clusters watching in series ro 44 '4+7' and graphical pictures of global clusters in M20 basing on common local clusters. First 4 numbers: 1- pass free (0 – M1, 1-M7, 2-M13, 3-M19, 4-M20). If this global cluster turns to be assembled of two simultaneous local clusters, then it becomes inactive which is denoted by adding 5.) 2- number of appearances in this pass free. For M20 it cannot be greater than number of accumulation (not PAS saved=), below it number of all accumulations from the beginning of pass N1 to end of pass M20. 3- number of nodes in this global cluster. 4- number of different periods. These periods are then listed to right. Triangles are shown only in range of active nodes (see fig.16) always in the same scale – one pixel shows common presence of 2 nodes in local cluster. For identification line with number of net, net type, s,K and series (ro is omitted). In the event 12bf (12 f 4, 3 met5b44) in M1 first and second clusters disintegrated but can be shown: on which two. First after 1 appearance (58 nodes), second after 493 times of appearance (11 nodes). Early clusters in pass have greater chance to divide, which is visible in third example (26bf). In M20 of this (26bf) net 2 clusters (second and third) appear 495 times, i.e. in each accumulation.

Fig.19. Results of series met5 ro 44 '4+7' 100M20 in a range of statistics of local and global clusters which create ro-modularity – type of half-chaos state based on mechanism of ro-modularity.

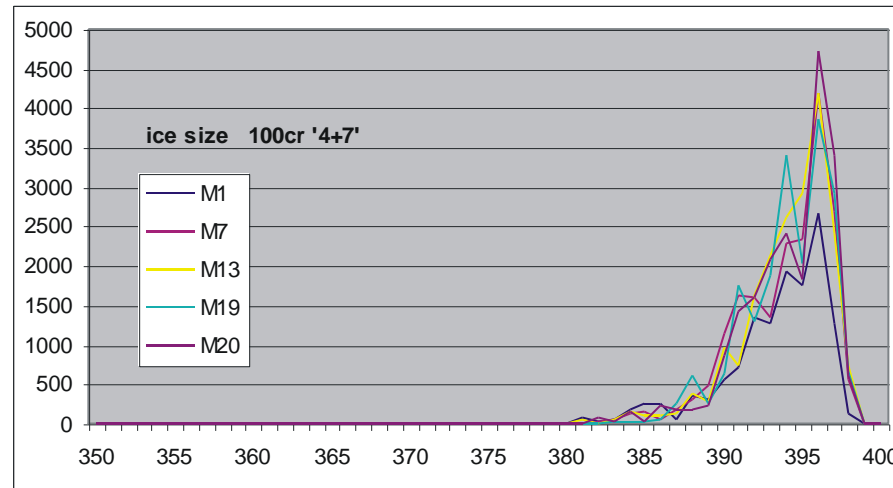
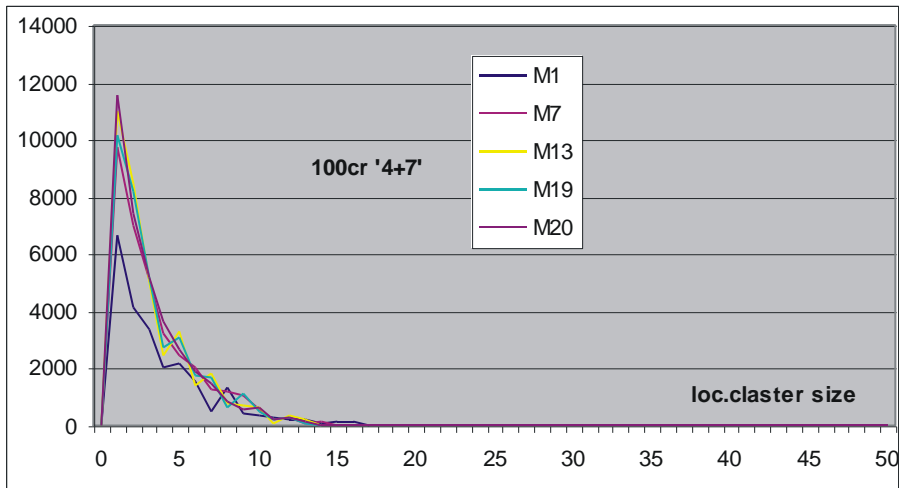
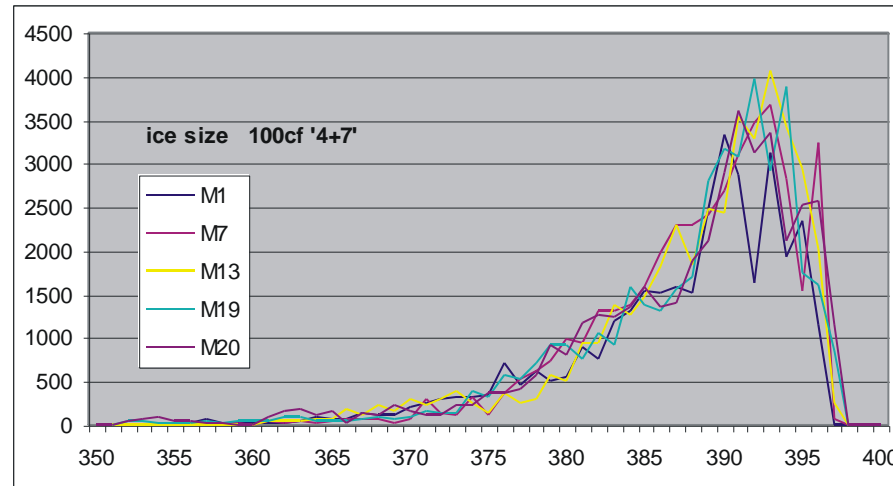
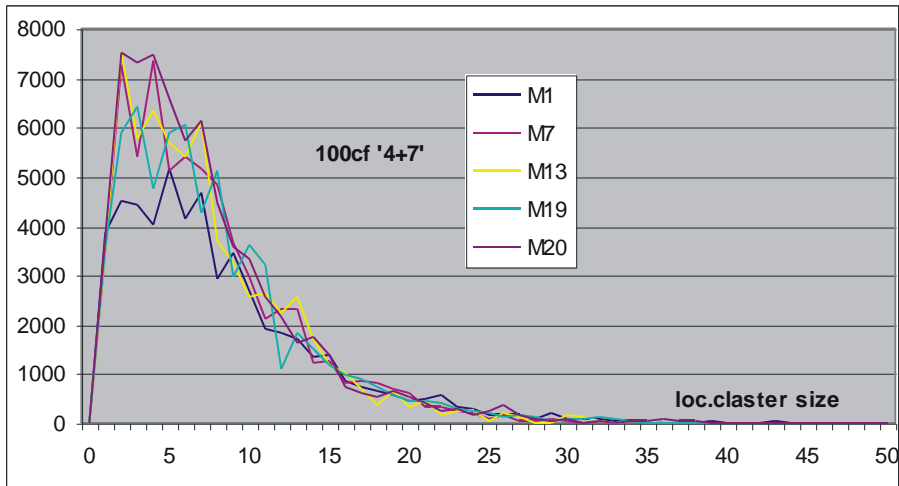
- (a) – Distributions of size of local clusters and ice for formulas bf,br,cf,cr in dependency on M - passes free describing level of advancement of shift from PAS0.
- (b) – Average size of local clusters and ice and average number of local and global clusters for formulas in dependency on M.
- (c) – Distributions of numbers of local clusters for formulas in dependency on M.
- (d) – Distributions of numbers of periods in global clusters for bf in dependency on M and average number of periods for formulas.
- (e) – Distributions of periods for formulas bf,br,cf,cr from M1-20, for model b also from M7-20 because M1 is different.



(a) – Distributions of size of local clusters and ice for formulas bf (above),br,cf,cr (below) in dependency on M - passes free describing level of advancement of shift from PAS0. In case of bf ranges of distributions are greater, i.e. tails are cut. The ranges are shown below in separate figure.

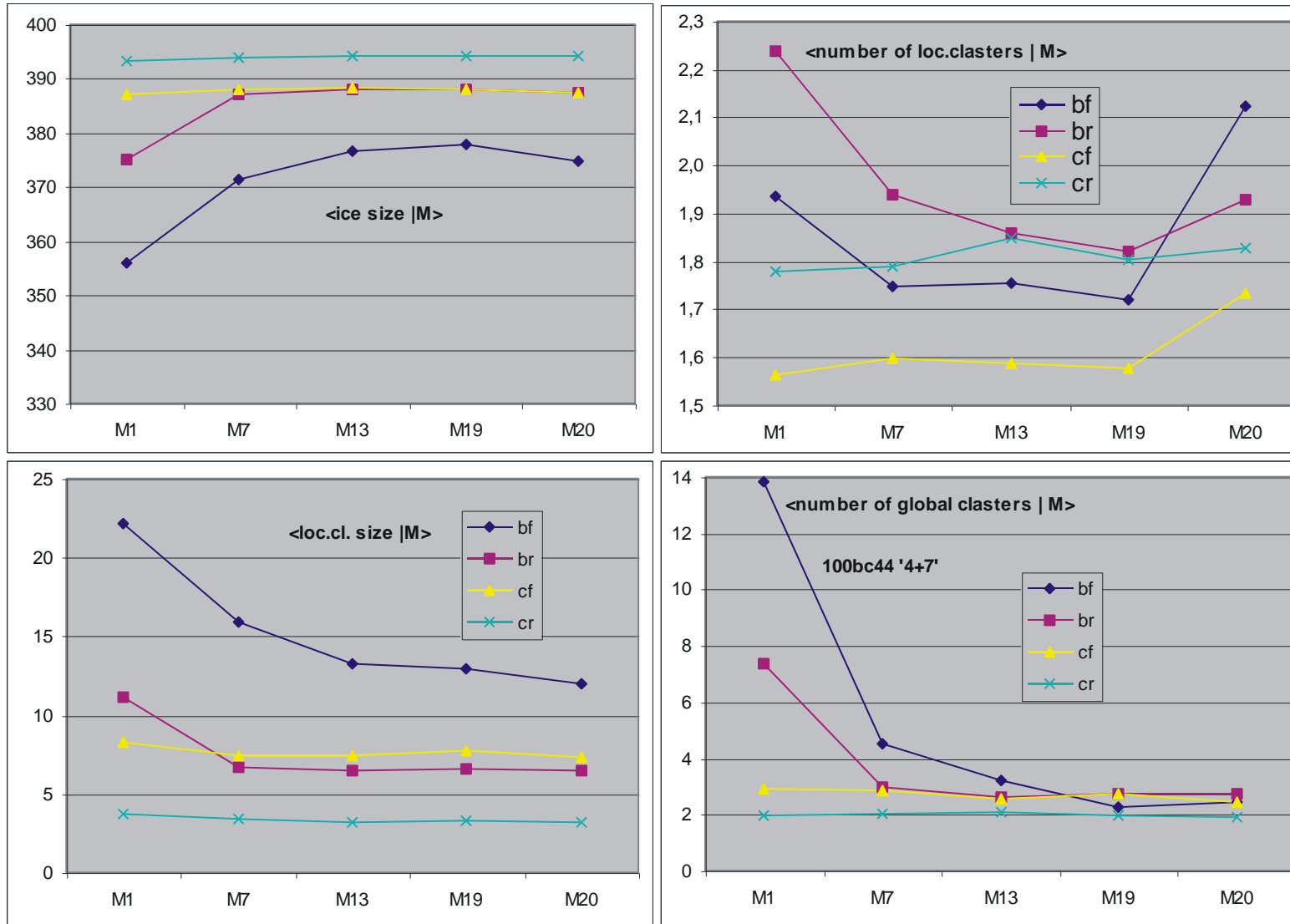


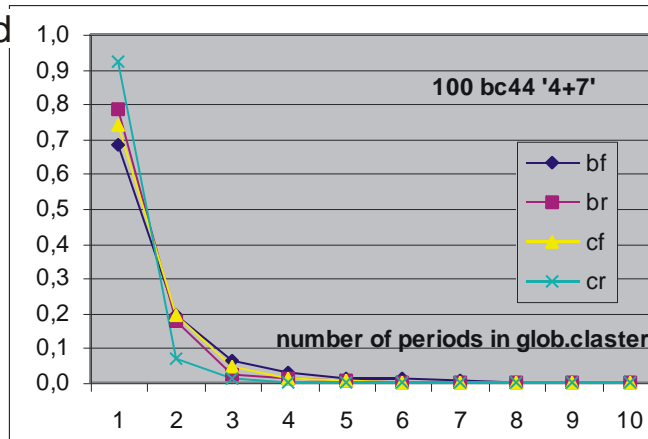
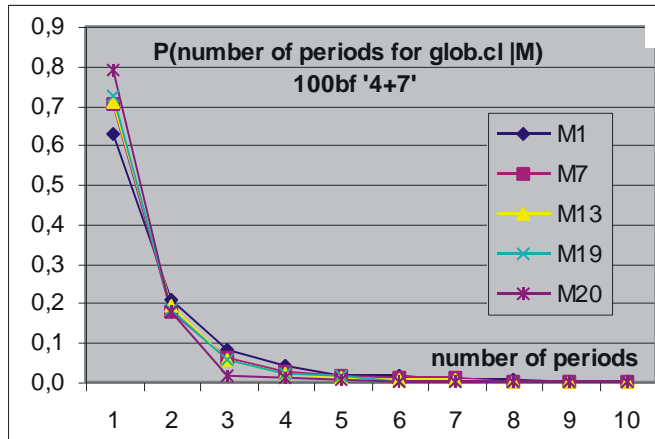
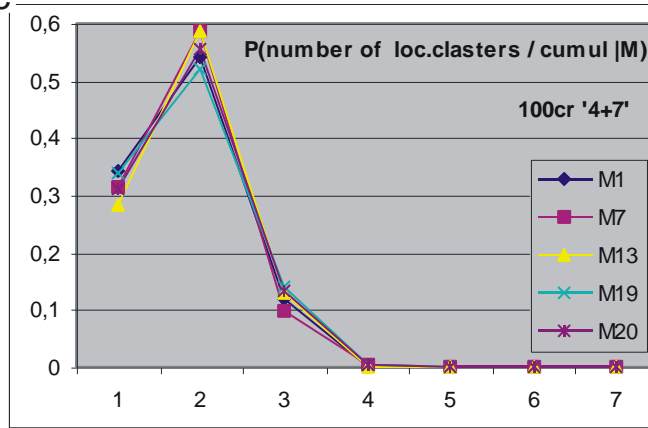
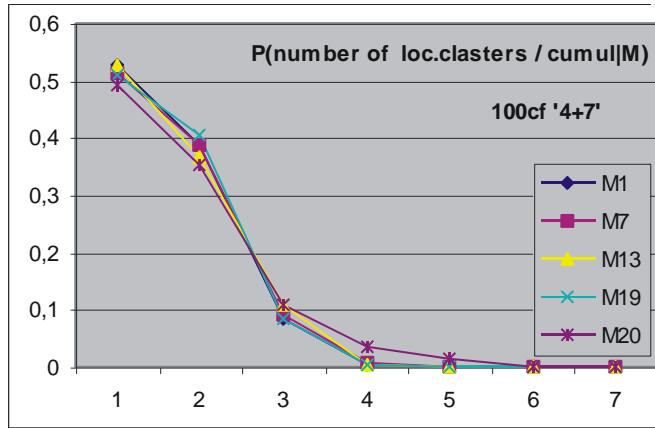
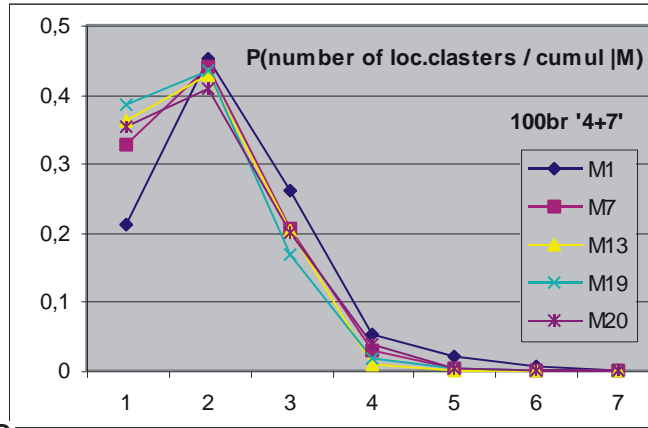
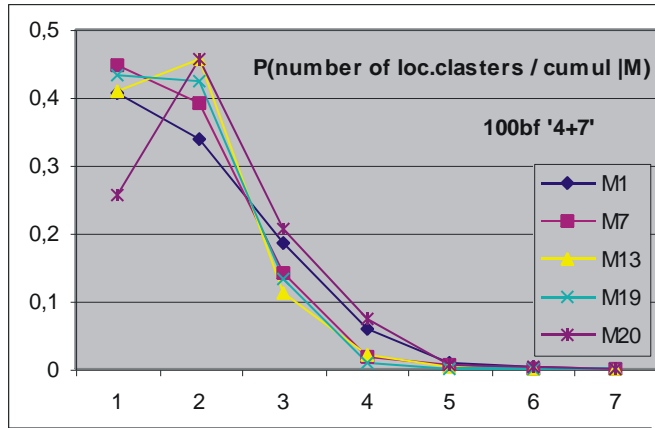
Range of sizes of local clusters and ice. It is first point where counts in tail is greater than 5. For cluster the range is from 0 to indicated value but for ice it is from the value to top=400. As is seen, only in bf M1 ice and clusters overcome, in remaining cases is a gap. Distributions above not always are full, e.g. in bf the tails are cut.



(b) – (below) Average size of local clusters and ice (in left) and average number (in right) of local (upper) and global (lower) clusters for formulas bf,br,cf,cr in dependency on M.

Distributions of size of local clusters and ice are shown above in (a). Because typically number of local clusters is near 2, then sum of average ice and average local cluster size does not give 400. For pass M1 in model b the number of global clusters is especially high. This initial diversity later vanish and all formulas end on number 2. Average number of local clusters also go to circa 1.7, but in M20 this average number rapidly grows. Forced ‘not to decrease’ of attractor length is the only difference to M19 then it is the cause.



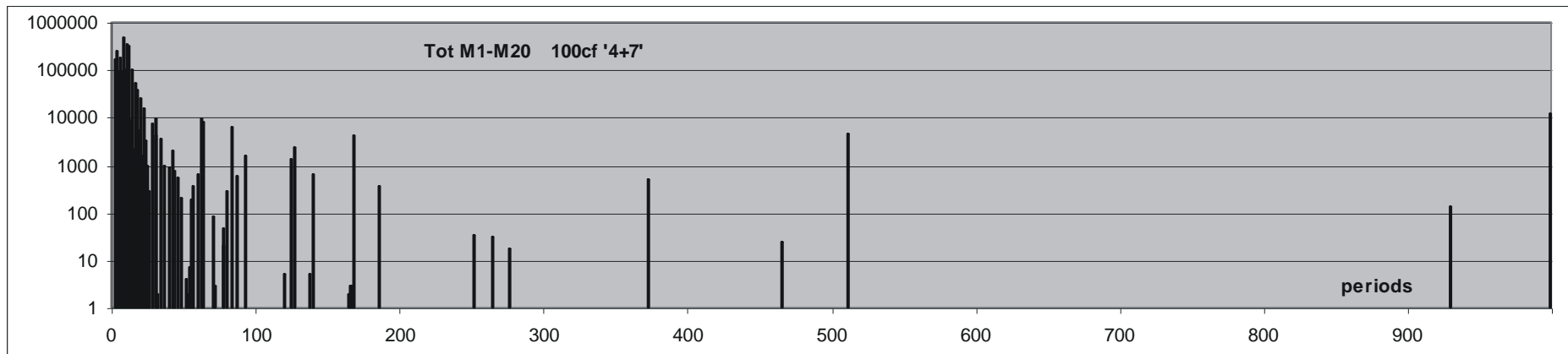
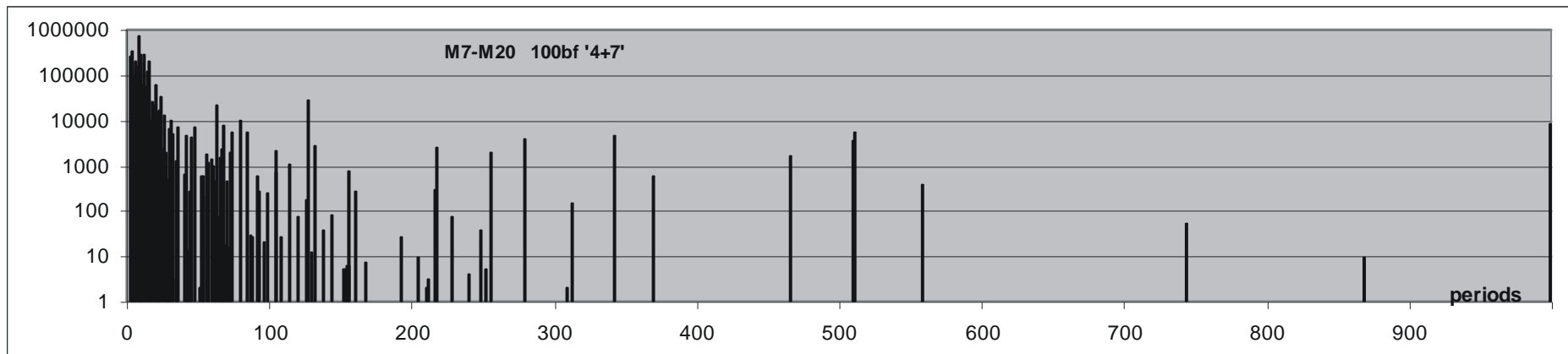
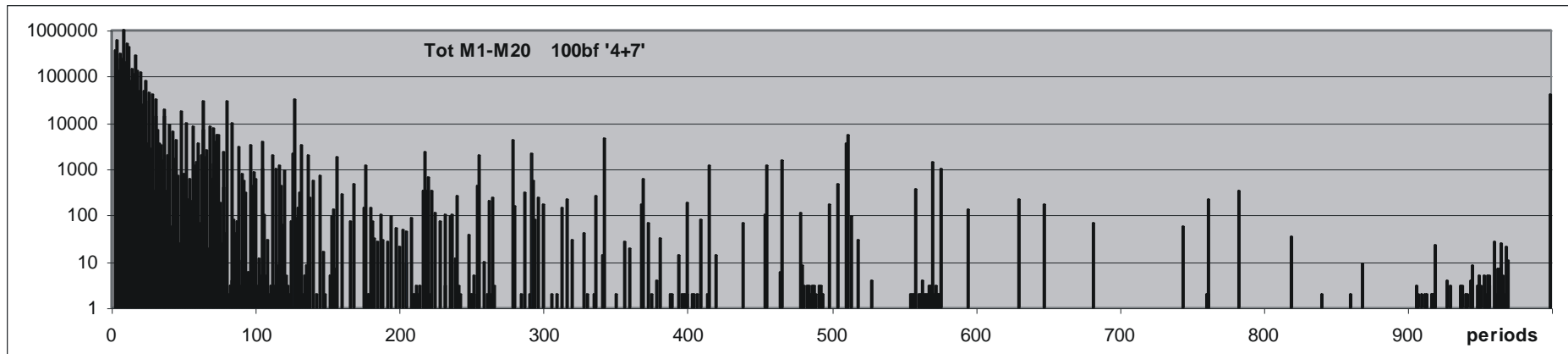


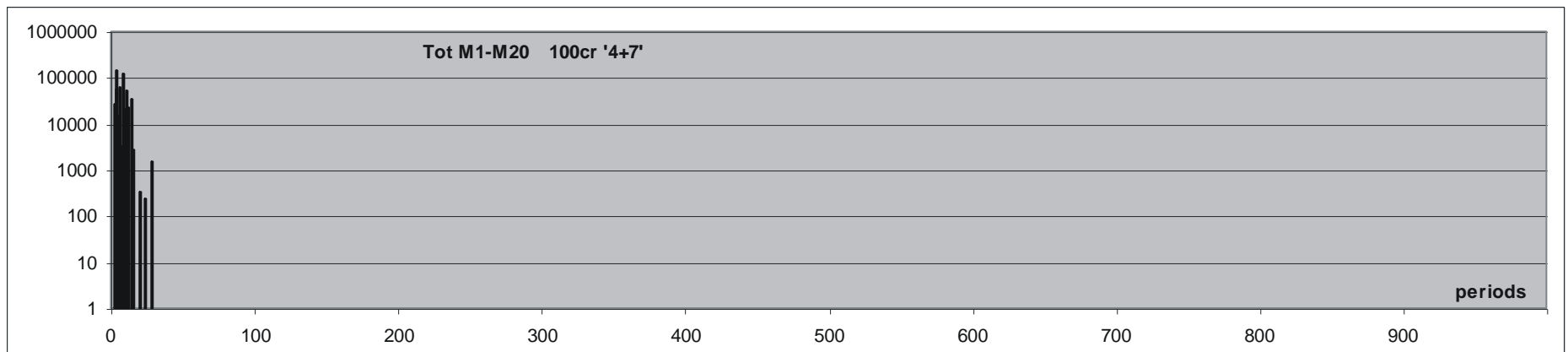
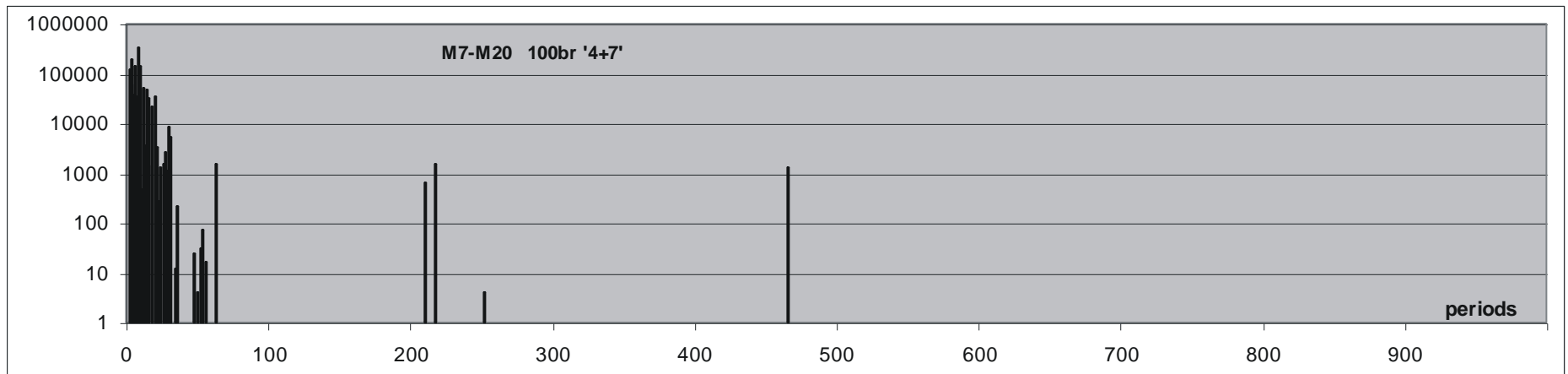
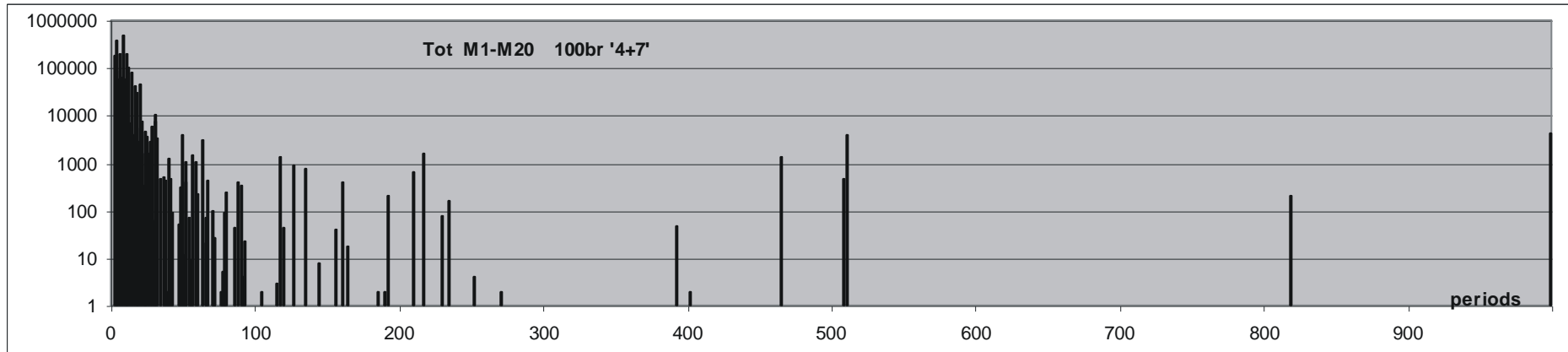
(c) – Distributions of numbers of local clusters for formulas bf,br,cf,cr in dependency on M.

Picture for formulas differ significantly. Net type have the strongest influence, next model but pass excluding M1 – the smallest.

(d) – Distributions of numbers of periods in global clusters for bf in dependency on M (in the left). It is a case of formula with the biggest differences between passes, therefore for remaining formulas these distributions are omitted, only showing averaged by M distributions of average number of periods for formulas bf,br,cf,cr (in the right). Here formula cr is extreme.

(e) – (below) Distributions of periods for formulas bf, cf, i br, cr from M1-20, for model b also from M7-20 because M1 is significantly different. Attention should be put that cr and bf are extreme.





5.8 Conclusion and summary

The main aim of investigations met5 was proving that long accumulation of small changes (small effects of small initiations) does not lead out of state ‘half-chaos’ found in met4 for point attractor, in which characteristic for chaotic network peak (in damage size distribution) of large damage in Derrida equilibrium and left peak of very small damage characteristic for ordered network are simultaneously present and contain similar part of results of small initiations. Such the picture is shown in fig.20, which is a sum of results from passes free M7,13,19 i 20 in series ro 44 ‘4+7’. Pass M20 100 nets and with numbers of accumulated in formulas bf,br,cf,cr respectively: 408693, 236527, 328056, 171677. These changes are selected to direct process in opposite direction to needs of safe stability (without return to PAS, even to attractor<7). Assembling of data in fig.20 from indicated section of process is based on their practical identity (fig.4a), way to this stable state in passes N1 to M1, also not free passes M, where results are disturbed by blockade of smearing (fig.4b) is neglected.

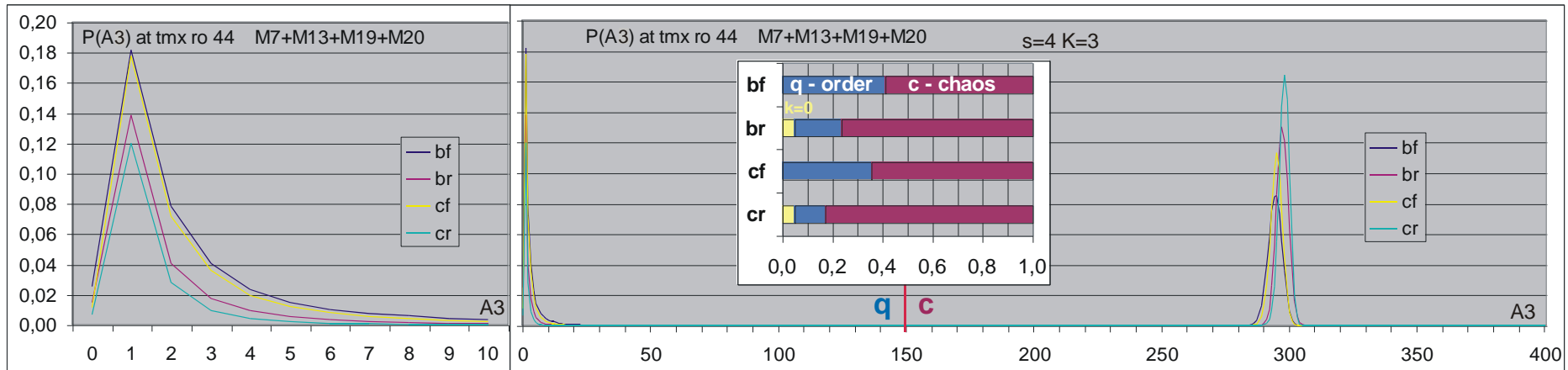


Fig.20. Two peaks in damage size distribution. Series ro 44, ‘4+7’ 100M20, passes free M7,13,19 & 20. Variant ‘4+7+20’ gives visually identical results. Left peak for very small effective changes of function contain ordered events. Right peak contains classic chaotic events of Derrida equilibrium. Both these types of reactions on small disturbance exist here simultaneously in one net created starting from PAS by accumulation of small (up to half of Derrida level, threshold ‘q|c’) changes. In addition return to attractor smaller than 7 is not accumulated. In passes between indicated passes free blockade of smearing is used. Remaining parameters, as node connections, functions and states (excluding initial force of PAS0 (model c & b) and minimal initial regulation (model b)), are random. In the figure a diagram of chaos and order proportion is included, where is clearly seen that degree of order q is similar to degree chaos c. For r network a part of the order (yellow) is an effect of blind nodes i.e. without output (k=0).

Presence of right peak – Derrida equilibrium shows chaotic character of network. Random network with used here parameters s=4, K=3 is strongly chaotic. One acceptance of chaotic change (of small change of function in one node which leads to large damage) is enough to network become typical chaotic. However, presence of left peak, which contains respectively for formulas bf, br, cf, cr: 41, 24, 36, 17 % of all initiations (which is shown in diagram of proportion of order q and chaos c included in fig.20) shows possibility of long biological evolution of such the network. This experiment proves (see fig.4a, fig.5a, 8 & 10a) that accumulation of small changes does not lead to vanish of left peak and full fall to chaos, and shown proportion of order and chaos degrees are stable with enough certainty. Differences between network without regulation (model c) and network with minimal regulation (model b) are distinct, but not fundamental. This shows the basic meaning of mechanism of keeping half-chaos state by accumulation small change during evolution. Regulation is not needed mechanism, additional but not the basic which is a surprising result of these investigations. As additional mechanism it can radically increase stability, i.e. order, but always changes must be small and this is enough to keep half-chaos, which must be the initial state.

The second aim of met5 was to reach boundary of half-chaos on the way from PAS0, by selection of process parameters, and to see of character of the boundary. The rules of series 44 turn to be not enough to this aim, therefore a complementary series 45 was done intensifying circumstances which should destabilize: shift was decreased from 50 to 2, attractor cannot decrease, fade out of damage was limited by condition $A3h > 2$ which replaces blockade of smearing. Despite these new stronger conditions the condition

of small changes turns to be enough to keep stability and even the most shaky formula bf does not reach chaos. However in bf a time range of explosions to chaos becomes much longer which needed to check for more extreme cases much longer section of tmx. Only one bf 176, (fig.9b,c) of 200 nets not reached stable state in longer tmx, it may be chaotic, but more probable is that also this event ends on increased level of stability. Lack of fulfilling of this aim, i.e. lack of reaching of chaos, does not mean failure, rather it is more awaited effect which shows power of so simple condition (small change) and reality of investigated variant of half-chaos called “ro-modularity”.

The third aim of met5 was to check thesis of „ro-modularity” that specificity and mechanism of observed half-chaos is based on many short, nearly independent loops. Here investigations of node state periods give a final answer. It turns out that most of nodes do not change their state, which follow Kauffman is call “ice”. It is characteristic for ordered systems, but if they are random. Here parameters of system make random system chaotic, but investigated systems are not random. Typically in the net there are simultaneously several (average circa 2) local clusters (set of nodes with the same state period of average length circa 10) which contain several nodes (fig.19b). Very similar clusters (as sets of nodes) typically are observed in consecutive accumulations, this create global clusters, which may change period, disappear (become frozen, i.e. period=1) and appear even after a long time of evolution. This stability shows their reality, clear identity but with changeability. This experimentally observed clusters (fig.15-19) correspond to hypothetical ro-modules. Area of ice as local cluster take most place in the net (over 370 nodes of 400, fig.19b). In case of PAS it was all nodes, in ro-modularity lot of them remain ice. The ro-modularity differs from the modularity in fact - the basic factor here is the ice, which isolates ro-modules whose essence is activity as a distinction from this ice. Modules, which in [met8](#) proved to cooperate with this phenomenon, significantly support and locate it, but the modules themselves are not enough. Observed increased stability (half-chaos in version ‘ro-modularity’) is not an effect of functions only, because one accumulation of explosion to chaos in enough to ro-modularity vanish, despite function remain without change of functions (exclude one function of one node for one input state). **Ro-modularity is a specific state of functions and node states**, but detection of the state by statistic investigation of static properties of network (distributions of states or function parameters) is not possible. In described simulations it was looked after the distributions looks like random. Ro-modural state correspond to liquid region in Kauffman approach, but it is not a random network. Presence of property of order and chaos simultaneously together with possibility to keep this state during evolution by simple limitation of effective changes initiated by small permanent accumulated changes are the main observed features of half-chaos. Ro-modularity is a mechanism of these here investigated features. As will be seen in met6, half-chaos is a wider term than ro-modularity – in system investigated in met6 half-chaos will be detected, but ro-modularity is absent.

6 Start from the short attractor instead PAS0 – met6

6.1 Introduction

In met4 was proved, that in point attractor (PAS) system exhibits half-chaos instead of chaos. Parameters $s, K=4,3$ and $2,4$ are used for investigation which makes system chaotic for random network. Most of effects of small disturbance, when limiting to small effective change, are also PAS, therefore in such state evolution can be long without need to leave this state. Limitation to state PAS is too extreme and question arise: if we allow to accumulate other changes than only PAS, but still small, will evolution can be also long or it must entry chaos? Investigation met5 was done to answer this question. In met5 only $s, K=4,3$ was investigated, networks start from PAS, only not PAS changes, even with attractor ≥ 7 were accumulated (if effective size of change was $<$ threshold which is about half of Derrida level), also other selected parameters are used to direct process to chaos, but condition of accumulation ‘small effective change’ turn to be stronger and chaos was not reached. State of network was evidently shifted from initial PAS. This state was deeply investigated and in effect probably known and understood – it was called ro-modular state due to it is based on ro-modularity. Earlier as a base of half-chaos a short attractor was taken, from such idea PAS was investigated as the extremely short attractor, but for mechanism of ro-modularity it is not enough. Therefore it should be tested, is short attractor enough or not? This is the main aim of met6, it correspond to main aim of met4.

It is sure, that using shift=50 like in met5 44 and starting from very short attractor, we will get significantly increased stability, but what is ‘very short attractor’?. We can include such mechanism to half-chaos, but not to ro-modularity.

The second aim is to check, similarly like in met5, what is an effect of long accumulation of small effective changes initiated by small disturbance. How long can be such evolution without reaching chaos? Here we cannot expect so many ice and mechanism of ro-modularity cannot help to keep stability. We hope, that here evolution is impossible and ro-modularity is the only explanation of phenomena observed in met5. However, this expectation turns to be false on the end of met6.

The third aim arise from such the effect: is the mechanism of observed stability similar to ro-modularity?

6.2 Short attractor

6.2.1 Creating of short attractor

To reach short (small) attractor similar method to met1 & 2 was used: from particular indicated time tax **if not used node input state occurs, then function value for this state is defined to value from step earlier by tax**. This way in second revolution of proposed cycle of $\text{length}=\text{tax}+1$ trajectory become more similar to first revolution. A point of initiations is shifted into the range of attractor.

Similarly like in met5, network f & r, $N=400$ nodes, $s=4$ and $K=3$ are used.

In early investigation attractor length = 200 on $\text{tmx}=10000$ was forced but for 200 nets f & r no one occurs – number of not used input state was not enough. Then smaller tax for small $\text{tmx}=200$ were checked. For tax=50 also was lack of effect, but for tax=40 in 3 nets f attractors occur, for tax=35 already 23 attractors happened, but only for f. For tax=30 and 200 nets f it founds 96 ($95*31+1*62$) attractors, and for r 9 attractors. Length of attractor near 30 looks to be enough to investigation, then tmx was enlarged to 10000, but no one more attractor occurs. For tax=19 all nets f and r have an attractor. Typically length of attractor was 20 but for f $22*40$ happened, and for r $25*40$ and $1*60$. Provisional results of stability for attractor =31 were similar to results for attractor=20, then investigations were limited to the last.

6.2.2 Stability investigation of system with short attractor

First complete of initiations was investigated without accumulation to check stability state got by forcing of short attractor. It correspond to met4. On this provisional stage of investigation only crocodiles were observed. Statistical investigation of initial state without of accumulation will be done in pass N in next simulations. Shift into range of attractor did not give an increasing of q, but shift was leaved.

6.3 Investigation of evolution – accumulation of changes as in passes M of met5 ro 44

For investigation of evolution the program for met5 ro 44 ro '4+7' was adapted which make comparison to met5 results easier. It is: 5 passes M free (1,7,13,19 & 20) without blockade of smearing and remain passes with this blockade; attractor length ≥ 7 , in M20 attractor cannot diminish. In pass N accumulations are not done, only stability is measured.

Provisionally simulation of 10 nets f,r 4,3 for tax=19 was done, but shift=50 and attractor length=20 interference every second time which introduced not needed effects (fig.1f). In final series were 200 nets f & r; s,K=4,3, tmx=1000 with tax=20, then attractor length=21 and not interferes with shift. Only for 2 nets f attractor is not found. Accumulation conditions for attractor length never were used – always attractor length was at least =21 and in M20 never happened double, which happen sporadically in other passes (in 3 nets r - one time, in 1 r and 1 f - 3 times).

The basic results are shown in fig.1. Chosen attractor length =21 turns to be practically the larger offered by algorithm. Obtained stability is not an effect of function narrowing which is essential by-product of the method (the last conclusion is from provisional investigations). Fig.1d concern explosion directly after ini without fade out. There is no significant differences to explosion after second ini or after third and later ini (fig.2.e). Small shift of later distributions to right shows that only very short cycles of fade out and secondary ini give later explosion. During accumulation process there is no difference in aspects of explosion time (fig.1c,d,e), then there is no base to expect that average explosion time will shift on larger time. Also the basic watched parameter – degree of order $q(M)$, i.e. probability of acceptance $P(akc|M)$ does not change with M (fig.1.a,b). Ranges of distributions in fig.1 are the same as in met5 for comparison and because program of simulation taken from met5 expects such ranges – they are not corrected. The same concern fig.2 where data are summarized without M1, this exclusion now may be omitted.

Shown in fig.2 shape of left peak is very different to peaks obtained in met5 for the most similar model c where only PAS was assumed. In met6 the left peak in all passes M practically contain only events, where damage fade out (to $A1=0$, but typically with secondary ini – see blue curve of $A1=0$ in fig.5) (see fig.1b & f). $A3$ is a average $A1$ on the last 50 steps, after explosion only 70 steps are calculated. For accepted it is an average from 2.5 revolution of attractor, see blue curve of $A1=0$ in fig.5. $A3$ allows to free from problem of $A1$ fluctuation in tmx, but these fluctuation have important meaning for interpretation, are real effect of ini. In tmx $A1=1$ have 0.005 of all events of f and 0.001 event of r, but $A3=1$ have only 0.001 and 0.000015 events respectively (tab.1, for explanation see fig.5). In met6 these evolutionary effects ($A1>0$) are very small and despite large fraction of ordered events (fig.2) practically is lack of evolution of function, which is observed in met5.

Tab.1. Exact values of probability for first 3 values of $A1$ and $A3$ in fig.2. Accepted changeability (initiations) forcing effective changes in met6 practically give no changes of function, i.e observed and working evolutionary effects. Assessed change size =0, there are lot of such “changes” and they create here left peak – ordered part of reactions.

A	3f	3r	3cf	3cr	1f	1r	1cf	1cr
0	0,252857	0,125226	0,011190	0,006678	0,213921	0,086347	0,019797	0,004277
1	0,001170	0,000015	0,177810	0,119833	0,005165	0,001120	0,107508	0,083801
2	0,000037	0,000001	0,071677	0,027884	0,000494	0,000038	0,044812	0,019729

Mechanism of acceptance is here based on fade out to $A=0$, despite shift=50 which in met5 removed such fade out. In phenomena of fade out and explosion probability a secondary initiations play an important role. They direct investigations on small attractors. Explosions are earlier than ends first revolution of attractor (more exact – than second revolution starts, but way to attractor entry is similar to attractor length). However, parameters of secondary ini shows, that they are different than for first ini, means that fact of fade out significantly change probability of the next fade out (we know, that this process can fade out). It can be seen in tab.2, where effects of consecutive (first, second, third together with later) initiations are shown in details. After ini the process can explode to chaos or remain “saved”. Saved may be in form PAS, fade out to $A1=0$ or other which wait on tmx with small $A1>0$. Fade out may be total, i.e. without later ini. Comparison to model c from met5 shows significant differences in mechanism of acceptance. Comparison of passes N and M shows lack of changes of this mechanism generated by accumulations. In met5 fraction of PAS decreases but here is lack of PAS from the beginning, when in met4 it was the main element of saved. In met6, however, constant manner of fade out become such the main mechanism of acceptance. The ice is a base of PAS and of ro-modularity, lack of ice in met6 make impossible PAS and total fade out.

Tab.2. Effects of initiations first - **1**, second - **2**, third together with later - **3**. After ini process can **explode** to chaos or remain “**saved**”. Saved may be in form **PAS**, **fade** out to A1=0 or **other** which wait for tmx with small (may be variable) A1 (threshold>A1>0). Fade out may be total (despite permanent change) – **tot.fade**, i.e. without later ini. First, second and later ini have different effects – division on these fractions but these differences have one direction. comparison to model met5 c shows significant differences in mechanism of acceptance. Especially lack of PAS in met6 is visible, the PAS were the main elements of saved in met4. In addition fraction of total fade out in fade out after first ini is shown. Such events were observed in met5 where ice was present, but in met6 they are absent. Fraction of fade out after next ini circa 100% shows that mechanism is repeated, it is not random after each next ini. fM & rM – results for M1-M20, not as in fig.2.

1	77,69	91,52	66,19	72,10	85,09	89,17	expl	%ini
	22,31	8,48	33,81	27,90	14,91	10,83	saved	%ini
	2,73	1,85	0,00	0,00	0,00	0,00	PAS	%saved
	10,75	17,00	99,99	99,99	100,00	100,00	fade	%saved
	86,52	81,16	0,01	0,01	0,00	0,00	other	%saved
	44	59	0	0	0	0	tot.fade	%fade
2	1,3542	0,2688	14,6427	21,0043	12,6006	20,5334	expl	%ini
	98,6458	99,7312	85,3573	78,9957	87,3994	79,4666	saved	%ini
	0,1317	0,0634	0,0000	0,0000	0,0000	0,0000	PAS	%saved
	93,4856	86,9896	99,9985	99,9994	100,0000	100,0000	fade	%saved
	6,3827	12,9470	0,0015	0,0006	0,0000	0,0000	other	%saved
	cfM	crM	fN	fM	rN	rM		
3	0,0004	0,0000	0,0259	0,0404	0,0114	0,0193	expl	%ini
	99,9996	100,0000	99,9741	99,9596	99,9886	99,9807	saved	%ini
	0,0260	0,0354	0,0000	0,0000	0,0000	0,0000	PAS	%saved
	99,6558	99,7125	99,9479	99,9519	99,9717	99,9758	fade	%saved
	0,3182	0,2521	0,0521	0,0481	0,0283	0,0242	other	%saved

Explosions after first fade out happened relatively often then about ¼ of second ini are earlier than end of first attractor. Distribution of explosion time nearly not changes (fig.1e). An average period of loops estimated from number of secondary ini (after subtraction of explosion) is for all passes M free and for N similar circa 17.6. Follow this, secondary ini happened more frequently than one time on attractor revolution, then in some attractors there are 2 ini and fade out in each attractor cycle up to tmx.

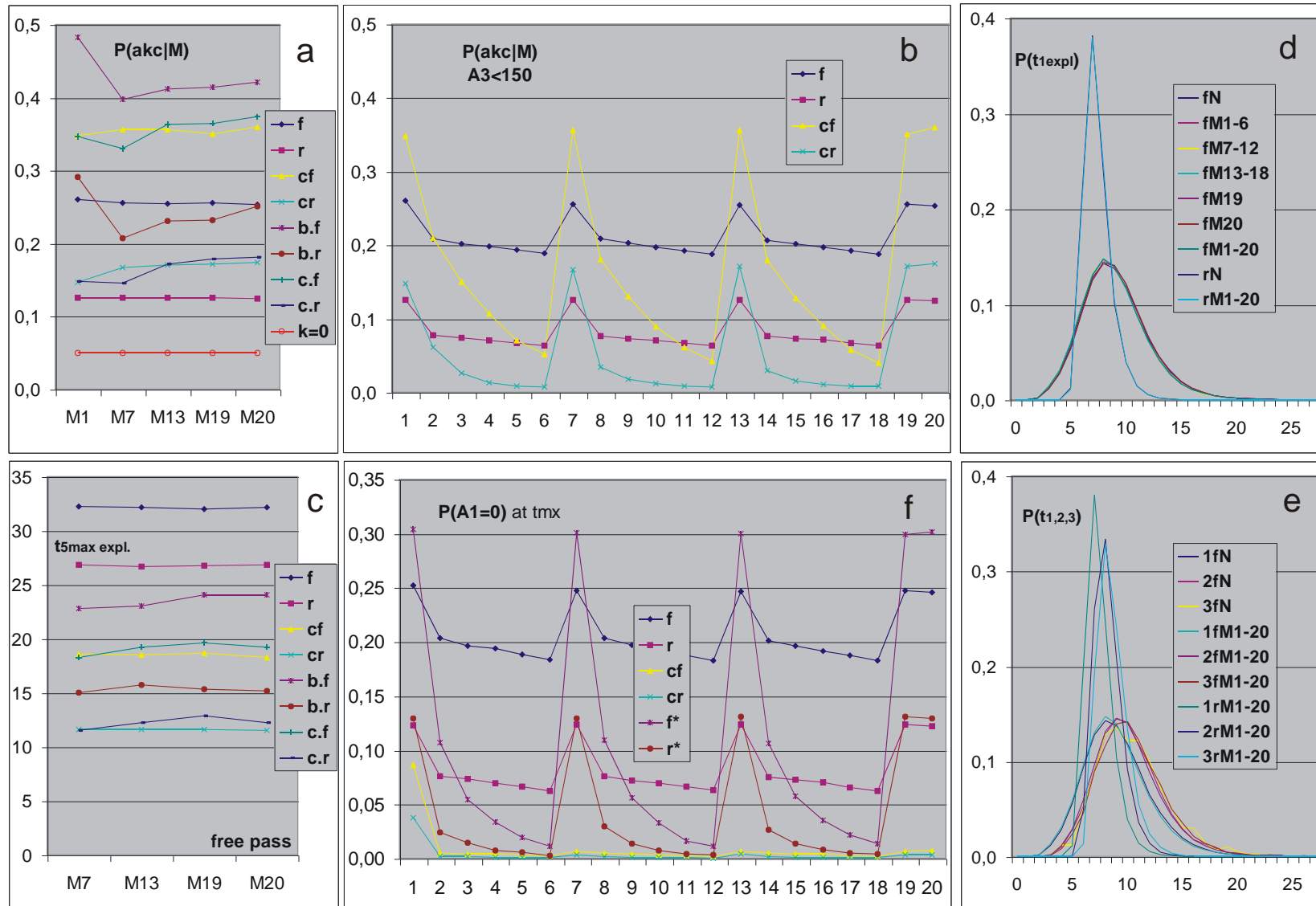


Fig.1. (a,b) Probability of acceptance: $A1 \ \& \ A3 < \text{threshold} = 150$, attractor ≥ 7 for M1-19 and it not diminish in M20. cf & cr – comparison to model c in met5 ro 44 ‘4+7’, dot inside concern met5 series 44 ‘4+7+20’. (a) – passes free, level effected from k=0 for r is shown. (b) – all passes M. (c,d,e) Explosion time (time of cross of threshold). (c) average explosion time for 5 the latest in free passes. (d,e) distribution of explosion time (d) directly after first ini, (e) comparison of 1- directly after first ini, 2-after first secondary ini, 3-after second secondary and later ini. More exactly for f to show identity of this distribution during all process, for r it is similarly identical. See also m7.fig.6 & 17. Small shift to right for explosion after later ini. (f) $P(A1=0)$ in tmx, i.e. that in tmx damage fade out. Series with stars concern met6 for tax=19 i.e. attractor =20. Difference is an effect of interference with shift=50, they are rejected by tax=20.

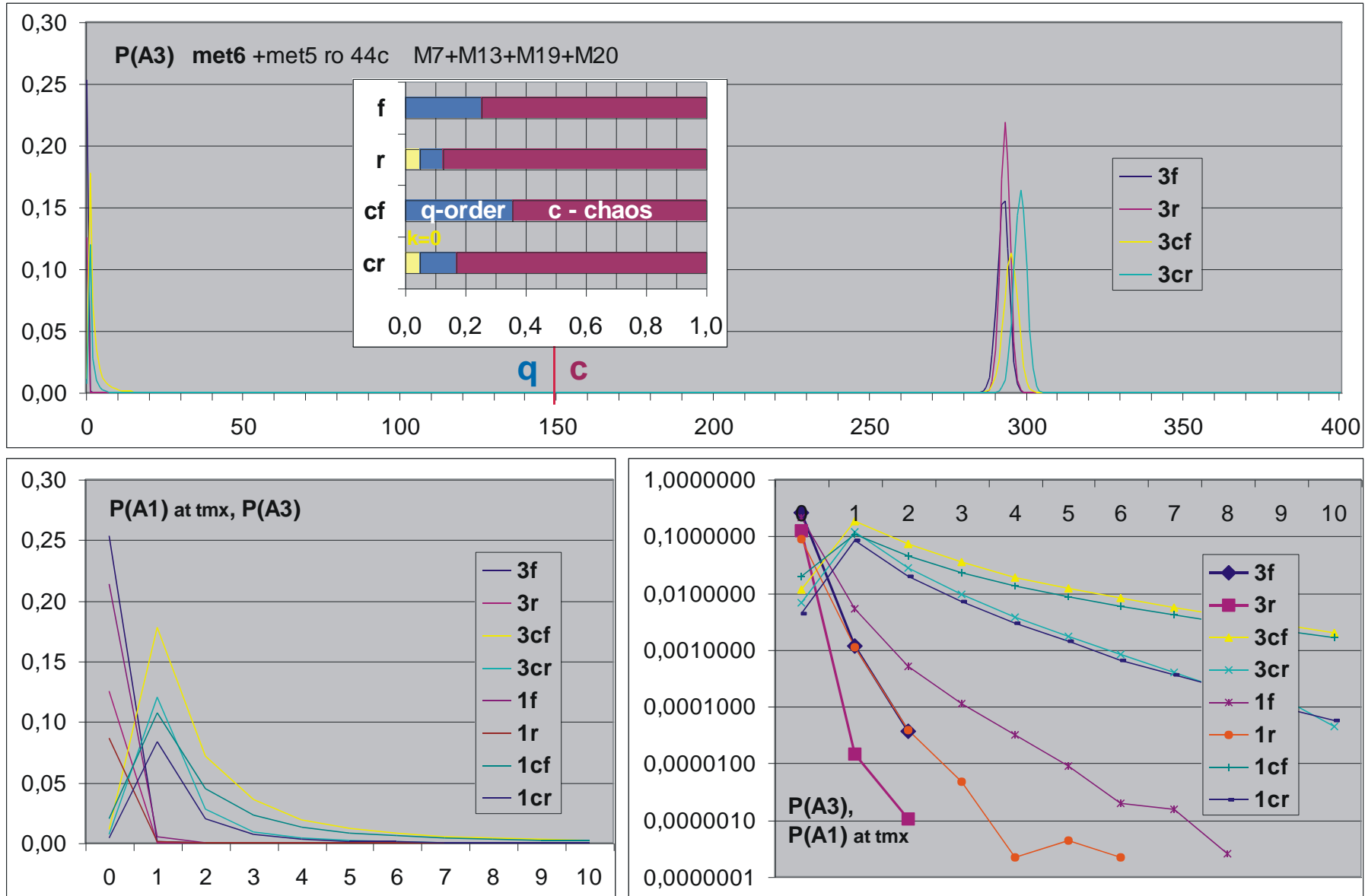


Fig.2. Distribution of damage size after small disturbance. Horizontal axis: A1 in tmx and A3 – average A1 in last 50 time steps. A1 collected in whole accumulation process with not free passes, A3 in passes free from M7 to M20, as in summary of met5. Differences are an effect of not free passes which is visible in fig.1b, however in met6 the tail behaves in opposite way. Left peak is shown more exactly (also tab.1), because just presence of it is the main theme of investigations. Its shape is here essentially different than obtained in met5. Upper diagram is included, in it degrees of chaos c and order q are shown. Yellow part of order effects of presence of k=0 in net r.

6.4 Half-chaos in met6 and conception of ro-modules

6.4.1 In met6 is lack of ro-modules

In met6 is exactly lack of ro-modules. Nearly always in pass free only one cluster occurs containing all 400 nodes with one period=21. Exceptionally, when double attractor=42 happened, then 2 clusters occur (4 events in M free for r). In 3 of the 4 cases one of them contain 399 nodes with period=21 and second – one node, period=42. In one case in M1 this cluster of period=42 contains 110 nodes and appears 39 times of 138. In such the reason the ice cluster essential for ro-modularity does not exist.

6.4.2 Clusters A4

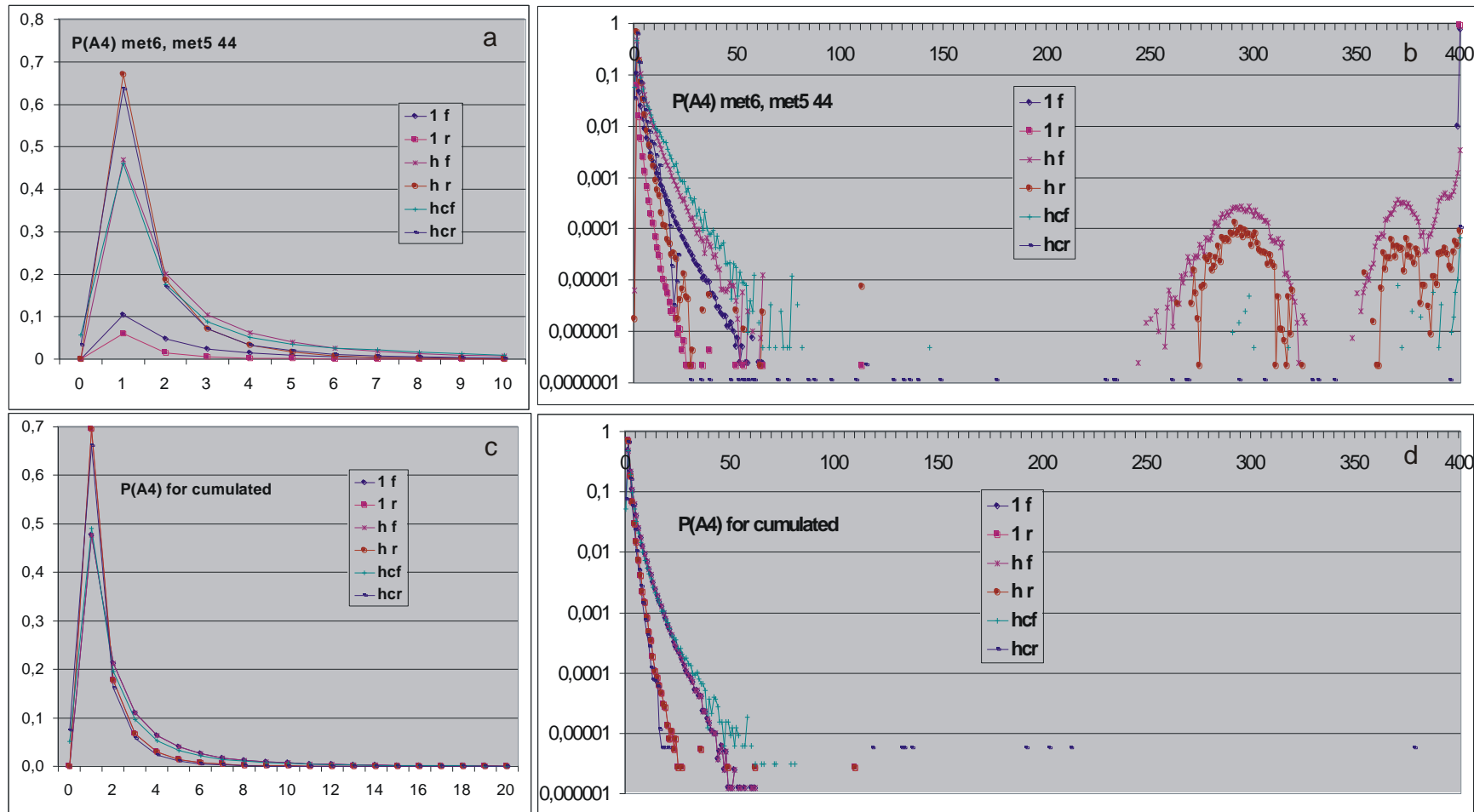


Fig.3. Distribution $P(A4)$ based on A4l collected on whole section tmx, and on A4h collected without first 100 steps t, where system is less stable an contain explosions. A4 – number of disturbed nodes as measure of size of local clusters A4 - hypothetic ro-modules which should be stable – as global clusters A4. Results of model met5c ro 44 ‘4+7’ are added for comparison similarly like in remaining fig. The picture is different than in met5 45 (see also m5.fig.13) (except cr) – it has no tail, which suggest greater similarity to expected picture of clusters A4, however similarity to model c in met5 44 ro is clear.

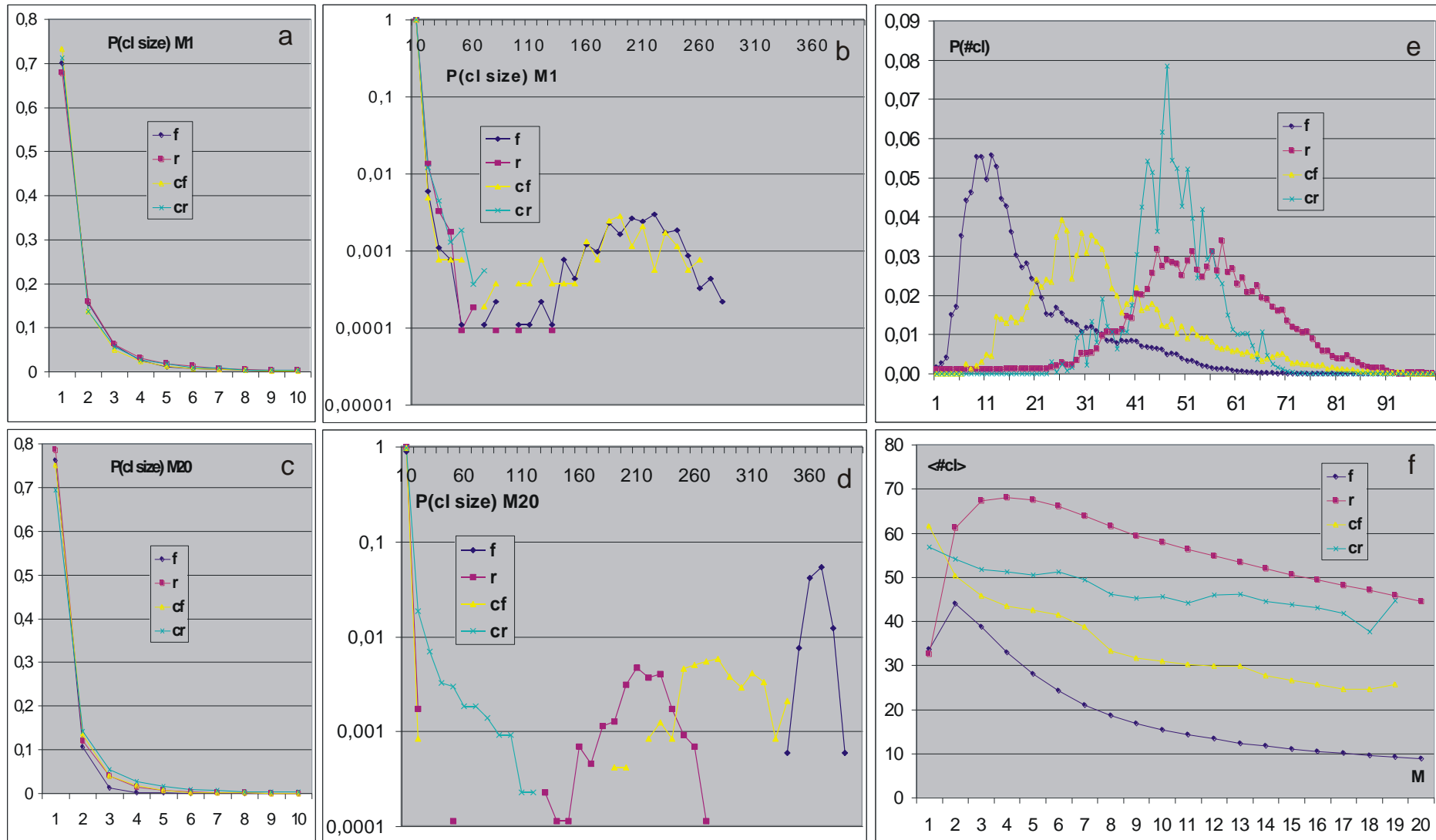


Fig. 4. Size distributions of global cluster A4 at the beginning (a,b) and at the end of accumulation process (c,d). For statistics increase in (b,d) 10 consecutive values are added. Local clusters are connected (included) to global cluster when they have common node. Despite lack of tails in fig.3d, in (d) right peaks for both nets appear and picture is not similar to cr. Distribution of number of global clusters (e) and average number of clusters for passes M (f). (compare to m5.fig.14, attention, that was series 45 but not 44 ro '4+7', from which cf & cr are taken; for f should be remembered that in met5 in passes N accumulations and clusters are already collected but here they start from M1). In (f) in model c differences of passes free and not free are visible, in met6 is lack of them but difference between f & r in number of clusters and cluster sizes in M20 increase (see also fig.5).

In met5 conception of clusters A4 turns to be not effective, clusters ro were better and they are developed. Only formula cr in both series (44 & 45) gave picture near expected. Investigated in met6 model is connected to model c in met4 & 5, because it not assume regulation, only small attractor. In [fig.3](#) (corresponding to [m5.fig.13](#)) where P(A4) is divided into A41 and A4h, even picture for net f is similar to cr. However, after deeper analyse, only net r gave results more similar to expected, but net f comparatively to met5 44 ro cf is shifted in direction of met5 45 b, which disappoint expectations.

Presence of clusters A4 in met5, as premise of ro-modules, when these ro-modules turn to be present and real, creates no reservations. However in met6 clearly is lack of ro-modules in that sense, which was expected and found in met5. But half-chaos is present, however [the shape of left peak poorly correspond to interpretive needs of biological evolution description](#). Simultaneously the picture of clusters A4 better correspond to expectations, than model b in met5.

In this reason investigations of clusters A4 become more interesting, because they give a hope to find another, weaker version of ro-modularity, which will explain obtained picture of clusters A4 and half-chaos. However it is weak premise. Problem stays open, but now we close investigations met6.

6.5 Conclusion

Start from short attractor forced by function selection gave half-chaos on other way that in met5. This mechanism of stop of melting of set not yet exploded processes was the first premise to put attention into small attractors and to test in met4 the point attractor system (PAS) as the shorter attractor. This idea turn to be effective and stable state of half-chaos was found. Investigations met6 have to weaken such extreme conditions to short attractor. Premise for this gave met5 in which stability of half-chaos did not need PAS. Such weaker condition turn out to be enough for half-chaos, however, character of effected half-chaos is much more worse for biological evolution description than of ro-modularity.

Long accumulation process of small changes does not come out of half-chaos also here, but it not change of system function. [Keeping of stability in met6 is a surprise, because there is no conditions for ro-modularity. Ro-modularity as a form of half-chaos occurs more useful to life description and this shows, that not short attractor is the most important, but causes of ro-modularity. However, mechanism found in met6 should be added to "box of tools" of evolution, but it is not well and effective tool.](#)

Working in met6 mechanism of stability increasing gives not transition to ro-modularity observed in met5. It was tested that it is not an effect of function narrowing, which is needed by-product of method. It is based on cyclic fade out and secondary initiations. Effectively used method to reach short attractor may be applied to create state of ro-modularity in controlled manner, without of starting from PAS. This is the aim of met7.

7 Controlled creation of ro-modules – met7

7.1 Introduction

Investigation met5 has led to indication of mechanism of half-chaos observed in met4 – it is ro-modularity based on majority of ice, i.e. nodes, which not change their state. It is not only the modularity, because it not base on density of connections. In the ice there are isolated lakes of activity, called ro-modules. Ro-modularity is a particular variant of half-chaos. In met6 half-chaos occur to be wider term than ro-modularity. After chaotic change ro-modularity vanish without change of node function (except small ini, later X and S experiments). Kauffman shows practically identical view for random systems near phase transition between order and chaos, mostly in ordered phase and calls it liquid. These both system states differ substantially, because in ordered phase the damage explosions to Derrida level of chaotic equilibrium are exceptional but in ro-modularity such the explosion are natural and typically state majority of events. Ro-modularity may be compared to overheated liquid easily changing to gas which in Kauffman approach represents chaos, or supercooling also, because lakes often freeze. System in ro-modularity is simultaneously ordered and chaotic because both these form of reaction on small disturbance are present in similar scale. Famous thesis “life on the edge of chaos and order” get another meaning than for random systems. Living objects cannot be modelled as random systems, especially in aspect of stability, because just for stability natural selection accumulates changes. Ro-modularity is more adequate for life description than area near phase transition between order and chaos of random systems. Explosion to chaos correctly models death of living object, without this elimination mechanism of natural selection does not work, but just this mechanism seems to be base of life definition. Small change receives here a natural definition based on damage size distribution, retains ro-modularity and system identity, then evolution can go on. This simplify definition of basic Darwinian mechanism.

Mechanism of ro-modularity was observed as an effect of accumulation of small changes starting from point attractor. As was above mentioned, it bases on ro-modules separated by ice. Presence of ro-modularity was proved, it seems, that all important elements of ro-modularity were taken and we understand its mechanism and results, but there is no proof, that just the ro-modularity is the main base of stability and the cause, that small changes does not lead out of it. Controlled constructing of the ro-modularity as the only change from random state and showing, that it similarly keep stability, can be such the proof.

This is the aim of met7. This aim is assembled from three parts: 1- controlled constructing of the ro-modularity as it was described in met5; 2- testing of its stability directly after constructing (met7a & b, correspond to met4); 3- and next during accumulation small changes (met7e – evolution, connected to met5).

From the beginning of half-chaos search the length of attractor is an important parameter. After permanent change damage may fade out, but secondary initiation of the node gives new damage avalanche, which develops in different circumstances. Probability of fade out in each case is similar (in first approximation), then chance to stay saved depends on number of secondary ini, but this number depends on section length to circumstances repetition, i.e. – on length of attractors of pattern and current ad on way to entry into the attractors. Investigations of met4 & 5 confirm this view and met6 even shows that short attractor has essential meaning. In met7 we wait confirmation of ro-modularity mechanism, in which short attractors of ro-modules are quickly reached and block explosions but global attractor assembled of them may be long. For this stage the accumulation is not needed yet. For investigation of accumulations program from met5 ro 44 can be used, similarly like in met6.

Expectation that random build ro-modules using chaotic parameters $s, K=4,3$, assembled from N_{ro-m} = few dozen of nodes will typically have a short attractors sees to be lack of bases. For $s=2$ and $K=3$ Kauffman expects length about 2^{125} for $N=100$, and 2^{32} for $N=25$. For $s=4$ they should be much longer, then at the beginning assumption was taken that short attractors must be forced. Much later testing of „clean ro-modular state” without such forcing shows surprising result that this assumption is wrong and the forcing is not needed. Description of conceptions and results should be ordered, then „clean ro-modular state” will be described first as met7a, however sequence of investigation was another. Elaborated in met6 method of creating small given attractor may be applied to forcing small attractors in ro-modules. This “additional” investigation before evolution creates series met7b. The met7a gives a little bit worse results than met7b which allow to show earlier investigation with stronger assumptions. Evolution investigation of such optimised ro-modularity is called met7eb. For view completing also series met7ea - evolution simulations without forcing of short attractors in ro-modules are done. In [table 2](#) in names the series are ordered content-related but not historically. However, before the simulations ro-modules separated by ice must be created. This part of first aim is a new and it is the main technical aim in met7.

7.2 Constructing of ro-modules

7.2.1 Basic algorithm

Autonomous network particular type is typically generated as from met1 to 6 before, it is random connection of N nodes. Net types f, s, r (scale-free, single-scale, random; see [\[arj, brj, it\]](#)), are used in met7. Always number of node inputs is $K=3$ and number of equally probable signal variants is $s=4$. Initial states of nodes are also random drawn.

Next, analysing node connections a set of ro-modules is created, in effect each node is dedicated to particular ro-module or to separating ice.

In order to increase chance of greater ro-modules, after the dedication of node its input and output nodes are investigated as the first.

The node creates a new ro-module, if no one its link (input or output) does not connect to node dedicated to already defined ro-module.

If the node is already connected to nodes dedicated to one ro-module, then it is dedicated to this ro-module.

If the node is connected to nodes already dedicated to different ro-modules, or limit of ro-modules ($=10$) is reached, or limit of ro-module size is reached ($=100$ nodes in met7a & met7b; 100, 40, 25 nodes in met7eb; 25 nodes in met7ea, [tab.2](#)), then the node is dedicated to ice.

Next trajectory is calculated with selection of function: for current node input state, if it was not used yet, nodes of ice get value 0 (can be any, but always the same), and nodes dedicated to ro-modules get (initially) random values.

7.2.2 Increasing active ro-modules number

This random value is tested to decrease number of ro-modules which are totally frozen: if it is the same as one step before, then it is changed by 1. It was estimated, that this method is not enough and there was less active (non point attractor) ro-modules, than assumed number 3.

In order to increase number of active ro-modules up to 9 correcting iterations are imposed until more than 3 of 10 are inactive. In such iteration new initial state are drawn for all frozen nodes and nodes from ro-modules without found attractor. Next their functions are defined ones more. In series met7b and met7eb, where tax is used for particular attractor forcing, next tax from table is taken – position in table is shifted to right, then next dozen (this is stable - tax: 6,4,2,1,10, 12,16,18,22,28) of these number is reached (see [tab.2](#)).

In “clean ro-modular state” (met7a and series fe,se,re in met7ea) the smaller limit $=1$ on minimum number of active ro-modules is used, to system be not PAS, because this case was already tested in met4 and met5. In met7b the limit is 3 (event with less than 3 active ro-modules is rejected). In final series met7eb and series fe2 & ff in met7ea at least 2 are allow ([tab.2](#)). In series fi, fu met7eb influence on results of this parameter in range 2 – 4 are tested.

7.2.3 Short attractor forcing, tax in met7b and met7eb

Forcing of short attractor turns to be not so needed as initially was expected, but this correction influences left peak shape in damage size distribution, which bring it near to picture from met5, which in met7 should be recover in controlled manner. When number of steps cross tax for given ro-module (as in met6) and input state is still not used, then function value is defined to node state tax step earlier. In result of testing for consecutive ro-modules tax was defined to: 10,6,4,2,1, 10,6,4,2,1; which means that attractors are forced to prime numbers: $tax+1=11,7,5,3,2$. In met7eb also tax =6,10,4,2,1, 6,4,10,12,6; and in final simulations: 1,2,4,6,10, 4,6,2,1,6 ([tab.2](#)) are used. Sequence in table of tax is substantial because typically earlier ro-modules are the biggest. In met6 the algorithm ‘tax’ was very effective for whole net and $tax=19$ and 20, but now it is effective in middle (typically tax now is much less) and great part of ro-modules falls to point attractor (is frozen – inactive). Forcing smaller attractors ([fig.4e](#)) effects multiple forced length of local attractor. Larger values from end of tax table (6,4,2,1,10, 12,16,18,22,28) used during correcting iterations seems not more effective and their influence is not seen, however, they are used for later ro-modules, which are much smaller.

7.2.4 Limitations for algorithm of ro-modularity creation

Beginning of trajectory, where point change of function is initiated, is shifted to the latest start of local (of ro-module) attractor, to all ro-modules be in their attractors. In met7a and met7ea without ff, where local attractors are not limited, in rare cases they are not found and in such cases their start point is not known and cannot be taken under consideration while shift.

Algorithm selects functions only in range tmx and if this section not contain full revolution of global attractor, then it cannot test all existing interactions between ro-modules and ice walls. Shift to the latest start of local attractor incorporates such untested section into range tmx and lost of ro-modularity may happened already during extension of pattern trajectory – it is ‘invisible explosion’ to chaos. In the place of this invisible explosion each process after ini exhibits explosion, but it is not true lost of ro-modularity. It was already observed in crocodiles in met5 ([m5.fig.9e](#)), and in early met7b ([fig.8a](#)) only for net s (for f and r it not occurs). Limitation on shift to attractor begin

was introduced for version b up to 500 (for $tmx=2000$) in met7b and 150 (for $tmx=1000$) in met7eb and ff, and local attractors were limited to 100. This radically decreased number of global attractors crossed tmx and probability of lost half-chaos in pattern trajectory, so in initial and final series met7b in over 1600 calculated nets each type f,s,r no one such event happened. In version a, without limitation to small local attractors this phenomena happened much more frequently (tab.2: for 600 effective sa 12 rejected events happened). Algorithm was extended – after shift local point attractors were watched and event of pattern trajectory which lost such attractor was rejected. It was effective.

7.3 Ro-modules investigations directly after creation – met7a and met7b

In experiments without evolutions (without accumulations) $N=800$, $tmx=2000$, threshold=300, $s=4$, $K=3$ are used. Simulations stop when indicated number of effective nets (fulfilling conditions) was reached.

7.3.1 Assumptions

Obviously, simpler assumptions are more desirable, but ‘clean ro-modular state’ without forcing of short attractors (tax) occurs sufficient on the end of investigations which are reported here. The whole way was not repeated, only completed, especially because version with more assumptions gives results more close to met5, which met7 have to recreate in controlled manner. Therefore simpler series met7a become the main and series with additional assumptions met7b become its extension in searched direction.

Condition for global attractor to be greater than 200 when local attractor is not greater than 100 effects from need to proof thesis that not length of global attractor is a base of mechanism of ro-modularity, but local attractors of ro-modules. In met6 was shown that short global attractors (=20 to 31) give half-chaos. In met7a & b 600 effective nets are simulated in 2 series: 300 nets with investigation N,X,S,T,F, and next 300 only for N, but result for N are assembled from both. This allow additionally for estimate of exactness of results. To reach 600 effective nets 4387 nets f, 1420 nets s and 1179 nets r were started. In met7a conditions: lack of chaotic collapse of pattern trajectory and at least one active ro-modular state are the only, they are fulfilled in near all cases than numbers of generated and effective are similar (tab.2).

Proving that constructed ro-modularity is responsible for got half-chaos needs to show that it is not an effect of function narrowing during method. For this 4 additional experiments of stability measure were done on each effective net of 300: X – after acceptance of one ini which gave chaotic explosion; S – after draw new random initial states; T – after shift functions to another node but with old initial states; F – after random draw of new functions. Always structure stays not changed. Exclude F statistical features of functions become not changed, the same as in N with ro-modularity, but always they gave picture as F – typical chaotic. Comparison of experiments X,S,T,F (fig.1c,d, 2right, 6, mainly 3d,e, tab.1) shows small systematic differences, but N is radically different.

7.3.2 Damage size distribution as the main result of met7

Damage size distribution, i.e. $P(A1)$ at tmx is the main result. In ro-modularity should exist (as in met4 & 5) two peaks: Left containing ordered events, this peak is the goal of all these investigations. Chaotic systems practically are lack of this peak, also here results from experiments X,S,T,F. Right peak is an effect of classic chaotic equilibrium shown by [Derrida](#). It is present in each experiment, also in N, but it is absent in ordered random systems. Results are shown in fig.1-3 and in tab.1.

Degree of order for net r contains effects of nodes without output ($k=0$) present in this net type. In fig.1c,d – diagram in fig.1a,b fraction of such nodes is shown (0.0498), their ini is always accepted. It is not a full effect, which is circa 0.01 greater, these phenomena are a cause of order increasing in experiments met7b X,S,T,F for net r, which is not seen for nets f i s. In experiments met7a X,S,T,F for nets f i s order is greater, but it not reach level effected from $k=0$ in net r.

All 4 control experiments (X,S,T,F) in both series: a i b exhibit classic chaotic picture, which explicitly hold constructed ro-modularity responsible for half-chaos (increased level of order) in N experiment. The ro-modularity is based on functions an states selecting to set of nodes creating network be divided into ro-modules with short attractors separated by walls of ice – nodes which for input states received in these attractors send constant signals to another ro-modules. Despite connections between ro-modules across the walls; and many different input states of nodes of walls; damage has small chance to penetrate the walls to neighbouring ro-modules. So small, then chaotic avalanche initiated and growing in the ro-module may not come out from it. Such the events are observed (especially dynamically) in crocodiles (fig.8a,d,g,j). They also have created a hump seen in fig.2a left. Also global explosion may not reach all ro-modules. Such the events have effected extension to left of right peak of Derrida equilibrium and decreasing its high for N experiment which is shown in fig.2a,b right, and fig.3e and tab.1. In this reason especially surprising is result q for X (fig.3d), which instead more than S bring near to N exhibit systematically (exclude r, for which the effect is not seen) less q than F. It is not fluctuation, because the effect occurs in many independent simulations. Acceptation of chaotic explosion (X) leads to greater disorder than spontaneous (F).

The shape of left peak (fig.2a,b left, 3a,b,c) is especially important. For description of biological evolution it must allow significant, however – small, changes of function, i.e. it cannot be so small like in met6 (m6.fig.2) and experiments X,S,T,F, which in fig.2a,b left are identical to X. In this aspect obtained results (fig.3b) are more “correct” than in model c in met5 44 ro, which correspond to N in met7a & b.

Tab.1. Degree of order $q = P(akc)$ where $akc = (\text{threshold} > A1 \text{ at } tmx)$; $N=800$, $\text{threshold}=300$; experiment N: 600 nets in met7a & b; X,S,T,F: 300 nets; degree of chaos $c=1-q$; also indicated in fig.1.c,d (diagram in fig.1a,b). Lower: $\langle \text{Derrida} \rangle$: average of Derrida peak (fig.2 a,b right), this peak is separated from left peak by section without counts (fig.1a,b); maximum of Derrida peak (fig.2a,b right) in results, not from fitted curve. Fig.1a,b, 2a,b and ‘max Derr’ in table from results summed by 4 consecutive A1.

	Nf	Ns	Nr	Xf	Xs	Xr	Sf	Ss	Sr	Tf	Ts	Tr	Ff	Fs	Fr
q a	0,273	0,204	0,230	0,0026	0,000124	0,0598	0,0128	0,000411	0,05987	0,0148	0,000188	0,05985	0,0021	9,7E-05	0,05984
q b	0,279	0,198	0,228	0,0014	7,64E-05	0,0591	0,0050	0,000263	0,05918	0,0027	0,000132	0,05910	0,0018	0,00015	0,05912
c a	0,727	0,796	0,770	0,9974	0,999876	0,9402	0,9872	0,999589	0,94013	0,9852	0,999813	0,94015	0,9979	0,99990	0,94016
c b	0,721	0,802	0,772	0,9986	0,999924	0,9409	0,9950	0,999738	0,94083	0,9973	0,999868	0,94090	0,9982	0,99985	0,94088
$\langle \text{Derrida} \rangle a$	492,6	550,3	563,8	550,6	580,3	584,3	551,1	580,2	584,3	562,3	582,5	585,2	586,2	587,3	587,4
$\langle \text{Derrida} \rangle b$	521,5	554,3	565,7	570,5	582,0	584,9	570,5	582,1	584,8	576,7	583,8	585,6	586,2	587,3	587,3
max Derr a	504	552	564	560	580	584	560	580	584	572	584	584	588	588	588
max Derr b	524	556	564	572	584	584	572	584	584	580	584	588	588	588	588

Fig.1. (In next page.) The basic results: $P(A1)$ and fraction of degree of order q and degree of chaos c . They show stability after controlled creation of ro-modularity met7a & b for nets f, s, r, $N=800$, $tmx=2000$, $\text{threshold}=300$, $s,K=4,3$. Results summed by 4 A, then ‘0’ contains original $0+1+2+3$.

Result are from 600 nets for experiment N (in Naaj called J) and 300 nets for X,S,T,F.

They explicitly show that expected radical increasing of stability (half-chaos) is reached in N experiment and it is not an effect of statistical feature of function or initial states changed during this creation – result of X,S,T,F are classically chaotic.

Upper - fig.(a,c) concern model a of clean ro-modular state without forcing of short attractors (tax) and limitations on length of local and global attractors and on number of active ro-modules.

Lower - fig.(b,d) is a result of simulation with forcing of short attractors ($\text{tax}=10,6,4,2,1, 10,6,4,2,1$); global attractor ≥ 200 , $\text{loka} \leq 100$, minimum 3 active ro-modules, shift to latest starting local attractor < 500 . It is model b.

More exact analysis influence of particular differences between models a and b will be made while analyse full model e with evolution (simulation fe,fe2,ff, see tab.2).

(a,b) - full range tmx of damage size distribution $P(A1)=q$ at tmx . As is seen in fig.8 “crocodile” in tmx value q is stable. A gap between peaks is exactly lack of counts. In the middle of this gap (taking right peak as in X,S,T F near 600) $\text{threshold}=300$ is arbitrary defined. Crossing the threshold by $A1$ - measure of “Avalanche” is a criterion of chaos reaching, the avalanche is too large to come back into ordered range, it only can reach Derrida level in right peak.

Both peaks are shown more exactly in fig.2 & 3.

(c,d) – share of ini results between q and chaos c (more exactly in tab.1); For net r influence ini for nodes with $k=0$ on ordered part is indicated in yellow. For N and X share of chaos on explosion directly after first ini (0 fade); after 1 fade out and first secondary ini; after more than 1 fade out are shown. For remaining experiments S,T,F this share is identical to X.

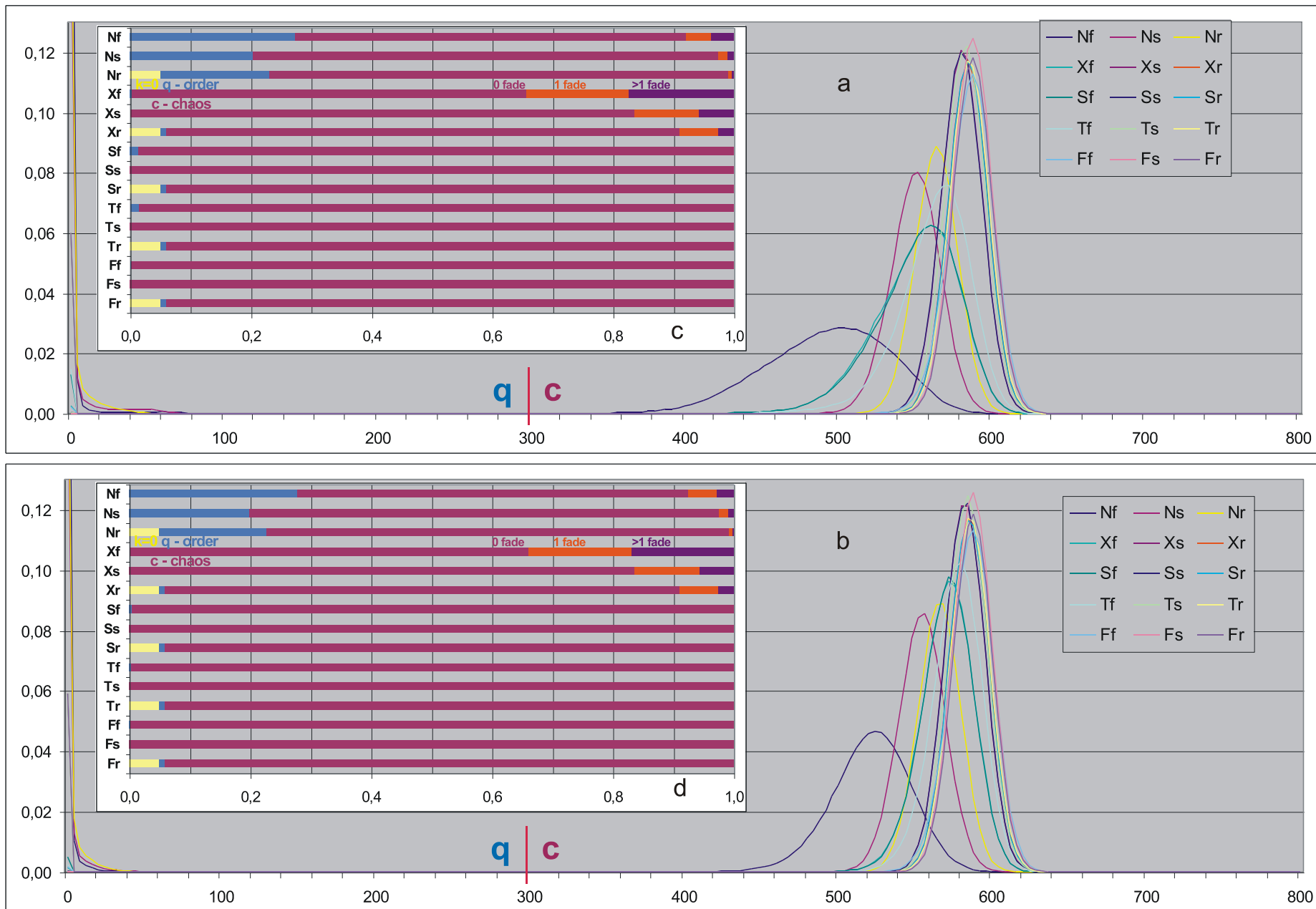


Fig.1. Description above.

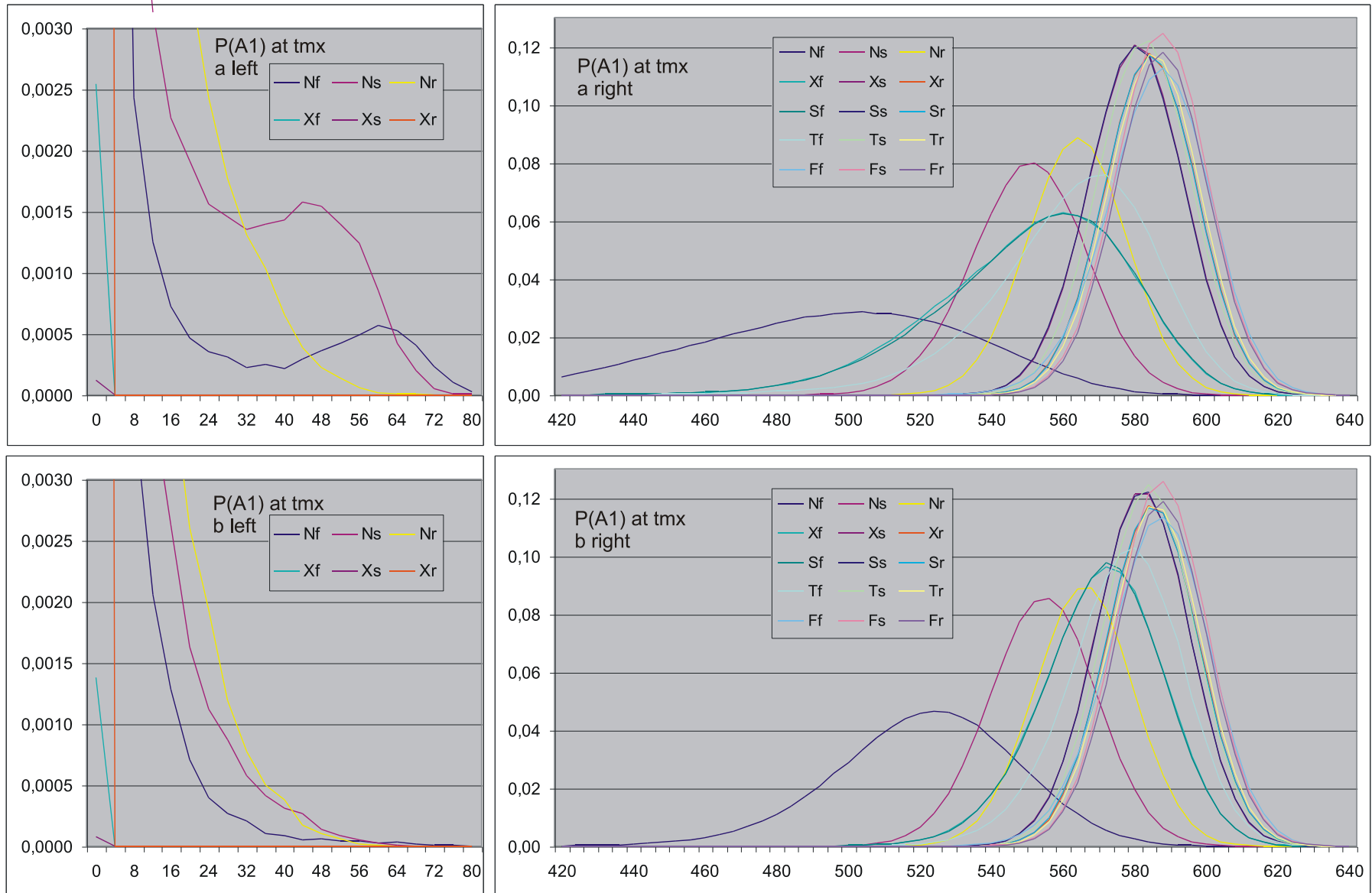


Fig.2. More exactly peaks left and right of damage size distribution shown in fig.1 (4A in 1 point). Similarly like in fig.1, upper row concern model a, and lower - model b. On the left lower range of left peak for ro-modularity (N) and for chaotic state on example (X) - chaos reaching by acceptance of one explosion. In (a left) for nets f & s additional peak is seen and in r change of shape effected from chaotic process in single larger ro-modules. More exact analysis of left peak in fig.3a,b,c. Right peaks (N) exhibit stronger flow to left – here damage after explosion does not reach all ro-modules. Differences between models a & b and experiments N,X,S,T,F more exactly in fig.3d,e.

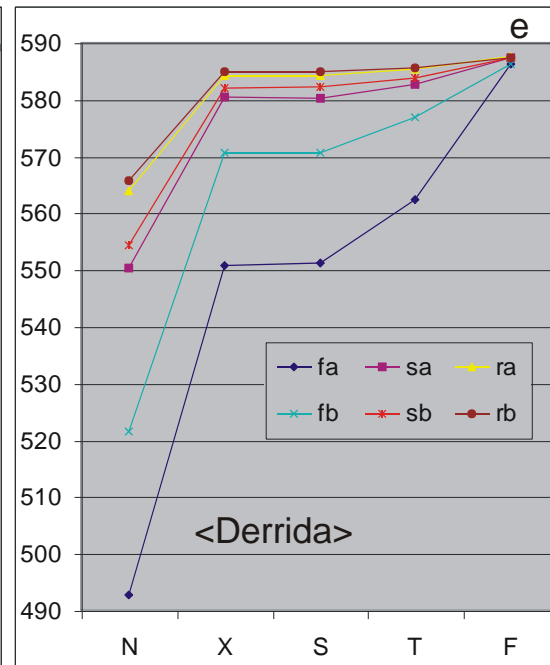
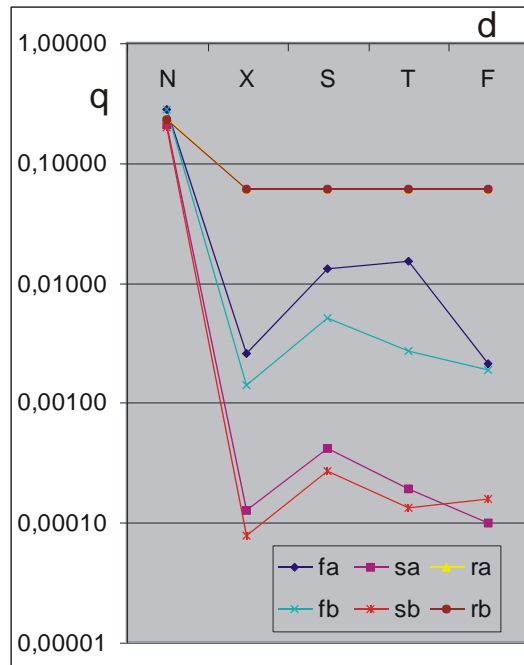
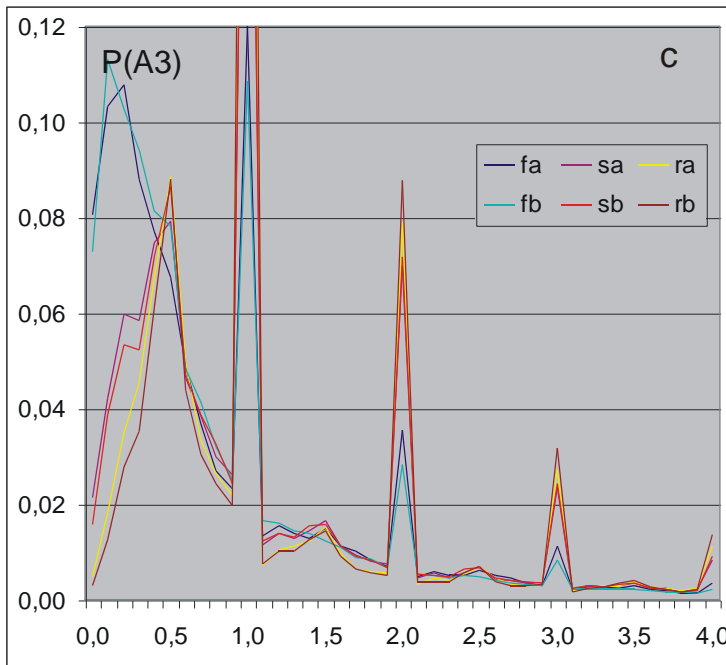
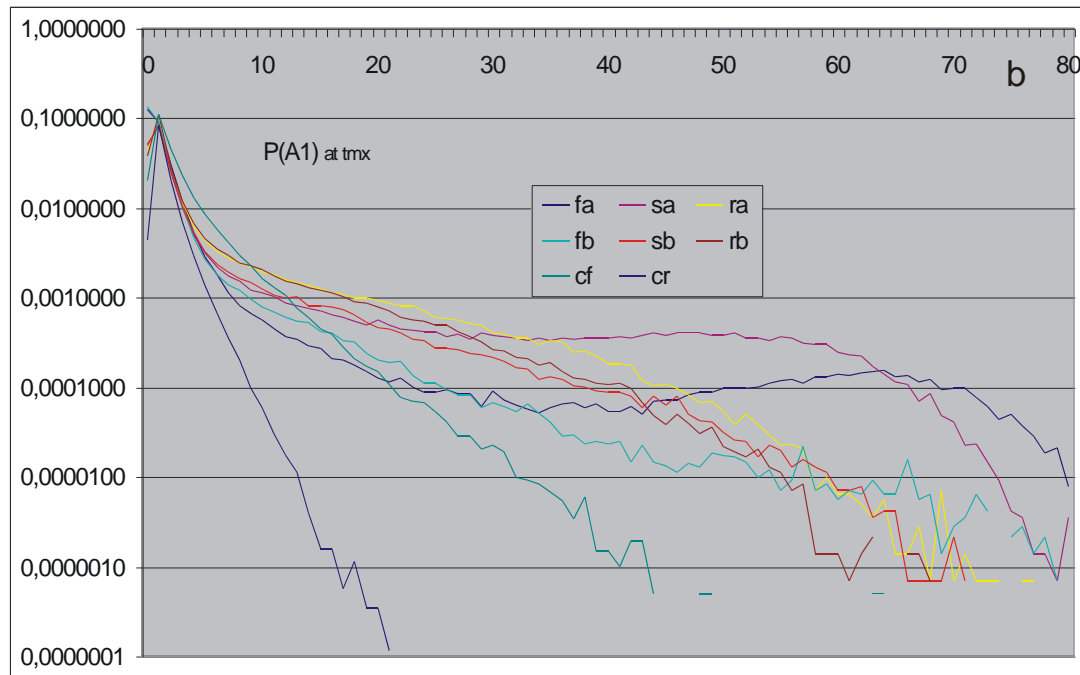
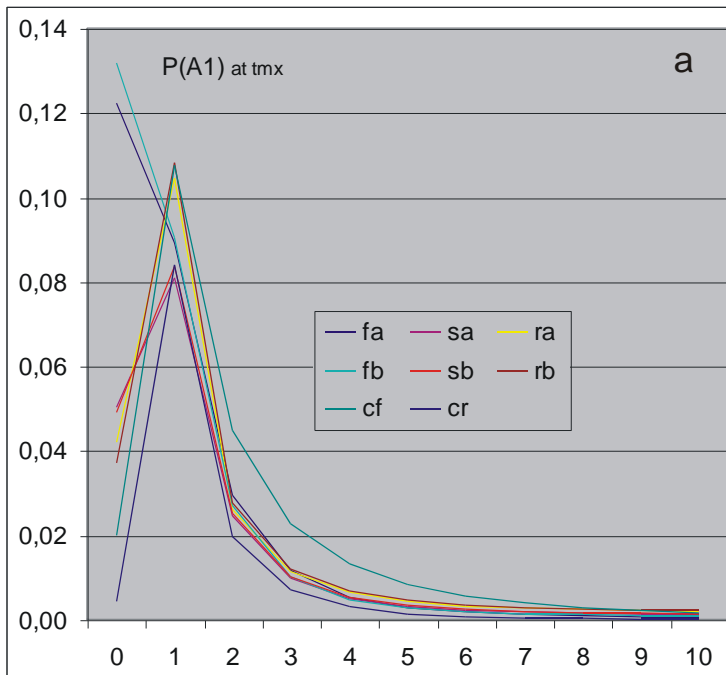


Fig.3. Left peak more precisely (a,b,c) and differences in results of N,X,S,T,F in q and average Derrida level (d,e), for both models a & b.

(a) - Completion to [fig.2 left](#), beginning of left peak in full range. It is the most important section of this peak, comparison of it for models met7a & b and met5c.

(c) - Disturbing difference of $A1=0$ and 1 for net f in met7 to remaining nets is shown using $A3$ – average $A1$ on last 500 steps. It is wider discussed in model met7eb ([fig.9](#)). It turns out that events with multiple fade out where $A1=1$ happened every few steps and in remaining steps $A1=0$ are often included to $A1=0$.

(b) - Left peak in log scale to show tail. For stability this tail has small importance but it show presence of additional, different than in met5c mechanism. This mechanism is especially seen in model a ([fig.2a left](#)). Its presence in model b is only seen here. The mechanism “corrects” stability in comparison to met5c, where is not seen. As was indicated in description of [fig.2a left](#) It bases on chaotic avalanche in larger ro-modules but this mechanism is created by accumulation which only in [fig.11](#).

(d) - Degree of order q for experiments N,X,S,T,F. It is surprising that q for X is so low. It is not a fluctuation, because in lot of independent simulation this effect is always present, here it is present in independent simulations of models a & b for different nets f and s. For net r it is not seen due to $k=0$. In model a for net f significant increasing q is also puzzling. Events of large q for T are observed in crocodiles ([fig.8f](#)): when for remaining chaotic experiments number L reach only: F -27, X -52, S -156, then for T it happened 5 times (of 300) crossing value 250: (256, 274, 362, 421, 511). In model b number L for T reached only 111. T is a shift of each function to another node without change of initial states.

(e) - Averages of right peaks, i.e. of measured Derrida equilibrium. Their relative location in range of net type and model is understandable: X and S (random node state) are identical. Shift of average N to lower value suggests that chaotic avalanche not always reaches all ro-modules. Differences between models a & b effects from lack of limitation for local attractor in model a ([fig.4g](#)), which leads to stronger narrowing of wall node functions.

Shown in (d,e) results confirm effective reaching ro-modularity in N, and that half-chaos in N is not an effect of statistical features of function set (saved in X, S, T), nor initial states changed while correcting iterations for increasing number of active ro-modules (saved in T and F). Differences to random functions of X,S,T are very small.

7.3.3 Testing effectiveness of algorithm

In [fig.4a](#) distribution of number of active ro-modules is shown for models a and b. Algorithm of model a has limits: up to 10 ro-modules with maximal size 100 nodes, up to 9 iterations decreasing number of inactive ro-modules. Limitations for model b contain in addition: forcing short attractors using tax table ; global attractor >200 ; maximal local attractor ≤ 100 ; shift to the latest starting local attractor <500 ; number of active ro-modules ≥ 3 . In model b the limitations, especially for number of active ≥ 3 , change the distribution comparatively initial one, then this generated is shown with letter ‘t’. As is seen, initial distributions in both models not differ, however, change of the distribution can influences a results. Rest of [fig.4](#) for model b considers nets fulfilling the conditions.

As is shown in [fig. 4b,c,d](#) ice nodes state majority of net nodes, nodes of inactive ro-modules shown separately in [fig.4c](#) should be included to the ice.

In [fig.4e](#) is shown that forcing (tax+1) has small effectiveness for 2,5,7, better for 3 and 11. It is not clean, why 5 and 7 are worse than 3. For 2 and 7 its multiples are present (4, 6,... 14, 16...), but not for 5. Avoiding value 5, seen also in [fig.4f](#), was observed already in met5. Fraction of local attractors >30 is very small.

First, or 2 first ro-modules typically grow to maximal size 100 nodes, remaining are small, typically less 20 nodes ([fig.4b](#)).

Fig.4. (In next page.) Structural features of algorithm of ro-modularity creation. (b-g) for calculated networks, (a) - Distribution of active ro-modules after conditions: 10 ro-modules not greater than 100 and up to 9 iterations decreasing fraction of inactive or without found attractor. In model a it is end of conditions - such network ia calculated. For model b (with letter t) in addition - after forcing short attractors using tax table, but before check next conditions: active ≥ 3 , global attractor >200 , local attractors ≤ 100 , the latest local attractor start before $t=500$. Letter b indicates such network, they are calculated.

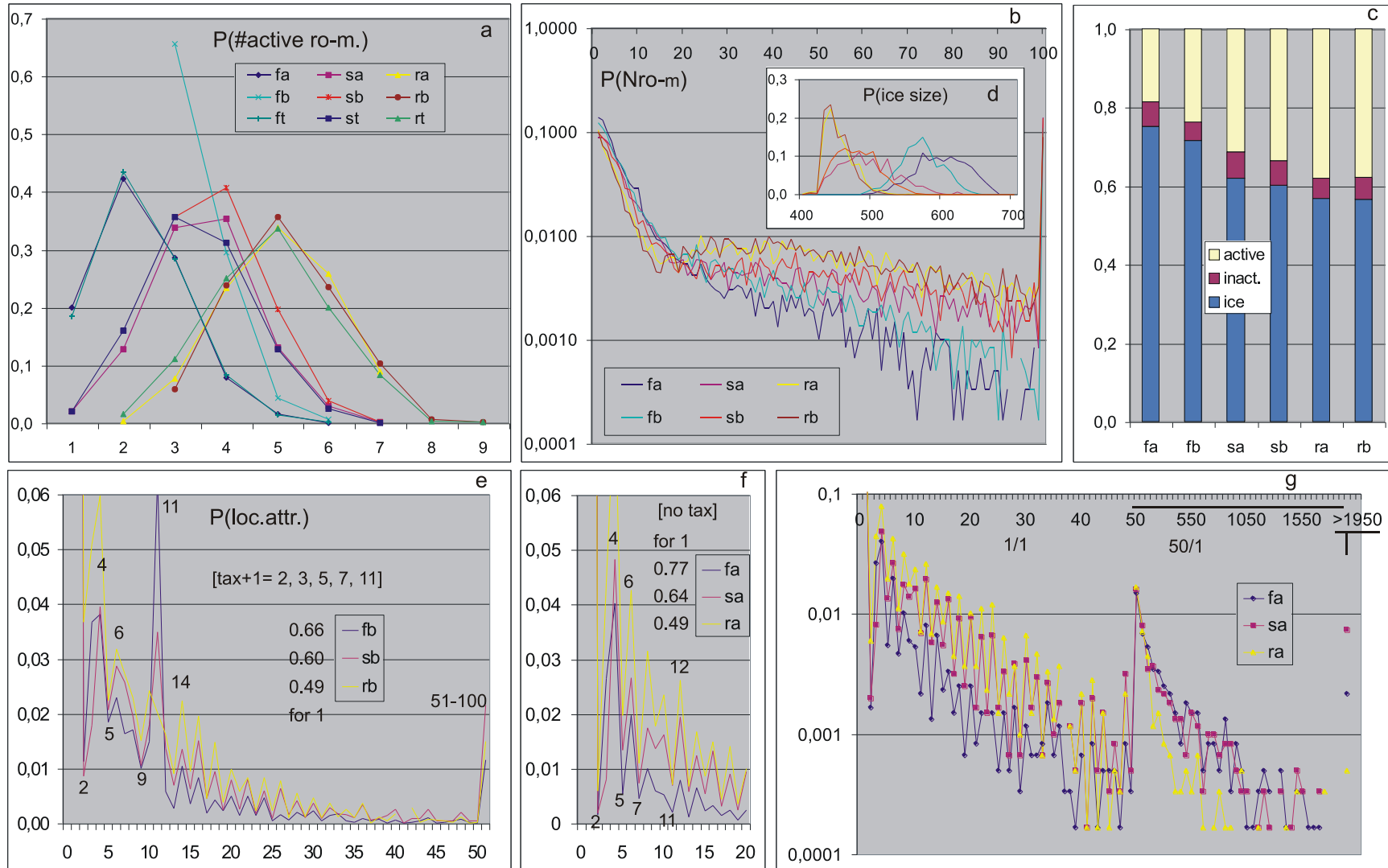
$P(\#active\ ro-m.) = (\text{number of nets where number of active ro-modules} = x) / (\text{number of nets})$.

(b) - Distribution of ro-module size: N_{ro-m} = number of nodes in ro-modules. For both models and all net types it is similar, only net f has small departures. Most ro-modules are smaller than 20 or =100 (upper limit typically reached by first) (see crocodiles [fig.8](#)).

(c) - Share of network nodes in: active, inactive ro-modules, walls (ice).

(d) - Distribution of ice size (in node number) for nets and models indicated in (b). Here points are a sum of 10 consecutive sizes. Picture of this problem is later analysed in [fig.11,12,13a](#) during evolution when it significantly changes. Presence of these changes of created state similar to observed in met5c shows work of some different mechanisms discussed in ch. 7.4.2.

(e,f,g) after fig, on next page.



(e,f,g) - Distribution of local attractor length for ro-modules. Compare [fig.5e, 7](#). Fraction >30 is very small. Values for point attractors are cut and separately written.
(e) - For model b. Forcing (tax+1) turns to be effective in small range for 2,5 and 7, but multiples are present for 2 & 7 (4,6,14, 16...) however not for 5. Attractors >50 are summed in last point (51-100).
(f) For model a in line form as in (e) but to 20, and in log scale (g) full range, where greater than 50 are shown summed by 50 consecutive values, last point indicates >1950 including not found. Distribution for model a without forcing short attractors is similar to model b with the forcing, which was surprised. The tails of these distributions practically have no influences, but they seems to be the only explanations of differences in [fig.3e](#).

7.3.4 Basic mechanism of ro-modularity

Ceasing of chaotic explosions in range of few first revolutions of small attractors of ro-modules is the basic mechanism of ro-modularity. New trajectory must not have the same attractor, in addition the way to attractor entry need typically a few time. However, typically time to the entry is short and attractor is similar (which is shown in ch.7.4.4), then new trajectory quickly (in time of 2 revolution of middle attractor statistically) reaches already tested section and explosions cease. This picture is a great approximation which assumes that new trajectory inside ro-module will not create not prepared state in ice walls and damage will not cross them.

Initiation of frozen nodes of wall has other conditions. It may initially introduce damage to one or more ro-modules, but damage may also spread inside ice, in such the case it exhausts variants to explode much later than in one ro-module. If inputs of particular node of wall take its signals from two different ro-modules with attractors – different prime numbers, then all variants ends after product of these numbers, practically – global attractor. In other hand functions of wall are more narrowed which help to fade out.

In this reason a simple expectation that small attractors of ro-modules limit explosions to 2 their revolutions turns out to be only a first approximation which neglects abundance of possible phenomena of small probability. In simulations initiations in ro-modules and in node of walls are distinguished, generally ini in ro-modules are observed. For ini in the walls is taken, that they are not limited by ro-modularity mechanism which also is a simplification.

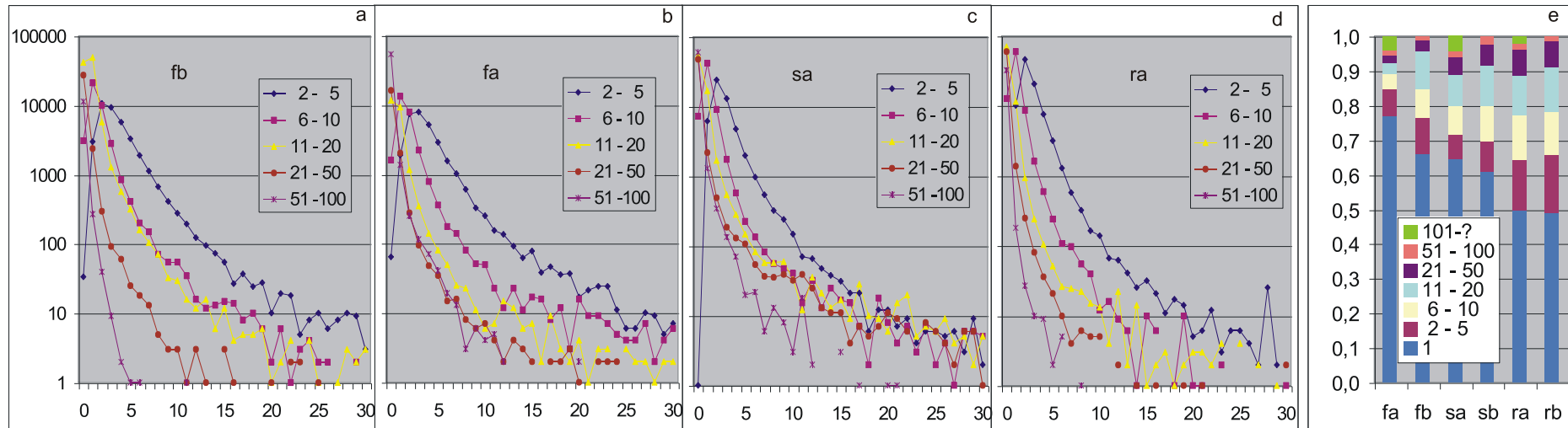


Fig.5. (a-d) Horizontal axis – number of local attractor revolutions up to chaotic explosion of ro-module which contains initiated node.

Vertical axis – counts in log scale. Data from 600 nets divided to ranges of local attractor length.

For ice and inactive ro-modules all explosions are in range of first revolution of global attractor.

(b,c,d) for nets f,s,r in model a. (a) - Net f in model b gives slightly other results than in model a. Nets s and r in both models are similar.

It is obvious that for very small local attractors number of revolutions is more, here time to reach threshold=300 by exploding avalanche (in average circa 10) is important (fig.6g). Comparison concerns pattern attractors, but after ini attractor must not to be the same. Typically also time to reach new attractor must not to be so short.

(e) – Share in ro-modules of local attractor ranges used in (a-d) and point attractor. The main part is taken by point attractor (inactive ro-module) not used in (a-d).

Results of comparison of these expectations and reality are shown in fig.5a-d for nets f,s,r and model a, but net f is shown also for model b. Because 2 revolutions of small local attractors (=2,3,5) rather will not be enough for way of avalanche to threshold, even the avalanche grow fast from ini, then test is divided to few ranges of local attractor length. Really, small attractors have more revolutions to explosion, which justify distribution of time for growth of avalanche to size = threshold shown in fig.6g. Therefore in fig.5a-d for range 2-5 explosions practically not occur in first (0 in fig.) revolution of attractor, and for range 6-10 also the first revolution takes much lower fraction than second one. These data are for any explosions, also after secondary initiations (always start from first ini), but little less precise measures (only to t=20) for explosion after

first ini are identical only tail is minimally lower. This very small difference is effects from secondary initiations which shift absolute time of explosion into slightly larger values, but fraction of such explosion in N experiment is also small which is seen in [fig.1c,d](#), greater for X. It indicate a cause of flat tail for chaotic X,S,T,F ([fig.6a,b,d,e](#)).

For N maximum in [fig.6g](#) for f,s,r, is in 12, 9.7, 8.5, but the distribution is not symmetrical and the time is smudged to right. After ini small attractors often become longer. If we respect these few different correction for very small attractors, then really **explosion later than 2 revolutions of local attractor have small probability which confirm view of ro-modularity. In this simplification first revolution” contains way to attractor and for greater attractors also way to threshold, which for short attractors it not hold.**

In [fig.6a,b,d,e,g](#) distribution of explosion time is shown. Data from 300 nets for X,S,T,F and from 600 nets for N. 2 mechanisms are visible, rapid change of domination (indicated in [fig.6a i d](#) for net f) – of fast into slow fallen curve the secondary initiation respond. Without ro-modularity they meet random circumstances, which lead to explosion if not now, then next time. However, in ro-modularity they meet already tested circumstances, it means – without explosion like last time. It is clearly shown in [fig.6c,f](#), where from this point explosions practically not happened and $q(t)$ level stays constant, But for X,S,T,F systematically falls to tmx and we can expect that after increasing tmx it will fall to 0. **Then another than typical situation of secondary initiations is an important element of ro-modularity mechanism.**

In ro-modules with very short attractors there is small number of input states for which function of walls should be the ice. Comparing [fig.4c](#) and [fig.5e](#) we can conclude, that inactive ro-modules are smaller. Similar estimation of linear connection between ro-module size and local attractor length can be taken from crocodiles observation. Then in [fig.7a,b](#) connection of average size of ro-module and range of local attractor length is shown. It really confirms such connection, but it mainly effects from number of ro-modules with maximal size 100. After removing this size=100 - series with star in [fig.7a,b](#) show entirely another picture. More information in [fig.7e,f,g](#) for nets f,s,r, (assembled from models a and b) where size of ro-module N_{ro-m} measured in nodes (5 indicates range 0-9, similarly 15, ... 95, but 100 indicates only 100) is indicated in condition of local attractor length. Strong preference of small sizes by inactive ro-modules and avoiding of small sizes when attractor is greater is seen. However, they are not simple connections and they depend on network type.

Connection of ro-module size and its attractor length is interesting to estimation explosion probability after ini in particular ro-module and to compare it to the probability for ice walls. It can confirm mechanism of stability increasing and role of ro-modules. In [fig.7c,d](#) $q = P(akc)$ of initiation in ice and in ro-modules with indicated range of local attractor length is shown. Fraction of the ro-modules (series with star) are added. There is seen that nodes of ice walls take the main fraction but they have small degree of order (high probability of explosion) despite they have more narrowed functions. However, ro-modules have small fractions (compare [fig.4c](#)), but greater q , which creates left peak in [fig.1 i 2](#). However, results of condition q and range of local attractor in [fig.7c,d](#) is surprising, because q grows with attractor length in both models a and b, but it should be expected much greater q for range e.g. 6-10, and significantly lower for range 51-100. Also q is significantly greater than expected. However, q for ice is few times lower than for active ro-modules, which confirm importance and general view of mechanism. The picture is much more complex than expected.

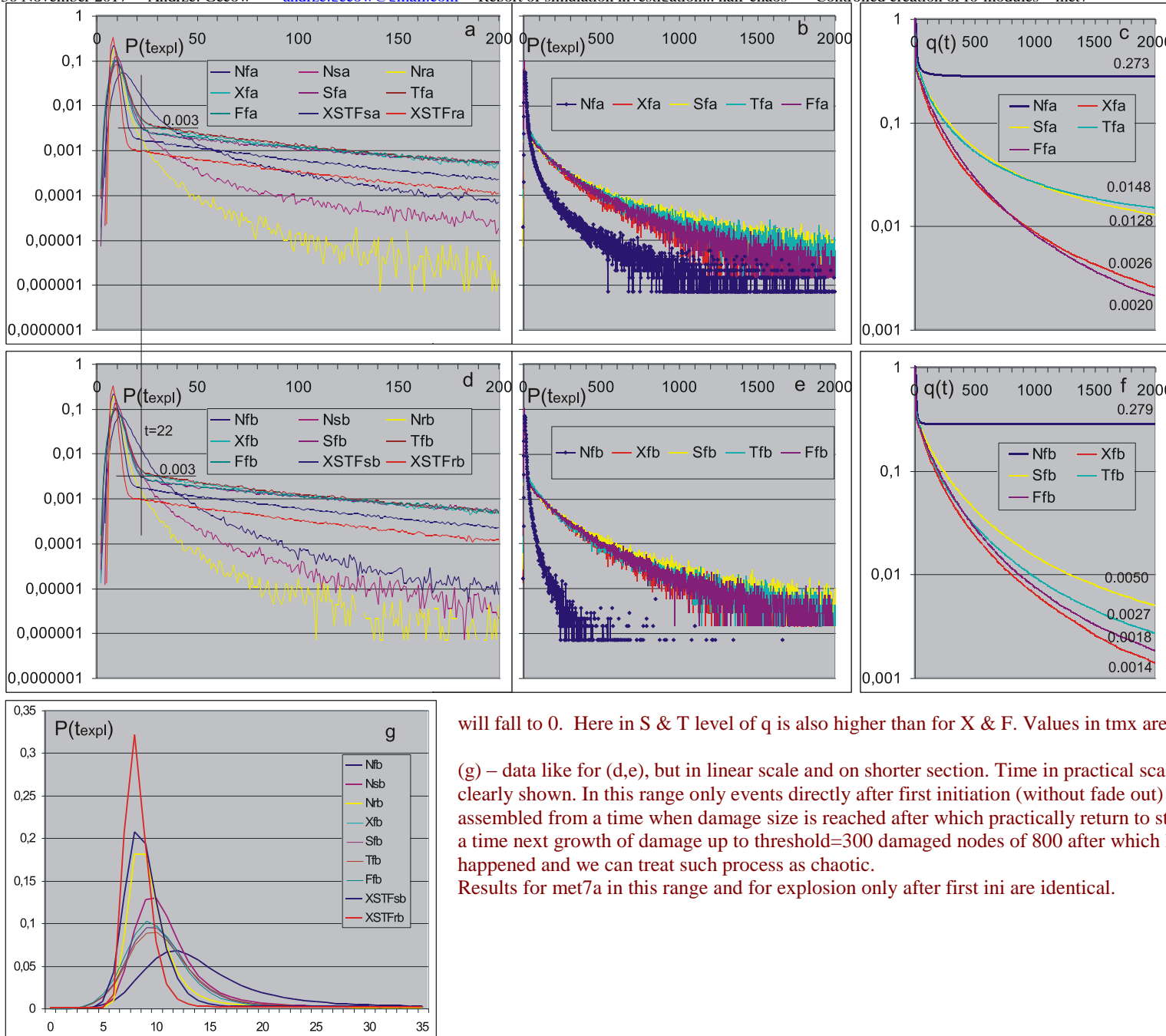


Fig.6. Distribution of explosion time (i.e. time of reaching of threshold by avalanche) for models a & b. Time to explosion is important due to its connections to ro-modularity mechanism of explosion blocking.

(b,e) – for fa & fb in full range of tmx.

(a,d) – beginning part of section tmx for all nets with separate X,S,T,F for f and sum of them for s & r. Point (t=22, P=0.003) of change of dominate mechanism from first ini to secondary ini is indicated for net f and X,S,T,F

(c,f) – decreasing of ordered processes q(t) on example net f. for N it practically ends at t=100, but for X,S,T,F it does not stops in effect of secondary ini and probably for greater tmx it

will fall to 0. Here in S & T level of q is also higher than for X & F. Values in tmx are written.

(g) – data like for (d,e), but in linear scale and on shorter section. Time in practical scale to threshold reaching is clearly shown. In this range only events directly after first initiation (without fade out) practically exhibit. The time is assembled from a time when damage size is reached after which practically return to stability does not happened, and a time next growth of damage up to threshold=300 damaged nodes of 800 after which level explosion never happened and we can treat such process as chaotic.

Results for met7a in this range and for explosion only after first ini are identical.

7.3.5 Comparison of met7a and met7b models

Fact, that local attractor length distribution with and without forcing of short attractors (by tax method) is similar (fig.4e,f,g) was a large surprise. Obviously, simpler model a without forcing is “first” and more important and despite model without evolution is only a step to more complete model with evolution, comparison of both models should be done already, on more simple models and due to more exact results based on larger $N=800$ and $tmx=2000$ than used in model with evolution ($N=400$, $tmx=1000$). Already starting from fig.1 and tab.1 result are shown for both models. The model b would be omitted however some small but important differences are detected. Models a & b differ also in not important limitations: in b local attractors are ≤ 100 but global > 200 .

The main result – level of q shown in tab.1 and in fig.1c,d is very similar: slightly lower in model a for net f, but slightly higher for nets s & r. In fig.1a,b the greater width and shift of right peak (Derrida chaotic equilibrium) especially for net f is the main difference of the models. It is better visible in fig.2 right, but the best in fig.3e. When only for experiment N the presence of ro-modules is the best explanation, then for X,S,T the same explanation of similar departures in fig.3e is not possible. It is clean, then it is still departure from full randomness of functions effected from strong narrowing in walls between ro-modules, but difference between X,S and T suggests that in X and S some trace of ro-modules remains (wall nodes remains with their functions). In T only function narrowing can act. In model a there is no limitation on attractor length and we can expect its larger length which would explain larger function narrowing, but in fig.4g fraction of larger local is small.

Picture in fig.2 left, fig.3b is an important difference. There for model a in left peak tail of nets f & s an additional hump is visible. Comparing model met7b to met5c such “new” mechanism may be suspected, but only the results of model a prove its presence. In other hand, the controlled recreating of met5c results is the goal of met7, then direction of modification model a to b is compatible to the goal. However, for the initial aims of investigation – search for mechanisms increasing stability of “chaotic” systems, this additional mechanism would be one of them because it adds events creating hump, but observed in fig.3b decreasing of fraction of smaller A1 makes balance negative. Chaotic explosion in ro-modules which does not come out of the ro-module is an explanation which is compatible with observation in fig.11, 12 i 13a that in effect of ini accumulations the ice melt and ro-modules grow, and it is stronger in model a than b and the weakest in met5c. In met7a & b there is no accumulation but peak effects from initiation.

Behaviour of T for net f shown in fig.3d is especially surprising. It is not a fluctuation, events with large q in T are observed in crocodiles (fig.8f). Much smaller, but similar in character departure from F exhibit S – should be remarked that graph is in log scale. When for chaotic X & F number L (processes without explosion) reaches maximally 52, that for T cross value 250 happened 5 times (of 300) and for S – 4 times value 100. This phenomena is also visible in fig.6c,f, where for model a degree of order $q(t)$ for S & T are much higher than X & F in all the range. Experiment T is a shift of function into another nodes but initial states (and connection structure as ever) stay without changes. Experiment S is a random change of initial states. In both cases and in X the set of functions stays without change, but they work in other circumstances. It may leads to indication of interesting remains of creating process of ro-modularity, but scale of these remains is so small and concern right peak, then it not influence conclusion from met7 investigation and deeper investigation of these phenomena are given up.

Results shown in fig.5 are similar in models a & b, excluding small difference for net f shown in fig.5a,b and effected from it difference in fig.5e. The last concern fraction of local attractor length ranges seen here clearly, but not so easy however present in fig.4e,f,g.

In fig.6, especially in fig.6b,e different behaviour of net f in experiment N in both models is clearly seen. In model a distribution of explosion time is much more “chaotic”. This difference is connected to secondary ini which level for net f in N in model a is significantly higher (fig.6a,d). Differences in fig.6c,f are described above.

In fig.7a,b,c,d differences effect from forcing mainly local attractor=11 then smaller fraction of range 2-5, which is seen also in fig.4e. This factor in met7eb is modified by another tax table. In effect f large similarity of results shown in fig.7e,f,g in both models for decreasing of fluctuation they are summed.

Summarising, model a is sufficient for main aims of met7 but model b and comparison both the models give deeper view on investigated problems. Model b shift picture in direction of model met5c, which has to be recreated, then it is the next step in correct direction. Comparison also shows that net f is especially sensitive on changes of model parameters, therefore limitation of investigation to one network type may give extreme results. Network s, despite similarity to f, is more stable regards model parameters and near net r.

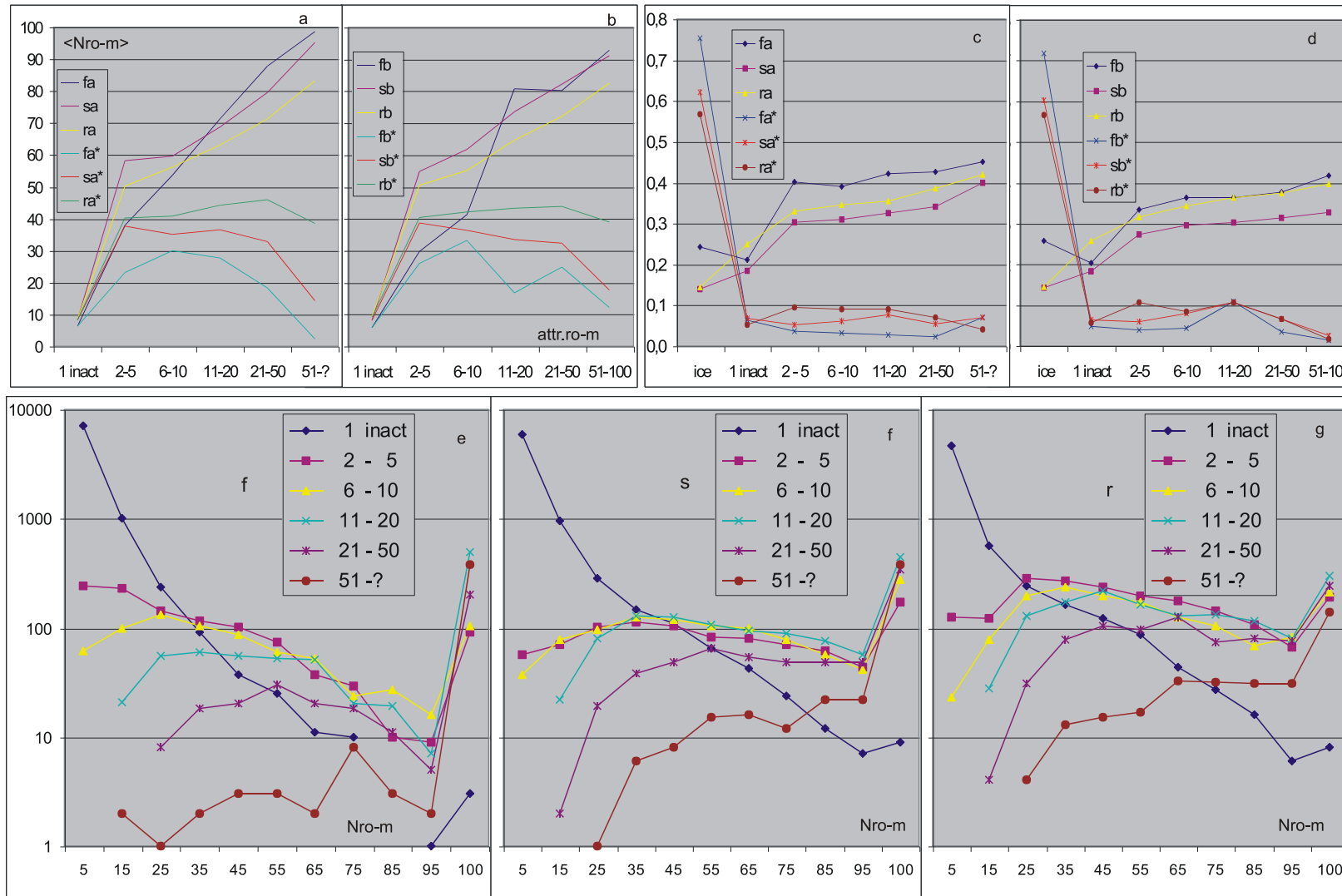


Fig.7. Connections of ro-module size and length of its (local) attractor. (a,b) – average size of ro-module $\langle N_{ro-m} \rangle$ in dependency on range of its attractor length. If $N_{ro-m}=100$ is excluded (series with *) the dependency become not more approximately linear. (e,f,g) – in other form for particular net type f,s,r, summed from both models a & b. $N_{ro-m}=5$ indicate range 0-9, similarly 95 range 90-99, but 100 - only 100. Strong preference of small sizes for inactive ro-modules, avoiding small sizes when local attractor is larger. (c,d) – $q = P(akc)$ probability of

acceptance of initiation in ice and in ro-modules in dependency on range of local attractor length. In addition - fraction of nodes of ro-modules (series with *). Nodes of ice walls are the main fraction, but despite function narrowing they have large probability of explosion. Ro-modules, especially active, have small fractions (see fig.4c), but larger q which creates left peak of ordered events in fig.1.

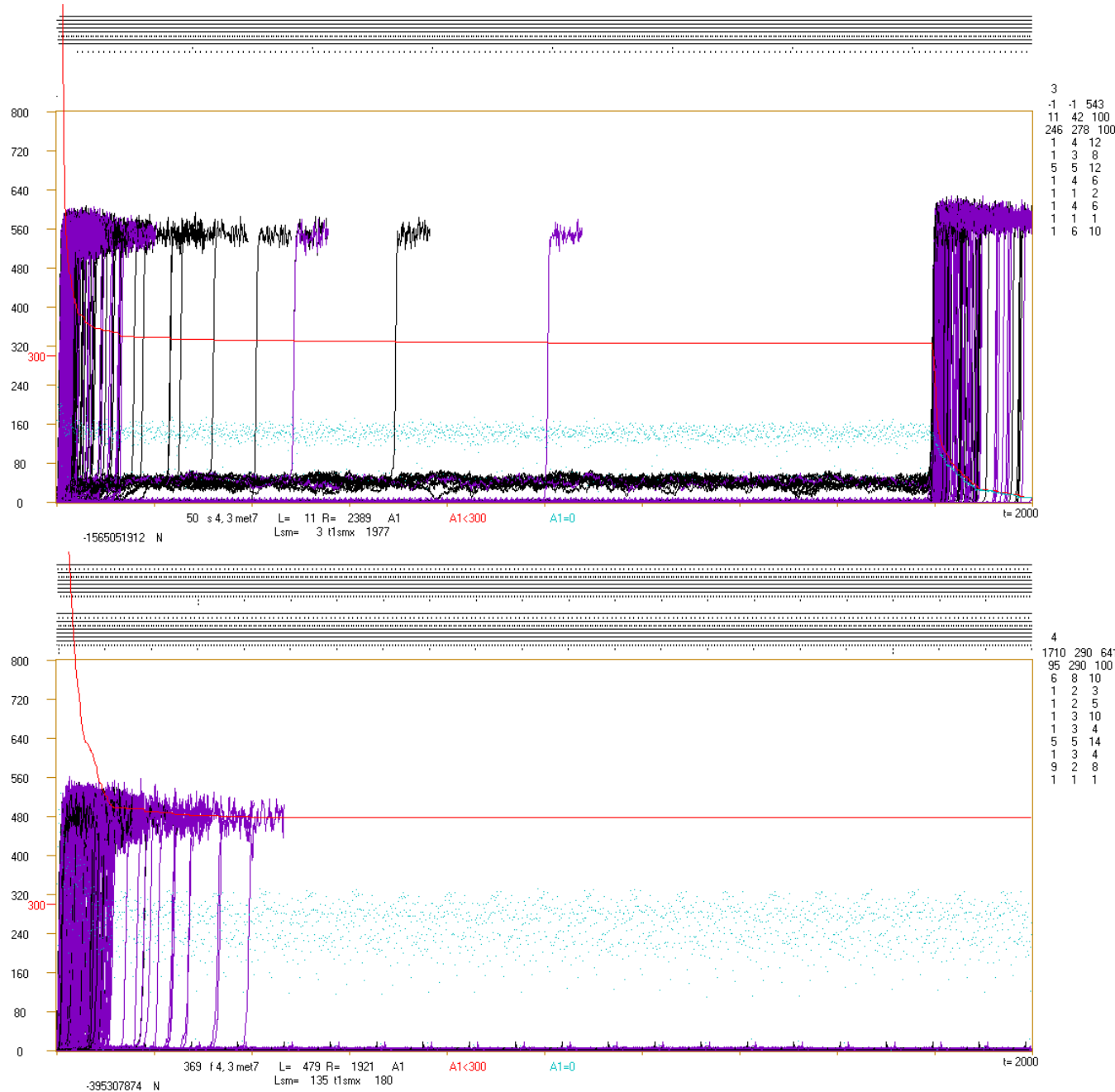
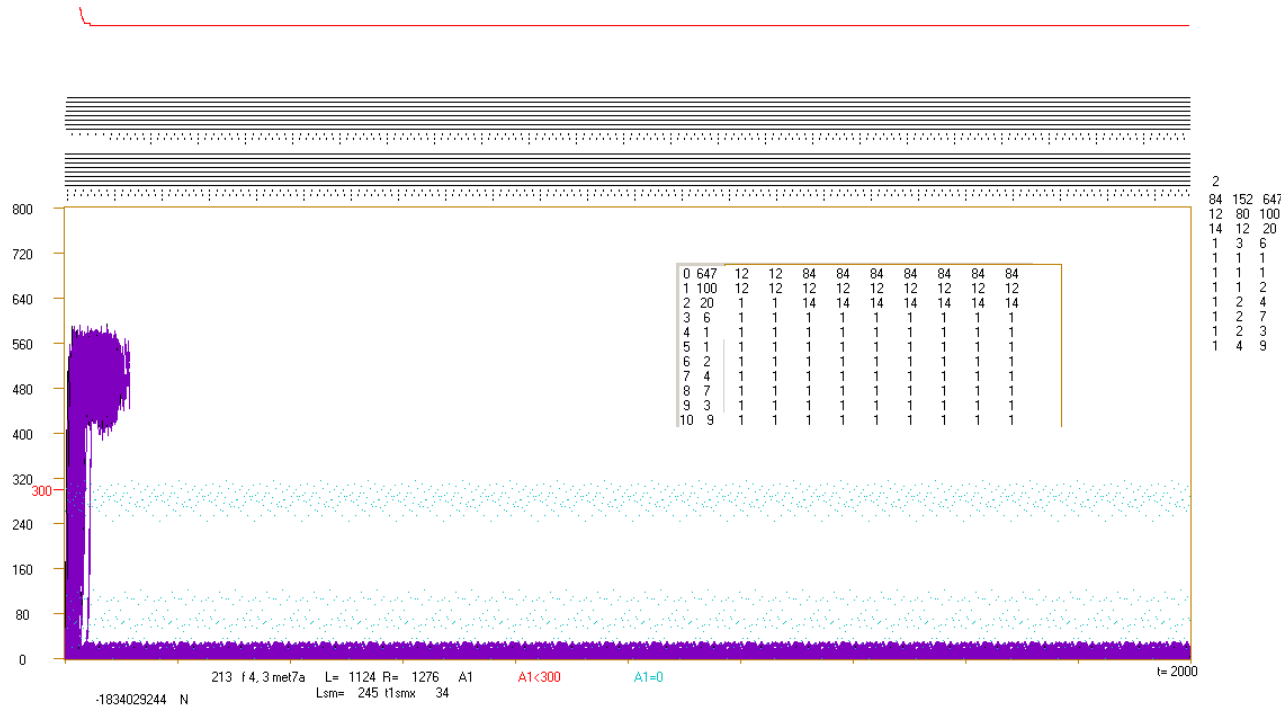


Fig.8. Examples of crocodiles. (a) - Event from provisional series where after shift of initial point to the latest begin (in 278 state from tmx) of local attractor (246 length) chaotic collapse happened (near t=1800). It is 'chaotic explosion' in added section of pattern trajectory, leaving of ro-modularity. In this point even processes which do not leave ro-modularity look like exploding ones. In the range of pattern ro-modularity (to 1722) one of 2 ro-module with size 100 nodes often reaches 'local' chaos and Derrida balance (level 40 – 65). Black concern ini in ro-module. There are 3 active ro-modules of 10 generated, global attractor not found (-1), 543 ice nodes. Below 10 ro-modules: local attractor length, its begin, number of nodes in ro-module. Above box attractors of ro-modules (state from tmx) before shift. (b)- Typical picture for net f in final simulation series. Higher set of 'attractors' before shift (state from tmx) lower after shift (state from t=4). Here global attractor length = 1710, however explosions stop near t=400. The latest explosion after initiation in ro-module: t1smx=180, in which ro-module was initiated is unknown, but the greatest local attractor=95 then 180 is less than 2 its revolutions. Red line shows number of which not cross threshold =300 (see fig.6cf), in tmx=2000 it is L=479. In each 800 nodes of net there are 3 ini, together 2400, therefore the red line is higher than left scale at the beginning. Number of A1=0 for particular t (blue) is here shown in point. It shows level of



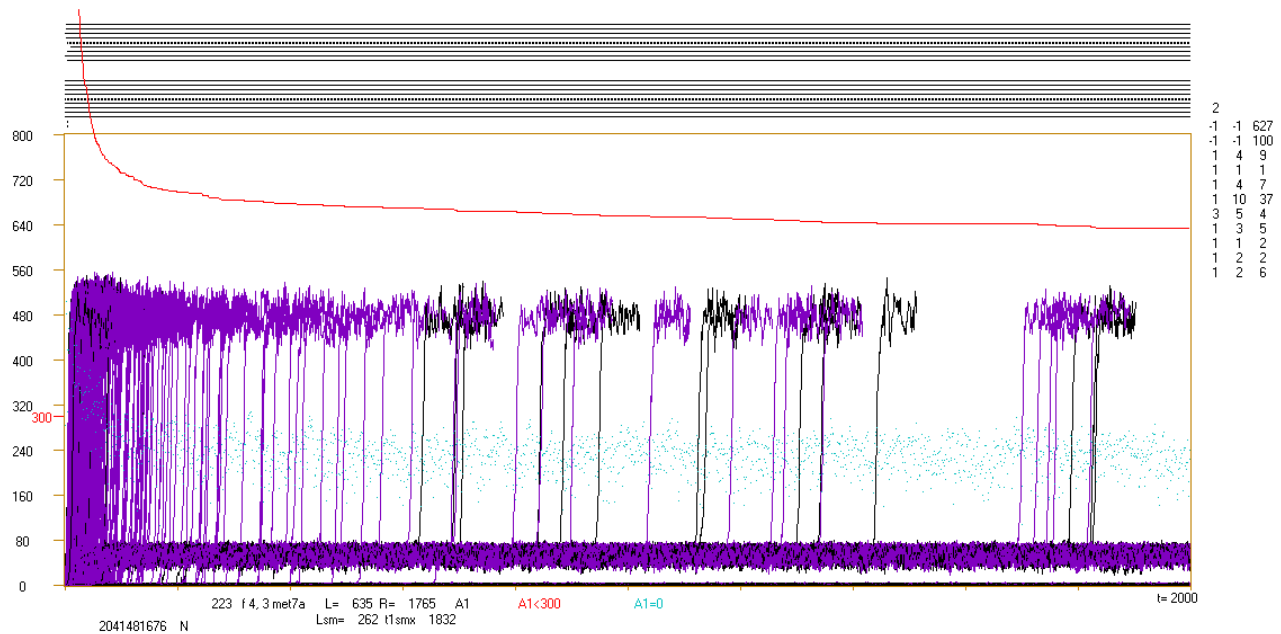
fade out and secondary initiation.
(c) - Often met form of very ordered event. Here level L=1124 is one of the higher. Blue points of A1=0 create here horizontal belts. Horizontal line even often happens.

Into box a table of correcting iteration (fight for active ro-modules) is copied. In effect one inactive become active. Global attractor is here product of prime number $84=2*2*3*7$ where one '2' is common for both active.

In the left lower corner, before 'N' indicating experiment type there is an initial number for random number generator allowing to repeat this event of net simulation.

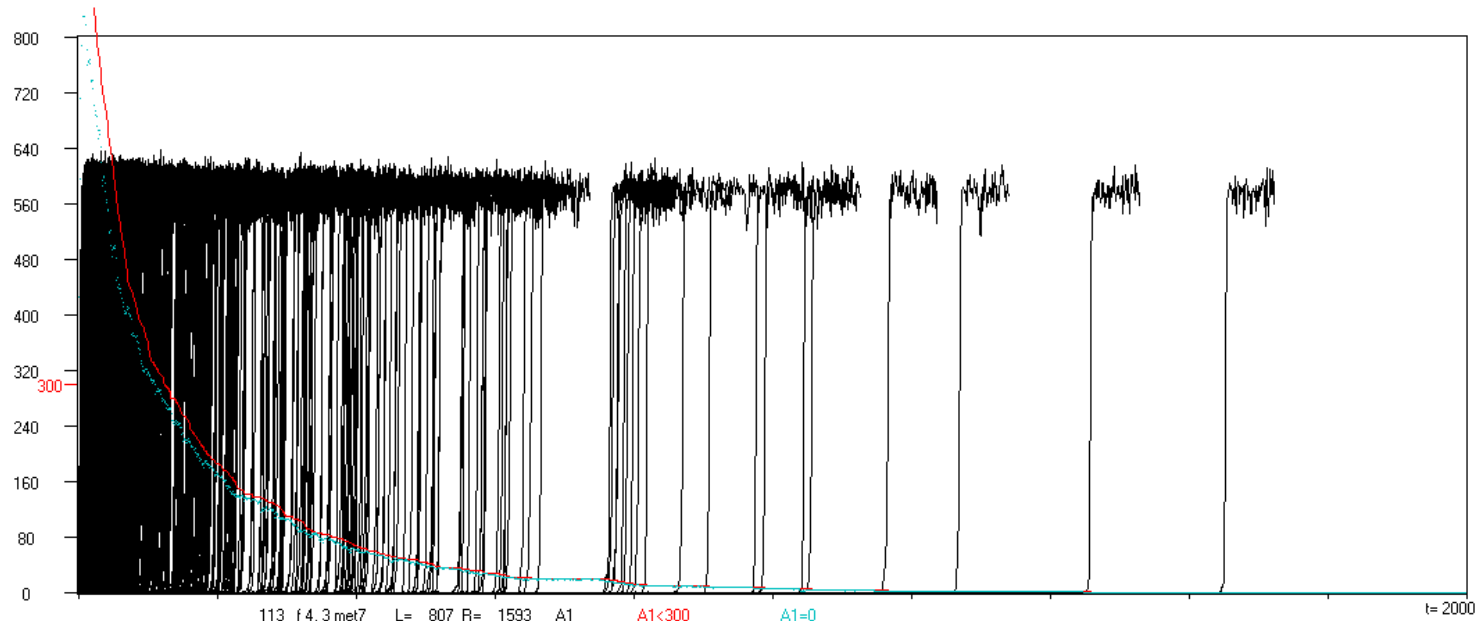
```

2
84 152 647
12 80 100
14 12 20
1 3 6
1 1 1
1 1 1
1 1 2
1 1 2
1 2 4
1 2 7
1 2 3
1 4 9
    
```

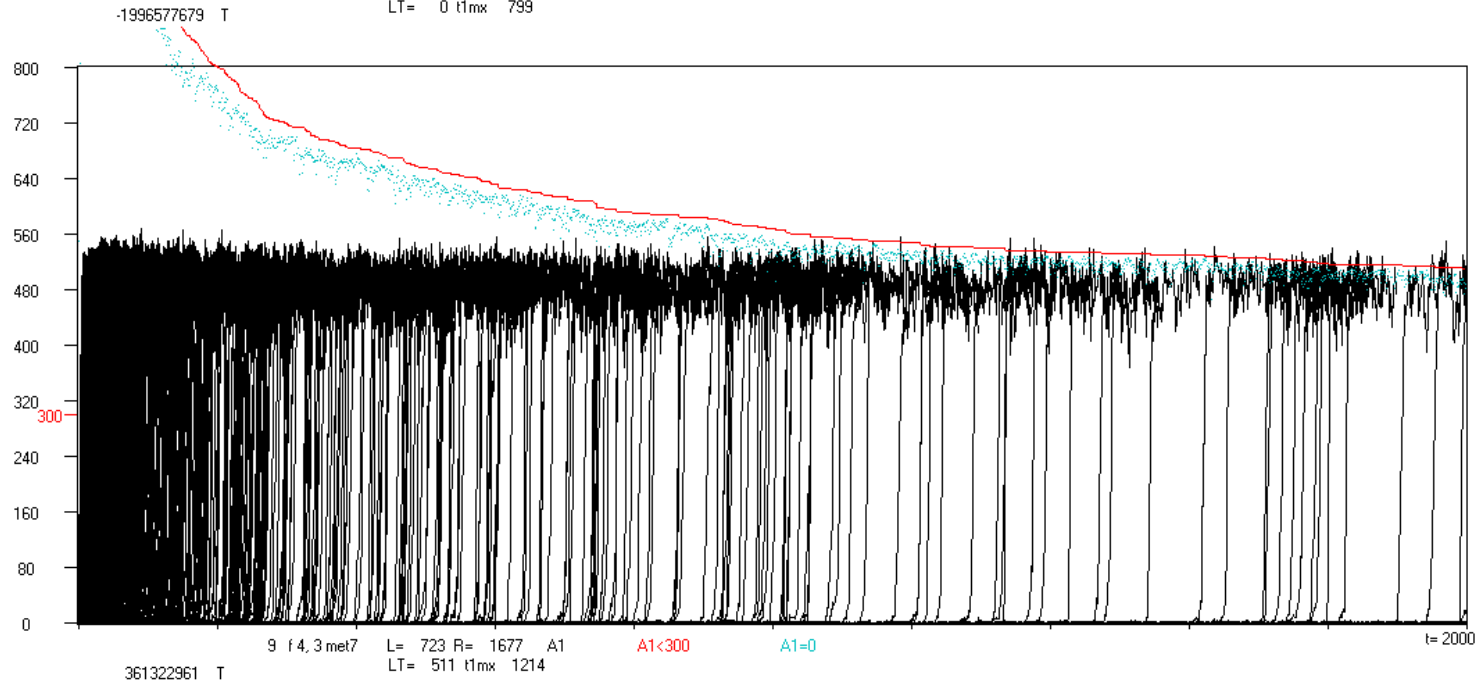


(d) - One of 2 active ro-modules has attractor greater than $tmx=2000$ and it is not found. The event looks like chaotic in range of tmx , but it differs from chaotic (e,f) in low level of fade out and high level of L (not yet explored).

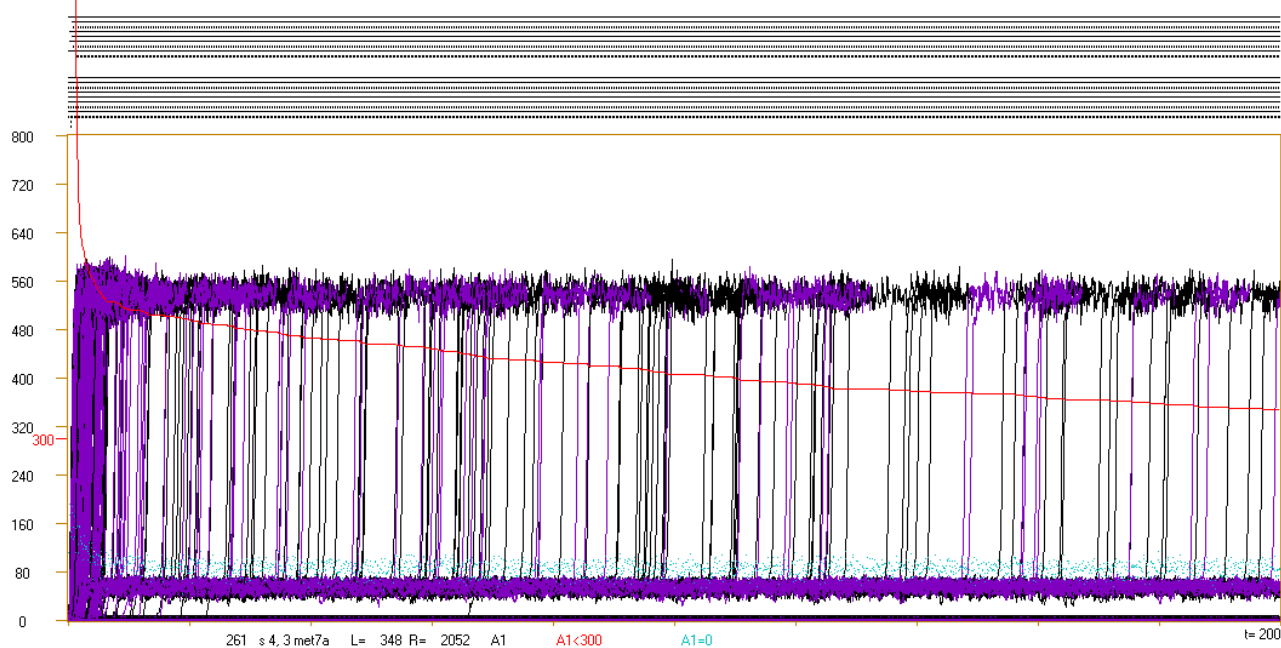
In level 30-70 the belt of Derrida level in ro-module with 100 nodes and not found attractor is seen. In this belt may be 300 ini in this ro-modularity, but L=635. Lot of the ini concern wall nodes (purple) but typically they are late, therefore purple are on the top. Thin belt as line on level 1 also contain lot of processes which become blue 'A1=0' (their number 160-280), probably initiated in initially inactive ro-modules.



(e) - Chaotic result of T experiment (shift of functions to other nodes) for net f. Here $LT=0$, but typically for f it reaches a few or a dozen or so, for s & r it rarely cross 4.



(f) - For net f often happened in experiment T that level L (LT) is especially high as it is visible in extreme event in left, where $LT=511$. Despite similarity to (d) mechanism is different and here we should not expect keeping of the level if t_{mx} will be larger. Typically as for chaotic events the level of fade out (blue $A1=0$) is near equal to level L. For T, 5 nets f of 300 cross level $L=250$ (see description fig.3d).

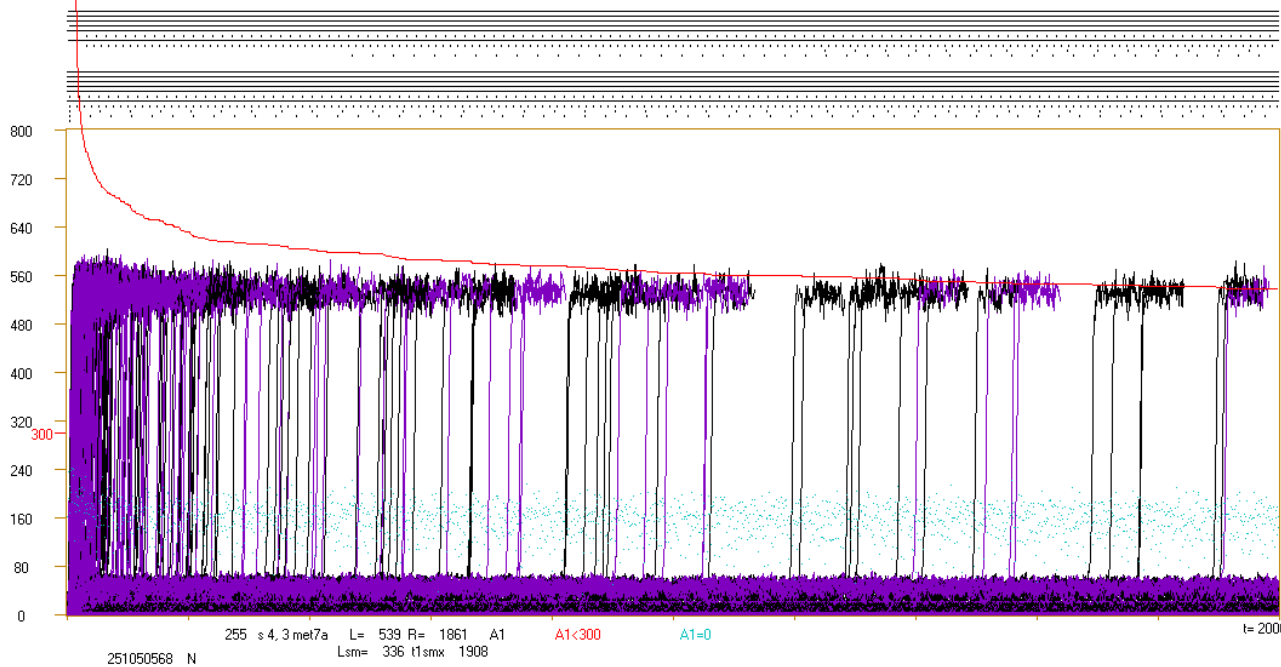


```

4
-1 -1 564
-1 -1 100
3 14 32
1 1 1
4 8 32
1 2 3
1 7 14
1 2 7
4 8 26
1 6 20
1 1 1
    
```

(g,h) - Supposedly chaotic events occurring mainly for net s.

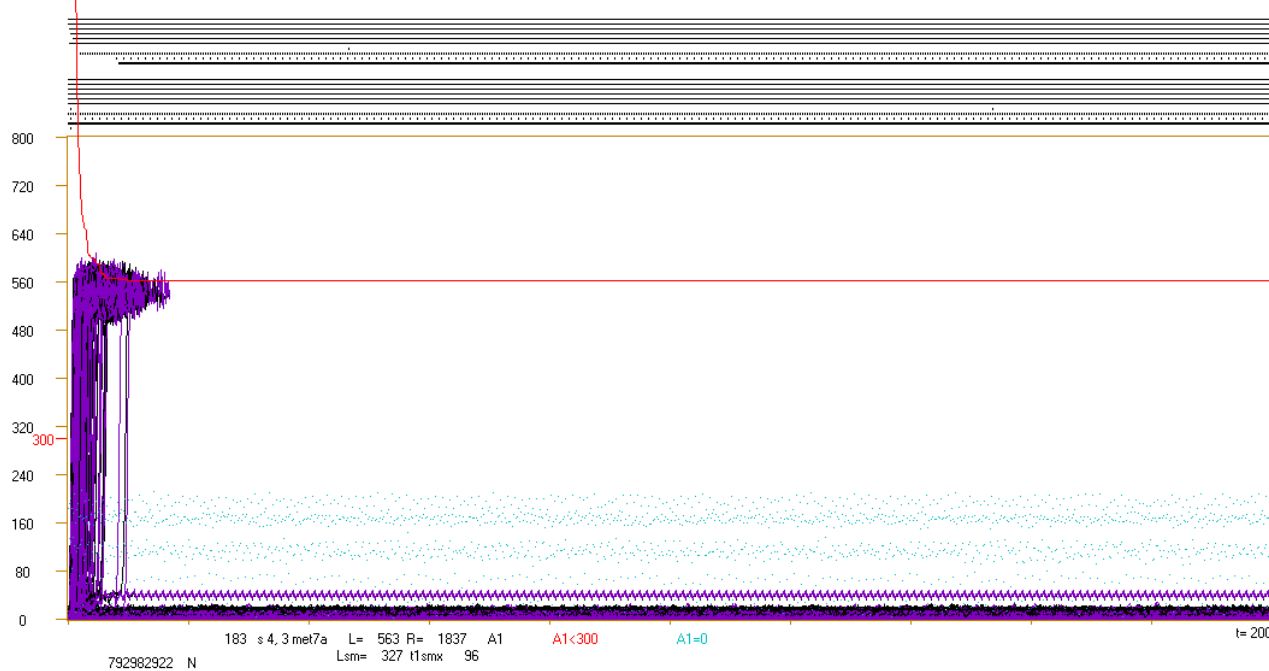
(g) - Expected effect of large local attractor. Here we can expect that after extending of tmx section over local attractor length explosion will stop. However, level L is already low and will be lower. Similarly to (d) explosions come out from belt of Derrida level in ro-module. Low level of fade out differ this event and typical chaotic one.



```

4
-1 -1 473
34 470 100
50 1250 100
12 32 83
1 2 2
16 16 16
1 1 1
1 5 14
1 0 1
1 1 1
1 3 9
    
```

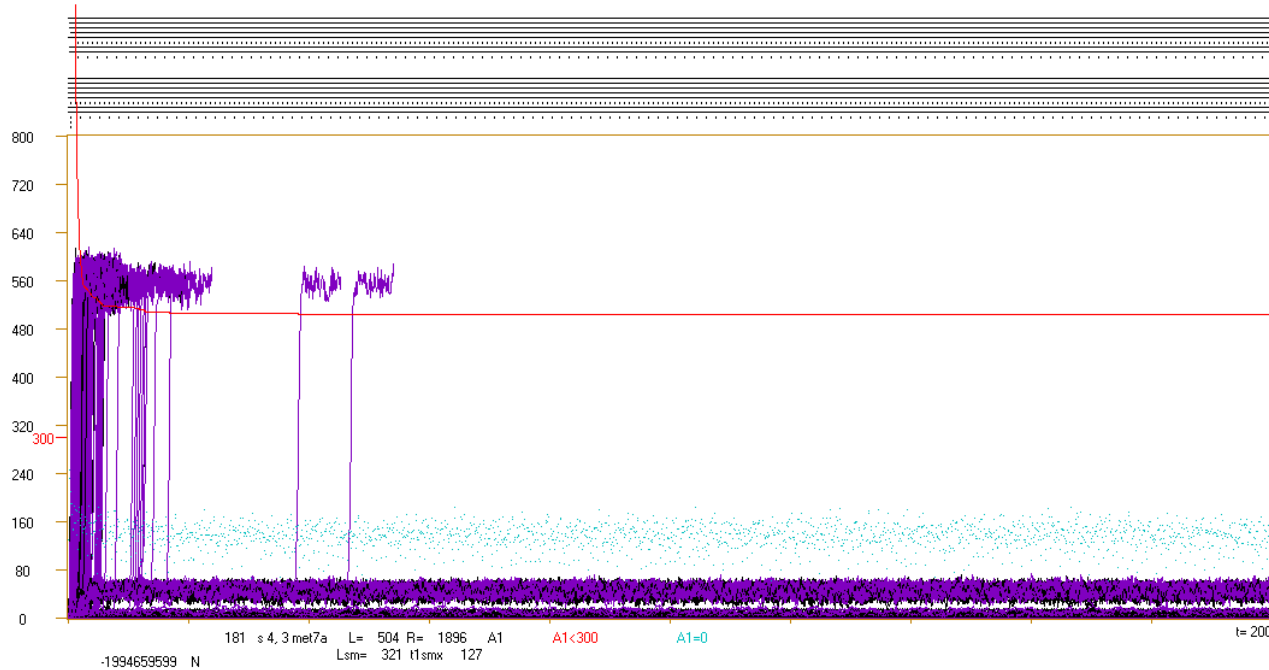
(h) - Here is lack of great local attractor but picture is similar to (g). Remark however, that minimal global attractor is $17*25*16*3=20400$ which is important for ini and process in ice. Under belt of Derrida level for ro-modules is lack a gap, probably one of ro-module is=83. Such ‘non-typical’ events with late explosion to chaos up to tmx happen rarely, mainly in net s. We can conclude – investigated connections and mechanisms are statistical and very complex. Almost each indicated mechanism exceptions happen, but statistical effect is clean.

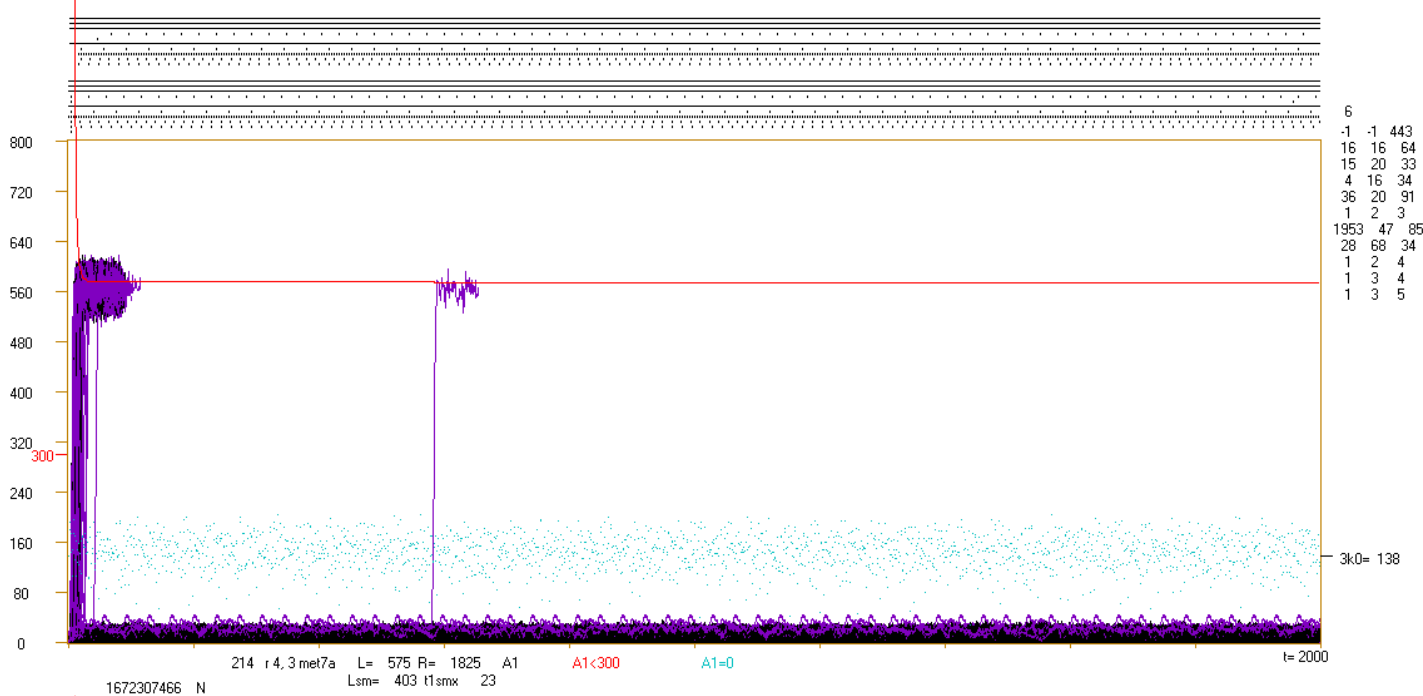


(i,j) - Influence of local attractor size happens small, especially in net r, but these example are for net s.
(i) – despite local attractor length=1533 and minimal global attractor>6000 the latest explosion initiated in ro-module happens at t1smx=96.

Lower in

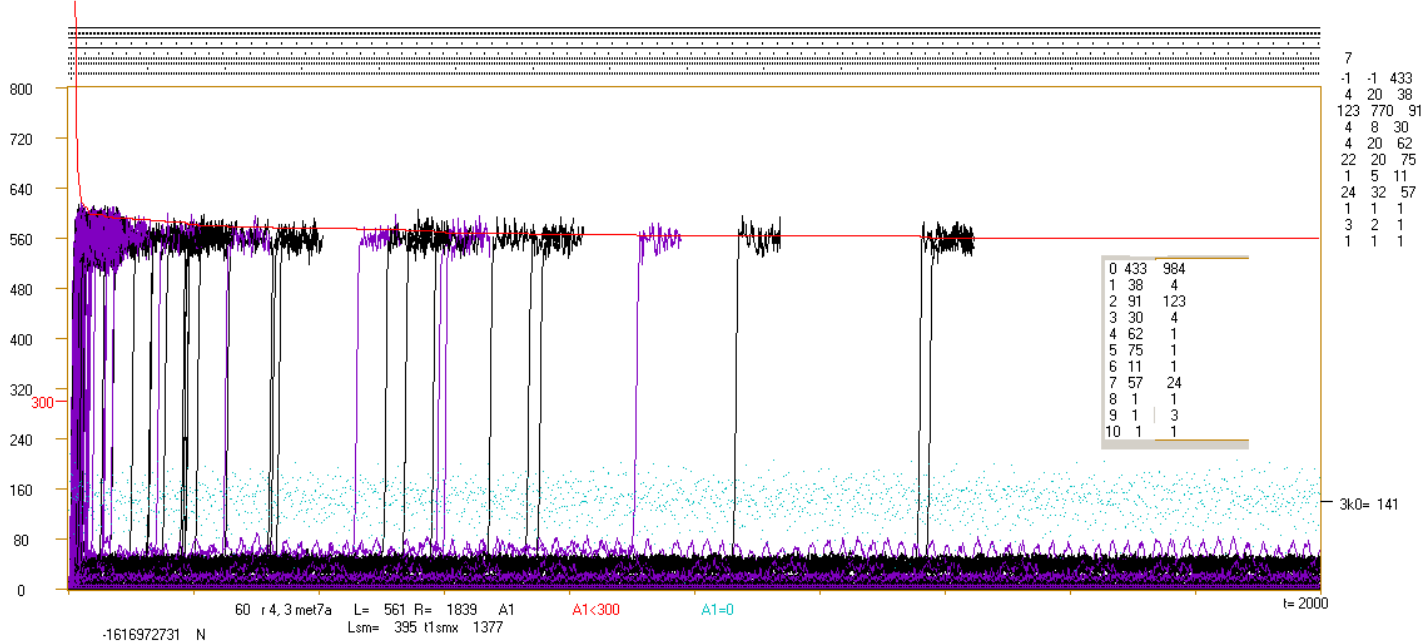
(j) with one attractor larger than tmx the latest explosion initiated in ro-module happens at t1smx=127, and seen explosion initiated in ice - at t<500.





(k,l) - Examples for net r. They are not typical for r, where typically they are similar to (c) or (i), or (k) without explosion near 600. On right wall of box minimal level of $L= '3k0'$ effected from ini in blind nodes ($k=0$) is indicated.

(k) - the greatest local attractor found in met7a for net r. Despite this the process is very ordered. This shows essential differences in behaviour of different net types.



(l) - belongs to exceptional events of net r. Despite that here is lack of large local attractor and there are 7 active ro-modules (for net r it is often but for s and f rather rare), that explosions happened late and typically are an effect of ini in ro-module (as last at $t1smx=1377$). In addition, in the case only one iteration was enough, which happened only ones. In net r happened events with smaller number of iteration than 9.

7.4 Investigation of evolution – accumulation of changes – met7e

7.4.1 Left peak and parameters selection

Simulation of evolution in met7 (met7e) was done for nets f,s,r with parameters $N=400$, $tmx=1000$ used earlier in met5 and met6, changed in comparison to met7a,b described in ch.7.3 where $N=800$ and $tmx=2000$ were used. It is for better comparison to met5 & 6 and for simulation time reducing. As in met5 44 ‘4+7’ ro and met6 after initial pass N (without accumulation in met6 & 7), 20 passes M is calculated, from which 5 (1,7,13,19,20) are „free”, i.e. without blockade of smearing but with full statistics. Rules of passes M are the same as in met5c 44 ‘4+7’. As was mentioned, firstly was made series met7eb, where maximal shift to the latest begin of local attractor is reduced from 500 to 150, because tmx is reduced. Before final series with 400 effective nets were made many provisional small series were done for recognition and parameters selections. Near end of investigations met7eb it turn out that forcing tax is not necessary which forced to create model met7a. Parameters of more important simulation series are listed in [table2](#). Those series results and their names are used in discussion and in figures.

For provisional simulation (1) 30 nets conditions: global attractor >200 , local ≤ 100 , ro-module size ≤ 100 leaved without changes. Shape of left peak in linear graph for nets f & s shown in [fig.9e](#) (range $A=0-3$) looks more similar to results of met6, but not of expected met5. Searching parameters to correct the shape also conditions were changed to: global attractor >40 (aim of limitation to 200 was already reached in ch.7.3), ro-module size ≤ 40 , tax table from [10,6,4,2,1, 10,6,4,2,1] to [6,10,4,2,1, 6,4,10,12,6] for chance of local attractor =7 increasing and addition 13 because most M20 ended on 11 which explain similarity to met6. This changes (2) significantly bring the shape near to expected for net s, and a little for net f. Next experiment (3) with change of active ≥ 3 on ≥ 4 gives small improvement for s and small deterioration for f. This change was not used later. The shape of left peak for net r was satisfactory from the beginning, and for net s after correction (2) also, but for f it was very different than in met5, then searching was continued. Limitation of ro-module size was shifted to 25 (4) with reorganization of influence of number of active ro-modules and allowing 2 active. Next tax table was changed to [1,2,4,6,10, 4,6,2,1,6] to prefer shorter attractors, but ro-module size ≤ 40 comes back (5), but next ≤ 25 was used with last tax table. This last variant turn to be the best and using these parameters final simulation for 400 effective nets are done. When simulation was repeated with the same parameters but other sequence of pseudo-random number, then it turn out, that results, e.g. q, have large dispersion, which is shown in [table 2](#). The strongest change turns to be tax redefinition. It is complex parameter, hard to interpretation and not adequately approximating real circumstances in met5. It is possible that more complex model of this aspect can give more similar results to met5cf. Investigating this aspect lack of necessity of tax was found and simpler model should be the main, then investigations come back to model without evolution (met7a) and later ones more to evolution (met7ea – series fe,se,re), but with simpler assumptions. For comparison to model b for net f series fe2 (active ≥ 2) and ff (like basic series f model b, but without forcing tax).

Results – Shape of left peak is shown mainly in [fig.9e](#), and also in [fig.9c,e,f,g](#). Log scale graph ([fig.9f](#)) clearly showing slope for greater A which is similar to observed in model met5 c 44 ro 4+7, but not in met6. Comparison for passes free ([fig.9g](#)) and similar level q in [fig.9h](#) allow summing in range M7 to M20. Pass M1 has slightly different results. Later investigations, especially picture of stabilising ice level ([fig.11, 12](#)) confirm this conclusion – in pass M7 evolution practically reaches its stable state, however, visible part of events of net f slowly converts to mechanism from met6. Differences of left peak in different passes M are shown in [fig.9g](#) for net s & f in both models a & b. The pictures for nets s & r in both models are practically identical.

All distribution $P(A)$ also excluding M1 is shown in [fig.9a](#) for measure A3 at tmx . In comparison to A1 it is more exact. Obtained share of initiated processes on ordered (including ini in nodes with $k=0$ for net r) and chaotic is shown in [fig.9b](#) typically included to [fig.9a](#). In final simulations results for nets s & r are very similar which is shown in [fig.9](#). For simulation with parameters (1) they were different, and in simulations 30 nets with parameters like final series are not so similar.

In [fig.9d](#) right peaks for met5c are slightly shifted to right for both nets f & r, which also (shape of left peak for f – [fig.9c,e](#)) suggests some difference of mechanism. In right peak for fe,f,& ff additional gibbosity occurs in left slope, it is better seen in log scale (see in [Naaj](#)). However, generally these differences are very small in comparison to differences to random network and we can state, that generated in met7 ro-modularity is very similar to obtained in met5.

Differences to met5 in left peak picture for net f in direction met6 suggest participation of mechanism met6, here called mech2, for which many basis are found. Similarity to met5 of evolution in non-free passes seen in [fig.9i](#) is clear, much greater than in met6 ([m6.fig.1b](#)), however, here also differences to met5cf in direction met6 f are seen.

Tab.2. Parameters of simulations described in ch.7.4 called met7e investigations, and comparison the parameters to used in met7a & b, met6 and met5c. Remain parameters: $tmx=1000$; $N=400$, $threshold=150$. In tax table only first 10 values are listed, because they are changed, next 10 values used in iteration increasing number of active: 6,4,2,1,10, 12,16,18,22,28 are constant. Precision of statistical results are indicated by number of assumed effective nets (**calc.nets**), i.e. fulfilled all conditions (in met7e ended in M20). Because not all **generated** nets fulfil the conditions then effective nets are less. Next columns: **description** – names used in figures; values degree of order **q**. All next columns indicate the main parameters of simulations: number of **active** ro-modules must be \geq than listed below; **tax** table (first 10). Conditions for already **generated ro-modules**: **Nro-m** - number of nodes in ro-module; **local attractor** length; **shift** of initial point to begin of attractor; **global attractor** length for passes **N** (initial and **M**, in M20 attractor cannot decrease.

As is seen, values q differ despite the same parameters for simulation are used, which indicates precision of such measures. The degree of order q for net f is the greatest for met5 but for r the greatest q is in met7. It suggests slightly different mechanisms (see also fig.9b,h). Significantly lower values q gives met6 (fig.9b), but here differences of mechanisms are known. Model a only without evolution for nets s & r give slightly greater values q , after evolution results of both models are practically identical and only difference for net f remains. In fe2 & ff model a and b with evolution differ in 3 factors: minimal number of active (change 1 to 2 increase q), remain set of limitations (decrease q back) and the main difference between ff & f – lack of tax in ff (model b turn to be “better”, i.e. giving greater q). Models met7a and b without evolution are indicated by colour.

met	calc. nets	generated			description			q			act \geq	tax	generated ro-module			glob. attr. >	
		f	r	s	f	r	s	f	r	s			Nro-m \leq	loc.attr \leq	shift \leq	N	M
7a	600	602	600	612	fa	ra	sa	0,273	0,230	0,204	1	no tax	100	no limit	1	no pass M	
7ea	400	459	408	414	fe	re	se	0,256	0,210	0,206	2		25			150	40
	210	344			fe2			0,268									
	400	1570			ff			0,251						500	200	no pass M	
7b	600	4387	1179	1420	fb	rb	sb	0,279	0,228	0,198	3	10,6,4,2,1, 10,6,4,2,1	100	100	150	40	7, M20
7eb	30	889	76	168	f1		s1	0,270	0,220	0,176		4	6,10,4,2,1, 6,4,10,12,6				
		313		67	f2		s2	0,257		0,188							
		1295		227	f3		s3	0,262		0,199	2	1,2,4,6,10, 4,6,2,1,6	40				
		102			f4			0,258									
		1011			f5			0,329									
	400	10768	625	852	f	r	s	0,313	0,210	0,211	3	25	do not concern	4			
	30	770	40	59	fi2			0,301	0,209	0,212							
		1021			fu2			0,322									
1572				fi3			0,329										
1318				fu3			0,330										
6129				fi4			0,337										
4477			fu4			0,326											
5c ro	100	165	434		cf	cr	0,355	0,171			no tax	do not concern	4				
6	200	200	200		6f	6r	0,254	0,125			20			20			

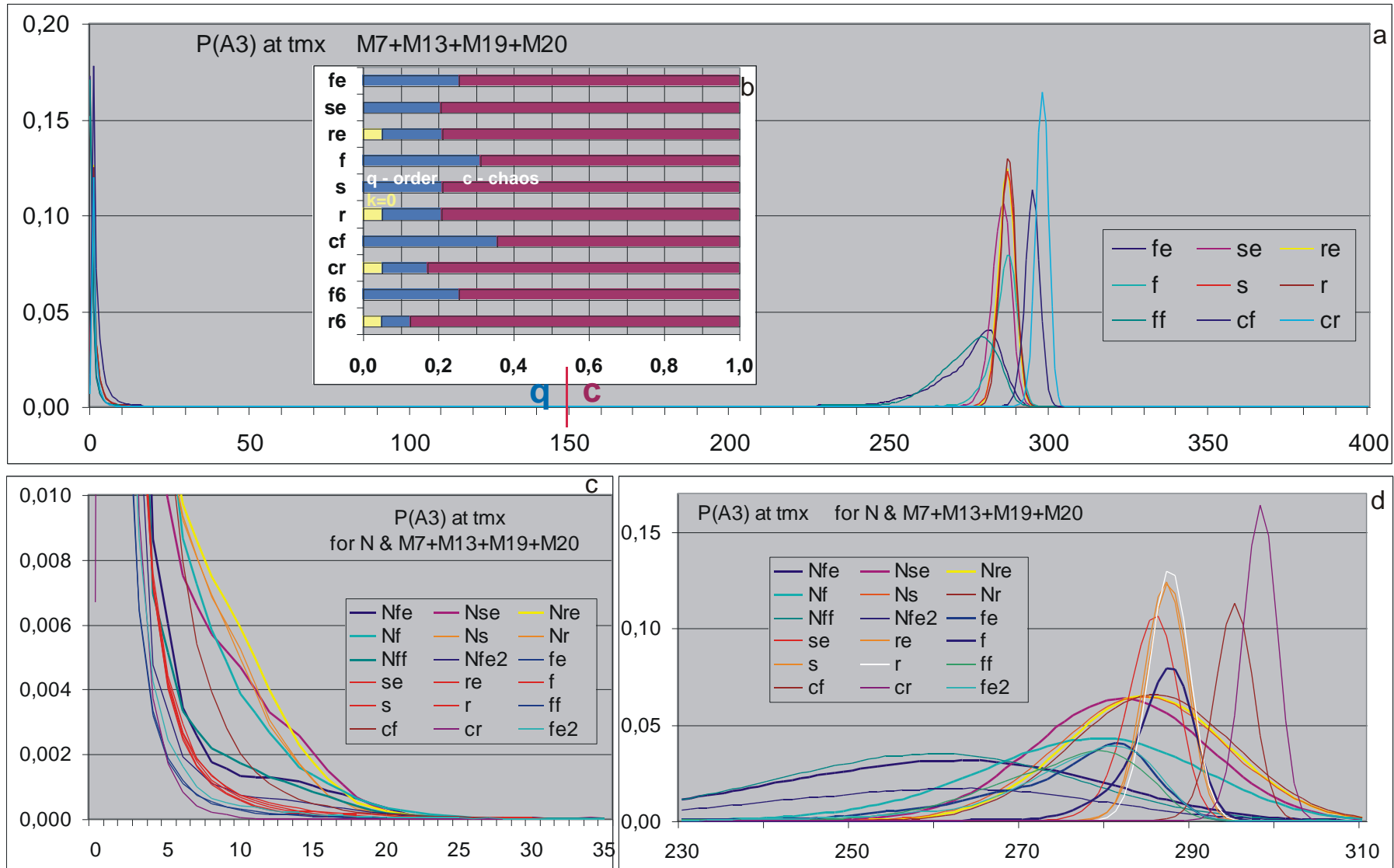
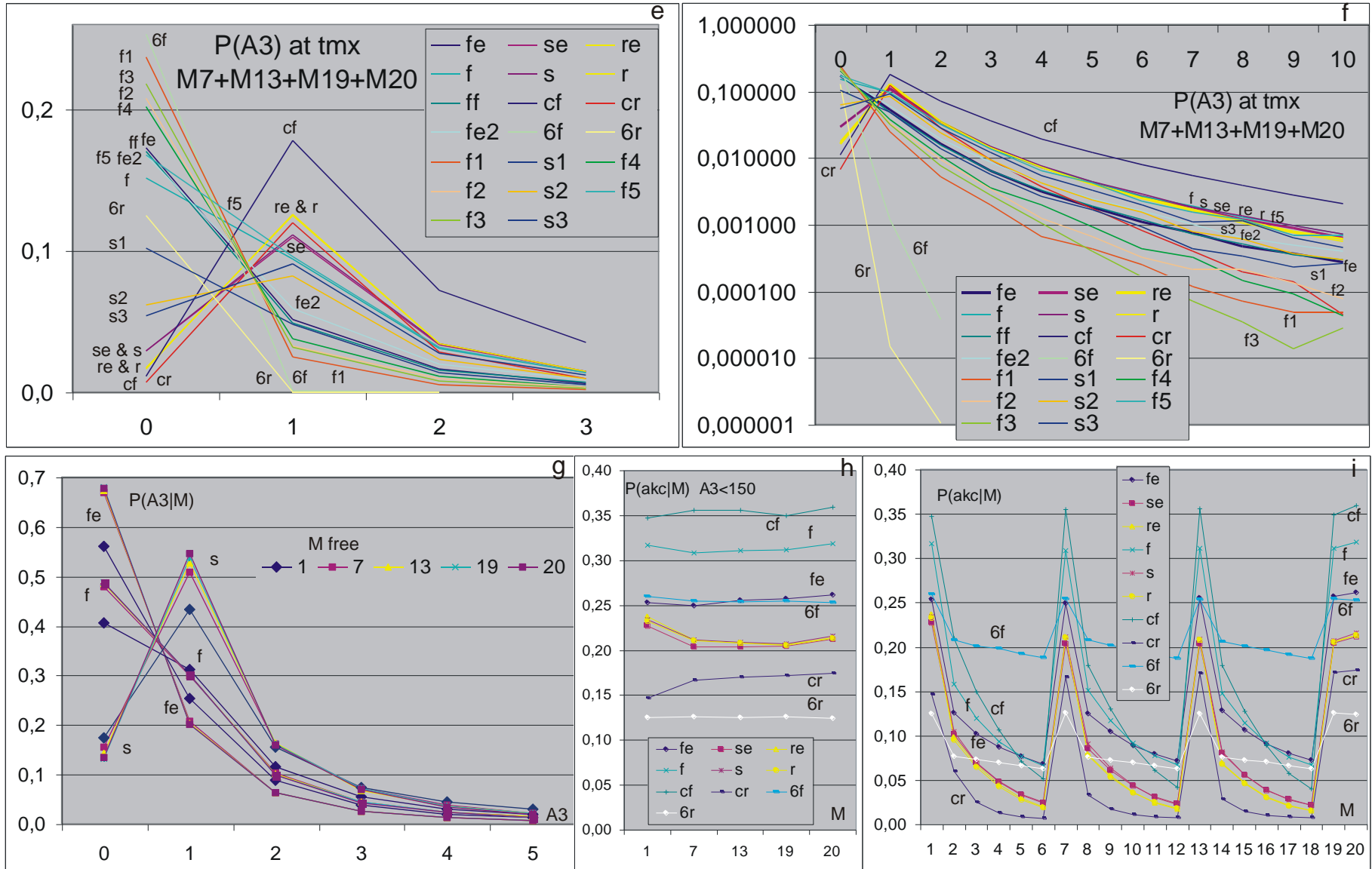


Fig.9. Basic results from met7e. They show keeping of half-chaos (obtained by controlled creating of ro-modularity) during evolution (accumulation of changes: accepted, not PAS, M1-19 global attractor ≥ 7 , M20 global attractor not decrease). Relationships (a-f) are an effect of sum of results from passes free M7 to M20 on a base fig.9g,h, which shows that only pass M1 is slightly different. In (g) passes free M7-20 cover earlier so exactly that exclude A3=1 for s only last M20 is visible. Shift of right peak (a,c) is not disturbing about basic mechanism of ro-modularity, but significant distinctness of left peak for f (e) to shape observed in met5cf is disturbing (compare m5.fig.3). This distinctness effects from admixture mechanism of met6 for net f, which for nets s & r in the most important range A3=0 to 3 in (e) is not visible. In (c), in range A3=5 to 20 for experiment N complex effects earlier observed in fig.2a left in met7a are visible. Near value 0.001 all N (exclude Nfe2) lie on the right from cf but results of evolution



on the left. This shows change of network state during evolution, i.e. generated state is not stable. The tail seen in (f) which is satisfactory and radically different than in met6 is a basic feature of left peak necessary for interpretation connected to life. Obtained q (degree of order) is similar to met5 and higher than in met6 (h,i). In (h,i) $q(M) = P(\text{acceptation}|M)$ is shown for passes free and for all. Similarity to met5 is clear (compare m5.fig.4; m6.fig.1.a,b), however in (i) for net f, especially series fe, shape flow in met6 direction. Large number of compared results make problems to read, therefore for near identical curve the same colours are used. (e) contains especially lot of information which are used to select parameters for model eb. There in points A3=1 & 2 fe and ff similar to fe2 is fare from f and f5 but they should be similar to cf.

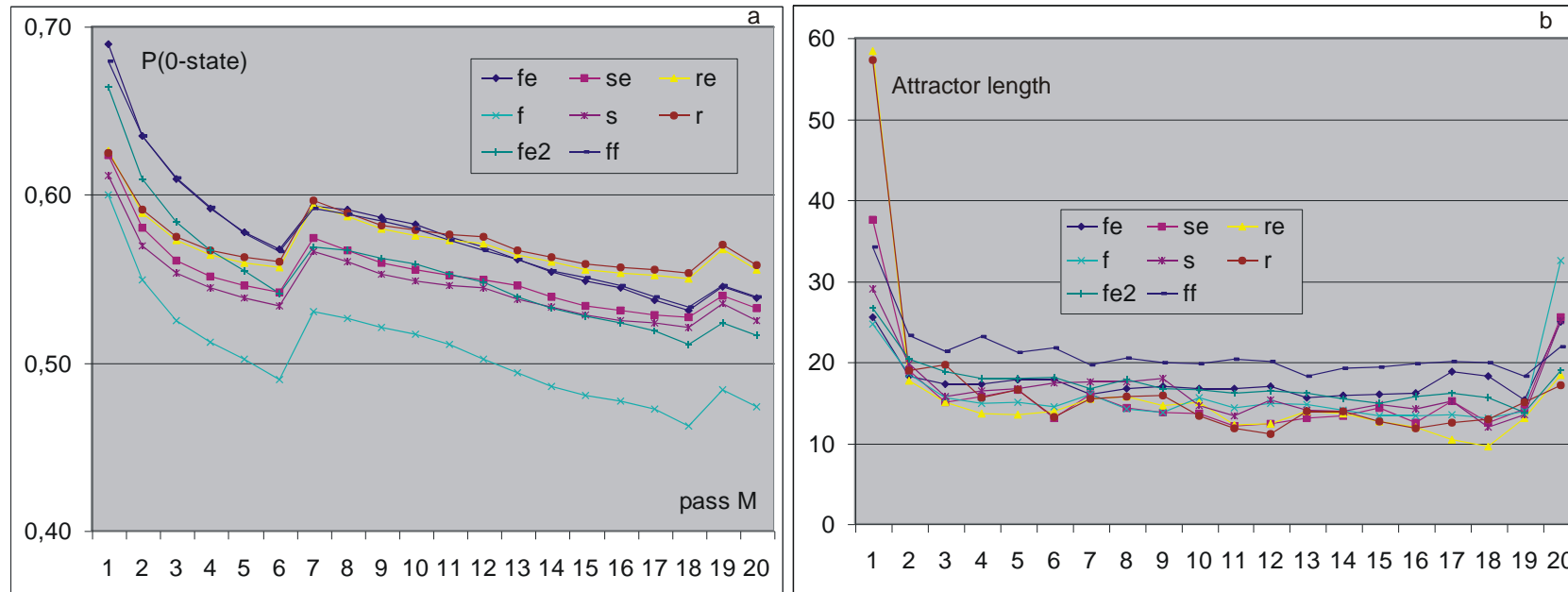


Fig.10. (a) Probability of state 0 during evolution (on section $100 < t < 900$ from trajectory after last ini in given pass, not from function), as level of evolution process advancement. Similarly like in [m5.fig.6b](#) the parameter shows degree of shift from specific initial state. In met5 it was PAS0 where all states =0, in met7 states 0 are given to nodes of walls but it is most of nodes. It is important that they are used states, not a potential possible from function statistics. Fraction of states 0 decrease despite increased stability. Similarly like in met5, the fraction very slowly decreases and is far from expected random =0.25, despite from M7 picture is stable ([fig.11-13](#)). It not prevent reaching chaos in experiments X,S,T,F met7a,b.

(b) Average length of global attractor. In met5 (compare [m5.fig.5c,d](#)) process starts from small attractor and looking after it to be not too small was necessary, in met7 after ro-module generation in model b global attractor is greater than 40 in final series, and in model a no other limitation than 'not PAS' is used.

7.4.2 Clusters ro – ice and local cluster size distribution, additional disturbing mechanism ‘mech2’ similar to met6

Investigation of clusters ro in met5 allows to confirm hypothesis of ro-modularity. Experiment met7e has to check, if ro-modular state generated under control keeps presence during evolution similarly like in met5, means, are known all its basic features. For this aim clusters ro are observed in similar way like in met5 and met6. The met6 is lack of cluster ro and necessary ice.

Local cluster ro is described in met5 ch.5.7. It is a set of nodes with the same period of node states in given process after ini which is accumulated. If period was not found, then ‘period is 999’ and it also makes cluster. Algorithm for node period searching is complex, global attractor length plays important role in it, but it is not always found. In such reason a certainty of found period decreases, especially for periods longer than half of tmx. In met5 larger global attractors are rare but in met7 they happened often (in met7ea spontaneously, in met7eb forced, see [tab.2](#)). This difference forced a small correction of algorithm. Periods<12 must repeat on section =90 steps, periods so large, that tmx not hold its second revolution, must repeat first revolution at least in 90 steps. (Periods, as attractors, are searched from tmx to begin of trajectory.) However still certainty such findings are significantly lower and they give slightly different picture, therefore events lack of global attractor are separated. Remark, that finding global attractor (even near tmx=1000, it was searched up to 900) is sure, because it is meeting of all N=400 node states as in tmx at once, but state of node has only s=4 variants and neighbour nodes must not have the same period.

The main version global clusters was build when global attractor was found. If local cluster in new event had similarity to global cluster $>1/2$, then it could be connected to this global one. From set of such candidate global cluster with the highest similarity was indicated. The similarity was calculated as number of common nodes + period is from set already used by this global cluster. Next this was divided by number of nodes in local cluster. When several simultaneous local clusters have to be connected to the same global cluster, then this global cluster becomes inactive and new global clusters were created from those local clusters. Such event was indicated in crocodiles by adding 5 to free pass number (M1=0;M7=1; M13=2; M19=3; M20=4). If global attractor was not found, then all found local clusters are connected to one specific global cluster, which never becomes inactive, it was indicated by adding 30. It is complex algorithm, but very simplified comparing to investigated problem. Its aim is only first reconnaissance of phenomenon.

Let us start of comparison from discussion of distributions of ice and local cluster sizes ([fig.11](#)). They are shown as in [m5.fig.19a](#) in form of count number. To obtain probability for passes, counts should be divided by number of accumulated – it is number slightly different for particular pass. For pass N it is number of “able for accumulation, because in N there is no accumulation. These differences are connected to probability of acceptance ([fig.9h](#)), but it not this number. For cluster size these number are greater by factor indicated in [fig.13b](#), because in average is more than one local cluster in event. For each net type (f,s,r) apart full distributions of ice and local cluster sizes a distribution of greater local clusters rarely happened is shown in larger scale, because for net f the distribution significantly differ to expected one. For net r there is no such departure, however it is not so extreme like met5 cf – in met5 cr the tail ends practically in 17 and 380; cf in 40 and 350, but here r in 80 and 300. Net s is halfway, the tails ends in 140 and 220, but we can state, that picture agree with ro-module view. Unfortunately, about net f it is hard to state this. **For net f, apart ro-modules, significantly some other mechanism is here present, which becomes stable already in M7, i.e. fare from the end of evolution simulation. Larger local clusters create clear peak ([fig.11 for f down](#)) with maximum near 175, separated from typical for ro-modularity left peak by minimum near 70. In ice distribution also appear separated hill in range 60-290.** This departure form expectations effects more exact analysis of net f in this aspect which is shown in [fig.12](#). Remark that for all three net types the distributions in [fig.11](#) for pass N is clearly different, for M1 is in halfway, than rest which are similar. It is especially clear for ice. This shows that generated ro-modularity is not stable in generated form and evolution change this form. That is **not all aspects of ro-modularity are known and used while generation**, and additional rule should be found to make stable state at once, which is aim of met7. Next in ch.7.4.7 an attempts of indication additional conditions to eliminate this departure are described, but they occurs small effective.

In [fig.12](#) differently averaged ice states for accumulated mainly for net f are shown in condition of free passes. In [fig.12a](#) average ice states for each one net of all 60 nets from series fi2 and fu2 are shown. Large discrepancy is visible, but practically all quickly and definitely evolve from initial state in N (where accumulation is yet absent) to near stable state already in M7. It effects from accumulation during M1-M6. Except state of full range it is hard to deeper analyse in this tangle. In [fig.12b](#) average ice for particular simulations are shown. Here graphs for nets s and r are added – in opposition tu net f ice grows (compare [m5.fig.19b](#)). On the right crucial last section of evolution net f is shown in larger scale. Generally in met7 for net f ice melt in range M7-20 and ro-modularity mechanism slowly is replaced by mechanism observed in met6, however, as is seen in [fig.12a,c,f](#), part of nets f keep ro-modularity. Simulations using parameters the main series ‘f’ done for 400 effective nets (for this aspect summed only up to 300) are also made 2 times (fi2,fu2, i - first, u as ii - second) for 30 effective nets but with another chain of pseudo-random numbers. It is also repeated for different number of

active ro-modules (digit on the end of series symbol, see [tab.2](#)). Because each net is specific, average in is not an average of all accumulation directly, but an average of averages for nets. Graphs for f and fu2 are near identical, but fi2 is significantly different despite parameters are the same. Similarly, fi3 & fu3 and fi4 & fu4 differ, but much less. For easier comparison the same colours are used for the same parameters. Dispersion for different assumed number of active turn to be only slightly lower than experiment of 30 nets resolution. Simulations f4 and f5 are clearly out of the main concentration, but fi2 is similar.

Dispersion seen in [fig.12a](#) is deeper analysed in [fig.12c,d,e](#) where as criterion of selection range of ice in M20 is taken. There averages in shown range of indicated number of events of about 300 events of series fe, se, re are shown. In [fig.12f](#) the shares of events in the ranges are shown. Here also additional provisional simulation are assembled, that fe has 900 effective nets, and f - 689. It turns out in agreement with [fig.11](#), that **distributions of shares are systematically uneven with clear minimum in range 349-250. Maximum in lower ranges effects from additional mechanism “spoiled” expected picture of ro-modularity mechanism for net type f. let’s call it in short “mech2”**. Separated net types s & r ([fig.12b,d,e,f](#)) do not exhibit presence of mech2 (lack of minimum in [fig.12f](#)), but comparison [fig.11](#) to met5 cf i cr ([m5.fig.19a](#)) suggests its presence, however in much lower degree than in net f. So **analysis of distributions of ice and local clusters sizes also clearly showed presence of the mech2**.

Direction of departure observed in [fig.9e](#) in left peak shape **suggests similarity mech2 to mechanism from met6** keeping small global attractor. It would be lost of ro-modules multitude replaced by single one, which spill on the rest of net melting ice. Such picture also effects from [fig.11, 12 i 15b](#). **However, number of local clusters on accumulation (fig.13b) and number of global clusters in final passes free (fig.13c) not confirm such explanation of departure from met5 picture**. Their equivalent ([m5.fig.19b](#)) is similar in this aspect. In [fig.14a,b](#) such picture (of flow to met6) is well confirmed in M20 in series se & s, where mech2 is weakly seen, easily can be agreed for fe, where mech2 is the strongest, but for f with slightly weaker mech2 than in fe maximum is in 2 clusters but not in 1. Taking such explanation we should expect that larger number of active ro-modules significantly decreases participation mech2, but in [fig.12f, 21a i tab.5a](#) this parameter has not clear meaning. It was not surprising because in met5c Average number of local clusters on accumulation for f is 1.6, and for r 1.8. In met7e these values are similar, even higher: r - 1.7, f - 2.3 ([fig.13b](#)). Allowing one active ro-module as in fe, se decreases averages making them more similar to met5c, but not cut events which exhibit presence of mech2, even increases their frequency.

The tax table has the strongest influence on similarity to met5, but it deeper investigations has been postponed.

Summarising, **in picture of conditions creating ro-modularity some important parameter is omitted**, which in met5c is in “correct” range, but in generated ro-modularity in met7 sometimes happens out of “correct” range, especially for net f. For now, I can not indicate how this parameter is.

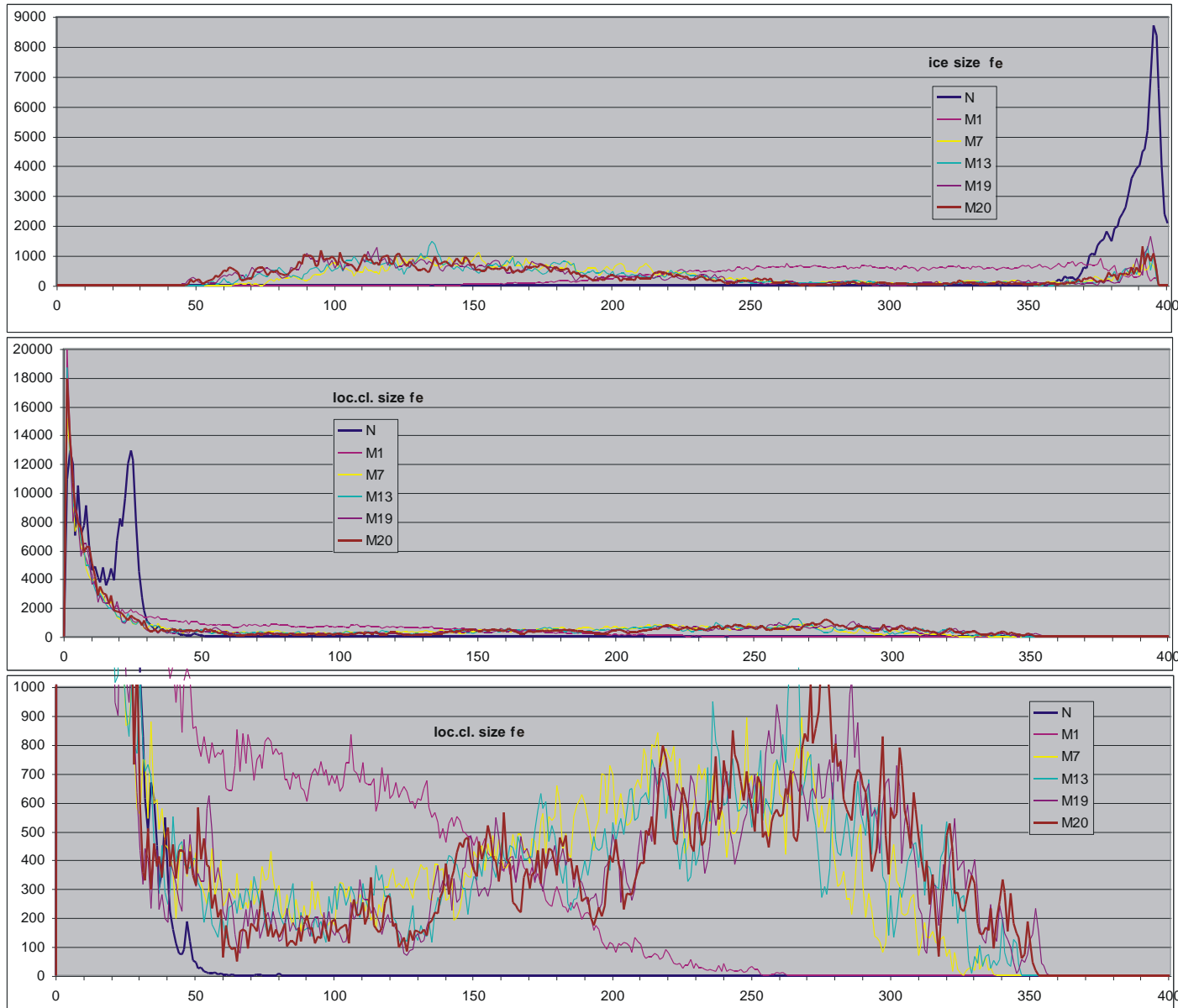
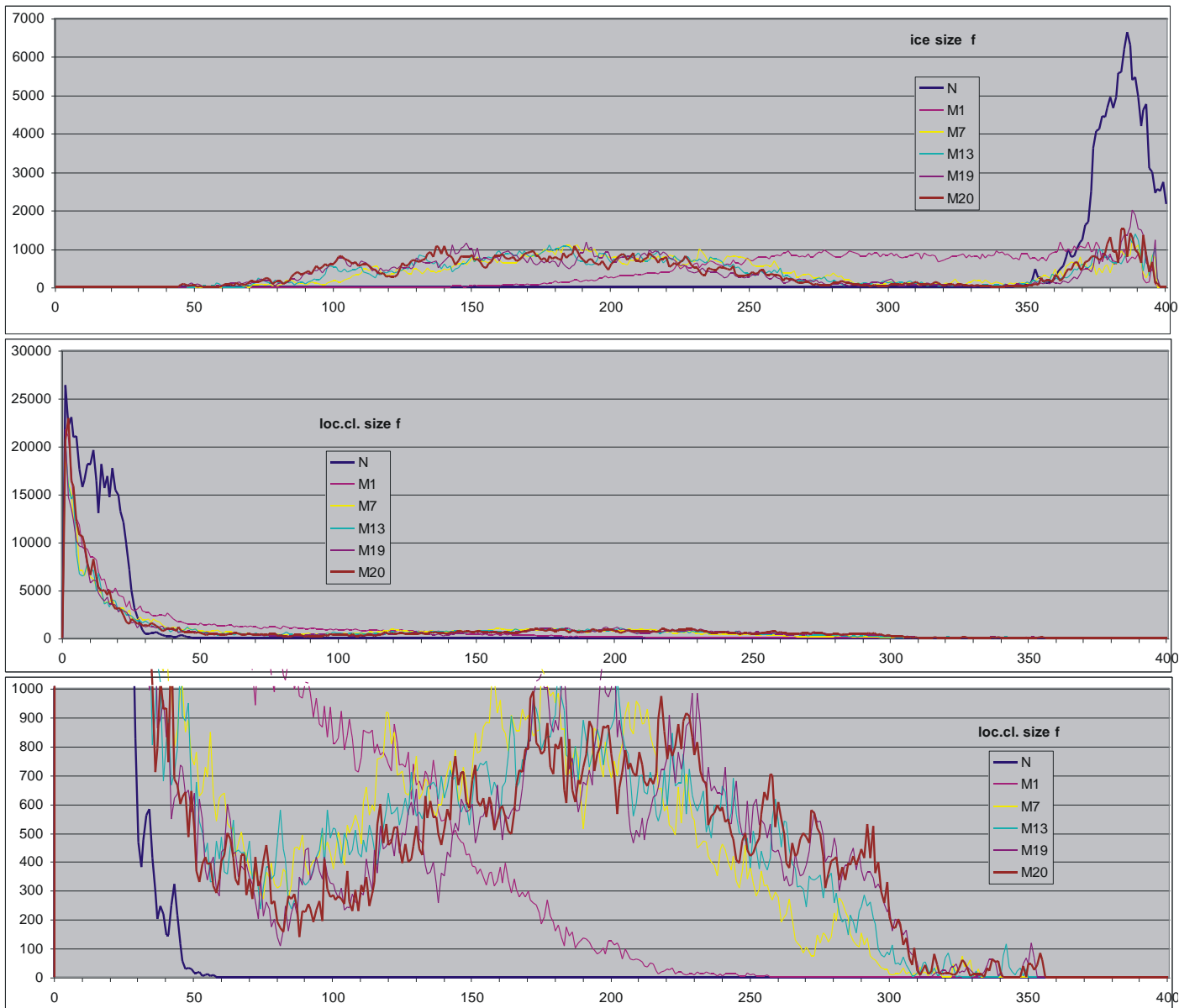
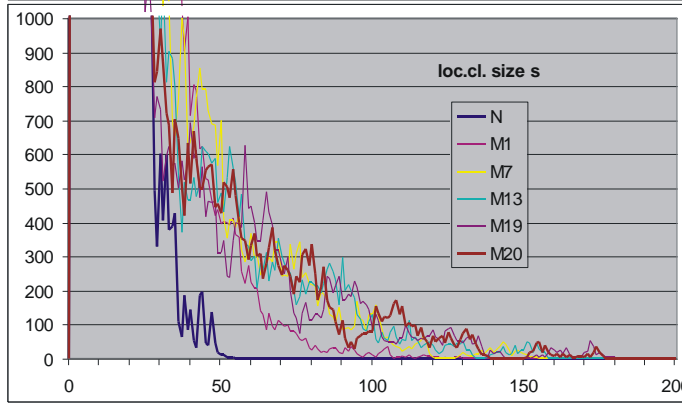
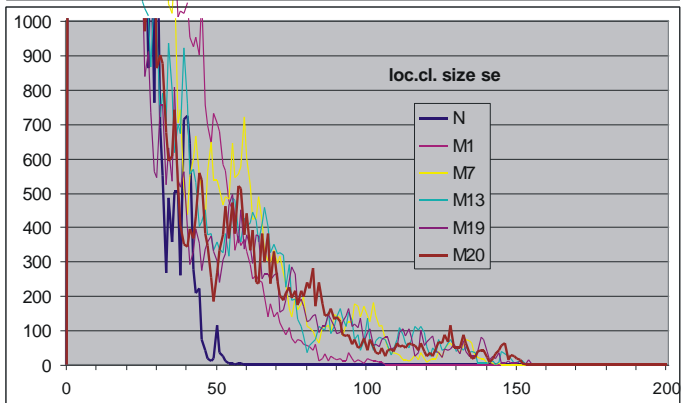
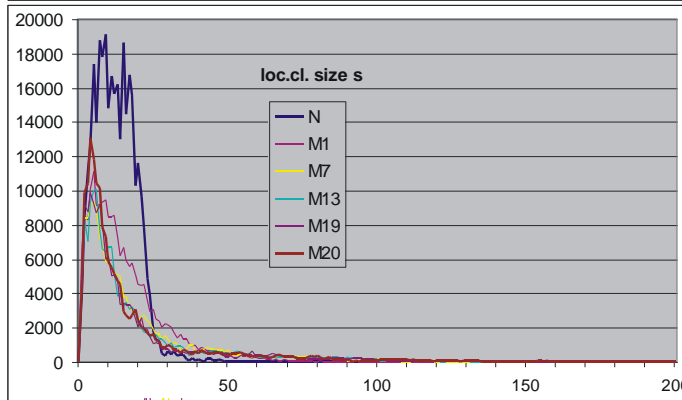
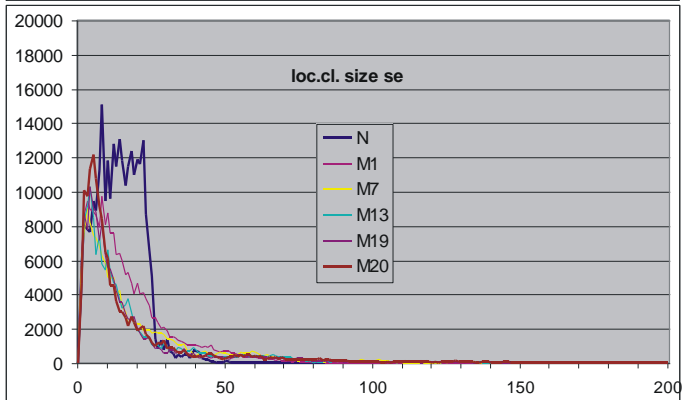
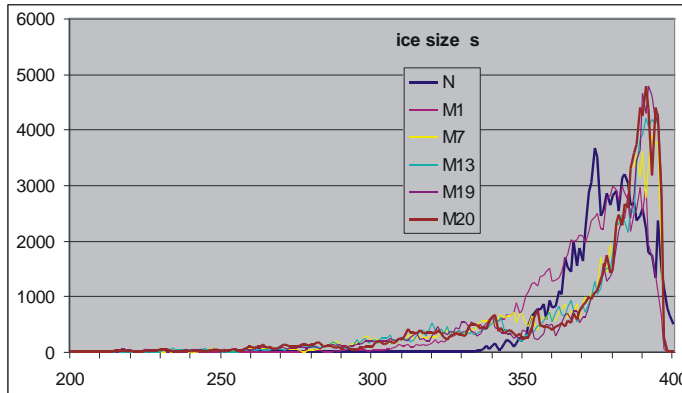
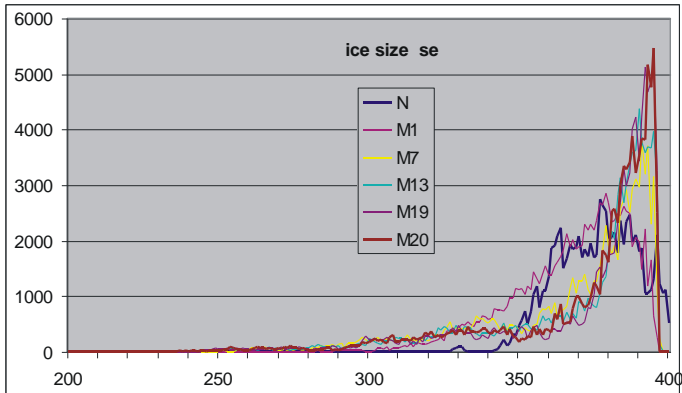
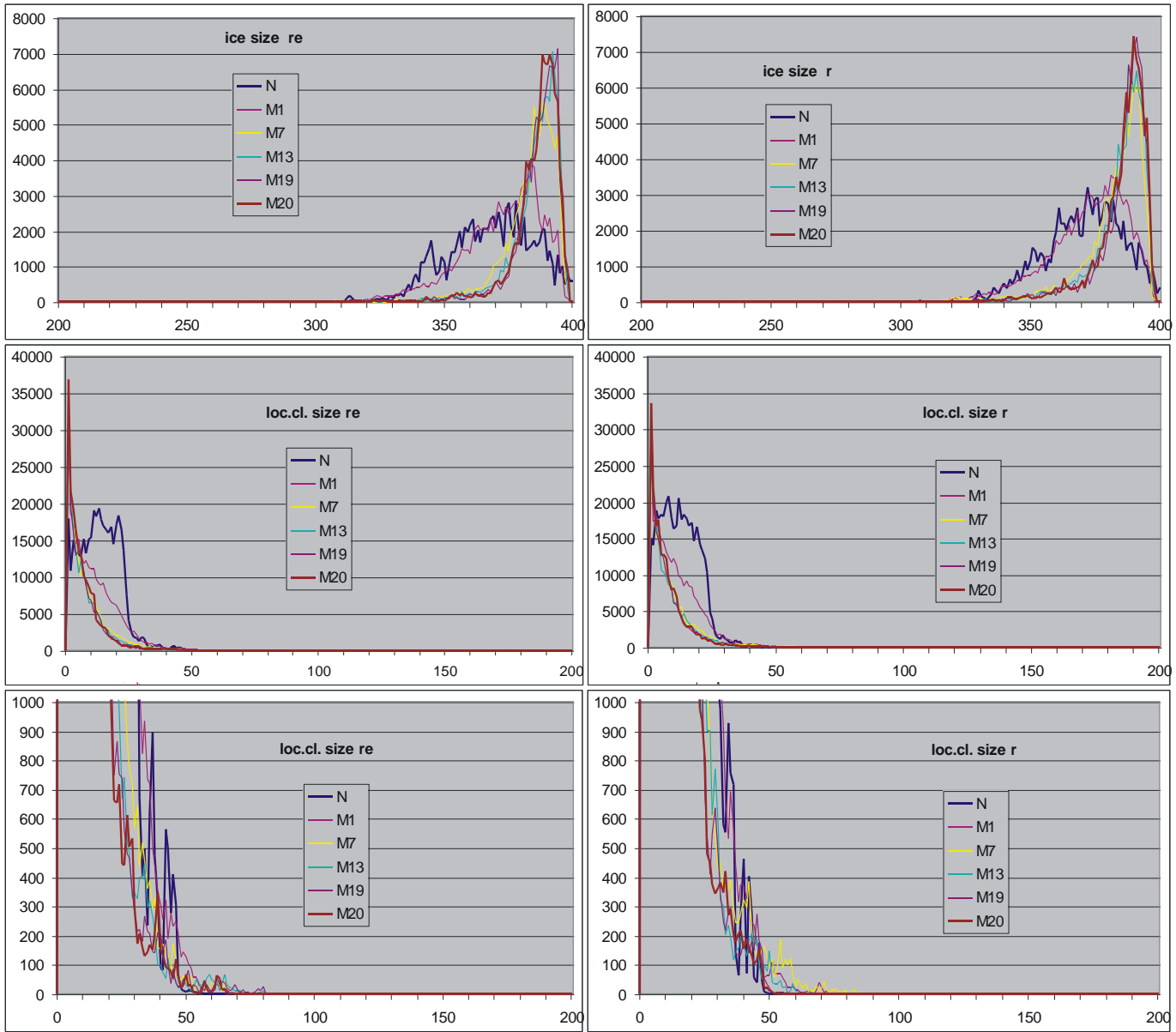


Fig.11. Distributions of ice and local clusters sizes in form of number of counts (as in m5.fig.19a), for accumulated (N lack of accumulation). For each net type (f,s,r) full distributions of ice and local cluster sizes is shown. In addition a distribution of greater local clusters rarely happened is shown in larger scale, because for net f the distribution significantly differ to expected one. An additional maximum separated from typical peak appears which suggests additional mechanism (mech2).

For nets r and s there is no such departure (lack of minimum and additional maximum), however, in met5 cr the tail ends practically in 17 and 380; cf in 40 and 350, but here r in 80 and 300. For net s the tails ends in 140 and 220. This demonstrates the diversity mechanism and presence of mech2. For all 3 net types picture for pass N is clearly different, M1 is in halfway and remaining passes are similar. It is seen especially clearly for ice. This shows that generated ro-modularity form is not stable and evolution build another form, which contains met2 not observed in met5c.







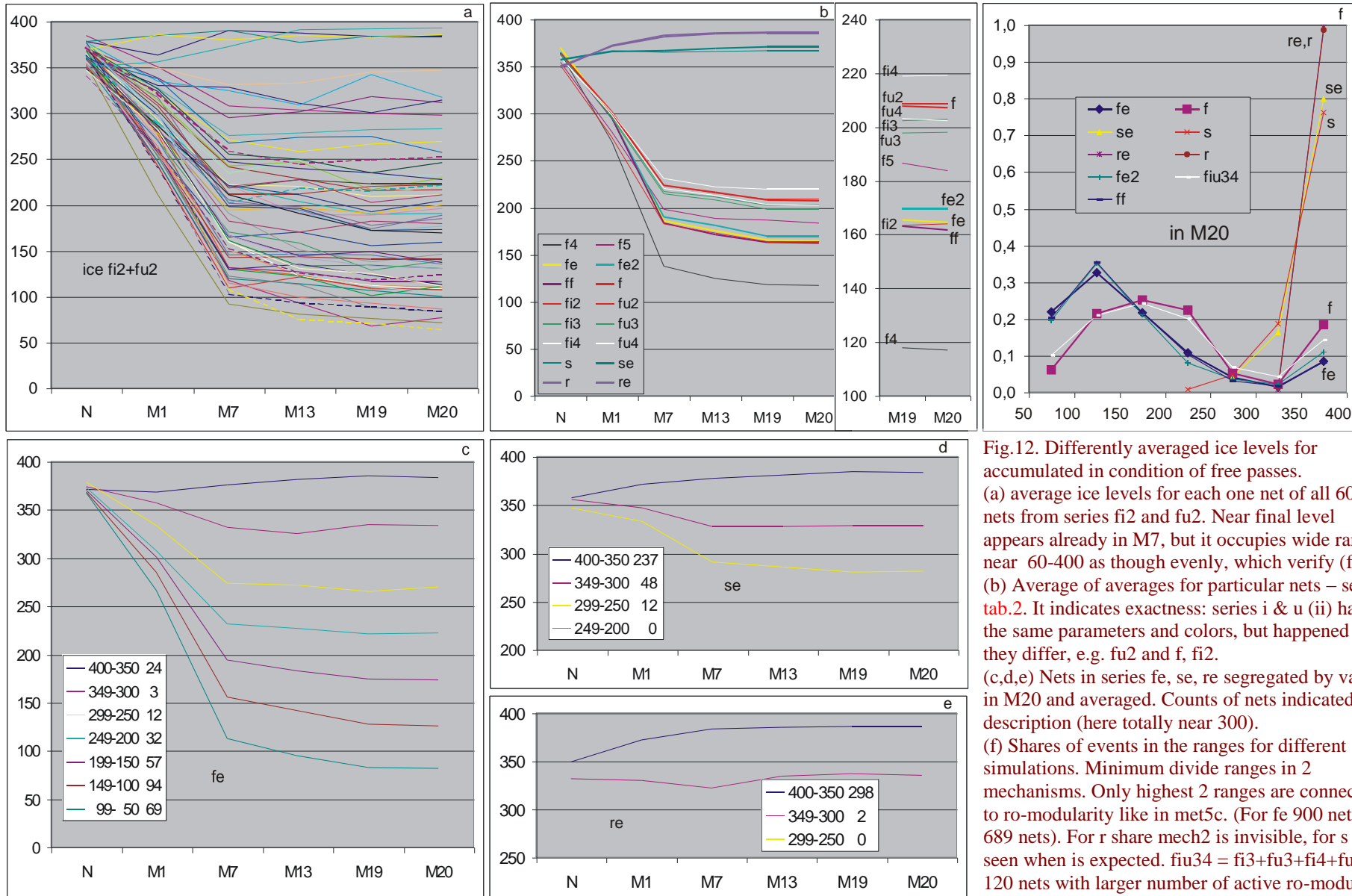


Fig.12. Differently averaged ice levels for accumulated in condition of free passes. (a) average ice levels for each one net of all 60 nets from series fi2 and fu2. Near final level appears already in M7, but it occupies wide range near 60-400 as though evenly, which verify (f). (b) Average of averages for particular nets – see tab.2. It indicates exactness: series i & u (ii) have the same parameters and colors, but happened that they differ, e.g. fu2 and f, fi2. (c,d,e) Nets in series fe, se, re segregated by value in M20 and averaged. Counts of nets indicated in description (here totally near 300). (f) Shares of events in the ranges for different simulations. Minimum divide ranges in 2 mechanisms. Only highest 2 ranges are connected to ro-modularity like in met5c. (For fe 900 nets, f 689 nets). For r share mech2 is invisible, for s it is seen when is expected. fiu34 = fi3+fu3+fi4+fu4 120 nets with larger number of active ro-modules.

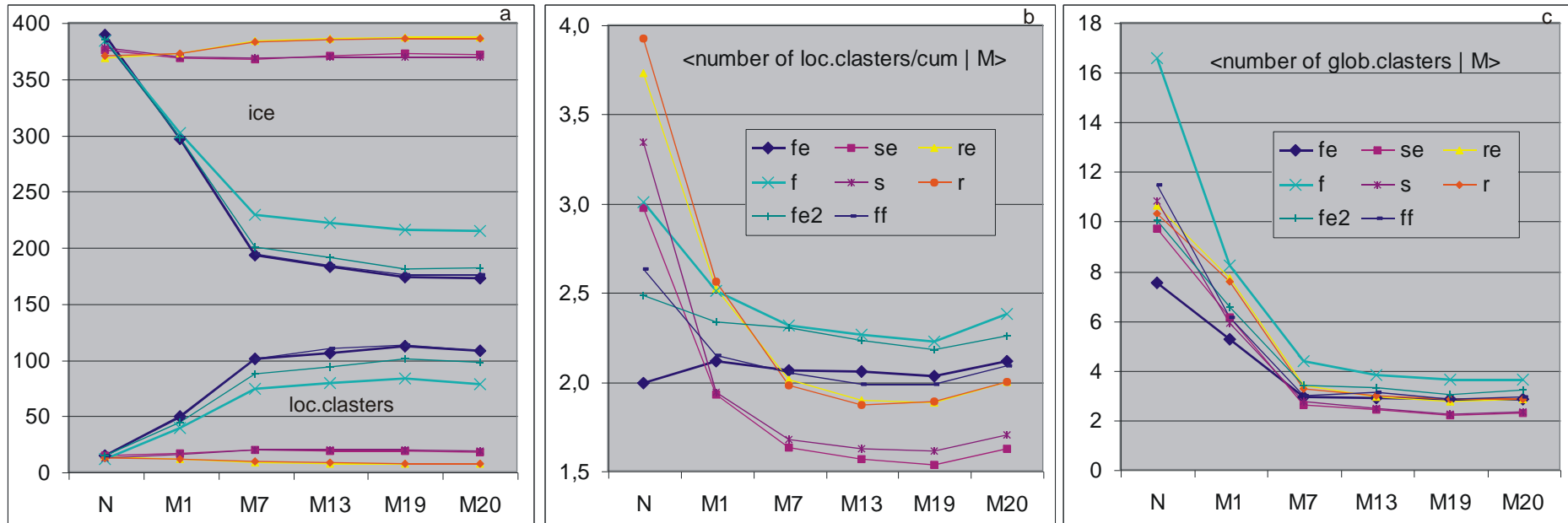


Fig.13. (a) Average (on accumulated, i.e. sum of frozen nodes for accumulated in all nets / sum of accumulated in all nets) ice and local cluster size in passes N and M free. Description as in (b) & (c). Results for nets s & r models a & b overwrite, they agree with mechanism of ro-modularity. Net f is different, models a & b give little different results. Points for fe and overwritten ff are especially fare from expectations, f model b gives results shifted in direction of ro-modularity expectations comparing model a. (b) Average number of local clusters on accumulation. Here departure of series fe is also large, however this series has the lowest variation during evolution. Decreasing of number of local clusters during evolution shows lack of stability generated form of ro-modularity. Nets s & r in both models the strongest change this parameter coming from N to M7, but later it is stable in all nets. (c) Average number of global clusters in passes N & M free. Here also on the way from N to M7 changes are great but later stabilisation becomes.

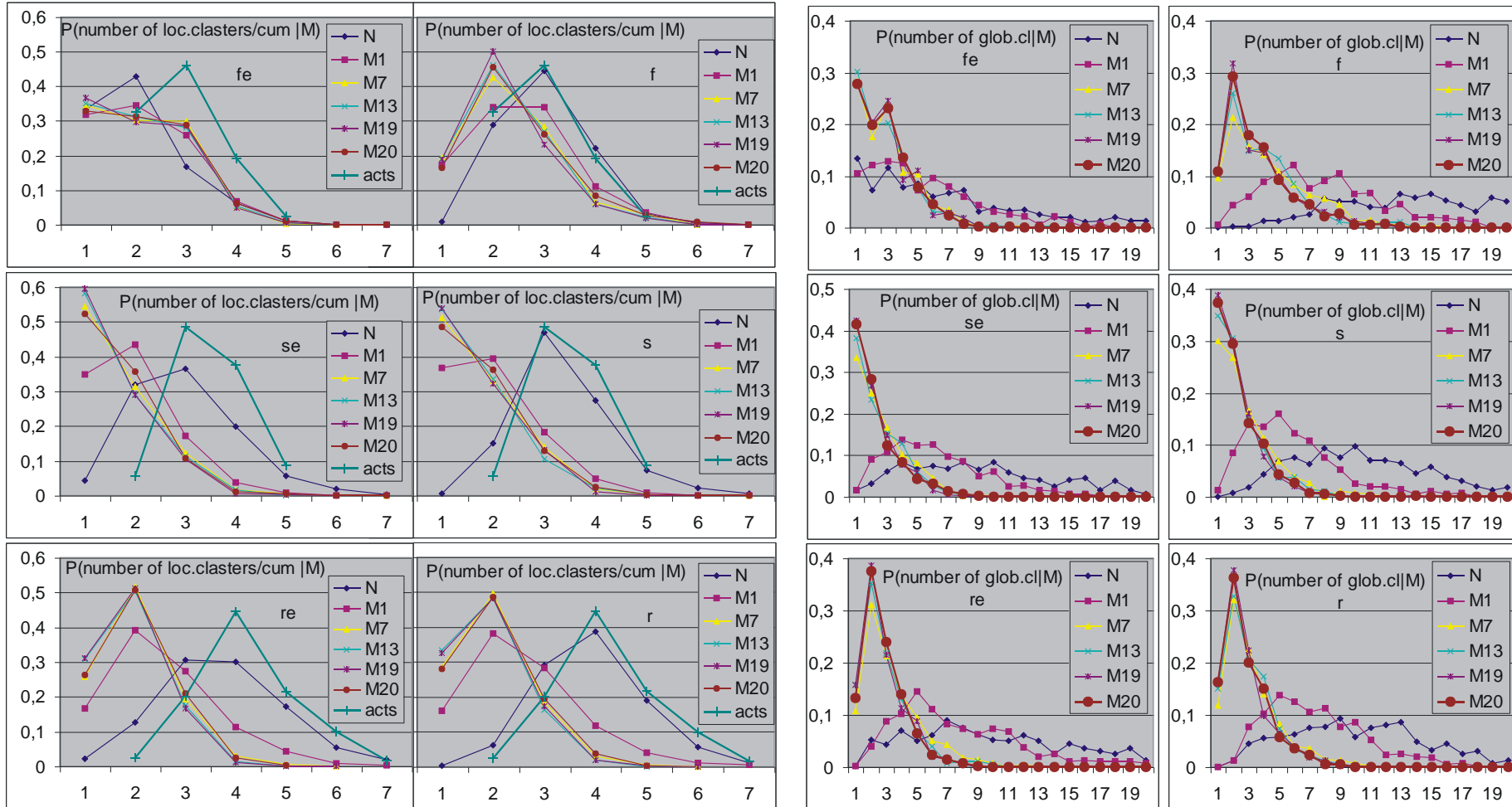
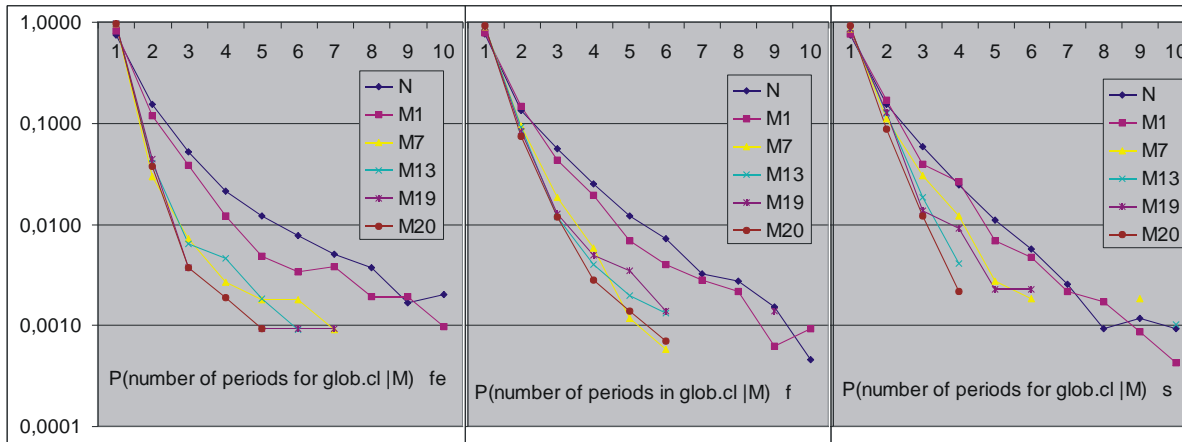


Fig.14. Distributions of numbers of local and global clusters ro, and of number of periods of global clusters, in condition of passes N and M free.

(a) (Left 2 columns) Distributions of number of local clusters for accumulated. Distribution of number of active ro-modules (acts) directly after generation is added.

As is seen, acts & N are not identical, however are similar. Measure for N is done after change which can be accumulated, but it is not accumulated.

(b) (Right 2 columns) Distributions of number of global clusters. In both cases (a,b) distinctness of pass N, halfway of M1 and similarity of remaining are seen. It is clear change of generated state of network to another state, but stable. Interpretation, that mech2, seen mainly in series fe & f, is a form of mechanism from met6, which the main property is single cluster on near all net get confirmation in these graphs, however, as typically, situation occurs more complex. Number of global and local clusters for f in M20 (bold) has maximum in 2 but not in 1. In net s mech2 has small share, however here such hypothesis have no this problem.



(c) Distribution of number of periods in global clusters for passes N and M free in log scale. The graphs are similar for sets of simulations then they are shown on examples. Series fe is similar to fe2 & ff; f is in halfway; and remaining se, re, r are similar to s. There is no additional hills. Clear difference between N & M1 and rest is seen, which is also seen in other investigated parameters.

7.4.3 Global clusters ro and their comparison to generated ro-modules

Two method for global cluster detection was used: graphic by ‘triangle’ (described in me5 ch.5.7.2) and automatic connection of local clusters by complex algorithm described in ch.7.4.2 (previous) dedicated to statistical analysis. Both the methods character is simplified due to abundance of phenomena, variants and circumstances. As is seen in fig.15 generated ro-modules are detected in pass N as global clusters, then algorithm works effectively. However, during evolution division on particular global clusters becomes blurry especially for net f in triangle method. Typically number of clusters decreases. In net f clusters typically grow melting ice, but in nets s & r inversely – rather decrease and ice grows.

In opposition to met5, here wall nodes have statistically different functions than ro-module nodes. In met7 accumulated changes have small probability to build new ‘wall’ and divide greater ro-module. This is probably the main mechanism of ice melting in net f where hubs are the greatest. Evolution in nets s & r lead to frozen which makes situation more similar to met5 and makes easier to create new walls. In net f also such evolutions happen, which is shown in fig.15d.

Generally. the picture is similar to known from met5 (m5.fig.18), however it have slightly different parameters, especially for large part of event for net f.

One of more interesting and convincing picture of function of local clusters ro is dynamical size distribution, which from necessity is shown in static form in fig.15b,g,h creating during passes M free. Appearance in accumulated event of local cluster ro of particular size in range 150 is recorded by adding pixel to left. Colour of pixel is connected to pass M, which show sequence of growth.

Dynamic image shows how to change the momentary preferences: concrete pillars are growing rapidly, followed by a shift, usually close by. Usually it happens several local clusters ro (fig.15g,h), so a few pillars grows at the same time and there are more such counts here than for a similar dynamic image of size of clusters A4h (located on the left side and growing to the right), where after one ini is only one result A4h. The non-uniformity of growth in the distribution Ah4 is small, because the range of size of such clusters is small. But the size distribution of clusters ro grows particularly unevenly, which on a static result is hard to see. It is seen, however, that increases in certain passes M free (fixed colour) are not proportional, mostly not due to the low statistics. For various nets it is more or less visible, in fig.15g events of net f model b are shown where it is visible particularly clearly. In the first figure particularly small global clusters happened, which allows to include the "triangles". Larger (more than 150) clusters ro do not fit in the picture, and cases sometimes happen mainly for fe, as in fig.15b or last in fig.15h where almost nothing in this graph does not happen.

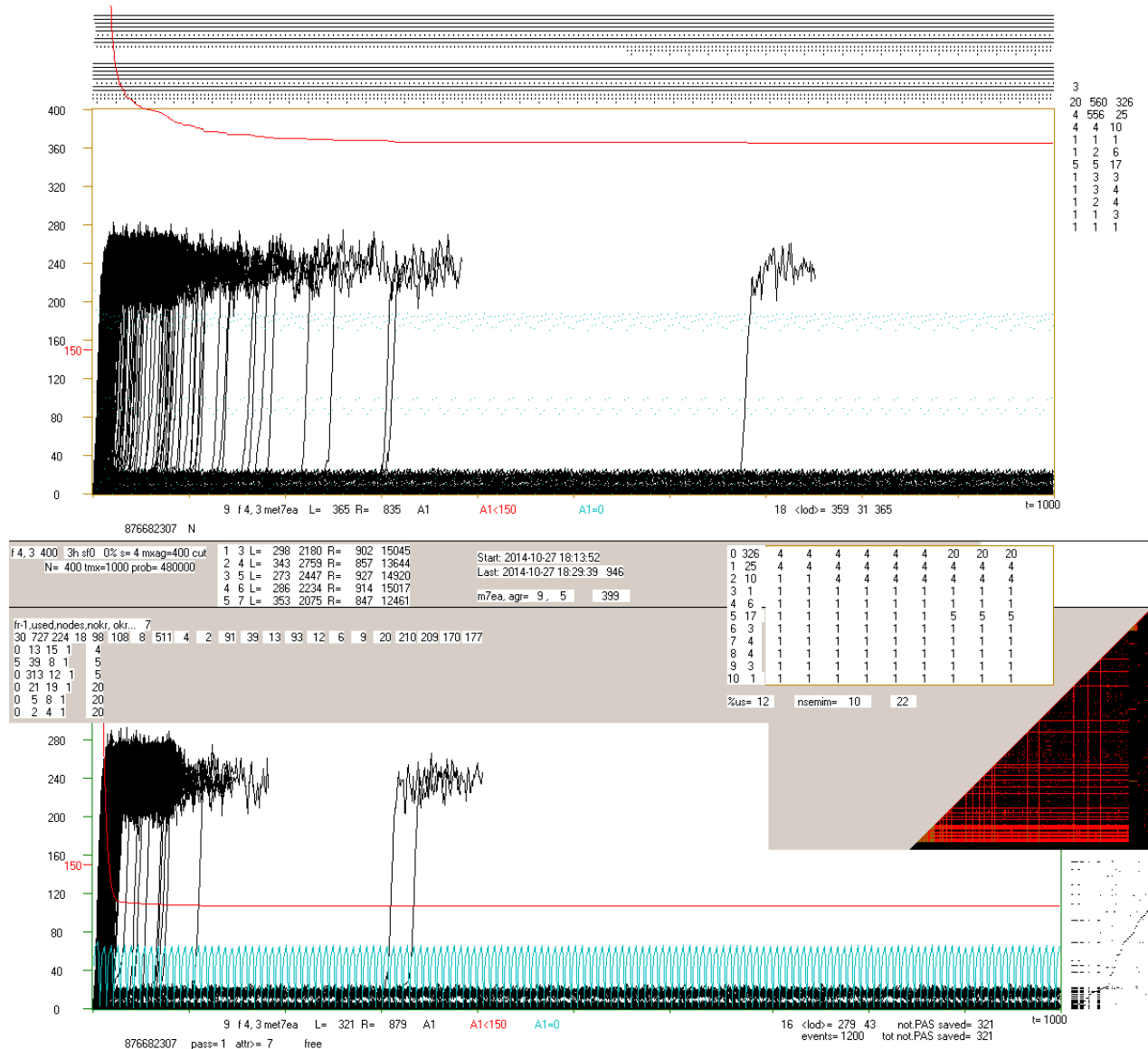
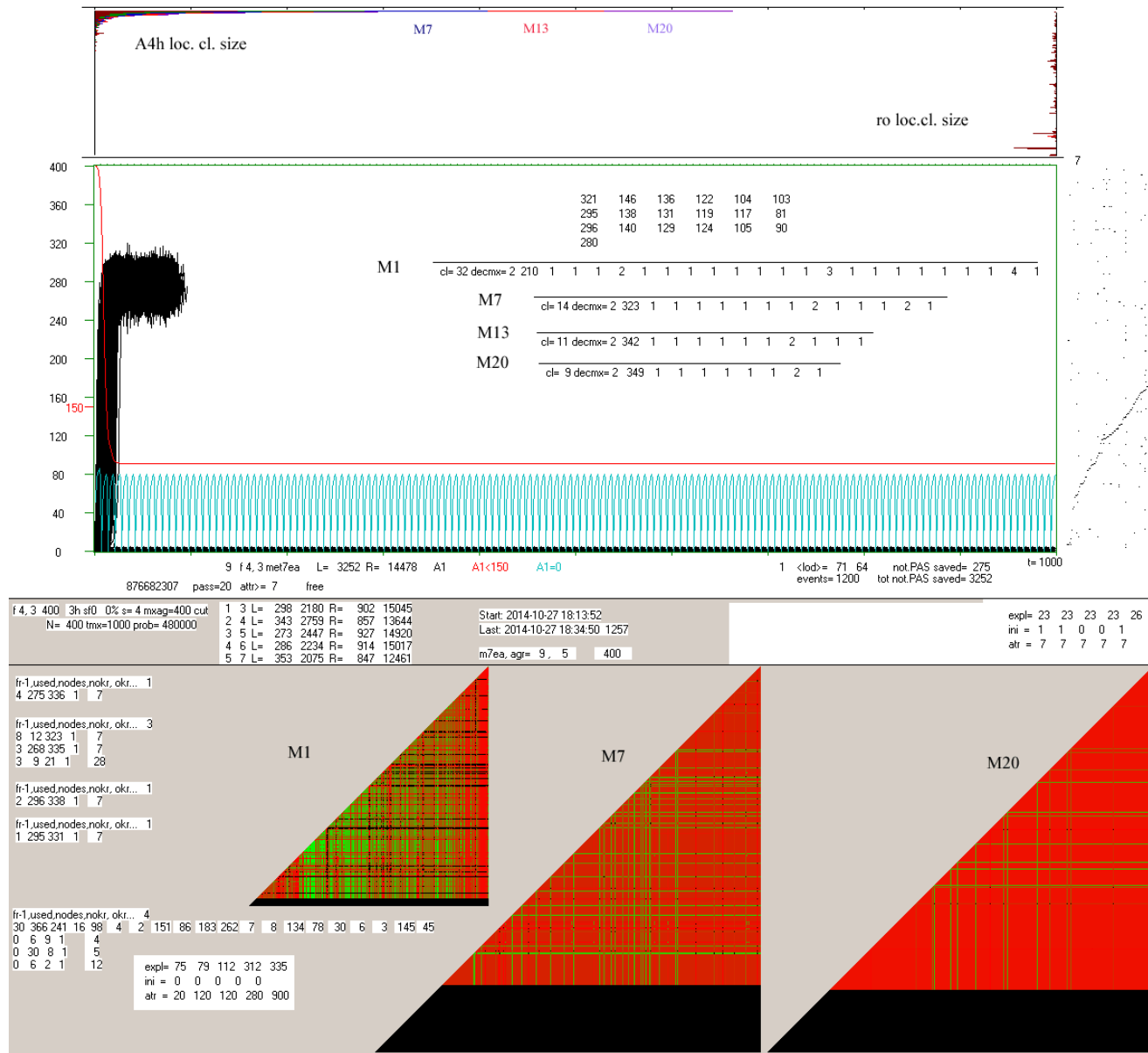


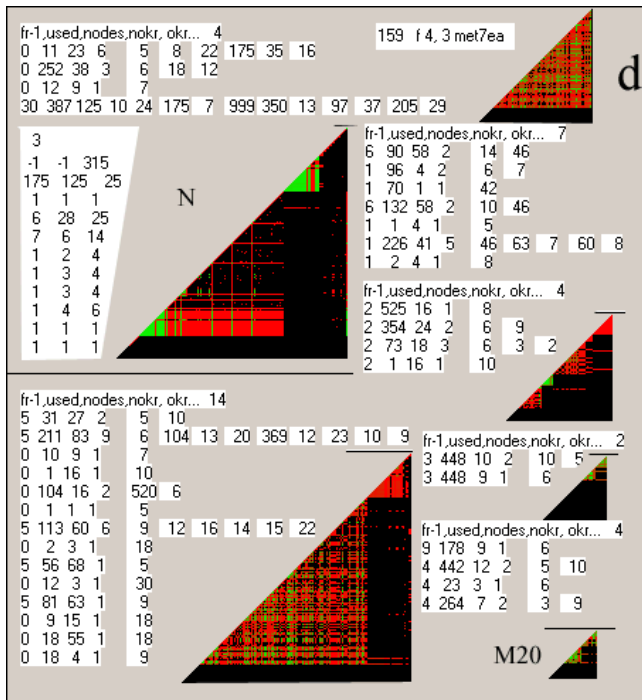
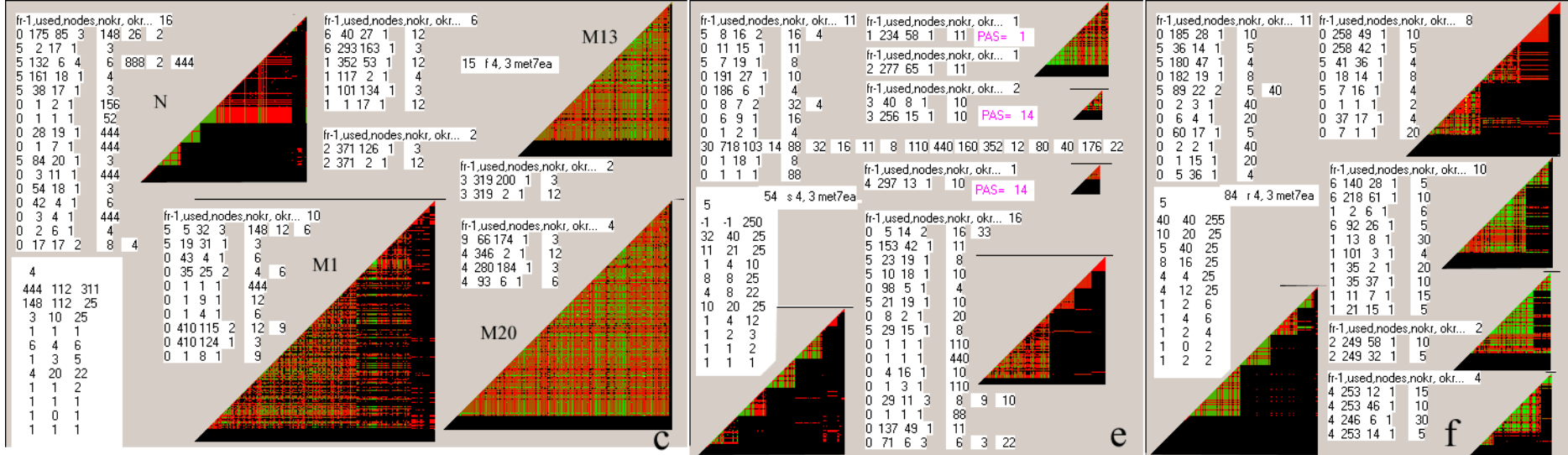
Fig.15. Graphical results obtained with the 'crocodiles' refer to the particular passes N or M. They are packed here to save space, and the less important elements have been omitted. Left side (a) net 9 fe2 pass N is entirely shown with the crocodile of pass M1 copied in the bottom. The exact description of the pass N is in fig.8 , but here the results are from evolution simulation met7e of model a (without forcing tax). In the lower part of N an analysis clusters ro is included - on the right: 'triangle' originally described in ch.5.7.2 and there in m5.fig.16. On the left global clusters are listed, they are used for statistical analysis, described in ch.7.4.2. Four initial numbers indicate : pass , how many times used in this pass, the number of cluster nodes, the number of periods of the cluster, further all periods are listed. For N and M1 pass symbol is the same = 0. Deactivated cluster has added 5 to the pass symbol, and the cluster of little certain diagnoses arising from lack of detection of the global attractor has added 30. As you can see in pass N occurred this situation. On the right at the top generated ro-modules are listed. The highest single number indicates the number of active ro-modules, here 3. The next line is: global attractor, its begin, the number of ice nodes. Lower 10 ro-modules: period, beginning, number of nodes (up to 25). In the middle, over the triangle –similar list for subsequent iterations trying to increase the number of active. Observing periods the generated ro-modules detected in global clusters can be seen. As in fig.8, for pass N red line indicates the number of ini, which did not explode into chaos. For passes M as in met5 in m5.fig.7 & 9, this value is divided by 3 to show the share of order and chaos by treating the left scale as 1. Similarly share of fade out is indicated in blue: in N by points and in M by line.



(b) – Continued accurately show the evolution of net 9 fe2, here final crocodile from pass M20. Numbers of accumulated in consecutive passes M (each line begins with free pass) and statistics of clusters A4 for subsequent passes free are copied into box. Statistics A4 contain: number of clusters, the largest number of simultaneously connected clusters and next a list of sizes of clusters from the first, which is usually the largest.

At the top - distributions of counts the sizes of local clusters A4h (left to right) and clusters ro (right to left) in the range of up to 150 nodes in size. Here ro clusters usually are larger than this range (see (g,h), fig.20). This is a typical picture for the series fe, sometimes also f.

Colours marked increases in passes free. Below in the middle bar to the right a table of 5 latest explosions: t, the value of ini, global attractor of pattern at the time of the explosion. For M1 the table is copied bottom left to show that there is global attractor '900', i.e. 'attractor is not detected', which justifies the presence of a global cluster marked '30'. It also started in pass N, but it has not more occurred in the later passes M7-20. Sets of global clusters detected in passes M are copied in left. Skipped copying 'triangles' for pass M13 & 19 because they are practically identical to those shown for M7 & 20. As can be seen the triangles for N and M1 are similar in size, but M1 are more fulfilled. Next in M7 active nodes already constitute the vast majority, and the ice 'melted' (black belt at the bottom of the triangle, M7 and M20 are shown all, the remaining triangles are on the same scale, but the ice has been truncated to save space).



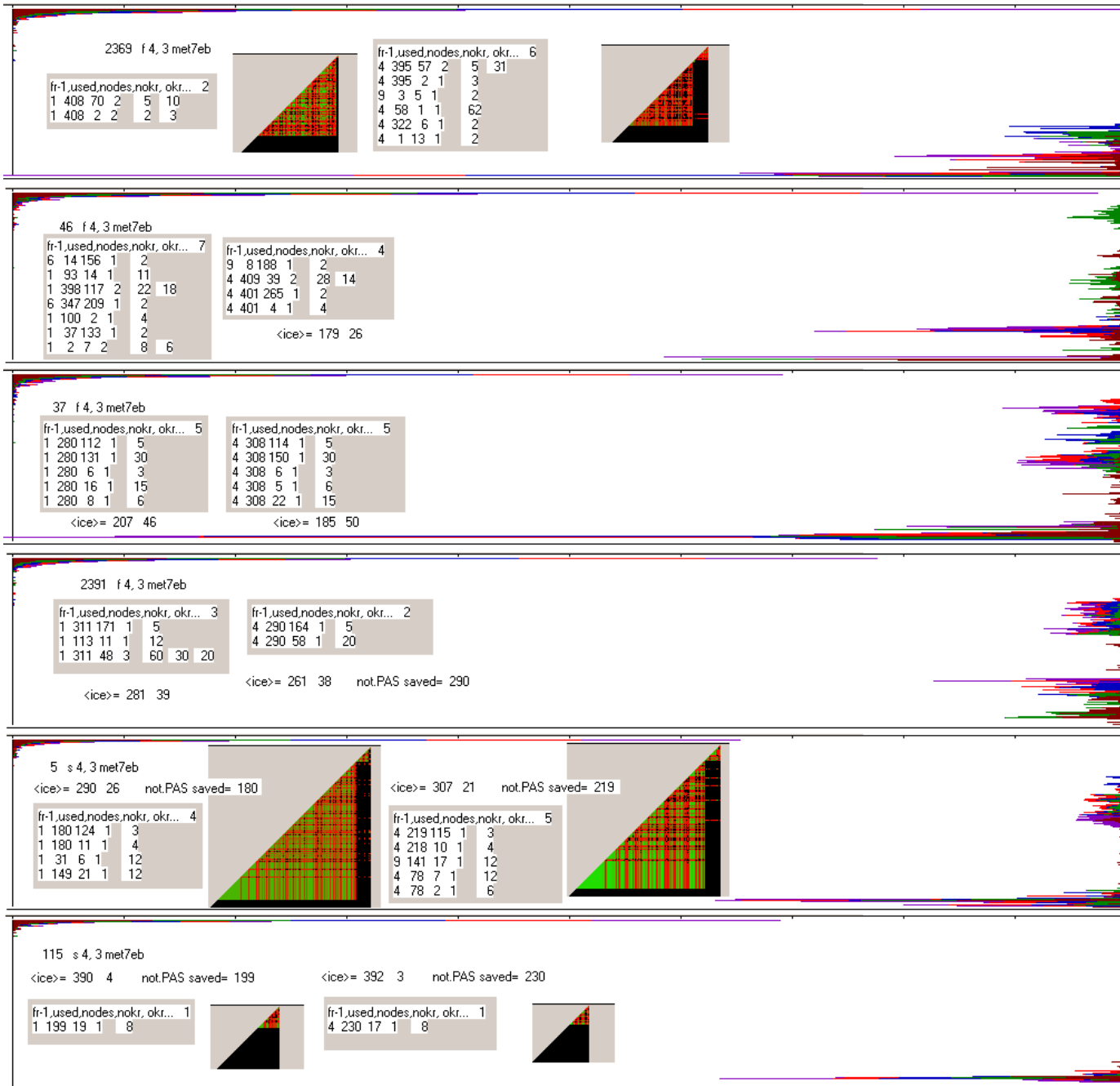
History of evolution of clusters ro on examples fe2 nets 15, 159; se 54; re 84. In (c - f 15) 4 active ro-modules are generated with periods: 148, 3, 6, 4. In pass N first 4 consecutive global clusters have precisely those periods. The number of nodes are not the same, because not all nodes of ro-module have such a period, as ro-module, part is an ice.

Also initiations cause activation of wall nodes, often also adjacent ro-modules. Such activation of the neighbours effects taking them as members of the global cluster, and next it turns out that they are at the same time in another local cluster, which leads to deactivation of the erroneous global cluster and create it from the beginning (add 5 to the pass symbol M1=0, M7= 1 ... M20= 4). Triangle for N detects global clusters by other means. Consecutive from the bottom 2 green triangles have 21 and 18 nodes, may be they correspond to periods 3 and 4, although it may instead of 4 is 444.

All initial periods appear in M1, cluster referred to period 3 grows to great size, period 148 disappears, 6 change to 12. Triangles for M7 and 19 are not shown, because they are almost identical to M20, only for M13 it is strangely smaller. Unfortunately, triangles do not show what global clusters. In (d - f 159) in N global attractor is not detected, it amounts to at least $175 \times 6 = 1050$. Three active ro-modules have periods: 175, 6, 7, which are detected in 3 initial global clusters. Periods 7 and 175 also appear in cluster '30', where 999 means no detection of the period.

Period 175 disappears in M1, 7 in M13, but 6 is kept to the end. In this case (though a net f) the ice increases, and finally practically two tiny clusters remain which triangle well illustrates.

(e and f) concern series re & se. Generally, in the image analysed here they are almost identical. Selected examples differ mainly end result - the number of active nodes. For re (f) it is clearly higher than for se (e), but opposite examples can be easily selected. In (e) is PAS (Attractor Point System) which in net s is more frequent. As can be seen, during evolution the initial quite clear images of division on ro-modules are blurred, usually followed by the loss of their differences. The network f typically produce one cluster on the triangle (although the example (d) shows that it can be different).

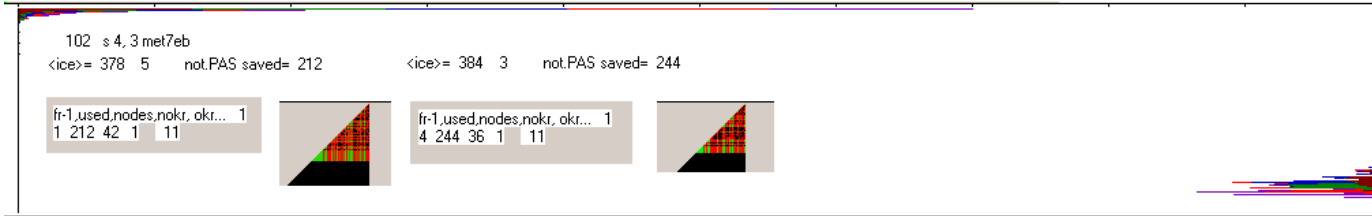


(g) –Dynamic distributions in M20 of counts the size of local clusters A4h (left to right) and of clusters ro (right to left) in the range of up to 150 nodes (see (b)). Supplemented by "tag": net number, net type and model; global clusters ro for M7 in left and for M20 in right; <ice>= average size of ice, average % of fade out (A1=0) on accumulation in the last 200 steps before tmx (A1h0); the number of accumulated in this pass (not PAS saved=).

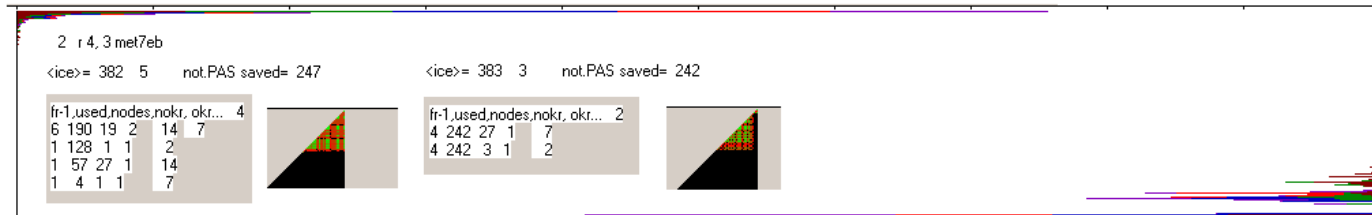
The resulting size distribution of clusters A4h is small interesting. Dynamically increases are significantly more uneven than this is due to randomness, it can be assessed painstakingly analysing the size of the growth of a specific colour assigned to the pass, but it does not reflect the image of a dynamic inside the pass. This non-uniformity is associated with the presence of different ro-modules also changing during the accumulation. For clusters ro whose size can vary considerably, the resulting image is largely retains traces of the dynamic non-uniformity increases. Here, for a deeper analysis the pasted information about global clusters ro should be used, especially about their size (nodes) which is slightly larger than the constituent local clusters and about the number of appearances (used) which may be compared to the number accumulated in the pass. Additionally the "triangle" showing a different form of global clusters ro supports the image. Only a small "triangles" can be pasted here (see (c-f)). Both, triangles and presented here size distributions of the two types of local clusters should be analysed on greatly enlarged picture in pixels.



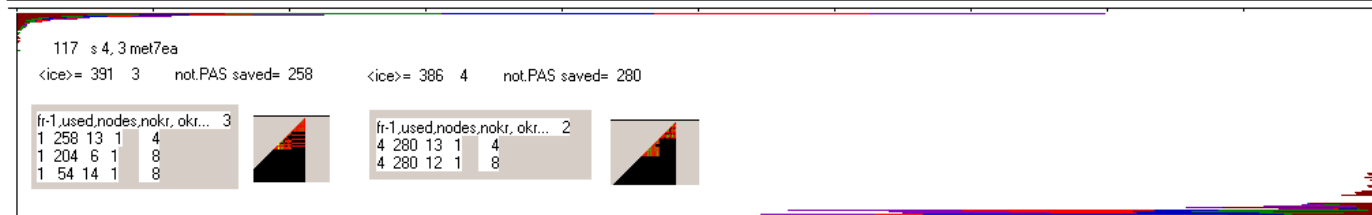
The results presented here from model b (with tax) are identical with those obtained from the model a (no tax) (see the last 3 examples in (h) and example (b)). These models in this respect differs only statistic types such images, which better show other drawings.



(h) – Continued examples of (g). The sequence of imaging is f,s,r,se,re,fe. For f the majority of clusters ro is in the range of 150, which allows them to analyse and image here is the most interesting. In fe clusters ro are typically larger (fig.13a) and the image such as in (b), or the last here occurs more frequently.



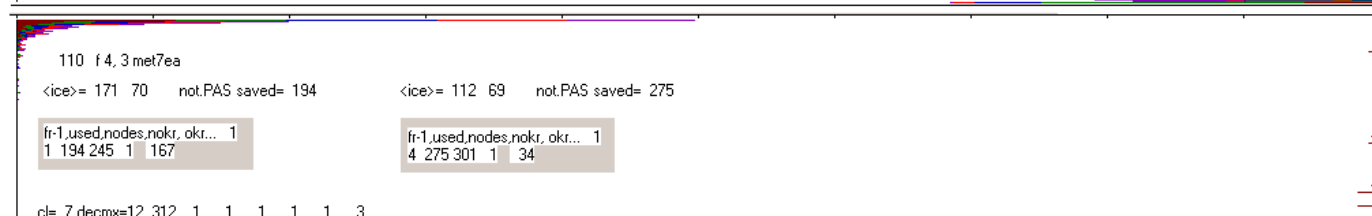
Network s and r in both models vary considerably - in the r and re larger local clusters ro are very rare. The differences in the pictures between the models a and b for the net types s and r are almost imperceptible.



Presented image for clusters ro, especially in the form of a dynamic in part reproducible through colours, is a strong, eye- argument for the existence and functioning of ro-modules. As can be seen, ro-modules may even be considerable, but the size of the changes depicted by clusters A4h is small, and such events are under the threshold of acceptance is not leading to a chaotic explosion.



As befits for complex networks, the image of conditions is very complex and simple explanations appear to be generally too simplistic. The analysis is entering deeply into various aspects of the process, providing a strong basis for the proposals in so "slippery and treacherous" area.



7.4.4 Similarity of ro-modules attractors after accumulation

In ch.7.3.4 in vision of basic ro-modularity mechanism a hypothesis is used that after accumulation a time to come to a new attractor of local ro-module is usually short and attractor usually similar. In met5 it was difficult to verify this hypothesis, there the view was based on a review of local clusters ro and impression from this review. Generation of ro-module and their attractors, allows now in pass N without accumulation on automatic testing the hypothesis with high statistics. Such investigations were performed in met7e and they confirmed roughly above hypothesis, but as usual, the reality was more complex. We studied 3 elements of ro-modules, in which was made initiation, in dependency on the range of local attractor size before the change suitable for accumulation: 1- size of a new attractor; 2 - change the size of the attractor; 3 - the time to come to a new attractor (here come to the state of tmx).

The results are difficult to clear present mainly due to the heterogeneous size distribution of the attractor, as shown in fig.4e,f,g, but also due to many parameters that influence here, such as 3 types of networks, 2 models, and many options to discuss. Of necessity, the main results are presented in table 3, for their representations of would take inadequately much space and would be not more readable.

The results description in tab.3 is no repeat here, only note that there are also indicated the average time to come to the attractor, which turned out to be really small. The distribution of attractor changes in dependency on the attractor range before change is shown, however, in fig.16. The same size ranges of decreased or increase attractor are here arguments (e.g. -2 means a reduction in the length by the value from the range 2-5). A separate position is no change in length (0).

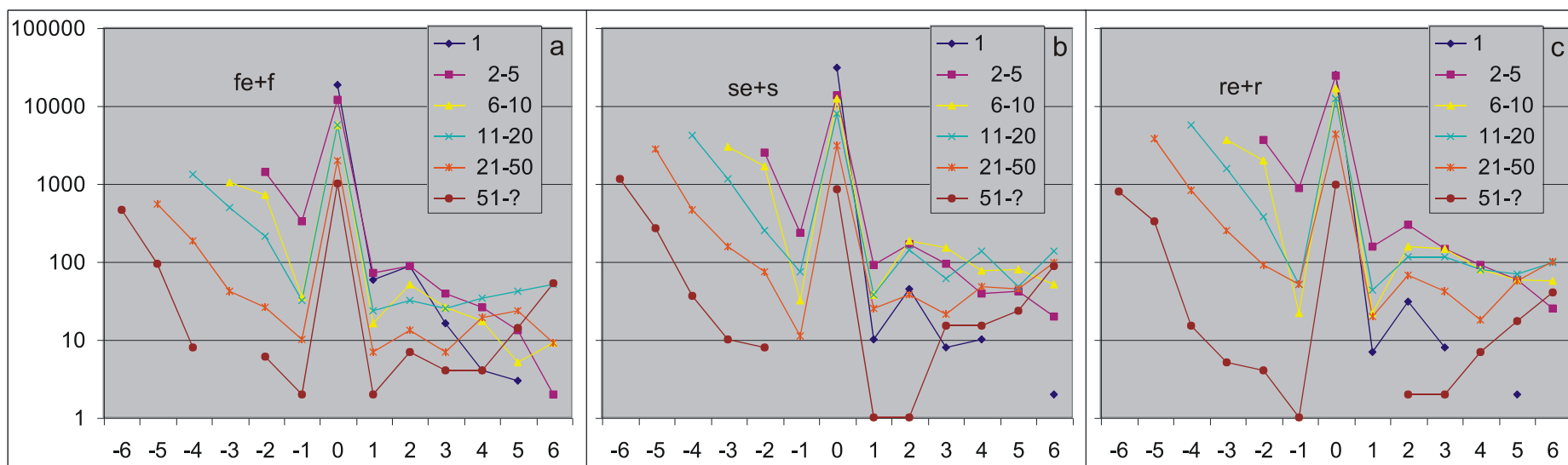


Fig.16. Distributions of local attractor length changes of ro-module after accumulated initiation made in function of node belonging to the ro-module. The relationship is given from size range of the ro-module attractor before initiation. The same size ranges of decreased or increase attractor are here arguments (e.g. -3 means a reduction in the length by the value from the range 6-10). A separate position is no change in length (0). The presented results are a sum of the results from the models a and b to increase statistics and readability, as they were similar. The asymmetry of changes reducing and increasing the attractor is visible. Reducing changes are in large part (see tab.3) a transition to point attractor, i.e. inactivation of ro-module. Reducing has an obvious limitation, but increasing has not. Overall, the picture for all 3 types of networks is qualitatively similar. Remaining unchanged in length strongly prevails, which is also seen in tab.3.

Tab.3. The similarity of local attractors before and after accumulated change initiated in the given ro-module, in pass N, met7ea and met7eb, nets f,s,r (400 effective nets). In the upper line the headlines concern the size range of local attractor prior to the change. Values except 'count' and 'attr.start' - share in the range (vertical). The exact identity of the length of the attractor occurs usually (**equal**) is the basic effect. The lowest share in model a (0.334) has net s, in model b (0.415) has net r, both in the range of largest attractors 51-?. This is an essential element of staying in the initial range (**same range**) . The transition to the point attractor (**to 1**) is the second to the significance the phenomenon (warning on interpretation for range 1). Together, these two phenomena (**same+1**) always account more than half. Also move to the adjacent range on both sides (**to range ne.** from nearby or neighbour) is the similarity, but not always on both sides, and sometimes it is already indicated specific range 1 (for range 2-5). For larger attractors than 6, which no longer includes range 1, this phenomenon has a negligible share. On the occasion the shares of increasing (**inc**) and decreasing (**dec**) the size of the local attractor are shown. It turns out that there is a strong disproportion (almost 10 times) which prefers reducing of attractors. Line (**count**) shows the number of counts, and (**fraction**) - the share of compartments in able for accumulation, which allow to calculate column '**globally**' . The last line (**attr.start**) shows the average time to reach a new attractor - indeed it is negligible. The more that this is the emergence of the tmx, not the real entry to the attractor, which usually was before, it should be assumed that on average about half the interval. In this situation it is a result that indicates that initiation usually not throws ro-module from the attractor, but only slightly modifies. On the basis the hypothesis established in ch.7.3.4 about similarity of attractor after accumulation and about a short time to come to the attractor should be considered justified. Models a and b here give qualitatively identical results, but quantitatively there are differences, mainly for the biggest attractors, which in the model b are initially limitation to 100 but in model a there is no such limitation. Series fe (model a) in comparison to f (model b) has significantly stronger participation of 'equal'.

	f	1	2-5	6-10	11-20	21-50	51-?	globally	s	1	2-5	6-10	11-20	21-50	51-?	globally	r	1	2-5	6-10	11-20	21-50	51-?	globally
a	equal	0,991	0,864	0,841	0,777	0,807	0,626	0,888	0,998	0,812	0,726	0,573	0,442	0,334	0,775	0,997	0,818	0,741	0,598	0,457	0,449	0,756		
	same ra.	0,991	0,893	0,853	0,803	0,850	0,786	0,912	0,998	0,820	0,747	0,600	0,480	0,517	0,796	0,997	0,846	0,755	0,626	0,498	0,508	0,777		
	to 1	0,991	0,093	0,102	0,088	0,021	0,013	0,474	0,998	0,154	0,187	0,277	0,308	0,038	0,498	0,997	0,129	0,190	0,268	0,304	0,098	0,379		
	to ra.ne.	0,007	0,099	0,042	0,063	0,058	0,069	0,043	0,001	0,169	0,051	0,067	0,106	0,139	0,063	0,002	0,143	0,045	0,055	0,087	0,086	0,066		
	inc	0,009	0,017	0,011	0,042	0,032	0,055	0,019	0,002	0,029	0,040	0,047	0,054	0,064	0,028	0,003	0,029	0,025	0,033	0,040	0,031	0,024		
	dec		0,119	0,148	0,181	0,160	0,319	0,093		0,159	0,234	0,380	0,504	0,601	0,198		0,153	0,234	0,369	0,503	0,520	0,220		
	count	9471	4374	2791	2274	1508	1376	21794	15866	7050	7838	6471	3553	2120	42898	12306	13501	12184	10152	5224	1538	54905		
	attr.start	2,1	4,4	7,7	16,4	19,8	98,5	12,0	2,2	6,0	9,1	15,5	24,1	82,7	11,9	2,3	5,2	8,8	12,11	23,3	51,2	9,6		
b	equal	0,991	0,852	0,695	0,691	0,545	0,523	0,824	0,996	0,807	0,674	0,558	0,457	0,438	0,769	0,999	0,817	0,724	0,606	0,445	0,415	0,766		
	same ra.	0,991	0,881	0,723	0,715	0,576	0,544	0,843	0,996	0,813	0,689	0,584	0,483	0,459	0,780	0,999	0,841	0,735	0,621	0,478	0,445	0,780		
	to 1	0,991	0,107	0,218	0,193	0,202	0,091	0,414	0,996	0,165	0,263	0,338	0,365	0,097	0,498	0,999	0,140	0,222	0,302	0,385	0,120	0,403		
	to ra.ne.	0,008	0,116	0,055	0,049	0,079	0,057	0,059	0,002	0,178	0,040	0,052	0,067	0,032	0,061	0,001	0,149	0,038	0,040	0,068	0,092	0,065		
	inc	0,009	0,017	0,020	0,020	0,022	0,027	0,016	0,004	0,026	0,028	0,033	0,026	0,021	0,020	0,001	0,024	0,019	0,018	0,022	0,032	0,017		
	dec		0,130	0,286	0,289	0,433	0,450	0,160		0,168	0,298	0,409	0,517	0,541	0,211		0,159	0,256	0,376	0,533	0,554	0,218		
	dec -1		0,023	0,068	0,096	0,231	0,359	0,049		0,003	0,035	0,071	0,151	0,444	0,034		0,018	0,034	0,074	0,148	0,434	0,043		
	sam+1	0,991	0,988	0,942	0,909	0,778	0,634	0,955	0,996	0,978	0,953	0,922	0,849	0,556	0,957	0,999	0,982	0,957	0,923	0,863	0,565	0,955		
	sam+ne.	0,999	0,996	0,778	0,765	0,655	0,601	0,902	0,999	0,991	0,729	0,636	0,550	0,491	0,841	1,000	0,991	0,773	0,661	0,547	0,536	0,846		
	count	9358	9290	4766	5608	1323	298	30643	14406	9509	9490	7706	3163	340	44614	12289	15701	10618	10379	4258	632	53877		
	fraction	0,305	0,303	0,156	0,183	0,043	0,010	1	0,323	0,213	0,213	0,173	0,071	0,008	1	0,228	0,291	0,197	0,193	0,079	0,012	1		
	attr.start	2,1	3,9	7,0	9,8	18,5	37,1	5,8	2,2	4,8	8,0	12,3	17,9	35,7	7,1	2,4	5,0	8,1	10,9	17,1	31,6	7,5		

7.4.5 Fade out as factor of mech2

In met5 presence of multiple fade out was significantly associated with the shift size of the trajectory beginning after accumulation. In met7e the shift =50 is the same as in met5 44, but for f in met7e fade out is significantly higher, whereas for r the opposite - slightly smaller, as shown in [tab.4](#). This table, analogous to [m6.tab.2](#), contains a division of histories of initiated processes on chaotic explosions and acceptable (saved). Next, division of 'saved' on point attractors (PAS), fade out (fade) and others, i.e. cases which not exploded, not fade out, are not PAS, but they came to tmx not exceeding the threshold A1=150. They are described in lines '1' in the sense of first initiation. If damage fade out, it could be stimulated by the secondary initiation: the second '2', a further third and next ini '3 & next' described together. Fade out can be complete (total fade), i.e. without secondary initiation, but this happened only in series met5c. It is also puzzling difference met5c and met7e. For comparison with previous simulations [tab.4](#) contains similar data for met5c and met6 which relate to passes M1 to M20 together. Now pass N is added separately and passes M free are examined separately, enabling network f to separate pass M1. Also falling in the point attractor (PAS) is in met7 clearly rarer than in met5c, but it happens, in met6 not occur.

Multiple fade out participates in mech2, which lowers the level of the ice, which was shown searching (ch.7.4.7 parameter A1h0, [tab.5](#), [fig.21](#)) an additional criterion to generate ro-modularity.

Tab.4. The division of the effects of the first initiation; of the second; and a third and further; between the explosion and acceptance (saved). Next division 'saved' on point attractors (PAS), fade out to A1=0 (fade) and (others) through the tmx with A1: threshold>A1>0, but variable in the process. Secondary initiations, however, have different proportions of these effects than first ini, and later than the second, and also change share in the same direction. Comparison with met5c and met6 points to significant differences in the mechanism leading to acceptance. A clear increasing fade out in nets f in comparison to met5 is a change in direction of met6 image. After the first ini also shown how % of fade out had no further ini, i.e. secondary ini, and remained as fade out to the end (despite the change is permanent). Such events were observed in met5, but did not occur in met6 nor met7. The share of nearly 100% fade out after next ini demonstrates the repeatability of fade out mechanism and this is the basis for the calculation of the length of such loops ([fig.17c](#)).

1	77,69	91,52	72,10	89,17	68,13	66,62	66,99	77,92	78,53	78,93	78,28	70,44	69,60	68,49	77,45	78,39	79,84	78,71	expl1	% ini1
	22,31	8,48	27,90	10,83	31,87	33,38	33,01	22,08	21,47	21,07	21,72	29,56	30,40	31,51	22,55	21,61	20,16	21,29	saved1	% ini1
	2,73	1,85	0,00	0,00	0,00	0,32	0,35	0,00	0,88	0,00	1,78	0,10	0,21	0,12	0,02	0,86	0,04	1,63	PAS1	% saved1
	10,75	17,00	99,99	100,00	50,68	48,45	55,46	31,24	11,87	31,39	17,16	70,39	69,94	79,32	32,50	11,65	36,54	18,88	fade1	% saved1
	86,52	81,16	0,01	0,00	49,32	51,23	44,20	68,75	87,25	68,61	81,05	29,52	29,84	20,55	67,48	87,49	63,42	79,49	other1	% saved1
	43,66	58,96	0,0000	0,0000	0,0013	0,0000	0,0000	0,0000	0,0000	0,0000	0,0000	0,0000	0,0000	0,0049	0,0000	0,0000	0,0000	0,0000	0,0042	tot.fade
2	1,3542	0,2688	21,0043	20,5334	9,8646	7,7095	7,6890	6,3744	1,5407	10,0239	3,3220	18,8882	16,8287	17,8431	6,7394	1,5968	12,8209	5,4342	expl2	% ini2
	98,6458	99,7312	78,9957	79,4666	90,1354	92,2905	92,3110	93,6256	98,4593	89,9761	96,6780	81,1118	83,1713	82,1569	93,2606	98,4032	87,1791	94,5658	saved2	% ini2
	0,1317	0,0634	0,0000	0,0000	0,0000	0,0056	0,0022	0,0000	0,0100	0,0000	0,0197	0,0037	0,0059	0,0008	0,0000	0,0235	0,0000	0,0166	PAS2	% saved2
	93,4856	86,9896	99,9994	100,0000	98,9210	99,0033	99,1897	99,1647	99,7093	98,7221	99,5086	99,0989	99,0328	99,2739	98,9546	99,6032	98,1609	99,3768	fade2	% saved2
	6,3827	12,9470	0,0006	0,0000	1,0790	0,9911	0,8081	0,8353	0,2807	1,2779	0,4717	0,8974	0,9613	0,7253	1,0454	0,3733	1,8391	0,6066	other2	% saved2
3 & next	cf M	cr M	6f M	6r M	fN	fM1	fM7-20	rN	rM	sN	sM	feN	feM1	feM7-20	reN	reM	seN	seM		
	0,0004	0,0000	0,0404	0,0193	0,0241	0,0103	0,0074	0,0112	0,0016	0,0210	0,0030	0,0992	0,0507	0,0446	0,0129	0,0019	0,0373	0,0049	expl3	% ini3
	99,9996	100,0000	99,9596	99,9807	99,9759	99,9897	99,9926	99,9888	99,9984	99,9790	99,9970	99,9008	99,9493	99,9554	99,9871	99,9981	99,9627	99,9951	saved3	% ini3
	0,0260	0,0354	0,0000	0,0000	0,0000	0,0001	0,0001	0,0000	0,0038	0,0000	0,0035	0,0000	0,0001	0,0001	0,0000	0,0035	0,0000	0,0042	PAS3	% saved3
	99,6558	99,7125	99,9519	99,9758	99,7893	99,8147	99,8357	99,7434	99,7560	99,7464	99,7831	99,7683	99,7795	99,8142	99,7293	99,7415	99,7275	99,7356	fade3	% saved3
0,3182	0,2521	0,0481	0,0242	0,2107	0,1852	0,1642	0,2566	0,2402	0,2536	0,2135	0,2317	0,2205	0,1857	0,2707	0,2551	0,2725	0,2602	other3	% saved3	

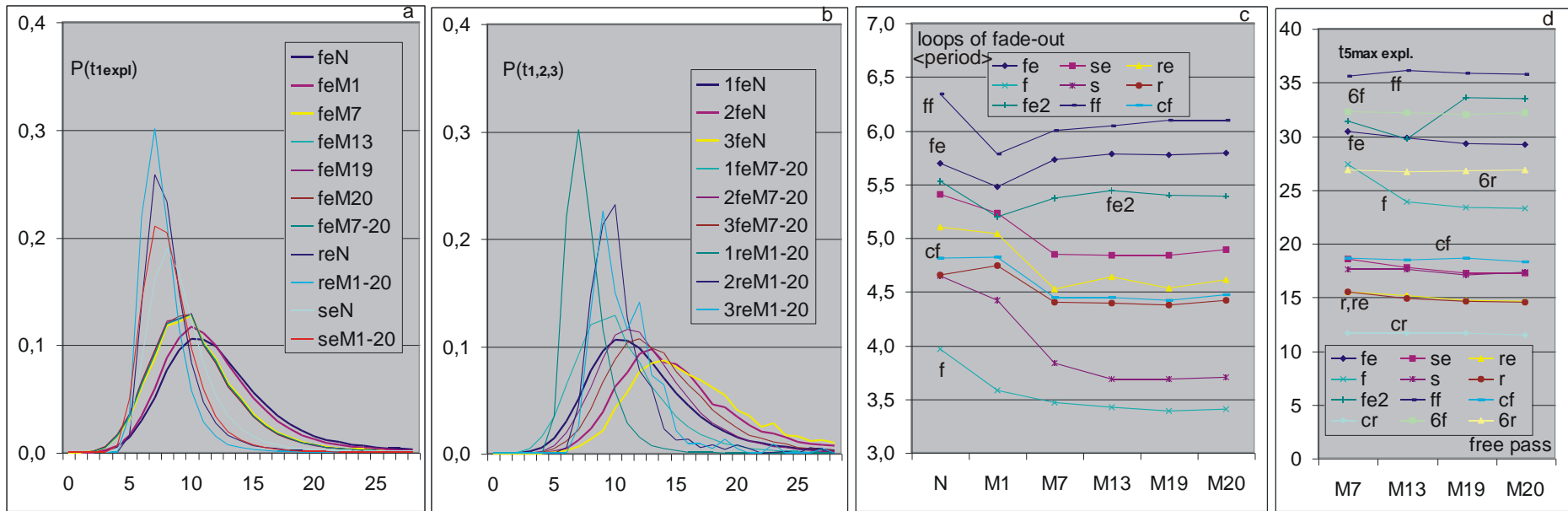


Fig.17. Multiple fade out suggests the existence of loops of a similar course, in which fade out to $A1 = 0$ is repeated and secondary initiation resulting from the reception on the input of modified node the initial state of the input, for which that point permanent change was introduced. In met5 it was one of the premises of ro-modularity (ch.5.6.1, m5.fig.11b), it corresponds to fig.(c), where obtained in met7e values are similar. Wonders here distinctly different deflection net f from the nets s and r. Models a and b give here departure from met5 cf in opposite directions. Clearly model a is closer to image of met6, which confirms similar findings from other results.

The theme of strongly connecting with the fade out is a moment of the explosion to chaos. Tab.4 also tracks participation of explosion. In (a,b) presented distributions of moment of explosion measured from the time of initiation (see m6.fig.1d,e and fig.6).

(a) Explosion after first initiation for fe in different passes. Only passes N and M1 differ from all other passes free, which practically coincide. For series re and se differences of passes M are smaller and separately only pass N is shown. In these networks, the explosion occurs earlier, the distribution is much less fuzzy.

(b) The difference in the time of the explosion for the secondary ini. As can be seen, the after later secondary ini explosions occur somewhat later, then the state of the secondary ini harder leading to chaotic explosion.

(c) Average period of fade out loops, see above.

(d) Average time of 5 of latest explosion (see m5.fig.5ab; m6.fig.1c). As usual, series r and re are the most similar, s and se also lie close together and close to the r, re. Nets type f have later explosions to chaos, which is consistent with the distribution in (a,b) and more resemble the image of met6. Model met5c, however, gives shorter end of the explosion.

7.4.6 Clusters A4 and their connection

Clusters ro quickly turns out to be effective and this stopped the development of concept of cluster A4. This left the concept in too simple form, especially in the algorithm connecting detected local clusters. The results indicate, however, that the concept of clusters A4 provides a tool to distinguish between the effects of small damage avalanche, changing depending on the type of network and other formulas constructing them. This simple diagnosis can be useful to design further studies. Recall: Local cluster A4 is a set of nodes which after one (later accumulated) ini for at least one step have a state different from the pattern. Their fulfilment is not the ice, but always remain consistent with the pattern. Nodes assigned to A4 may be ice. The nodes are thus constituting damage, but not in a moment as A1, only almost the whole trajectory to tmx. A41 from all trajectory; A4h from t=100, that is the stable section, this value is used for local clusters definition.

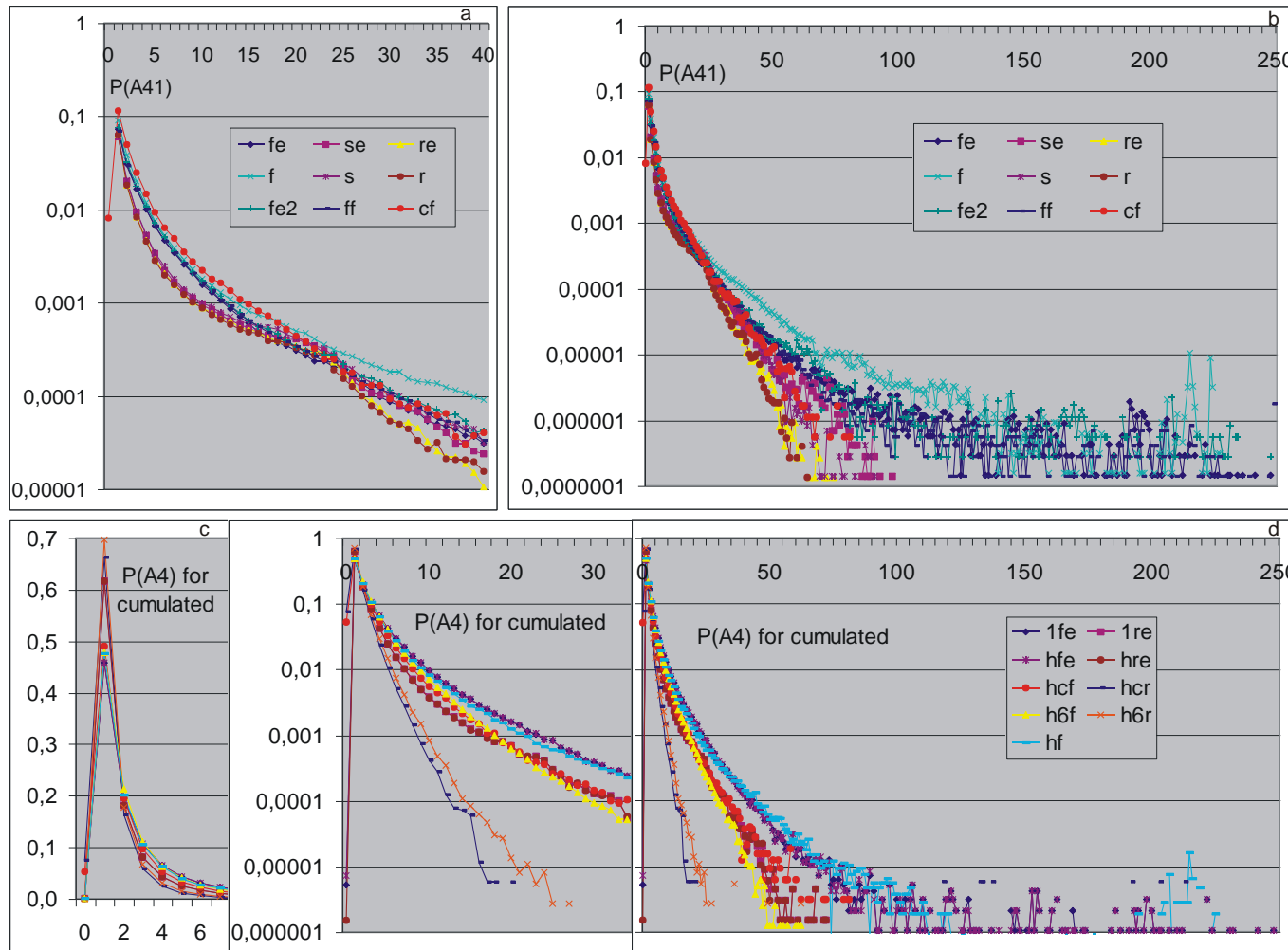


Fig.18. Comparison of local clusters A4 in met7 to met5 (m5.fig.13) and met6 (m6.fig.3) from the whole process from N to M20. In met5 for series 44 an A4h has not been studied, only A41 and data are collected for all cases, including the chaotic explosions. Research in met7 consider model similar to met5c 44 '4+7'. (a,b) Data are collected similarly like for m5.fig.13a,b. Series met5 cf is more similar here to the end of s and r in both models, however, does not have a bend in the area 24, as is best seen in (a). Series fe, f, fe2 and ff have a distinctly longer tail. (c,d) corresponds to m6.fig.3c,d. Here the picture is for accumulated, mainly for a more appropriate measure A4h (excluding the first 100 steps). Series s & se are omitted here for clarity, as they are close to r. Here, too, the above bending is visible, but smaller. In comparison to met5 and met6, the met7 results lie considerably more to right: cf and 6f almost coincide with re; fe and f have higher and longer tails. Peak in (c) looks almost exactly like in m6.fig.3c. In terms of cluster A4 the met7 slightly differs from met5 and met6 by higher levels of mostly infrequently occurring large local clusters A4.

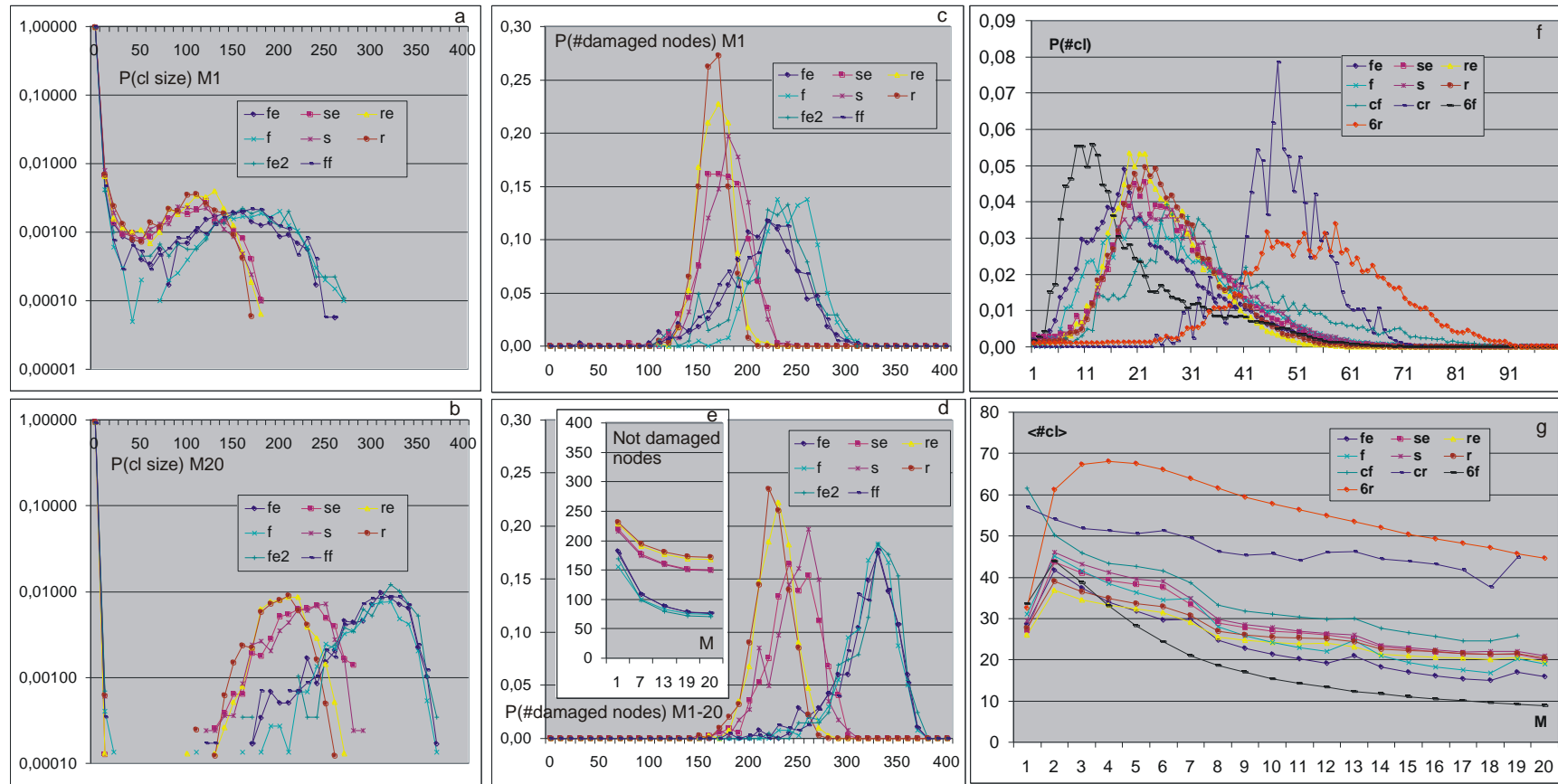


Fig.19. Size distributions combined (global) cluster A4 at the beginning (a) and at the end (b) of the process of accumulation. Here to increase statistics summed each 10 consecutive values. These results correspond to [m5.fig.14b,d](#), where cf looks similar (but there is a result for series met5 45, not for 44 '4+7', which is similar to met6 & 7) and [m6.fig.4b,d](#), where the image is roughly similar (here for comparison data from met5 44 '4+7' are shown). Usually (except cr) at the end is one big cluster and a dozen to twenty few tiny clusters. Probably improving criterion of combining the image would be much more diverse and interesting.

(c,d) - Probability that so much nodes has been damaged (in accumulated) at any time t from the start of accumulation, to the end of pass M1 (c) and to the end of the accumulation process (d). (Note, it is not $P(A4)$, A4 is for one accumulation only in one pass.)

(e) - Based on the data as in (c,d) for each pass free numbers of nodes that do not have suffered damage up to indicated pass free are determined. This result interpretatively is somewhat analogous to [fig.13a](#) which shows the size of the ice clusters ro (however, there is an average ice in the pass).

Next (f) distribution of number of clusters; and (g) the average number of clusters for subsequent pass M. They correspond [m5.fig.14e,f](#) (note the model 45 instead of 44 '4+7' and pass N) and [m6.fig.4e,f](#) (this data is inserted here). In met7 compared to met6 and 5 there was a results unification - they are now very close to the f and r.

It was expected that nodes participating in damage after one ini are clearly strongly related not only for this particular ini, they are therefore a quasi-module. The rule to combine these local clusters have as criterion a common node. This assumption turned out to be too simplistic, which resulted in the more advanced observation of clusters ro and problems in construction of global clusters ro. But that time, attention was focused clusters ro and the development of algorithms for clusters A4 are given up. This does not mean, however, that a deeper study of this concept are pointless, but for the main aims of the study they turn out to be unnecessary. Combining local clusters should be based on some similarity associated with a number of common nodes, so that the occasional participation of a small number of nodes in another global cluster did not damage the separation of these clusters. Both global clusters ro and A4 should be treated as the hills in the field but not as thoroughly separated island.

Global clusters image in used form typically differs from initial expectations, but for network cr was very close to expectations. There were many clusters of similar sizes, and in [m5.fig.14b,d](#) and [m6.fig.4b,d](#) this network in both models met5 45 and 44 did not have the right peak of clusters size. Probably the mechanism of the right peak was the cause of the left peak tail. In met6 and 7 net r has already right peak separated from the left ([fig.19a,b](#)) despite the absence of a bent tail ([m5.fig.13f](#); [m6.fig.3d](#); [m7.fig.18d](#)).

In met7 local clusters test are supplemented showing their presence in particular networks in range of pass free ([fig.15b,g,h](#)). Dynamic size distribution of local clusters A4h clearly growing unevenly - the same size appear in many subsequent accumulated initiations which indicates the presence of a real cluster of such size. A4h sizes of clusters, however, are small, they relate only changed nodes, not like in event of ro - active, do not arise so similarly pronounced peaks as for clusters ro.

Local clusters ro and A4h have quite a different interpretation and comparing them should be cautious - clusters ro are sets of nodes linked by a common period, usually lasting in several consecutive accumulations and appearing simultaneously with the similar period even after the ice break, so illustrate the functional relationship of these nodes but they not consider changes after initiation (although as a result of the ini are changed). They are tested and detected after each accumulation. Cluster A4h concerns only changes in the process after ini, it also illustrate the functional relationship, as common deviations from pattern, however, a piece of the cluster ro can change.

Similarly to ice in clusters ro, in study of cluster A4 there is a significant number of nodes that were not damaged during accumulation from pass M1 to M20 ([fig.19e](#)).

Similarly to met5 ([m5.tab.1](#)), A41 for exploding in se, re, f has only counts for 400, 399 and 398; for s and r even only 400. Network fe and fe2 go to 380 and ff to 390. Beyond that range counts exactly none. Chaotic avalanche therefore covers virtually the entire network, but in the model met7a (without tax) is sometimes more nodes is not affected by damage.

Accumulated events (i.e. accepted $A1 < \text{threshold}$ and not PAS and with a sufficiently large global attractor) have a distribution A4h shown in [fig.18d](#). The sum of all nodes that have been damaged in accumulating cases in pass M1 or in the whole process of accumulation up to the end of M20, has distribution shown in [fig.19c,d](#).

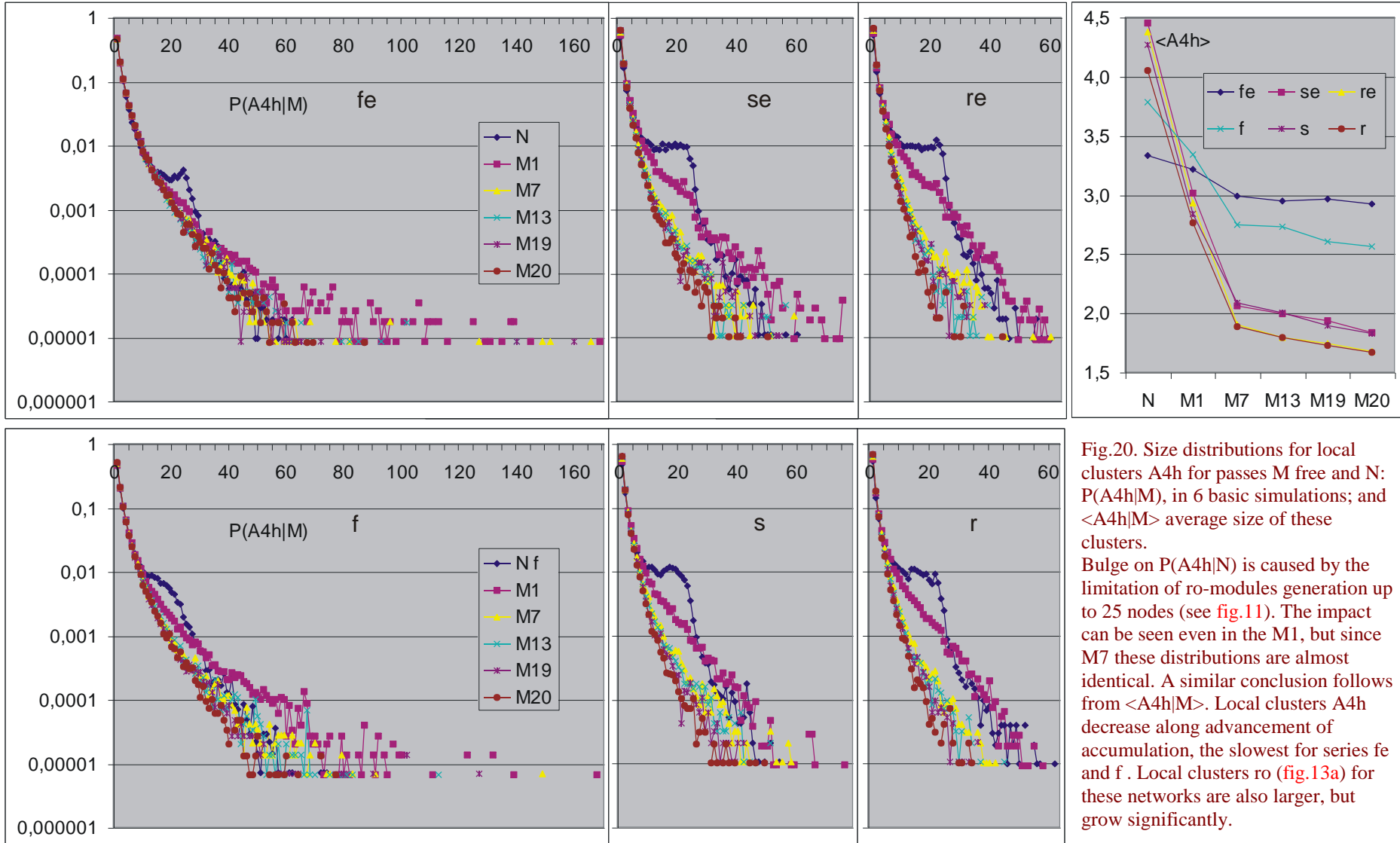


Fig.20. Size distributions for local clusters A4h for passes M free and N: $P(A4h|M)$, in 6 basic simulations; and $\langle A4h \rangle$ average size of these clusters. Bulge on $P(A4h|N)$ is caused by the limitation of ro-modules generation up to 25 nodes (see fig.11). The impact can be seen even in the M1, but since M7 these distributions are almost identical. A similar conclusion follows from $\langle A4h \rangle$. Local clusters A4h decrease along advancement of accumulation, the slowest for series fe and f. Local clusters ro (fig.13a) for these networks are also larger, but grow significantly.

7.4.7 Attempts to find in pass N an indicator of later deviations from met5 of net f

The search of parameter omitted when ro-modularity is generated should lead by indicating phenomena present in the initial pass N (or M1), the intensity of which correlated with mechanism mech2 detected by the range of ice in M20 (fig.12f). Such factors may include: 1- The number of active ro-modules immediately after they are generated. Here the similarity series f_i and f_u with different minimal numbers of active ro-modules (tab.2) suggests that it is not (fig.12f). Series f_{e2} moving in the right direction from the f_e (fig.12b), but minutely, substantially in the range of error. 2- Size of the ice in pass N (fig.12a). These parameters are available immediately after generation of ro-modularity and can be used to elimination such generation result.

Next, in crocodiles generally higher levels of fade out are observed in the cases, which later strong decrease of ice. Fact that the fade out here is significantly higher than in met5 supports this suggestion. Also in the chaotic case met7a and b (X,S,T,F) blue dots $A1=0$ in fig.8e,f are directly below the red line of accepted. This not enough accurate observation required a statistical check: 3- $A1h0$ is the average % of fade out ($A1=0$) on section 200 the last steps before tmx. In crocodiles M the blue curve shows level $A1=0$ (fig.15), in N there are blue points. Next, can be expected that 4- the size of initial attractor may also have an impact on the future process. 5- Occurrence of larger local clusters ro should indicate a lack of immunity of ro-module walls, which is probably the way to drift in the direction of mech2 as the liquidation of division on separate ro-modules and making one space as in met6. 6- The number of states 0 shows departure of network from random state as an undesirable side effect resulting from the algorithm for ro-modularity generating. The conclusion that the formation of mech2 is the result of the effect should be excluded.

Defining phenomena in M1 actively transforming the network from given ro-modular state into stable state since M7 is appealing, but it is not done and waiting for successors.

The results are shown in tab.5 and fig.21, especially in fig.21a, which shows using example of f the relative deviation of average parameter for ice range in M20 (horizontal axis) from the average over the entire M20. This allows to easily compare the ability to predict various studied parameters. Two of them are stand out: $A1h0$ and a number of local clusters ro, whose size exceeds the 80 nodes (>80). Somewhat weaker is the ' > 50 ', and similar ' >150 ' has already too small statistics. The number of active ro-modules is of little importance, while attractor in f seem attractive, but they are fluctuations, which reflects tab.5a: for f_e and f_{se} - image of f is not repeated for the other networks. As can be seen from the tab.5a, level states 0 does not correlate with the ice size in the M20. Thus, for further analysis only $A1h0$ and ' >80 ' remain.

The purpose of this study was to find an additional criterion for ro-modularity generating that can cut out the mech2 as mechanism virtually absent in met5. Such a criterion will cut part of 400 effective nets, it has to cut as little as possible, at the latest after pass N, so that the average ice in M20 be as large as possible. In fig.21g the range of such a criterion is shown - it should housed between the upper curve 'M20' showing the average in M20, if there is allowed only so many cases with the greatest ice, which indicates the horizontal axis; and the lower curve 'org', which results from a random set of cases, as occurred in this simulation. The main section of the largest ice the $A1h0$ criterion turns out to be better than ' >80 '. This is due to the size and nature of dispersion shown in fig.21b,c.

As shown in fig.21d, the phenomenon $A1h0$ increases dramatically with accumulation and in N has yet low strength but already is suitable for use, but only statistically due to dispersion (fig.21b). All tested parameters have such dispersion, there are not among them a decent standard deterministic factor in a well-conditioned mechanism. Preliminary results of effectiveness of criterion $A1h0$ are shown in tab.5b, and the results of the final simulations - in tab.5c. $A1h0$ parameter is not a priori known before allowing the generated state testing, and only after examining pass N. It shows that fade out is an important part in mech2 (see ch.7.4.5, tab.4 and fig.17).

Tables 5b,c show that allowing for the analysis of ro-modularity only cases which in N have a mean fade out less than 15 is enough that the image be similar to expected. Unfortunately, this parameter does not show how to build a network of such property. In addition, the parameter is statistical and a low power, which can be seen in tab.5b,c.

In addition to checking single parameters, it was performed a simple recognition of two-parameter correlation. For this purpose the 19 parameters formed as products of 2 single parameters. In fig.21e their strength in the same manner as in fig.21a are shown. It is not surprising that the product of the strongest single parameters here is the strongest, but it also shows that there is not found a better, double correlation, which could not be seen in the study each parameter separately. In fig.21f the dispersion of such product $A1h0 * '>80$ ' is shown, which looks more promising than shown above fig.21b,c. However, in fig.21g its efficacy was lower in the main section than the $A1h0$. It could be due to the initial value 0 in ' > 80 ', which liquidate the information contributed by $A1h0$. Therefore this parameter was revised to $A1h0 * ('>80'+1)$, which does, indeed, improve its efficiency, but it reached only a level similar to the $A1h0$ alone (fig.21g).

In network r the dispersion of ice in M20 was so insignificant that there is a lack of results, such as in tab.5a and fig.21, but they are in tab.5b, and the lack of a clear presence mech2, although in fig.11 a big difference between N and M7 is seen.

Tab.5. The search criteria for elimination mech2 by correlation with the ice level in M20 .

	range	ev	ice M20	ice N	A1h0N	>50	>80	act.ro-m.	attr	#0
f	400-351	83	381	370	15,23	1,90	0,77	2,76	111	337890
	350-301	10	325	369	18,90	1,40	0,70	2,70	121	339511
	300-251	23	269	370	17,91	1,96	0,65	2,57	65	337647
	250-201	77	222	366	20,06	2,30	1,14	2,91	78	336014
	200-151	108	176	363	22,63	2,68	1,54	2,91	84	337922
	150-101	74	123	360	27,22	2,73	1,70	2,82	72	338590
	100- 51	25	87	358	29,16	2,92	1,88	2,96	86	337543
fe	400-351	33	382	369	27,97	1,73	1,15	2,21	160	341615
	350-301	6	315	368	32,83	1,50	1,00	2,17	107	341927
	300-251	15	273	374	24,93	1,93	0,87	1,93	177	345973
	250-201	41	222	371	29,95	1,93	1,29	1,90	86	343624
	200-151	91	173	370	37,80	1,67	1,05	1,73	128	344957
	150-101	129	126	369	39,88	1,88	1,22	1,81	116	346002
	100- 51	81	85	366	43,67	2,02	1,42	2,00	208	344901
se	400-351	327	383	358	13,63	0,43	0,02	3,06	160	307666
	350-301	59	330	355	17,42	0,59	0,05	3,00	107	308454
	300-251	13	283	353	18,54	0,77	0,08	3,08	177	308908

(a) The search for a correlation between the range of ice at the end of evolution in M20 (ev - number of events, ice M20 - average ice in M20) and the average on accumulation of:
 1- ice size in pass N (ice N);
 2- A1h0 - % of fade out (A1=0) in pass N on the last 200 steps;
 3,4- number local clusters ro whose size is greater than 50 or 80 nodes;
 5- the number of active ro-modules after creation;
 6- length of the generated global attractor;
 7- the number of node states =0 in trajectory after accumulation.
 To estimate the accuracy of the results given the number of events (ev), which for some compartments are very small (fig.12f). The results of the simulation f, fe and se . For s they are similar to se, analysis of network type r is omitted, since virtually all events are in the highest range.

As can be seen, only A1h0, '>50' and '>80' show a clear correlation (fig.21).

range A1h0 in N	f		s		r	
	ice in M20	events	ice in M20	events	ice in M20	events
1 - 9	314,3	12	376,4	54	387,0	49
10-14	312,3	19	369,4	95	385,1	82
15-19	215,3	43	352,2	43	383,2	58
20-24	195,6	47	335,4	8	375,4	11
25-29	171,2	35				
30-34	172,1	25				
35-52	173,0	19				

(b) Criterion A1h0 effectiveness measured in pass N for ice level in M20 for nets f, s and r (one of the initial simulation up to 200 nets). As can be seen, limiting A1h0<15 gives the average ice for f at a level above 310. For nets s and r the A1h0 works monotonically. However, it is an a'posteriori indicator (after pass N) but not algorithmic condition in the phase ro-modularity creation. The number of events of 200 is given to evaluate the accuracy, but the spread of ice is significant, e.g. for range f 10-14 here is 218-390 and for range 15-19 f: 114-389, s: 270-395, r: 341-396, which is typical. The minimal ice for f: 68, s: 220, r: was 341. Indicator A1h0 is therefore a factor of low statistical power. See also fig.21.

	range	ev	ice M20	ice N	A1h0N	cut M20	cut ev	act.ro-m.	>50	#0
f	1-9	28	343	377	6,21	343	28	2,71	1,43	337246
	10-14	51	287	370	12,18	306	79	2,96	2,24	335987
	15-19	90	231	365	17,02	267	169	2,96	2,62	335910
	20-24	95	207	364	21,89	245	264	2,82	2,45	338392
	25-29	72	187	362	27,08	233	336	2,74	2,58	339369
	30-34	32	168	359	31,81	227	368	2,84	2,25	337322
	35-52	32	153	357	38,19	221	400	2,72	2,41	340078
fe	1-9	5	229	381	8,20	229	5	1,40	1,40	343504
	10-14	9	319	376	12,67	287	14	2,00	2,22	342673
	15-19	15	238	375	16,87	262	29	1,93	2,33	345541
	20-24	29	217	369	21,86	240	58	2,14	2,24	341102
	25-29	44	198	369	27,14	222	102	2,05	2,05	343598
	30-34	59	169	369	31,86	202	161	1,75	1,92	343385
	35-67	239	142	368	45,62	166	400	1,85	1,71	345983
se	1-9	73	382	371	7,19	382	73	2,52	0,34	306480
	10-14	150	375	360	12,20	377	223	2,91	0,44	307120
	15-19	115	368	351	16,86	374	338	3,45	0,53	307687
	20-24	42	357	348	21,52	372	380	3,31	0,57	310349
	25-29	16	355	341	26,44	372	396	3,44	0,63	312732
	30-34	4	355	348	32,25	371	400	2,50	0,50	316501

(c) The effectiveness of elimination criterion A1h0. **Range** of A1h0; **ev**- number of events in the range; **ice** in **M20** or **N** - average ice level; average **A1h0** in **N**. If the elimination of higher ranges events would be done, then average level of the ice in M20 would be the '**cut M20**', and included events of 400 would be '**cut ev**'. Comparison with (b) shows the accuracy of such methods. In this ranges division the average of: the number of **active ro-modules**, of local clusters **ro >50** and the number of states of zero (**#0**) are indicated in the last columns.

range	ev	A1h0*>80	ice M20	cut M20	cut ev
1-9	83	0,87	296	296	83
10-19	72	15,26	257	278	155
20-29	84	24,11	225	259	239
30-39	49	33,94	179	246	288
40-135	112	60,69	158	221	400

(d) The sequence for f basing on A1h0 * '> 80'. It is presented more exactly in fig.21g. Using submission criteria A1h0 and >80 turns out to be less effective than single A1h0.

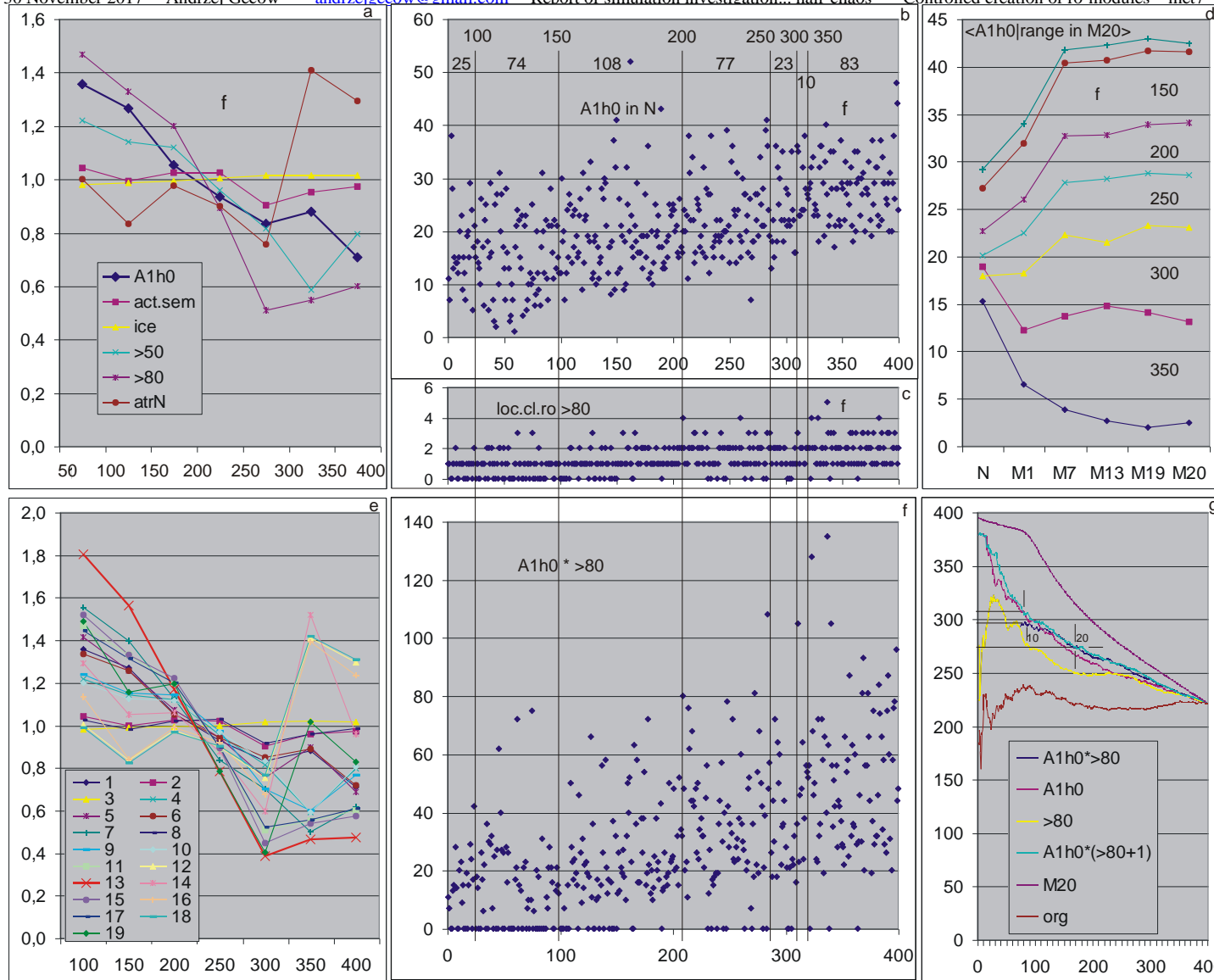


Fig.21. Results of searching in pass N of additional criterion rejecting mech2, on example of f. (a) - Deviation of averages for ice compartments in M20 from the average for M20 for several tested parameters in pass N. The most important of them, A1h0 - (see tab.5) average % of fade out (A1=0) for the last 200 steps before tmx. For chaotic cases it is usually close to 90, so if mech2 was associated with chaos, should also have a relationship with A1h0. As is shown in (a) a connection A1h0 and mech2 is determined, and in (d) is shown that strongly grows with consecutive passes. However, the criterion is poorly suited, because the dispersion is too large, as shown in (b). Value about 25 could be used, but it left too large number of cases of small ice in M20 and also cut out a large number of cases with a big ice. The second candidate for the criterion could be a number of local clusters ro larger than 80 nodes, but this parameter has a weak statistics and better illustrates this phenomenon number greater than 50 nodes. Here, too, the dispersion (c) is too large. In (c,d) the horizontal axis is the number of net ordered by the ice size in M20. The vertical lines divide the results on ice size ranges in M20 described at the top of the lines and lower - the number of nets in each of the ranges (fig.12f). In (d) the boundaries of

these ranges are given between the graph lines described in this way. The problem of dispersion consider all tested parameters, and it mostly makes impossible to add a satisfactory criterion. The level of ice, the number of active ro-modules and size of the attractor in N have no relation to the state of ice in M20. The level of ice after ro-modularity generation in the graphs of type (a) in all tested networks is similarly almost equal to 1, two remaining parameters show random fluctuations and e.g. deviation of attractor size in (a) for f is not repeated for fe or for se the examined more closely. The nature of these results for fe and se is very close and there is no reason to show them here.

7.5 Summarising

The jobs of met7 defined in ch. 7.1.Introduction are:

1 – controlled creating of ro-modularity (ch.7.2) indicated in met5;

2 – testing of its stability indirectly after creation (ch.7.3) and

confirmation of ro-modularity mechanism: small attractors of ro-modules quickly introduce into already tested trajectory and block next explosion, but their assembling into global attractor of system gives not so small attractors;

3 – checking of stability of generated state and mechanism of ro-modularity during accumulation of small effective changes (ch.4 - met7e from evolution).

Ro-modularity is a specific form of half-chaos based on particular mechanism, similar to modularity, but it is more than just modularity, it requires ice in which the lakes of activity are formed with the help of modules. Half-chaos concern not fully random network. The network because its parameters would be chaotic, if it would be random. In half-chaos similar parts of small disturbance give ordered and chaotic effect (small or near Derrida level damage - effective change of system function). Autonomous Kauffman networks are investigated, but number s of equally probable signal versions is not limited to 2, as in Boolean networks, but may be greater, in met7 $s=4$ is used. Number K of input links to each node of net are fixed to $K=3$ for any net type. Parameters $s, K=4,3$ make random network strongly chaotic, but creating ro-modular network becomes not fully random and gets 'left peak' of ordered events which make it half-chaotic. In met7 3 types of network are investigated: scale-free (f), random Erdos-Renyi (r) and single-scale (s). Coming out of ro-modularity in effect of very small change of function of one node makes network classically chaotic. For keeping ro-modularity an acceptance of small effective change, smaller than half of Derrida level, is enough. Natural division on chaotic and ordered events is radical, section of middle damage has no counts, then threshold can be defined in wide range (fig.1a,b; 9a).

7.5.1 Ro-modularity creation

Indications of construction of ro-modularity from met5 turn to be approximate and to get the algorithm had to make many simplifying assumptions. They are mostly arbitrary choices of limiting parameters (the maximum size of ro-module, local attractor size, the minimum number of active ro-modules, minimal global attractor); and the arbitrary choices of parameters tax to force the local period, which, however, turned out to be unnecessary. These parameters are indicated in tab.2, but moreover, the algorithm is simplified. These parameters in nature should not be rigid, but given by distributions, which so far nothing is known. Even if it were determined from met5, it resulted from the unique, arbitrary initial condition which was PAS0. An important difference to met5 is the design of ro-module walls, which imposed severe narrowing of function. This approach resulted from the assumption possibly different primes forcing ro-module periods. These two design assumptions have a strong influence on the results, as is demonstrated by the selection of tax (tab.2) and probably cause a noticeable results difference between met7e and met5c. The big surprise was that forcing small attractors in ro-modules (procedure using tax table) is unnecessary. It forced repetition of research for the simpler model, which was named 'a' as the primary (see ch.7.3.5). It shows, however, higher deviation from met5, so the original model 'b' can be seen as attempt to bring the results to the desired form of met5.

Despite some differences to met5, including the presence of new mechanisms (meh2) and severity negligible in met5 phenomena (not detected global attractor) it can be considered that the ro-modularity vision, on which basis in a controlled way it was built, was the right one. However, it seems that the ro-modularity character in met5 is "cleaner" and to its controlled obtaining, particularly for network f the algorithm should be further refined, probably for node functions of walls. The search for additional criteria to construct ro-modularity on the basis of the main feature of mech2 - significant 'melt the ice' observed in evolution, merely indicated that mech2 is associated with an increased incidence of multiple fade out, did not give an effective, algorithmic criterion for ro-modularity constructing.

7.5.2 Stability of obtained ro-modularity without evolution

The stability of the resulting ro-modularity is not the result of not completely random node functions neither of selecting the initial states, that is also not entirely random. This stability is due to the obtained state of the system. After leaving the ro-modularity (X), or after changing the initial states (S), or after moving functions to other nodes with the original initial states (T), despite leaving the functions, the system behaves as a chaotic (F), where the functions are random.

The graph (fig.1) of damage size (P(A1 at tmx)), the shapes of the right and left peaks and an empty region between them are very close to the expected indicated in met5. This confirms the presence in the generated ro-modularity state of ordered and chaotic modes at the same time in the same network and on a similar scale (fig.1c,d). The presence of the ordered response to a small disturbance on a scale similar to the alternative chaotic mode is the main novelty of the presented concept and the basic subject of research to confirm its existence and basic properties.

7.5.3 Confirmation of the blocking mechanism of explosion by small local attractors in spite of the large global attractor

The essence of the ro-modularity mechanism of explaining importance lies in the presence of short attractors of ro-modules, so short that the number of occurrences of the node input state for which a permanent change is introduced, is so small that probability of damage fade out for each of these cases substantially independent is not negligible.

During the study we found that the hope for one simple explanation is deceptive, and studied the phenomenon have a wealth of conditions and mechanisms. However, this simplified vision turned out to be (ch.7.3.4) roughly correct. Convincingly it is mainly shown in [fig.6abde](#) where for ro-modularity the probability of chaotic explosion falls steadily, but for the networks in chaotic state of the scope of the first initiation occurs much more slowly declining share of the explosions from secondary initiation.

7.5.4 Stability of ro-modularity during evolution - accumulation of 'small' changes

The attractiveness of the use of ro-modular state to describe living objects requires to demonstrate that the ro-modular state can evolve long enough without a systematic need to leave him by the system. This property has already demonstrated in met5 for PAS0 (generally the PAS - Point Attractor System) as initial state. Now the ro-modular state was generated by specific algorithm, it does not necessarily have all the properties obtained when starting from the PAS including the stability during evolution so it was necessary to check this major property in the new conditions.

In the evolution tested as in met5 stability remains similarly as in met5, however, in the initial stage the system state defined by the algorithm generating ro-modularity is explicitly switched to some other state that virtually no further changes. Although exploration (mainly in ch.7.4.7) failed to grasp a factor or condition which introduced the algorithm for ro-modularity generating would give the state immediately. This demonstrates the incompleteness of this algorithm and our understanding of ro-modularity, but the sufficiency of the algorithm, as well as the start from PAS, has been confirmed. Evolution leads to a state that already shows no further changes, and during the whole process system state displays basic properties of ro-modularity.

7.5.5 Other mechanisms detected

In addition to the mechanism specified in met5 and called ro-modularity, the state generated by studied algorithm shows the presence of other mechanisms, not observed in met5 and, it seems, that it is not directly related to understanding the mechanism of ro-modularity. Much stronger melting of ice in a large number of cases, mainly network type f is one of the most important symptoms. Networks type s and r almost do not manifest the presence of the mechanism. It is possible that found a variety of symptoms arise not from one additional mechanism, but rather they have a common cause and a common character. Thus it was assumed tentatively that this is one mechanism called 'mech2' and studied primarily correlation with its main feature. One can assume that this is the mechanism responsible for changing the system state at the beginning of evolution mentioned above.

It has been shown that it has a relationship with a significant increasing relative to met5 of level of multiple fade out (parameter A1h0 in ch.7.4.7). It leads to very large clusters ro and this is already at the beginning of the process (ibid parameter '>80'), which allows the use of these two criteria to predict the statistical deviations from the image of met5 at the end of the evolution met7e. Such large clusters are formed at the expense of ice wall between ro-modules and probably some ro-modules, which resembles the situation to the observed in met6, where for stability small attractor was enough without ro-modularity. It can be summarized as in met6, that the ability to create an evolutionary steady state half-chaos, from which small changes (characteristic in the evolution of living organisms) do not lead out, is not limited to ro-modularity (met4 & 5) or modularity (met3, met8), but the essence of this state is small attractor.

7.5.6 Clusters ro and A4 - check interpretation of ro-modularity

In met5 ro-modularity concept has been derived by observing the formation of node clusters so functionally linked that initiating changes rarely go beyond the cluster. Initially clusters A4, based on just such a concept were studied. Parameter A4 is the number of nodes, which took part in damage from initiation to t_{mx} - the end of the tested section of the trajectory. In met6 and met7 this range was limited, eliminating the 100 initial steps in which the waveforms were unstable, they on the way to the attractor. However, the method of connecting such local clusters in global clusters A4 - the objects more durable, better characterizing the system and summarizing the knowledge of its history – turns out to be too simple and create the image of a little adequate.

Finding in met5 the local clusters ro based on the same period of node state gave a much more effective tool. Focusing on it the methods of cluster A4 were not further developed. In met7 clusters ro local and global have been observed in many ways (mostly ch.7.4.2) and gave a broad base to the picture of the ro-modularity function. They fully confirmed the reality of the existence of ro-modules during evolution and the relationship of these global clusters with generated by algorithm at the beginning.

References

- Barabasi-Albert** A.-L. Barabási, R. Albert, H. Jeong, 1999. Mean-field theory for scale-free random networks. *Physica A* 272, p.173–187.
- Derrida** B. Derrida, Y. Pomeau, 1986. Random Networks of Automata: A Simple Annealed Approximation. *Europhys. Lett.*, 1(2), p.45–49.
B. Derrida, G. Weisbuch, 1986. Evolution of Overlaps Between Configurations in Random Boolean Networks. *Journal De Physique* 47, p.1297–1303.
- Erdos-Renyi** P. Erdős, A. Rényi, 1960. Random graphs. *Publication of the Mathematical Institute of the Hungarian Academy of Science*, 5, p.17–61
- Hughes00** T. R. Hughes et al., 2000. Functional discovery via a compendium of expression profiles. *Cell* **102**, p.109-126.
- Kauffman 1969-71** S.A. Kauffman, 1969. Metabolic stability and epigenesis in randomly constructed genetic nets. *J. Theor. Biol.* 22, p.437-467
S.A. Kauffman, 1971. Gene regulation networks: a theory for their global structure and behaviour. *Current topics in dev. biol.* 6, p.145.
- ooKauf** S.A. Kauffman, 1993. *The Origins of Order: Self-Organization and Selection in Evolution*. (Oxford University Press New York)
- Ramo06** P. Rämö, J. Kesseli, O. Yli-Harja, 2006. Perturbation avalanches and criticality in gene regulatory networks. *J. Theor. Biol.* **242** p.164-170
- Serra04** R. Serra, M. Villani, A. Semeria, 2004. Genetic network models and statistical properties of gene expression data in knock-out experiments. *J. Theor. Biol.* 227, p.149-157
- Serrajtb07** R. Serra, M. Villani, A. Graudenzi, S. A. Kauffman, 2007. Why a simple model of genetic regulatory networks describes the distribution of avalanches in gene expression data. *J.Theor.Biol.* **246** 449-460
- Iguchi07** K. Iguchi, SI. Kinoshita, H. Yamada, Boolean dynamics of Kauffman models with a scale-free network. *J. Theor. Biol.* 247, 138-151, (2007)
- arj** A. Gecow, 2010. More Than Two Equally Probable Variants of Signal in Kauffman Networks as an Important Overlooked Case, Negative Feedbacks Allow Life in the Chaos. [arXiv:1003.1988v2](https://arxiv.org/abs/1003.1988v2)
- brj** A. Gecow, 2010. Complexity Threshold for Functioning Directed Networks in Damage Size Distribution. [arXiv:1004.3795v1](https://arxiv.org/abs/1004.3795v1)
- it** A. Gecow, 2011. Emergence of Matured Chaos During Network Growth, Place for Adaptive Evolution and More of Equally Probable Signal Variants as an Alternative to Bias p. In: *Chaotic Systems*, E.Telo-Cuautle (ed.), ISBN: 978-953-307-564-8, pp 280-310, <http://www.intechopen.com>
- 1974** A. Gecow, 1974. Draft of deductive theory of biological evolution. III Polish Symposium of Biocybernetic, Biomathematic and Biotechnique. 9-11 May 1974, talk and paper PTC 1975.
- 1975** A. Gecow, 1975. A cybernetic model of improving and its application to the evolution and ontogenesis description. In: *Fifth International Congress of Biomathematics Paris*
- dgec** A. Gecow, 2008. Structural Tendencies - effects of adaptive evolution of complex (chaotic) systems. *Int.J Mod.Phys.C*, 19, 4, pp 647-664.
- bics** A. Gecow, 2008. A simplified algorithm for statistical investigation of damage spreading. *BICS 5-7 Nov.08 Tg.Mures Romania AIP Conf. Proc.* 1117 pp 133-141.
- fgec** A. Gecow, 2009. Emergence of Chaos and Complexity During System Growth. In : *From System Complexity to Emergent Properties*. M.A. Aziz-Alaoui & Cyrille Bertelle (eds), Springer, Understanding Complex Systems Series, pp 115-154
- Naaj** A. Gecow, 2016. Life evolves in half-chaos of not fully random systems. <http://vixra.org/abs/1612.0390>
- GdM** M. Nowostawski, A. Gecow, 2011. Identity criterion for living objects based on the entanglement measure. *ICCCI 2011, Studies in Computational Intelligence* 381, Radosław Katarzyniak, Tzu-Fu Chiu, Chao-Fu Hong, Ngoc Thanh Nguyen (Eds.) *Semantic Methods for Knowledge Management and Communication*, Springer, pp 159-170